UNIVERSITY OF BELGRADE

FACULTY OF CIVIL ENGINEERING

Anja Ranđelović

MODELLING TRANSPORT OF MICROPOLLUTANTS IN BIOFILTRATION SYSTEMS FOR STORMWATER TREATMENT

Doctoral Dissertation

Belgrade, 2016

УНИВЕРЗИТЕТ У БЕОГРАДУ

ГРАЂЕВИНСКИ ФАКУЛТЕТ

Ања Ранђеловић

МОДЕЛИРАЊЕ ТРАНСПОРТА МИКРОПОЛУТАНАТА У БИОФИЛТЕРСКИМ СИСТЕМИМА ЗА ТРЕТМАН КИШНИХ ВОДА

докторска дисертација

Београд, 2016

ПОДАЦИ О МЕНТОРУ И ЧЛАНОВИМА КОМИСИЈЕ

Ментори:

Проф. др Ана Делетић, Универзитет Monash, Факултет за инжењерство, Департман за грађевину

Доцент др Ненад Јаћимовић, Универзитет у Београду, Грађевински факултет

Чланови комисије:

Проф. др Ана Делетић, Универзитет Monash, Факултет за инжењерство, Департман за грађевину

Проф. др Душан Продановић, Универзитет у Београду, Грађевински факултет

В. проф. др Зорана Науновић, Универзитет у Београду, Грађевински факултет

Доцент др Бранислава Лекић, Универзитет у Београду, Грађевински факултет

Доцент др Ненад Јаћимовић, Универзитет у Београду, Грађевински факултет

Датум одбране докторске дисертације: _____

Захвалница

Посебну захвалност дугујем ментору, проф. др Ани Делетић, која ми је несебично пружала подршку у досадашњем научном и стручном усавршавању. Права је привилегија радити са њом и њеним тимом. Захваљујем проф. др Душану Продановићу јер су ми његови мудри савети помогли да будем бољи стручњак и човек. Захваљујем ментору, доц др Ненаду Јаћимовићу, на пажљивом исчитавању Дисертације. Велику захвалност дугујем свим члановима Комисије на подршци и на корисним сугестијама оком израде и прегледа Дисертације.

My eternal gratitude goes to my good friend and colleague dr Kefeng Zhang, without whom this Thesis would not be the same. It has been my privilege to endure this voyage with you. I am grateful to my colleagues in the Civil Engineering Department, especially to Cintia, David, Dušan and Sandy, who each, in their own way, helped me finish this thesis.

Захваљујем од срца и свим колегама са Института за хидротехнику који су увек били расположени за дискусију или спремни да ми помогну, међу којима бих издвојила Жељка, Андријану, Љиљу и Драгутина. Посебно бих се захвалила Буди и Душану, са којима сам дуго делила канцеларију и који су моји најстарији и највреднији саборци у овој дисциплини. Захваљујем се и Николи Златановићу на бројим корисним сугестијама и дискусијама.

Посебну, највећу захвалност дугујем мојим најближима, Урошу и мами, који су ми током година пружали безрезервну подршку. Немам речи којима могу описати колико ми је то значило!

У Београду, 2016

Ања

MODELLING TRANSPORT OF MICROPOLLUTANTS IN BIOFILTRATION SYSTEMS FOR STORMWATER TREATMENT

Abstract

Biofiltration systems, also known as bioretentions or rain-gardens, are widely used for stormwater treatment. In order to successfully design biofilters, it is important to improve models that can predict their performance. This thesis presents a rare model that can simulate removal of a wide range of micro-pollutants from stormwater by biofilters. The model is based on (1) a bucket approach for water flow simulation, and (2) advection/dispersion transport equations for pollutant transport and fate. The latter includes chemical non-equilibrium two-site model of sorption, first-order decay, and volatilization, thus is a compromise between the limited availability of data (on stormwater micro-pollutants) and the required complexity to accurately describe the nature of the phenomenon.

The model was calibrated and independently validated on two field data series collected for different organic micro-pollutants at two biofilters of different design. This included data on triazines (atrazine, prometryn, and simazine), glyphosate, and chloroform. The data included variable and challenging biofilter operational conditions; e.g. variable inflow volumes, dry and wet period dynamics, and inflow pollutant concentrations. The model was able to simulate water flow well, with slight discrepancies being observed only during long dry periods when, presumably, soil cracking occurred. In general, the agreement between simulated and measured pollutographs was good. As with flows, the long dry periods posed a problem for water quality simulation (e.g. simazine and prometryn were difficult to model in low inflow events that followed prolonged dry periods). However, it was encouraging that pollutant transport and fate parameters estimated by the model calibration were in agreement with available literature data. This suggests that the model could probably be adopted for assessment of biofilter performance of other stormwater micro-pollutants (PAHs, phenols, phthalates, etc.). The model, therefore, could be applied in practice for sizing of biofilter systems and their validation monitoring, when used for stormwater harvesting.

The model was run with laboratory data from batch studies (fluorescein as referent pollutant) and column studies (herbicides: atrazine, prometryn, simazine, glyphosate). A procedure was developed for the estimation of parameters from batch studies, and a regular calibration method was used for parameter estimation from column tests. Parameters for both sorption and degradation were found to be underestimated from batch studies. This is hypothesized to be due to differences in the water to soil ratio in batch studies, when compared to the field. The sorption parameters estimated from columns were also somewhat underestimated, and when used with the model produced higher outflow pollutant concentrations. This is especially the case with glyphosate, and only slightly with the triazines. Column studies also indicate less-kinetic-sorption behaviour when compared with the field data. It is hypothesized that kinetic sorption behaviour on the field may be apparent, and a consequence of the assumption that the flow is one dimensional, when in reality it is not, leading to conclusion that the kinetic behaviour is due to *structural* heterogeneity of the biofiltration material, rather than *chemical*.

Uncertainty analysis was conducted using GLUE methodology that pointed the most sensitive parameters: soil-water partitioning coefficient and fraction of sites prone to instantaneous sorption. Additionally, the predictive uncertainty was assessed by making 95% confidence intervals for model predictions, and it suggested that the model is sound.

Keywords

Stormwater biofilter, micropollutant modelling, atrazine, simazine, prometryn, glyphosate, chloroform, uncertainty analysis

Research area: Civil Engineering

Specific research areas: Ecological engineering, Fluid mechanics and hydraulics, Transport processes in hydrotechnical engineering

UDC: 628.1/.4(043.3)

МОДЕЛИРАЊЕ ТРАНСПОРТА МИКРОПОЛУТАНАТА У БИОФИЛТЕРСКИМ СИСТЕМИМА ЗА ТРЕТМАН КИШНИХ ВОДА

Резиме

Биофилтерски системи, познати и као биоретензије или кишне баште, се често користе за третман кишних вода. Да би биофилтери били успешно пројектовани, неопходно је побољшање модела који могу да предвиде њихово понашање. Ова дисертација садржи модел који може да симулира отклањање шире групе микрополутаната из кишних вода помоћу биофилтера. Модел је базиран на (1) методи линеарних резервоара којима се описује ток воде и (2) адвективно-дисперзивне транспортне једначине за транспорт микрополутаната. Транспортна једначина садржи и модел за хемијски неуравнотежену двостепену сорпцију, биоразградњу по реакцији првог реда, и волатилизацију, и тако представља компромис између ограничених података (о микрополутантима у кишном отицају) и неопходне сложености да се опише природа феномена.

Модел је калибрисан и независно верификован на две серије теренских података прикупљене за различите органске микрополутанте на два биофилтера. Подаци су о триазинима (атразин, прометрин, симазин), глифосату, и хлороформу. Подаци обухватају оперативне услове који су варијабилни и изазовни: варијабилне запремине воде на улазу у биофилтер, различиту динамику сушних и кишних периода и варијабилне концентрације загађивача у кишној води. Модел је успешно симулирао ток воде, са разликама у мереним и симулираним вредностима протока уочљивим у периодима после дугих суша, када је земљиште испуцало. Слагање између симулираних и мерених полутограма је било углавном добро. Као и са протоцима, дуги сушни периоди су представљали проблем и за симулације квалитета воде (нпр. симазин и прометрин нису најбоље моделирани у периоду маловодних кишних епизода које су уследиле после дугог сушног периода). Међутим, било је охрабрујуће да су параметри модел за транспорт полутаната оцењени путем калибрације били у сагласности са вредностима у литератури. Ово даје назнаке да би модел могао да се користи и за симулирање понашања других микрополутанта (полицикличних угљоводоница, фенола,

фталата, итд.) у биофилтерима. Модел би, дакле, могао да се примени и у пракси за димензионисање биофилтерских система и валидациони мониторинг.

Модел је испробан и са лабораторијским подацима са batch тестова (флуоресцеин као референтни микрополутант) и са колона (хербициди: атразин, прометрин, симазин и глифосат). Развијена је процедура за процену параматера модела коришћењем података са batch тестова, а подаци са колона су коришћени за калибрацију модела. Параметри модела који описују сорпцију и биоразградњу одређени помоћу batch тестова су били мало потцењени. Сматра се да је узрок томе различит однос земљиште-вода који је примењен у тестовима у односу на онај који се налазио на терену. Сорпциони параметри одређени са колона су такође били мало потцењени, и давали су веће излазне концентрације микрополутаната. Ово је посебно случај са глифосатом, и мало мање са триазинима. Подаци са колона су показали да се у њима одвија процес сорпције који има далеко мање карактеристику кинетике, него оно што су показали подаци са терена. Сматра се да је кинетика сорпције на терену вероватно привидна, и да је последица претпоставке да је ток воде кроз биофилтер једнодимензионалан. Такође се сматра да је један од разлога за привидно кинетичке карактеристике сорпције на терену структурална хетерогеност биофилтерског материјала, а не хемијска (што је претпоставка модела).

Анализа неодређености је спроведена коришћењем GLUE методологије која је указала на најосетљивије параметре модела: коефицијент партиције и проценат сорпционих места која су склона инстант сорпцији. Додатно, направљен је 95% интервал поверења, који је показао да је већина мерења добро обухваћена моделом.

Кључне речи

Биофилтер за третман кишних вода, моделирање микрополутаната, атразин, симазин, прометрин, глифосат, хлороформ, анализа неодређености

Научна област: Грађевинарство

Уже научне области: Еколошко инжењество, Механика флуида и хидраулика, Транспортни процеси у хидротехници

УДК: 628.1/.4(043.3)

Publication list from this research

Journal papers:

Randelovic A., Zhang K., Jacimovic N., McCarthy D., Deletic A. (2016) Stormwater treatment model (MPiRe) for selected micro-pollutants. Water Research, vol. 89, pp. 180-191 (Impact factor: 6.279)

Zhang K., **Randelovic A.**, Deletic A., Page D., McCarthy D. (2016) Stormwater biofilters: A new validation modelling tool. Ecological Engineering, vol. 87, pp. 53-61 (Impact factor: 3.231)

Zhang K., **Randelovic A.**, Aguiar L.M., Page D., McCarthy D., Deletic A. (2015) Methodologies for Pre-Validation of Biofilters and Wetlands for Stormwater Treatment. PLoS ONE 10(5): e0125979. (Impact factor: 3.702)

Zhang K., **Randelovic A.**, Page D., McCarthy D., Deletic A., (2014) The validation of stormwater biofilters for micropollutant removal using in-situ challenge tests. Ecological Engineering, vol. 67(1), pp. 1-10 (Impact factor: 3.231)

Randelovic A., Zhang L., Jacimovic N., McCarthy D., Deletic A. (2013) Eksperimentalno istraživanje transformacije mikropolutanta u biofilterima (raingardens). Voda i sanitarna tehnika, vol. 2/2013, pp. 9-16

Conference papers:

Randelovic A. Prodanovic V., Jacimovic N., McCarthy D., Deletic A. (2015, September 17-19) Assessing uncertainty of a water quality model for a stormwater biofiltration treatment system. Paper presented at the 7th IWA Young Water Professional Conference "East meets West", Belgrade, Serbia

Randelovic A., Zhang K., Jacimovic N., McCarthy D., Deletic A. (2014, September 7-11) Development of a transport and fate model for organic micropollutants at a stormwater biofilter site. Paper presented at the 13th International Conference on Urban Drainage, Sarawak, Malaysia

Randelovic A., Zhang K., Jacimovic N., McCarthy D., Deletic A. (2014, May 28-30) Preliminary study on transport and fate of selected pesticides at a stormwater biofilter site. Paper presented at the 6th IWA Young Water Professional Conference "East meets West", Istanbul, Turkey

Randelovic A., Zhang L., Jacimovic N., McCarthy D., Deletic A. (2013, 22.-24. maja) Eksperimentalno istraživanje transformacije mikropolutanta u biofilterima (raingardens). 13-a Međunarodna konferencija „Vodovodni i kanalizacioni sistemi", Jahorina, Pale, BiH

TABLE OF CONTENTS

1 INTRODUCTION 2

1.1 BIOFILTRATION WATER QUALITY MODELLING 3

1.2 OVERALL AIM 4

1.3 SCOPE OF THE THESIS 5

1.4 OUTLINE OF THE THESIS 6

2 LITERATURE REVIEW 8

2.1 INTRODUCTION 8

2.2 STORMWATER QUALITY 8

2.2.1 MICROPOLLUTANTS, PRIORITY OR EMERGING POLLUTANTS 8

2.2.2 NOTABLE STORMWATER QUALITY STUDIES 9

2.2.3 ORGANIC MICROPOLLUTANTS DETECTED IN STORMWATER 10

2.3 BIOFILTRATION SYSTEMS CHARACTERISTICS 19

2.3.1 BIOFILTER DESIGN 20

2.3.2 MODE OF OPERATION 22

2.4 REVIEW OF STORMWATER AND RELATED TREATMENT MODELS 23

2.4.1 OVERALL VIEW 23

2.4.2 STORMWATER BIOFILTER MODELS AND WATER QUALITY MODELLING 24

2.4.3 WATER QUALITY MODELS POTENTIALLY APPLICABLE TO STORMWATER ORGANIC MICROPOLLUTANT MODELLING 25

2.4.4 PROCESS MODELLING 28

2.5 UNCERTAINTY ANALYSIS 40

2.5.1 INTRODUCTION 40

2.5.2 UNCERTAINTY ASSESSMENT 41

2.5.3 SOURCES OF UNCERTAINTY IN STORMWATER QUALITY MODELS 43

2.6 CONCLUSION: IDENTIFICATION OF KEY KNOWLEDGE GAPS 47

2.7 RESEARCH AIMS AND OBJECTIVES 48

2.8 METHODOLOGY USED TO COMPLETE THE RESEARCH AIMS 49

3 EXPERIMENTAL DATA 51

3.1 INTRODUCTION 51
3.2 FIELD EXPERIMENTAL SITE 51
3.2.1 MEASURING AND SAMPLE COLLECTION SYSTEM 54
3.3 FIELD TRACER TESTING 60
3.4 FIELD ELECTRO RESISTIVE TOMOGRAPHY (ERT) 61
3.4.1 INTRODUCTION 61
3.4.2 ABOUT THE METHOD 62
3.4.3 FIELD SETUP 63
3.4.4 RESULTS AND DISCUSSION 64
3.5 FIELD "SPIKING" TESTING 67
3.5.1 EXPERIMENTAL SETUP 68
3.5.2 CHALLENGE TESTS CHARACTERISTICS 71
3.5.3 SAMPLING AND ANALYSIS 73
3.5.4 CHALLENGE TEST: RESULTS AND DISCUSSION 74
3.6 LABORATORY BATCH AND COLUMN TESTING 87
3.6.1 BATCH STUDIES 88
3.6.2 COLUMN STUDIES 89
3.7 CONCLUSIONS 90

4 MODEL DEVELOPMENT 92

4.1 INTRODUCTION 92
4.2 MODEL STRUCTURE SELECTION 92
4.3 FLUID FLOW 94
4.4 POLLUTANT TRANSPORT AND FATE 98

5 MODEL TESTING 104

5.1 INTRODUCTION 104
5.2 MODEL TESTING SETTINGS AND PROCEDURES 104

5.2.1 INPUT DATA AND BOUNDARY CONDITIONS 104
5.2.2 CALIBRATION PROCEDURE 106
5.2.3 MODEL PERFORMANCE ASSESSMENT 108
5.2.4 CONSERVATIVE TRACER TEST ANALYSIS 109
5.2.5 MODEL CALIBRATION AND VERIFICATION WITH FIELD DATA 110
5.2.6 MODEL PARAMETER ESTIMATION FROM BATCH STUDIES DATA 111
5.2.7 MODEL PARAMETER ESTIMATION FROM COLUMN STUDIES 114
5.3 MODEL TESTING RESULTS AND DISCUSSION 115
5.3.1 MODEL CALIBRATION AND VERIFICATION WITH FIELD DATA 115
5.3.2 MODEL PARAMETER ESTIMATION VIA LABORATORY TESTING 128
5.4 CONCLUSIONS 139

6 MODEL UNCERTAINTY ANALYSIS 142

6.1 INTRODUCTION 142
6.2 MATERIALS AND METHODS 142
6.2.1 CALIBRATION DATA SELECTION UNCERTAINTY PROCEDURE 142
6.2.2 GENERAL UNCERTAINTY PROCEDURE 142
6.3 RESULTS AND DISCUSSION 144
6.3.1 CALIBRATION DATA SELECTION 144
6.3.2 GENERAL UNCERTAINTY 145
6.4 CONCLUSIONS 152

7 CONCLUSIONS AND FURTHER RESEARCH 154

7.1 SUMMARY OF CONCLUSIONS 154
7.2 RESEARCH AIM EVALUATION 156
7.3 DISCUSSION ON MODEL DEVELOPMENT 158
7.3.1 MODEL'S USABILITY IN PRACTICAL APPLICATIONS 159
7.4 FUTURE RESEARCH 160

8 REFERENCES 162

LIST OF FIGURES

FIGURE 2-1 SOME OF THE COMMONLY USED PLANTS IN BIOFILTRATION SYSTEMS: *CEPHALANTHUS OCCIDENTALIS* (UPPER LEFT), *SALIX NIGRA* (UPPER RIGHT), *SCIRPUS MICROCARPUS* (LOWER LEFT), *EUPATORIUM PURPUREUM* (LOWER RIGHT). SOURCE: WIKIPEDIA.ORG 21

FIGURE 2-2 CONCEPTUAL PHYSICAL NON-EQUILIBRIUM MODELS FOR WATER AND SOLUTE TRANSPORT (AFTER ŠIMŮNEK AND VAN GENUCHTEN, 2009) 36

FIGURE 2-3 CONCEPTUAL CHEMICAL NON-EQUILIBRIUM MODELS FOR REACTIVE SOLUTE TRANSPORT (Θ – SOIL WATER CONTENT, C – POLLUTANT CONCENTRATION IN WATER, S^E – POLLUTANT CONCENTRATION SORBED ON SOIL AT EQUILIBRIUM, S^K – POLLUTANT CONCENTRATION SORBED ON SOIL KINETICALLY (AFTER ŠIMŮNEK AND VAN GENUCHTEN, 2009) 37

FIGURE 2-4 MAJOR UPTAKE PROCESSES OF ORGANIC SUBSTANCES BY PLANTS (AFTER COLLINS ET AL., 2006) 40

FIGURE 2-5 KEY SOURCES OF UNCERTAINTIES IN URBAN DRAINAGE MODELS AND LINKS BETWEEN THEM (AFTER DELETIC ET AL., 2012) 44

FIGURE 2-6 SUBJECTIVE ASSESSMENT OF THE EMPHASIS (INDICATED BY THE LENGTH OF BARS) GIVEN BY DIFFERENT MODELLING COMMUNITIES TO VARIOUS SOURCES OF MODEL INADEQUACY (AFTER GUPTA ET AL., 2012) 46

FIGURE 3-1 THE MONASH CAR PARK BIOFILTRATION SYSTEM – A SCHEME 52

FIGURE 3-2 CELL 1 AT THE MONASH CAR PARK BIOFILTRATION SYSTEM – A SCHEME 54

FIGURE 3-3 CELL 2 AT THE MONASH CAR PARK BIOFILTRATION SYSTEM – A SCHEME 54

FIGURE 3-4 THE FLOW MEASURING SYSTEM SCHEME 54

FIGURE 3-5 THE THETA PROBE – SOIL MOISTURE SENSOR TYPE ML2X 55

FIGURE 3-6 SOIL MOISTURE PROBES SCHEME 57

FIGURE 3-7 THE SAMPLING POINTS SHOWING THE CUSTOM SAMPLING PROCEDURE 58

FIGURE 3-8 POLLUTOGRAPHS OF FLUORESCEIN DURING TRACER TESTS AT CELL 1 AND CELL 2 60

FIGURE 3-9 POLLUTOGRAPH OF KCL DURING THE TRACER TEST AT CELL 1 AND CELL 2 61

FIGURE 3-10 SAMPLE ELECTRODE ARRAY PLACEMENT AND MEASUREMENT POINTS FOR ERT (AFTER KELLER AND FRISCHKNECHT, 1996) 62

FIGURE 3-11 ELECTRODE PLACEMENT AT THE BIOFILTER SITE - MONASH CARPARK 64

FIGURE 3-12 TIME LAPSE OF ERT INVERTED DATA FOR CELL 1 ON 9/11/2012 (10 MIN INVERVAL) 66

FIGURE 3-13 TIME LAPSE OF ERT INVERTED DATA FOR CELL 2 ON 8/11/2012 (10 MIN INVERVAL) 67

FIGURE 3-14 INFLOW AND OUTFLOW RATES MEASURED DURING THE 1^{ST} (TOP) AND THE 2^{ND} (BOTTOM) TEST SERIES 75

FIGURE 3-15 POLLUTOGRAPHS OF GLYPHOSATE DURING 1^{ST} TEST SERIES (TOP) AND 2^{ND} TEST SERIES (BOTTOM) FOR CELL 1 AND CELL 2 81

FIGURE 3-16 POLLUTOGRAPHS OF CHLOROFORM DURING 1ST TEST SERIES (TOP) AND 2ND TEST SERIES (BOTTOM) FOR CELL 1 AND CELL 2 82
FIGURE 3-17 POLLUTOGRAPHS OF ATRAZINE DURING 1ST TEST SERIES (TOP) AND 2ND TEST SERIES (MIDDLE) AND OF SIMAZINE DURING 1ST TEST SERIES (BOTTOM) FOR CELL 1 AND CELL 2 83
FIGURE 3-18 POLLUTOGRAPHS OF SIMAZINE DURING 2ND TEST SERIES (TOP) AND OF PROMETRYN DURING 1ST TEST SERIES (MIDDLE) AND 2ND TEST SERIES (BOTTOM) FOR CELL 1 AND CELL 2 84
FIGURE 3-19 POLLUTOGRAPHS OF NAPHTHALENE DURING 2ND TEST SERIES FOR CELL 1 AND CELL 2 85
FIGURE 3-20 POLLUTOGRAPHS OF PCP AND PHENOL DURING 2ND TEST SERIES FOR CELL 1 AND CELL 2 85
FIGURE 3-21 TPHS, PYRENE AND DEHP CONCENTRATION DETECTED IN SOIL SAMPLES TAKEN FROM SURFACE SOIL AT CELL 1 AND CELL 2 DURING THE 2ND TEST SERIES 86
FIGURE 4-1 THE MAIN BIOFILTER ZONES AND FLOW SCHEME 94
FIGURE 5-1 THE METEOROLOGICAL STATION NO. 086071 DISTANCE FROM THE BIOFILTER LOCATION (ADAPTED FROM WWW.BOM.GOV.AU) 105
FIGURE 5-2 SCHEME OF PEST "WRAPPING-UP" THE STANDALONE MODEL 108
FIGURE 5-3 POLLUTOGRAPHS OF KCL FOR CELLS 1 AND 2 - ESTIMATION OF DISPERSIVITY 110
FIGURE 5-4 EXAMPLE PLOT OF LABORATORY SORPTION DATA WITH CHARACTERISTIC CONCENTRATIONS USED FOR DETERMINATION OF SORPTION PARAMETERS IN THE TRANSPORT MODULE 111
FIGURE 5-5 INFLOW, MEASURED AND MODELLED FLOW AT THE OUTFLOWS OF CELL 1 FOR THE TWO TEST SERIES: CALIBRATION DATA FROM 2012, E = 0.876 (BOTTOM), VERIFICATION DATA FROM 2011, E = 0.611 (TOP). NOMENCLATURE TEST X-Y: X – CELL NUMBER, Y – TEST NUMBER 115
FIGURE 5-6 INFLOW, MEASURED AND MODELLED FLOW AT THE OUTFLOWS OF CELL 2 FOR THE TWO TEST SERIES: CALIBRATION DATA FROM 2012, E = 0.881 (BOTTOM), VERIFICATION DATA FROM 2011, E = 0.904 (TOP) 116
FIGURE 5-7 INFLOW AND OUTFLOW CONCENTRATION AND POLLUTANT FLUX TIME SERIES FOR GLYPHOSATE AND CELL 1: CALIBRATION, E = 0.575 (BOTTOM), VERIFICATION, E = 0.545 (TOP) 117
FIGURE 5-8 INFLOW AND OUTFLOW CONCENTRATION AND POLLUTANT FLUX TIME SERIES FOR GLYPHOSATE AND CELL 2: CALIBRATION, E = 0.736 (BOTTOM), VERIFICATION, E = 0.611 (TOP) 118
FIGURE 5-9 INFLOW AND OUTFLOW CONCENTRATION AND POLLUTANT FLUX TIME SERIES FOR ATRAZINE IN CELL 1: CALIBRATION, E = 0.876 (BOTTOM), VERIFICATION, E = 0.536 (TOP) 119
FIGURE 5-10 INFLOW AND OUTFLOW CONCENTRATION AND POLLUTANT FLUX TIME SERIES FOR ATRAZINE IN CELL 2: CALIBRATION, E = 0.776 (BOTTOM), VERIFICATION, E = 0.941 (TOP) 120
FIGURE 5-11 INFLOW AND OUTFLOW CONCENTRATION AND POLLUTANT FLUX TIME SERIES FOR PROMETRYN IN CELL 1: CALIBRATION, E = 0.730 (BOTTOM), VERIFICATION, E = 0.782(0.595) (TOP) 121
FIGURE 5-12 INFLOW AND OUTFLOW CONCENTRATION AND POLLUTANT FLUX TIME SERIES FOR PROMETRYN IN CELL 2: CALIBRATION, E = 0.907 (BOTTOM), VERIFICATION, E = 0.893 (TOP) 122
FIGURE 5-13 INFLOW AND OUTFLOW CONCENTRATION AND POLLUTANT FLUX TIME SERIES FOR SIMAZINE IN CELL 1: CALIBRATION E = 0.700 (BOTTOM), VERIFICATION E = 0.286(0.293) (TOP) 123

FIGURE 5-14 INFLOW AND OUTFLOW CONCENTRATION AND POLLUTANT FLUX TIME SERIES FOR SIMAZINE IN CELL 2: CALIBRATION, E = 0.511 (BOTTOM), VERIFICATION, E = 0.285 (TOP) 124
FIGURE 5-15 INFLOW AND OUTFLOW CONCENTRATION AND POLLUTANT FLUX TIME SERIES FOR CHLOROFORM IN CELL 1: CALIBRATION, E = 0.967 (BOTTOM), VERIFICATION, E = 0.705 (TOP) 124
FIGURE 5-16 INFLOW AND OUTFLOW CONCENTRATION AND POLLUTANT FLUX TIME SERIES FOR CHLOROFORM IN CELL 1: CALIBRATION, E = 0.947 (BOTTOM), VERIFICATION, E = 0.685 (TOP) 125
FIGURE 5-17 THE PREDICTED AND MEASURED POLLUTANT EVENT MEAN CONCENTRATION (EMC) WITH MARKED ZONES WHERE THE MODEL IS UNDER AND OVER ESTIMATING EMCS 126
FIGURE 5-18 PREDICTED AND MEASURED POLLUTANT EVENT MEAN CONCENTRATION (EMC) IN MG/L (LEFT) AND EVENT LOAD IN MG (RIGHT) FOR ATRAZINE 126
FIGURE 5-19 PREDICTED AND MEASURED POLLUTANT EVENT MEAN CONCENTRATION (EMC) IN MG/L (LEFT) AND EVENT LOAD IN MG (RIGHT) FOR PROMETRYN (TOP), SIMAZINE (MIDDLE) AND GLYPHOSATE (BOTTOM) 127
FIGURE 5-20 PREDICTED AND MEASURED POLLUTANT EVENT MEAN CONCENTRATION (EMC) IN MG/L (LEFT) AND EVENT LOAD IN MG (RIGHT) FOR CHLOROFORM 128
FIGURE 5-21 BATCH TEST RESULTS: SORPTION OF FLUORESCEIN IN DIFFERENT BIOFILTER SOILS – FLUORESCEIN CONCENTRATION IN WATER (LEFT) AND FLUORESCEIN CONCENTRATION ON SOIL (RIGHT) 128
FIGURE 5-22 BATCH TEST RESULTS ANALYSIS: ESTIMATION OF KINETIC SORPTION RATE OF FLUORESCEIN IN DIFFERENT BIOFILTER SOILS 129
FIGURE 5-23 BATCH TEST RESULTS: DEGRADATION OF FLUORESCEIN IN DIFFERENT BIOFILTER SOILS 130
FIGURE 5-24 BATCH TEST RESULTS ANALYSIS: ESTIMATION OF DEGRADATION RATE OF FLUORESCEIN IN DIFFERENT BIOFILTER SOILS 131
FIGURE 5-25 MEASURED AND MODELLED FLOW AT THE OUTFLOW PIPE FOR FLUORESCEIN TEST: CELL 1 (TOP), E = 0.284 AND CELL 2 (BOTTOM), E = 0.709 132
FIGURE 5-26 BATCH TEST RESULTS APPLICATION: MEASURED AND MODELLED FLUORESCEIN OUTFLOW CONCENTRATION FOR *IN-SITU* TEST FOR CELL 1 (TOP), E = -1.27, AND CELL 2 (BOTTOM), E = 0.67. FIELD MODEL PARAMETERS ESTIMATED FROM BATCH TEST RESULTS 133
FIGURE 5-27 MEASURED AND MODELLED FLUORESCEIN OUTFLOW CONCENTRATION FOR *IN-SITU* TEST FOR CELL 1 (TOP), E = 0.69, AND CELL 2 (BOTTOM), E= 0.90. FIELD MODEL PARAMETERS CALIBRATED ON FIELD DATA 134
FIGURE 5-28 MEASURED AND MODELLED OUTFLOW CONCENTRATIONS OF KCL DURING COLUMN TEST NORMALIZED TO INITIAL CONCENTRATION C/C_0 135
FIGURE 5-29 MEASURED AND MODELLED OUTFLOW CONCENTRATIONS OF GLYPHOSATE (LEFT) AND ATRAZINE (RIGHT) NORMALIZED TO INITIAL CONCENTRATION C/C_0 135
FIGURE 5-30 MEASURED AND MODELLED OUTFLOW CONCENTRATIONS OF SIMAZINE (LEFT) AND PROMETRYN (RIGHT) NORMALIZED TO INITIAL CONCENTRATION C/C_0 135
FIGURE 5-31 INFLOW AND OUTFLOW CONCENTRATION AND POLLUTANT FLUX TIME SERIES FOR GLYPHOSATE AT CELL 2 USING COLUMN TEST PARAMETERS: 2011, E = 0.205 (TOP), 2012, AND E = -1.410 (BOTTOM) 137

FIGURE 5-32 INFLOW AND OUTFLOW CONCENTRATION AND POLLUTANT FLUX TIME SERIES FOR ATRAZINE AT CELL 2 USING COLUMN TEST PARAMETERS: 2011, E = 0.929 (TOP), 2012, AND E = 0.478 (BOTTOM) 138
FIGURE 5-33 INFLOW AND OUTFLOW CONCENTRATION AND POLLUTANT FLUX TIME SERIES FOR PROMETRYN AT CELL 2 USING COLUMN TEST PARAMETERS: 2011, E = 0.736 (TOP), 2012, AND E = 0.452 (BOTTOM) 138
FIGURE 5-34 INFLOW AND OUTFLOW CONCENTRATION AND POLLUTANT FLUX TIME SERIES FOR SIMAZINE AT CELL 2 USING COLUMN TEST PARAMETERS: 2011, E = 0.193 (TOP), 2012, AND E = 0.502 (BOTTOM) 139
FIGURE 6-1 MATRIX PLOT OF CROSS-CORRELATION SCATTER PLOTS (OFF-DIAGONAL) AND POSTERIOR PARAMETER PROBABILITY DENSITY FUNCTIONS (DIAGONAL) FOR FLOWS AT CELL 2 USING GLUE AND LIKELIHOOD E > 0.6 (PRODANOVIC ET AL., 2014) 145
FIGURE 6-2 MATRIX PLOT OF CROSS-CORRELATION SCATTER PLOTS (OFF-DIAGONAL), EFFICIENCY DENSITY(UPPER LEFT CORNER) AND POSTERIOR PARAMETER PROBABILITY DENSITY FUNCTIONS (DIAGONAL) FOR ATRAZINE CONCENTRATIONS AT CELL 2 USING GLUE AND LIKELIHOOD E > 0.4 146
FIGURE 6-3 MATRIX PLOT OF CROSS-CORRELATION SCATTER PLOTS (OFF-DIAGONAL), EFFICIENCY DENSITY(UPPER LEFT CORNER) AND POSTERIOR PARAMETER PROBABILITY DENSITY FUNCTIONS (DIAGONAL) FOR SIMAZINE CONCENTRATIONS AT CELL 2 USING GLUE AND LIKELIHOOD E > 0.4 148
FIGURE 6-4 MATRIX PLOT OF CROSS-CORRELATION SCATTER PLOTS (OFF-DIAGONAL), EFFICIENCY DENSITY(UPPER LEFT CORNER) AND POSTERIOR PARAMETER PROBABILITY DENSITY FUNCTIONS (DIAGONAL) FOR PROMETRYN CONCENTRATIONS AT CELL 2 USING GLUE AND LIKELIHOOD E > 0.6 149
FIGURE 6-5 MATRIX PLOT OF CROSS-CORRELATION SCATTER PLOTS (OFF-DIAGONAL), EFFICIENCY DENSITY(UPPER LEFT CORNER) AND POSTERIOR PARAMETER PROBABILITY DENSITY FUNCTIONS (DIAGONAL) FOR GLYPHOSATE CONCENTRATIONS AT CELL 2 USING GLUE AND LIKELIHOOD E > 0.6 150
FIGURE 6-6 ATRAZINE, SIMAZINE, PROMETRYN AND GLYPHOSATE (TOP-BOTTOM) POLLUTOGRAPHS AT BIOFILTER OUTFLOW PIPE WITH MEASURED AND MODELLED CONCENTRATIONS INCLUDING A 95% CONFIDENCE INTERVAL FROM GLUE ANALYSIS 151

LIST OF TABLES

TABLE 2-1 ORGANIC MICROPOLLUTANTS DETECTED IN STORMWATER (LIST ADAPTED FROM P5: RISKS AND HEALTH (CRCWSC, AUSTRALIAN GOVERNMENT) AND ZHANG (2015)) 11

TABLE 2-2 MICROPOLLUTANTS DETECTED IN STORMWATER ABOVE AUSTRALIAN DRINKING WATER GUIDELINE VALUES 15

TABLE 2-3 THE KEY ORGANIC MICROPOLLUTANTS THAT EXIST IN STORMWATER RUNOFF WITH THEIR PHYSICOCHEMICAL PROPERTIES (MACKAY ET AL, 2006) 17

TABLE 2-4 PROCESSES ANTICIPATED IN STORMWATER BIOFILTERS AND THEIR IMPACT ON POLLUTANT MASS BALANCE IN EACH OF THE PHASES 29

TABLE 2-5 SOME OF THE KEY STORMWATER MICROPOLLUTANTS' PROPERTIES RELEVANT FOR FATE PROCESSES 30

TABLE 2-6 DEEP FILTRATION TYPES WITH POSSIBLE CAPTURE MECHANISMS AND DECOLMATAGE CHARACTERISTICS (AFTER HERZIG ET AL., 1970) 31

TABLE 2-7 SOME OF THE COMMON EQUATION FORMS/MODELS IN ENVIRONMENTAL MODELLING 32

TABLE 3-1 SOIL CHARACTERISTICS AND CONFIGURATIONS OF THE TWO FIELD BIOFILTERS, NOV 2013 53

TABLE 3-2 SUMMARY OF THE µPS' PHYSICO-CHEMICAL PROPERTIES, 95TH PERCENTILE STORMWATER CONCENTRATIONS, MEASURED INFLOW CONCENTRATIONS, AUSTRALIAN DRINKING WATER GUIDELINE (ADWG) VALUES, AND ANALYTICAL METHODS USED TO QUANTIFY THE POLLUTANTS IN THE COLLECTED WATER SAMPLES AND THEIR ASSOCIATED LIMITS OF REPORTING (LOR). 59

TABLE 3-3 SUMMARY OF THE MICROPOLLUTANTS' PHYSICO-CHEMICAL PROPERTIES, EXPECTED REMOVAL PROCESSES IN BIOFILTRATION SYSTEM, AND TARGET CONCENTRATIONS DURING TESTS 69

TABLE 3-4 DETAILED INFORMATION OF CHALLENGE TESTS 72

TABLE 3-5 WATER QUALITY OF THE SEMI-SYNTHETIC STORMWATER IN THE CHALLENGE TESTS 73

TABLE 3-6 THE SOIL SAMPLING SEQUENCE AND SAMPLE TYPE 74

TABLE 3-7 THE WATER BALANCE OF THE TWO TEST SERIES OF CHALLENGE TESTS: UNIT M^3 76

TABLE 3-8 MEASURED INFLOW CONCENTRATIONS AND OUTFLOW EVENT MEAN CONCENTRATIONS (EMCS) FOR MICROPOLLUTANTS DURING THE TWO CHALLENGE TESTS 79

TABLE 3-9 CALCULATED MASS BALANCES FOR MICROPOLLUTANTS DURING THE TWO CHALLENGE TESTS 80

TABLE 4-1 BIOFILTER GEOMETRY AND STATE VARIABLES 96

TABLE 4-2 WATER FLOW MODEL EQUATIONS 96

TABLE 4-3 WATER FLOW MODEL PARAMETERS 98

TABLE 4-4 POLLUTANT TRANSPORT MODEL EQUATIONS 99

TABLE 4-5 POLLUTANT TRANSPORT MODEL PARAMETERS 101

TABLE 5-1 BIOFILTER CHARACTERISTICS AND INITIAL CONDITIONS FOR THE TWO TEST SERIES 106

TABLE 5-2 THE NASH-SUTCLIFFE VALUES BETWEEN THE MEASURED AND MODELLED CONCENTRATION, E, AND THE MODEL PARAMETER VALUES AS CALIBRATED AND REPORTED BY MACKAY ET AL. (2006) 123
TABLE 5-3 TRANSPORT AND FATE MODEL PARAMETERS FOR FLUORESCEIN OBTAINED FROM LABORATORY BATCH STUDIES AND MODEL CALIBRATION 129
TABLE 5-4 VALUES OF SORPTION MODEL PARAMETERS CALIBRATED ON COLUMN TEST FOR HERBICIDES; E VALUES FOR COLUMN TEST (CALIBRATED) AND FIELD TESTS (PREDICTION) 136
TABLE 5-5 COMPARISON OF FIELD AND COLUMN CALIBRATED SORPTION PARAMETERS' VALUES 137
TABLE 6-1 PARAMETER RANGE FOR UNIFORM PRIOR PDS WITH THE E - THRESHOLD 143
TABLE 6-2 MODEL PARAMETER AND NASH-SUTCLIFFE VALUES FOR DIFFERENT PERIODS FOR HYDRAULIC MODULE ON CELL 2 144
TABLE 6-3 MODEL PARAMETER AND NASH-SUTCLIFFE VALUES FOR DIFFERENT CALIBRATION PERIODS FOR ATRAZINE ON CELL 2 144
TABLE 6-4 MATRIX OF PARAMETER CROSS-CORRELATION COEFFICIENTS FOR FLOWS AT CELL 2, USING GLUE, E > 0.6 146
TABLE 6-5 MATRIX OF PARAMETER CROSS-CORRELATION COEFFICIENTS FOR ATRAZINE AT CELL 2, USING GLUE, E > 0.4 147
TABLE 6-6 MATRIX OF PARAMETER CROSS-CORRELATION COEF. FOR SIMAZINE AT CELL 2, USING GLUE, E > 0.4 148
TABLE 6-7 MATRIX OF PARAMETER CROSS-CORRELATION COEF. FOR PROMETRYN AT CELL 2, USING GLUE, E > 0.6 149
TABLE 6-8 MATRIX OF PARAMETER CROSS-CORRELATION COEF. FOR GLYPHOSATE AT CELL 2, USING GLUE, E > 0.6 150

LIST OF ABBREVIATIONS

AGWR-ADWG - Australian Guidelines for Water Recycling - Australian Drinking Water Guidelines

BOD – Biological Oxygen Demand

COD – Chemical Oxygen Demand

CSTR – Continuous Stirred Tank Reactor

DBP – Dibutil Phthalate

DEHP – Diethylhexyl Phthalate

DOC – Dissolved Organic Carbon

EC – Electrical Conductivity

EMC – Event Mean Concentration

ERT – Electro-Resistive Tomography

FAWB – The Facility of Advancing Water Biofiltration

GLUE – Generalized Likelihood Uncertainty Estimation

LID – Low Impact Development

PAH – Polycyclic Aromatic Hydrocarbon

PCB – Polychlorinated Biphenyl

PCP – Pentachlorophenol

PD – Probability Distribution

PDE – Partial Differential Equation

PPCP – Pharmaceuticals and Personal Care Products

PV – Pore Volume

PVC – Polyvinyl chloride

SOM – Soil Organic Matter

SUDS – Sustainable Urban Design System

TDS – Total Dissolved Solids

THMs – Trihalomethanes

TN – Total Nitrogen

TOC – Total Organic Carbon

TP – Total Phosphorus

TPH – Total Petroleum Hydrocarbons

TSS – Total Suspended Solids

UVA - UV Absorption at 254 nm

WSUD – Water Sensitive Urban Design

CHAPTER 1: INTRODUCTION

1 INTRODUCTION

Micropollutants found in stormwater are becoming a noticeable issue, and an increasing number of studies illustrate their toxicological effects. Although micropollutant concentration levels are usually lower than what is the maximum allowed level (by regulations), and pharmaceutical products' levels are usually lower than therapeutic doses, adverse effects still exist while their cumulative effects are unknown. In some cases, harmful effects are caused by micropollutant byproducts. The presence of certain micropollutants or their byproducts at even low levels are sufficient to change the metabolism of living cells, which results in deterioration of cell self-protection, making them susceptible to illnesses and malignant degenerations. The effects are increased in high population density areas, as well as in industrial and commercial city zones. Micropollutants and their byproducts have been found in both surface and ground waters in such areas. These micropollutants are involved in sorption and degradation processes that eventually lead to their attenuation. Urban stormwater, a possible major carrier of micropollutants, can contain disinfection products, herbicides, hydrocarbons and other miscellaneous organic compounds. This is of particular problem for stormwater harvesting practices that aim to treat captured urban runoff for both non-potable and (in rare cases) potable uses.

Biofilters, wetlands and other Water Sensitive Design technologies are effective stormwater treatment technologies. They have been shown to efficiently reduce loads of nutrients, sediments and metals, but there is no understanding on whether these systems can remove common stormwater micropollutants. More importantly there are no reliable models that can predict micropollutant behavior in Water Sensitive Urban Design navesti puno ime skracenice pre prvog koriscenja u tekstu (WSUD) stormwater treatment systems. Even models for assessing micropollutant discharges from urban catchments are very rare. However, without such models, it is difficult to assess impacts of micropollutants on receiving waters and even more difficult to design and assess performance of the stormwater treatment and harvesting systems.

Water legislation regulates micropollutant concentrations in waterways either directly, by controlling their discharge (e.g. National Pollutant Discharge Elimination System,

US EPA) or indirectly, by setting requirements for achieving a good water status (e.g. EU Water Framework Directive). Lists of priority pollutants (a.k.a. emerging pollutants), such as the EU WFD 2008/105/EC, include a large number of organic micropollutants, some of which are often found in stormwater. To achieve legislative requirements that call for limiting pollutant discharge concentrations, and especially to achieve a good water status, it is necessary to collect a substantial amount of measurement data. The main issue with measurements related to micropollutants in various environments (water, soil, air) is that due to their very low concentrations (order of magnitude is μg/L) data uncertainty is quite high: representative samples are difficult to produce and sample analysis methods include operations that can induce large errors e.g. concentrating samples to get detectable amounts of micropollutants. This is why measurements of micropollutant concentrations require high technical and financial resources. The difficulties in conducting measurements give an additional value to the development of a micropollutant-biofilter model, as it can be used as a tool to optimize the monitoring procedure (that is necessary to demonstrate that treatment processes are capable of achieving the required water quality objectives) by selecting only the most valuable data points to be collected, thereby minimizing the total expenses (number of measurements).

1.1 Biofiltration water quality modelling

As previously stated, for biofilters to be used as an effective stormwater management measure, it is important to accurately model their performance: continuous simulations of biofilter hydraulic and treatment efficiencies allow for predictions of long-term impact on reduction of stormwater pollution levels and loads. Reliable modelling of biofilter performance is crucial for adequate sizing of biofiltration systems when used for both pollution control and stormwater harvesting.

There are not that many stormwater quality models that can be easily applied to stormwater biofilters without oversimplifying the processes. Some of the widely used stormwater software tools, such as MOUSE (DHI, 2009a-c), SWMM (Rossman, 2010) and STORM (US Army Corps of Engineers, 1977) use reservoir equations for modelling of biofiltration (i.e. bioretention) hydraulics, while they offer simple user defined regressions for the assessment of their treatment performance. These regression

equations need an abundandance of data, which in the case of micropollutants is quite difficult to obtain (technically and financially). Additionally, they lack the transferability between different variants of systems and do not perform well under different operational conditions. Even software specifically developed for stormwater biofilters, such as MUSIC software (eWater CRC, 2009), although includes a more complex biofiltration hydraulic model that continuously assesses outflows and moisture content within the systems, still relies heavily on regression equations for the transport and fate of pollutants (it uses first-order decay (USTM by Wong et al., 2006), but also experimentally derived regression curves (eWATER CRC, 2009)). It should be noted that, to the best of author's knowledge, none of the above models have been tested with micropollutants.

There are, however, models more physically based developed for biofilters (e.g. STUMP (Vezzaro et al., 2010)) or vertical flow constructed wetlands (e.g. CW2D (Langergraber and Šimůnek, 2005)), but they are either dependent on data shown to have low correlation with micropollutant concentrations (such as TSS, as shown by Zhang et al, 2015b), or are too complex (excessive data needed).

A more suitable model that is able to simulate the main treatment processes within the stormwater biofilter with parameters that are easily estimated is needed.

1.2 Overall aim

The aim of this study was to develop a general treatment model that allows for long-term simulations of stormwater biofilters and their performance for a wide range of micro-pollutants. The model needed to be reliable even when little data is available, which is almost always the case. Therefore, the model was required to simulate the main treatment processes within stormwater biofilters (at least volatilisation, sorption, and bio-chemical degradation) where the model parameters can be easily determined.

The aim was achieved through following specific objectives:

1. To develop a stormwater micropollutants model that includes the transport and fate of pollutants in biofiltration systems (the aim for the model was to be mechanistic, so that it can be easily transferred to other WSUD systems such as filters, infiltration trenches, swales, wetlands, etc.);

2. To conduct controlled lab and field tests to refine model components that simulate micropollutant treatment in biofilters;

3. To calibrate, validate, and assess uncertainties in the model using field data from two stormwater systems (two types of biofiltration design).

The developed model is anticipated to be used as a tool to ease the management of stormwater biofiltration systems when they are used for water harvesting or for control of the polluted urban runoff to water receiving bodies. The model can also facilitate the validation monitoring of biofilter systems (Zhang et al., 2015).

1.3 Scope of the thesis

The model developed in this study focuses on predicting micropollutants levels in urban stormwater treated by biofiltration systems of varying design. Model outputs include both micropollutant concentrations and loads. Although the model can be useful in water quality assessments, it does not include a specific part that can assist with that type of analysis (assessment criterias are not incorporated).

The development of the model and its testing was conducted on datasets that were collected throughout this research, as well with some data previously collected at the same sites. Data was collected from two different biofiltration cells, located at Monash campus in Melbourne and from several biofilter column testing tubes. Long term and high resolution flows, water levels, and soil moisture were measured. Composite and discrete inflow and outflow samples were analyzed to obtain data on TSS, TP, TN, total petroleum hydrocarbons, PAHs, glyphosate, triazines (atrazine, simazine, prometryn), phthalates (dibutyl phthalate, di-(2-ethylhexyl) phthalate), trihalomethanes (THMs) and phenols (phenol, pentachlorophenol).

The sensitivity analysis was performed using the less formal likelihood method GLUE (Generalized Likelihood Uncertainty Estimation, Beven and Binley, 1992), as it has no drawback when compared to the strictly Bayesian methods as shown by Dotto et al. (2010). The main focus of the uncertainty analysis was the module for the transport and fate of micropollutants.

1.4 Outline of the thesis

Chapter 2 provides a literature review as well as the identification of the key knowledge gaps, and presents the research aims and the main hypotheses. The review has four distinct parts: (1) stormwater quality and identification of key micropollutants, (2) biofiltration system operation characteristics, (3) review on existing models and modelling techniques, and (4) sources of uncertainty and uncertainty assessment in stormwater quality models.

Chapter 3 presents experimental data collected at the field and laboratory scale. It includes the field tracer tests, field electroresistive tomography, field spiking tests and laboratory column and batch studies. The column and batch studies were mostly performed by Kefeng Zhang (PhD thesis, 2015) and are only summarized here.

Chapter 4 presents the development of the MPiRe model, which includes both the adaptation of the water flow module, as well as the total development of the water quality part. This chapter includes governing equations and their solving techniques.

Chapter 5 includes model testing against field data i.e. calibration and verification. In addition to the input data and the boundary conditions, the calibration procedure is explained and model performance indicators are presented. This chapter also includes the methodology for estimating model parameters from column and batch tests. The initial testing includes analysis of the model performance against field data, and the meaning of parameter values.

Chapter 6 explores the model further via an uncertainty analysis. The calibration uncertainty is assessed by choosing different parts of dataset for calibration. The uncertainty of input data is visualized with impact of different scenarios (introduction of systematic errors to measurement data) on the probability distributions of model parameters. The results are used for the evaluation of sensitivity and predictive uncertainty of the stormwater quality model.

Chapter 7 provides a summary of the key findings, as well as a critical overview of the thesis' main strengths and weaknesses. A summary of necessary further investigations is given.

CHAPTER 2: LITERATURE REVIEW

2 LITERATURE REVIEW

2.1 Introduction

This chapter presents a literature overview of the broader research topic. The first topic is the stormwater quality in general with a focus on micropollutants, where different studies reported in literature are explored in search for the key micropollutants (their importance is estimated by their presence in the stormwater, as well as the hazard they present to humans and aquatic biota). This is followed by an overview of the major characteristics of stormwater biofiltration systems that includes their design and mode of operation. The major focus is the review of existing models and modelling techniques, which is the base for the development of the model in this thesis (Chapter 4). The final topic is the review of the uncertainty assessment methods applicable to stormwater quality modelling that present a theoretical background for Chapter 6. The literature review is concluded by identifying the key knowledge gaps and subsequently presenting the specific research aims and main hypotheses.

2.2 Stormwater quality

2.2.1 Micropollutants, priority or emerging pollutants

Micropollutants, priority substances, priority and emerging pollutants are terms that are sometimes used interchangeably; although the terms overlap to some extent, they have different origins. The term “micropollutant” is a scientific classification, while the terms “priority substance”, “priority pollutant” or “emerging pollutant” can be considered regulatory classifications.

Micropollutants are defined as compounds present in traces in the environment (with concentrations in the μg/L to ng/L range) that can affect the health of living organisms (Schwarzenbach et al., 2006). This broad definition does not limit the scope of substances that can be classified as micropollutants, so literature identifies micropollutants as various inorganic substances (metals, minerals) as well as different organic compounds (pesticides, polycyclic aromatic hydrocarbons, phenols, volatile organic substances, pharmaceuticals and personal care products, etc.).

Priority pollutants are defined in the US water quality regulatory programs under the Clean Water Act (CWA of 1977) as "toxic pollutants, with an available chemical standard test, that are found in water with a frequency of occurrence of at least 2.5% and are produced in significant quantities." The list contains a total of 129 pollutants, most of which are organic substances. The majority of priority pollutants, but not all, are also considered micropollutants, as they are detected in very low concentrations in the environment.

Priority substances are defined under the Annex II of Directive 2008/105/EC (EU Water Framework Directive, 2008). The list contains a total of 33 organic and inorganic substances, which are all considered to be micropollutants.

Emerging pollutants are a never-ending list of synthetic or natural substances that are "not commonly monitored but have a potential to enter the environment and cause adverse ecological and human health effects" (Geissen et al., 2015). These compounds are a new frontier in science; some do not have a long history of release into the environment and are only now becoming detectable due to advances in monitoring methods, while others are newly synthesized materials or are created by changes in use or disposal of existing chemicals (Geissen et al., 2015). The Norman-network (www.norman-network.net) lists more than 700 emerging pollutants. Most of these substances are considered to be micropollutants.

2.2.2 Notable stormwater quality studies

Stormwater as a major non-point pollution source can have a significant impact on receiving water bodies and as such has been a subject of many studies to date. Probably the most comprehensive and thorough study is the 1995 Makepeace et al. review of multiple physical, chemical and microbiological contaminants and indicators covering around 140 literature sources over a span of 25 years (1967 – 1992). The compilation's significant contribution is that it identified and quantified specific parameters (such as metals, organic compounds, microorganisms, temperatures, alkalinity etc.) rather than the traditionally used overall quality parameters. The reported levels of these parameters were compared to their regulated values and additionally to reported possible adverse effect levels. In addition to defining the most critical stormwater contaminants that

affect humans (through drinking water) and aquatic life, the study also helped in identifying the knowledge gaps in the toxicity of the combinations of certain organic and/or inorganic parameters. Duncan (1999) presented a statistical overview of reported urban runoff water quality and included interactions between stormwater quality with land use, population density, traffic density, and other catchment characteristics. The work by Duncan (1999) was based on data that covered a span of 47 years (1950 – 1997) and 21 specific water quality parameters: suspended solids, nutrients, COD, BOD, oils, TOC, pH, turbidity, heavy metal concentrations, and faecal coliforms. Göbel et al. (2007) went even further by developing a matrix for urban stormwater runoff concentrations for different types of surfaces (roofs, roads, etc.) that is usable in stormwater quality modelling. This includes event mean concentration range, as well as the representative average concentrations for 22 pollutants in 12 types of surface runoff (physico-chemical parameters, sum parameters, nutrients, heavy metals, main ions, and organic substances).

One of the first extensive priority pollutant specific studies was a monitoring programme conducted by Cole et al. (1984) across various cities throughout the United States, which included a total of 129 pollutants (pesticides, inorganic compounds, PCBs, halogenated aliphatics, phenols, etc.) and their potential risk to human health. A more recent and comprehensive two-part study was performed in the urban areas of Paris, France by Zgheib et al. (2012) and Gasperi et al. (2012). The named authors analysed a total of 88 priority pollutants in separate ("pure" stormwater) and combined storm sewers, such as metals, PAHs, PCBs, pesticides, volatile organic compounds, phthalates, etc., and presented their occurrence in particulate and dissolved phases.

2.2.3 Organic micropollutants detected in stormwater

Based on the results of Programme 5: Risks and Health of the Cooperative Research Center for Water Sensitive Cities (CRCWSC, Australian Government), a list was compiled that includes organic micropollutants detected in stormwater. The methodology for the formation of the list was to find whether regulated priority pollutants are detected in stormwater. The search lists included EPA and EU regulated priority substances from three major lists:

- The US EPA Priority Pollutants list (126 chemicals) (US EPA, 2009);
- The US EPA Unregulated Contaminants Monitoring Rule 2: Assessment monitoring list 1 and Screening survey list 2 (25 chemicals) (US EPA, 2010);
- The European Commission Priority Substances list (33 chemicals) (ECE, 2008).

Table 2-1 shows a list of 91 organic substances from regulated lists of priority pollutants that are reported to be detectable in stormwater, as well as their detection range.

Table 2-1 Organic micropollutants detected in stormwater (list adapted from P5: Risks and Health (CRCWSC, Australian Government) and Zhang (2015))

No.	Category	Compound	CAS No.	Detection Range	Reference
1	**Halogenated Aliphatics**	Tribromomethane (Bromoform)	75-25-2	1µg/L	[1]
2		Trichloromethane (Chloroform)	67-66-3	0.2-12µg/L	[1]
3		Chlorodibromomethane	124-48-1	2µg/L	[1]
4		Dichlorobromomethane	74-82-8	2µg/L	[1]
5		Dichloromethane	75-09-2	1.5-14.5µg/L	[1], [2], [14], [15]
6		Tetrachloromethane (carbon tetrachloride)	56-23-5	1-2µg/L	[1], [2]
7		Trichlorofluoromethane	75-69-4	0.6-27µg/L	[1]
8		1,1-dichloroethane	75-34-3	1.5-3µg/L	[1]
9		1,2-dichloroethane	107-06-2	<4µg/L	[1], [2]
10		1,1,1-trichloroethane	71-55-6	1.6-10µg/L	[1], [2]
11		Trichloroethylene	79-01-6	0.3-10µg/L	[1], [2]
12		1,1,2-trichloroethane	79-00-5	2-3µg/L	[1]
13		Tetrachloroethylene	127-18-4	4.5-43µg/L	[1], [2]
14		1,1,2,2-tetrachloroethane	79-34-5	2-3µg/L	[1]
15		1,1-dichloroethene	75-35-4	1.5-4µg/L	[1]
16		1,2-dichloroethene	156-59-2	1-3µg/L	[1], [2]
17		Trichloroethene	79-01-6	0.3-10µg/L	[1]
18		Tetrachloroethene	127-18-4	4.5-43µg/L	[1]
19		1,2-dichloropropane	78-87-5	<3µg/L	[1], [2]
20	**PAHs**	Total PAHs	Unspecified	0.24-33.7µg/L	[1], [2], [4], [8], [16]

No.	Category	Compound	CAS No.	Detection Range	Reference
21		Anthracene	120-12-7	0.005-10µg/L	[1], [2], [7]
22		Acenaphthene	83-32-9	0.013-0.044	[14], [15]
23		Acenaphthylene	208-96-8	0.027-0.126	[14], [15]
24		Benzo(k)fluoranthene	207-08-9	0.0012-103µg/L	[1], [2], [3]
25		Benzo(b)fluoranthene	205-99-2	0.0034-260µg/L	[1], [2], [3]
26		Benzo(k)fluoranthene	207-08-9	0.0012-103µg/L	[1], [2], [3]
27		Benzo(e)pyrene	192-97-2	4-6.1µg/L	[2]
28		Benzo(g,h,i)perylene	191-24-2	0.0024-1.5µg/L	[1], [2]
29		Chrysene	218-01-9	0.0038-10µg/L	[1], [2]
30		Fluoranthene	206-44-0	0.3-110µg/L	[1], [2], [3]
31		Fluorene	86-73-7	0.006-1µg/L	[1], [2]
32		Benzo(a)pyrene	50-32-8	0.0025-300µg/L	[1], [2], [3], [6]
33		Naphthalene	91-20-3	0.018-100µg/L	[1], [2], [3], [6], [7]
34		Phenanthrene	85-01-8	0.026-10µg/L	[1], [2], [7]
35		Pyrene	129-00-0	0.045-120µg/L	[1], [2], [3]
36		2-methylantracene	613-12-7	0.01-1.6µg/L	[2]
37		9,10-diphenylanthracene	781-43-1	1-1.4µg/L	[2]
38		Indeno[1,2,3-cd]pyrene	193-39-5	0.031-0.05	[2], [14], [15]
39	**Pesticides**	Aldrin	309-00-2	0.1µg/L	[1]
40		Atrazine	1912-24-9	0.0003-0.0016	[13]
41		Aminotriazole	61-82-5	0.14-0.53	[14], [15]
42		AMPA	74341-63-2	0.48-0.73	[14], [15]
43		α-BHC	319-84-6	0.0027-0.01µg/L	[1], [2]
44		β-BHC	319-85-7	0.1µg/L	[1], [2]
45		γ-BHC (lindane)	58-89-9	0.052-0.01µg/L	[1], [2]
46		δ-BHC	319-86-8	<0.1µg/L	[1], [2]
47		Chlordane	12789-03-6/ 57-74-9	0.01-10µg/L	[1], [2], [3], [16]
48		DDD (di-chloro-dipheny-ldichloroethane)	72-54-8	<0.008µg/L	[1], [2]
49		DDE (di-chloro-diphenyl-dichloroethylene)	72-55-9	<0.015µg/L	[1], [2]
50		DDT (di-chloro-diphenyl-trichloroethane)	50-29-3	<0.1µg/L	[1], [2]

No.	Category	Compound	CAS No.	Detection Range	Reference
51		Dieldrin	60-57-1	0.005-0.1µg/L	[1], [2]
52		Diuron	330-54-14	0.02-0.65µg/L	[13], [14], [15]
53		α-endosulfan	959-98-8	0.1-0.2µg/L	[1], [2]
54		Endrin	72-20-8	<0.005µg/L	[2]
55		Glyphosate	1071-83-6	<1.92	[14], [15]
56		Heptachlor	76-44-8	0.1µg/L	[1]
57		Heptachlor epoxide	1024-57-3	0.1µg/L	[1]
58		Isophorone	78-59-1	<10µg/L	[1], [2]
59		1,3-dichloropropene (DCP)	115-07-1	1-2µg/L	[1], [2]
60		Methoxychlor	72-43-5	<0.02 µg/L	[2]
61		Metaldehyde	108-62-3	<0.062 µg/L	[14], [15]
62		Pentachlorophenol (PCP)	87-86-5	1-115µg/L	[1], [2]
63		Simazine	122-34-9	0.06-0.17	[13]
64	**PCBs**	Total PCBs	Unspecified	0.03-1.12 µg/L	[2]
65		PCB 118	31508-00-6	<0.01-0.104 µg/L	[15]
66		PCB-1260 (Arochlor 1260)	11096-82-5	0.03µg/L	[1]
67	**Phthalates**	Diethyl Phthalate (DEP)	84-66-2	2-10µg/L	[1], [2]
68		Dibutyl Phthalate (DBP)	84-74-2	0.5-11µg/L	[1], [2]
69		Dioctyl phthalate (DOP)	117-84-0	0.4-1µg/L	[1], [2]
70		Diethylhexyl phthalate (DEHP)	117-81-7	0.45-60.9 µg/L	[1], [2], [9], [11], [14], [15]
71		Butyl benzyl phthalate	85-68-7	3.3-130µg/L	[1], [2], [3]
72	**Pharmaceuticals and personal care products (PPCPs)**	Ibuprofen	15687-27-1	<0.0026-0.674µg/L	[5]
73		Naproxen	22204-53-1	<0.0004-0.145µg/L	[5]
74		Triclosan	3380-34-5	0-0.029 µg/L	[5]
75	**Phenols**	Phenol	108-95-2	3-10µg/L	[1]
76		2-chlorophenol	95-57-8	2µg/L	[1]
77		2,4-dimethylphenol	105-67-9	<10µg/L	[1], [2]
78		Nonylphenol	104-40-5	0.01-9.17 µg/L	[6], [9], [12], [14], [15]
79		4-n-octylphenol	1806-26-4	0.018-0.24	[12]
80		4-nitrophenol	100-02-7	1-19µg/L	[1]

No.	Category	Compound	CAS No.	Detection Range	Reference
81		Bisphenol A	80-05-7	0.0015-0.113µg/L	[5]
82	**Ethers**	Bis(2-chloroethyl) ether	111-44-4	2.0-87µg/L	[3]
83		Bis(2-chloroisopropyl) ether	39638-32-93/ 108-60-1	3.0-400µg/L	[3]
84	**Other miscellaneous organic chemicals**	Benzene	71-43-2	3.5-13µg/L	[1], [2]
85		Chlorobenzene	108-90-7	1-10µg/L	[1], [2]
86		Ethylbenzene	100-41-4	1-2µg/L	[1], [2]
87		Toluene	108-88-3	9-12µg/L	[1], [2]
88		Perfluorooctane sulfonic acid (PFOS)	1763-23-1	0.051µg/L	[10]
89		Perfluorooctanoic acid (PFOA)	335-67-1	0.09µg/L	[10]
90		Perylene	198-55-0	0.05-0.5µg/L	[2]
91		m-cresol, p-chloro-	108-39-4	<1.5µg/L	[1], [2]

[1] Cole et al., 1984; [2] Makepeace et al., 1995; [3] Pitt et al., 1995; [4] Ngabe et al., 2000; [5] Boyd et al., 2004; [6] Eriksson et al., 2005; [7] Hwang and Foster, 2006; [8] Göbel et al., 2007; [9] Björklund et al, 2009; [10] Murakami et al., 2009; [11] Clara et al., 2010; [12] Bressy et al., 2011; [13] Page et al., 2011; [14] Zgheib et al., 2012; [15] Gasperi et al., 2012; [16] Gillbreath and McKee, 2015

The organic compounds identified in Table 2-1 were further classified according to whether they were detected in levels that are considered to have no detrimental effects to humans. The detection ranges of organic pollutants listed in Table 2-1 were compared to Australian Drinking Water Guidelines (ADWG, 2011), and Australian Guidelines for Water Recycling: Augmentation of Drinking Water Supplies (AGWR, 2008). Organic pollutants detected above AGWR-ADW guideline values are presented in Table 2-2. The exclusion of other detected organic micropollutants does not imply that their environmental presense and concentration levels are safe and that they can be neglected, as the AGWR and ADW guidelines mainly focus on hazards likely to be present in wastewater and potable water and may overlook a broader range of hazards that may be present in stormwater (especially for aquatic biota). The chemicals not identified by AGWR-ADWG as hazards should be further analysed for potential risk to humans and aquatic biota (Zhang, 2015).

Table 2-2 Micropollutants detected in stormwater above Australian drinking water guideline values

Category	Compound	Detection range	Guideline value
Halogenated Aliphatics	Dichloromethane	1.5-14.5 µg/L	4 µg/L [a]
PAHs	Benzo(a)pyrene	0.0025-300µg/L	0.01µg/L [a]
	Naphthalene	0.018-100µg/L	70µg/L [b]
Pesticides	Chlordane	0.01-10µg/L	2µg/L [a]
	Pentachlorophenol (PCP)	1-115µg/L	10µg/L [a]
PCBs	Total PCBs	0.03-1.12 µg/L	0.14µg/L [b]
	PCB 118	<0.01-0.104 µg/L	0.016 ng/L [b]
Phthalates	Diethylhexyl phthalate (DEHP)	0.45-60.9 µg/L	10µg/L [a]
Other MOCs	Benzene	3.5-13µg/L	1µg/L [a]

[a] Australian Drinking Water Guidelines (NHMRC-NRMMC, 2011)

[b] Australian Guidelines for Water Recycling: Augmentation of Drinking Water Supplies (NRMMC et al., 2008)

2.2.3.1 Halogenated aliphatics

Halogenated aliphatics are non-aromatic hydrocarbons. A total of 19 halogenated aliphatics is reported to be detected in stormwater with only one compound, Dichloromethane, detected in the concentration range above the AGWR-ADW guidelines (Table 2-2). However, having in mind that the AGWR-ADW guidelines do not consider all potential hazards to human health and aquatic biota, Chloroform (Trichloromethane) was also included as a compound of particular significance. This is due to the high toxicity of chloroform (e.g. stillbirths, Dodds et al., 2004), which is of particular interest if stormwater is to be harvested for potable use. Sources of dichloromethane and chloroform in stormwater include solvents, aerosols, fire-retardant chemicals, and products of reactions of chlorine with organic chemicals (Makepeace et al., 1995).

2.2.3.2 Polycyclic aromatic hydrocarbons (PAHs)

Polycyclic aromatic hydrocarbons (PAHs) have two or more aromatic rings. Some PAHs are volatile (e.g. naphthalene), while most PAHs are hydrophobic (non soluble in water). Depending on the number of rings, PAHs can be classified as light (3-rings and

less: naphthalene, acenaphthene, acenaphylene, fluorene, etc.) or heavy (more than 3-rings: fluoranthene, pyrene, benzo(a)pyrene, etc.). All PAHs are considered to be cancerogenous. A total of 18 PAHs are identified in stormwater, with only two surpassing the concentration levels prescribed by the AGWR-ADW guidelines: benzo(a)pyrene and naphthalene (Table 2-2). In addition, pyrene (a PAH with five benzene rings) is also considered to be a significant organic micropollutant as it contributes substantially to the total PAHs load, and is detected in concentrations (120 µg/L) close to the AGWR-ADW guideline values (150 µg/L). PAHs are ubiquitously present in the environment as they are produced by an incomplete combustion and many fuel processing operations.

2.2.3.3 Pesticides

Pesticides include: (1) herbicides that are chemicals used for prevention of growth or killing of certain types of vegetation, like weeds, and (2) biocides that are chemicals used for prevention of reproduction or killing of pest animals (insects, fungi, rodents etc.). Biocides are also referred to as fungicides, insecticides and pesticides. Pesticides, therefore, include various chemical compounds such as triazines, organophosphorus, organochlorines, amino-phosphonates, etc. Chlordane and pentachlorophenol (PCP) are the only two pesticide compounds detected in stormwater at concentrations above the AGWR-ADW guidelines (Table 2-2). Glyphosate, an active ingredient in many popular herbicides, including Monsanto's Roundup® brand herbicide, is probably the most used and most studied worldwide pesticide. Due to its classification as "probably carcinogenic to humans" by the International Agency for Research on Cancer (IARC, 2015) and its widespread use, it was selected as one of the key micropollutants. Triazines (especially atrazine and simazine) are also popular choices as pesticides due to their high efficiency in eliminating weeds. Although banned in many countries (e.g. Serbia, since 2008; EU, since 2003), triazines can still be found and are widely used in the US and Australia (SoE, 2011). Major sources of pesticides in stormwater are runoff from gardens, agriculture areas, and pesticide production and storage points.

2.2.3.4 Polychlorinated biphenyls (PCBs)

Polychlorinated biphenyls (PCBs) are very toxic substances that are persistent and readily transported from sites of contamination to remote areas (Beyer and Biziuk,

2009). Total PCBs and PCB 118 are found to surpass the set guidelines (Table 2-2). It should be noted that PCBs are found to be 100% particle-bound in stormwater (Zgheib et al., 2012). Main sources of PCBs in stormwater include leaching of lubricants, hydraulic fluids, landfills, and old transformer fluids.

Table 2-3 The key organic micropollutants that exist in stormwater runoff with their physicochemical properties (Mackay et al, 2006)

Category	Compound	Solubility (mg/L)	Log K_{ow}	Log K_{oc}	K_{Henry} (Pa m^3/mol)	Half-life (days)
Halogenated Aliphatics	Dichloromethane	16940	1.31	1.68	110-450	1.3-191 (sandy l) 54.8 (sand) 12.7 (sandy clay)
	Chloroform*	8452	1.95	1.65-1.90	200-700	100 (soil) 56-180 (grondw.)
PAHs	Benzo(a)pyrene	0.002	6.13	6.6-6.8	8-74E-03	229-309 (sandy l.)
	Naphthalene	32.2	3.33	2.30-3.17	35-125	80 (soil); 220 (gw)
	Pyrene*	0.1	5.13	3.11-6.50	0.5-0.2	199-260 (sandy l.)
Pesticides	Chlordane	0.1	2.78	4.19-4.39	0.2-10	476-2272
	Pentachlorophenol (PCP)	18.9	4.83	3.48-3.60	0.003-0.28	23-178
	Glyphosate*	12000	3.5	3.42-4.38	1.4E-05	4-210
	Atrazine*	29.8	2.65	2.09	2.7-6.2E-04	36-116
	Simazine*	5.7	2.18	2.13	0.3-3.4E-04	11-70
PCBs	Total PCBs	insoluble	>4.0	>3.7	20-100	3-100
	PCB 118	0.1-0.2	5.4	4.5-5.3	20-101.5	1-120
Phthalates	Diethylhexyl phthalate (DEHP)	0.029	7.48	4.0-5.0	0.004-4	2-69.3
Other MOCs	Benzene	1748	2.17	1.99	270-650	5-16 (soil) 10-720 (gw.)

* Micropollutant detection range in stormwater was not above selected guidelines, but is selected according to different criteria

2.2.3.5 Phthalates

Phthalates are esters of the phthalic acid and are mainly used as additives in the production of plastic compounds such as polyvinyl chlorids (PVC). Phthalates can be easily released from plastics, as they do not form a covalent bond, but rather only stay entangled (Wilkes et al., 2005). This is why many monitoring campaigns of human urine, food, and environment report the presence of phthalates (e.g. Griffiths et al.,

1985). As can be seen in Table 2-2, bis(2-ethylhexyl) phthalate (DEHP) is the only phthalate detected in concentration above the set guidelines. Sources of phthalates are plastic pipings, varnishes, safety glass and plastic food wraps.

2.2.3.6 Pharmaceuticals and personal care products (PPCPs)

Pharmaceuticals and personal care products (PPCPs) include various compounds and are usually found in the sewer (from showers, toilets, etc.). There is some evidence of PPCPs presence in stormwater (Boyd et al., 2004), but the detected levels are far below selected guidelines.

2.2.3.7 Phenols

Phenols are compounds that are derivatives of the phenol – carbolic acid. Due to their inexpensive production, phenols are used across different industries: production of plastics, polycarbonates, epoxide resins, precursor to different pharmaceutical products, cosmetics, herbicides, etc. The wide use of phenols results in their abundant presence in the environment. Although there are 7 different priority phenols detected in stormwater, only four of them have guideline values: 4-nitrophenol (30 µg/L), 2-chlorophenol (300 µg/L), nonylphenol (500 µg/L) and Bisphenol A (200 µg/L). None of the listed phenols are detected in stormwater concentrations that surpass the selected AGWR-ADW guidelines.

2.2.3.8 Other Miscellaneous organic chemicals

Of the many non-classified organic chemicals, only benzene is detected in stormwater in concentrations far above the guidelines (Table 2-2). Sources of benzene in stormwater include spills and combustion of fuels (especially from motor vehicles), and petrochemical and chemical manufacturing emissions.

2.2.3.9 Inorganic chemicals

Although not a research aim in this thesis, some inorganic chemicals are also considered to be micropollutants. The most studied of them are the heavy metals (elements starting with Sc, sometimes Na). The presence of heavy metals in stormwater is interesting as they are quite toxic and persistent (are not degraded chemically or biochemically). The main sources of heavy metals in stormwater are depositions throughout catchments (Djukić et al., 2016) or emissions in the atmosphere due to either anthropogenic

activities or natural causes. Anthropogenic sources include vehicle brake emissions, weathering of roof materials, petrol additives, paints, batteries, pesticides, etc. Natural sources are activities of volcanoes, forest fires, erosion of rock materials, minerals etc. Lead (Pb), copper (Cu), zinc (Zn), cadmium (Cd), chromium (Cr), mercury (Hg), platinum (Pt), and nickel (Ni) are identified as priority pollutants, while Zhang (2015) reports six more metals to be detected in stormwater at concentrations above the AGWR-ADW guidelines: antimony (Sb), aluminium (Al), arsenic (As), iron (Fe), manganese (Mn) and selenium (Se).

2.2.3.10 Summary

Table 2-3 presents selected key micropollutants present in the stormwater along with their physicochemical properties (solubility (S), octanol-water partitioning coefficient (log K_{ow}), soil-water partitioning coefficient normalized to organic carbon content (log K_{oc}), Henry constant (K_{Henry}), and biodegradation half-life ($T_{1/2}$). Possible transport and fate mechanism for the key pollutants are explored in Chapter 2.4.

2.3 Biofiltration systems characteristics

Stormwater biofilters, also known as bioretentions and rain-gardens, are soil-based filtration systems that contain a rich plant community that enhances their physical, chemical and biological treatment processes. Stormwater biofilters are widely used in the protection of waterways from polluted urban runoffs, and more recently for stormwater harvesting (Wong et al, 2012). Due to their attractive designs and good performance in removing sediments (e.g. Li and Davis, 2008a), nutrients (e.g. Hunt et al., 2006; Davis, 2007, Hatt et al, 2009), heavy metals (e.g. Li and Davis, 2008b; Feng et al, 2012), and faecal microorganisms (Li et al., 2012; Chandrasena et al., 2012), stormwater biofilters are popular Water Sensitive Urban Design (WSUD) measures (also known as Low Impact Development - LID technology or Sustainable Urban Drainage System, SUDS). Stormwater biofilters have also been tested for organic stormwater micropollutants at field scale; DiBlasi et al. (2009) showed good bioretention performance against 16 polycyclic aromatic hydrocarbons (PAHs). The importance of organic micropollutants comes from their harmful effect on both (1) aquatic systems (e.g. toxicity of pesticides to fish (Chopra et al., 2011)) and (2) humans (e.g. Australian drinking water guidelines regulate maximum allowed concentrations).

2.3.1 Biofilter design

Soils used as filter media in biofiltration systems need to be structurally stable, with moderate infiltration capacity, to promote stormwater treatment. The actual recommendations on compacted hydraulic conductivity rate differ slightly among regions and continents:

- In Australia and Asia infiltration capacities range between 100 and 300 mm/h, in temperate climates, and up to 600 mm/h in tropical climates (e.g. FAWB, 2009; ABC Waters – Design Features, 2014);
- In North America the recommended infiltration rates are between 50 and 100 mm/h for natural soils and up to 300 mm/h for engineered soils (soil mixtures) (e.g. Hinman, 2009; Maryland Stormwater Design Manual Volumes I and II, 2009),
- In Europe, the most comprehensive design manual for biofiltration systems is CIRIA's SuDS Manual (2015) form the UK, that adopted recommendations from FAWB (2009) and suggests infiltration rates of around 100 – 300 mm/h.

The infiltration rates allowed in tropical climates are usually higher, as rain episodes have larger volumes and are more frequent, and therefore pollutant concentrations are lower (diluted).

A loamy sand, either natural or engineered, is recommended by most design manuals, provided it is free of toxicants and weed seeds. The granulometry of the soil should be such that there is less than 5% clay and silt fractions (< 0.063 mm, w/w) and that the distribution curve is continuous (FAWB, 2009). The total porosity of the material should be more than 30% (e.g. The SuDS Manual, 2015). There are limits to organic matter content (up to 5%), pH (5.5-8.5), and contents of major plant nutrients (total nitrogen, total phosphorus, extractable potassium etc.).

The area of the biofilter depends on its filter media hydraulic rate, but as a rule of thumb, it corresponds to around 2% of the catchment area (Hatt et al, 2007). The recommended depths for different layers of the system are: extended detention 200-500 mm, filter media 400-700 mm (300-600 mm, in case a submerged zone exists),

transitional sand layers of 100-150 mm, and gravel (with perforated pipe) of around 150 mm (e.g. FAWB, 2009; The SuDS Manual, 2015). The perforated pipe should have a slope of at least 0.5% (5% the most) if it is freely draining, or no slope when a submerged zone is present.

Figure 2-1 Some of the commonly used plants in biofiltration systems: *Cephalanthus occidentalis* (upper left), *Salix nigra* (upper right), *Scirpus microcarpus* (lower left), *Eupatorium purpureum* (lower right). Source: Wikipedia.org

The choice of plants used in biofiltration systems depends on local climatic conditions, but all plants share a possession of a well-structured root system and a tendency to sustain wet/dry regimes. The plants have two major roles: (1) to help in the removal of nutrients and (2) to keep the biofiltration system from clogging (Read et al, 2008). The plants promote the microorganism and fungi growth in the filter media and the root

system that help with removal of various pollutants. The plants additionally help in water retention during dry periods and influence the pH level (e.g. Schnoor et al., 1995). FAWB, for example, recommends *Carex appressa*, *Melaleuca ericifolia*, *Juncus amabilis* and *Juncus flavidis* for effective nutrient removal. The Maryland Stormwater Design Manual (2009) lists multiple trees (*Acer rubrum, Betula nigra, Quercus spp., Salix nigra* etc.), shrubs (*Cephalanthus occidentalis, Hamemelis virginiana, Ilex spp.*, etc.) and herbaceous plants (*Eupatorium purpureum, Scirpus spp., Dichanthelium scopariu*, etc.) as commonly used species.

The additional features for biofiltration systems include the construction of a submerged zone, addition of organic matter to this zone (mulch, peat, etc.) and inclusion of specific materials in the engineered soil composition (e.g. Cu^{2+} - exchange zeolite, Li et al., 2014). These additional features enhance biofilter performance in terms of the removal of nutrients (e.g. Hatt et al, 2009, Bratieres et al., 2008), heavy metals (e.g. Blecken et al, 2009; Bratieres et al., 2008) and pathogens (e.g. Chandrasena et al., 2014; Li et al., 2014). The submerged zone additionally helps in maintaining the vegetation and microorganism community during prolonged dry periods.

2.3.2 Mode of operation

Stormwater biofilters function as intermittent treatment systems, consisting of:

- The *active phase*, when stormwater ponds and filtrates through the media during rain events, and
- The *passive phase*, when during dry weather pollutants retained in the soil and captured water are further treated by plants and microbes.

Good practices for biofilter design suggest a retention time in the range of 1 to 3 hours (FAWB, 2009) during the active phase, while the length of the passive phase depends on local climatic conditions which are highly variable. The removal of most pollutants occurs through three main processes (Hong et al., 2006; LeFevre et al, 2012; Zhang et al., 2014): volatilisation within the biofilters pond and sorption to the filter media and plant root system – predominate during the active phase, and bio-chemical transformation and degradation - predominate during the passive stage.

The hydraulic performance of biofilters decreases with time, as shown by an extensive study by Le Costumer et al (2009). Most of the change in hydraulic conductivity happens due to the formation of a so called surface cake i.e. surface clogging, caused by sediment deposition.

2.4 Review of stormwater and related treatment models

2.4.1 Overall view

A scientific model is an aproximation of the observed reality created to better understand its nature, underlying processes, and to allow for future predictions. Once the relevant processes for a particular system are observed, a set of mathematical equations is selected that transforms the input to output data. These equations represent only a part of a model's structure. The remaining structural components include a solving technique for equations (an algorithm or a numerical model), a procedural model (a code), and parameter values (estimated from measured data or calibrated). The model is then tested: (1) against an independent dataset (not used for its calibration) and (2) for robustness using uncertainty analysis (see Chapter 2.5). Depending on the knowledge on the system's processes and observed data, models can be:

- Empirical – completely data-driven models with parameters that do not have any physical meaning, and, therefore, need to be determined via calibration: regression equations (e.g. Biofilter treatment equations in MUSIC, eWater CRC, 2009), neural networks (Loke et al., 1997), etc.
- Conceptual – models with processes that have some physical meaning, but are represented by a highly simplified "concept"; parameters are estimated indirectly by calibration and directly from measured data (e.g. CITY DRAIN © by Achleitner et al, 2007; USTM by Wong et al., 2006), and
- Mechanistic – physically based process models with parameters reasonably determined from measured data (e.g. CW2D by Langergraber and Šimůnek (2005), FITOVERT by Giraldi et al. (2010))

Model equations may be deterministic, where a set of input data always has a unique output set, or may be stochastic, where the processes are described with random components, so different model runs on same input data give different model outputs.

The stochasticity in models serves to account for a process uncertainty that cannot be reduced by gathering new knowledge; this is known as aleatoric uncertainty (Beven, 2009). Although this quality gives stochastic models a certain advantage, it limits their calibration, validation and sensitivity analysis, as they do not give consistent results. Deterministic models are considered a standard approach in many fields, as well as in urban drainage (Butler and Davis, 2011).

2.4.2 Stormwater biofilter models and water quality modelling

Some of the widely used stormwater software tools, such as MOUSE (DHI, 2009a-c), SWMM (Rossman, 2010) and STORM (US Army Corps of Engineers, 1977) use reservoir equations for modelling of biofiltration (i.e. bioretention) hydraulics, while they offer simple user defined regressions for the assessment of biofilter treatment performance. The MUSIC software (eWater CRC, 2009) is widely used in Australia and New Zealand and includes a more complex biofiltration hydraulic model that continuously assesses outflows and moisture content within the systems. MUSIC can predict treatment of only sediments and nutrients by biofilters; it is based on a combination of the first order decay treatment equation (USTM by Wong et al., 2006) and experimentally derived regression curves (eWATER CRC, 2009), and is therefore a conceptual-empirical model. The problem of this approach is in the amount of data needed for their calibration, and its poor transferability between systems used under different operational conditions. These models are also seldom, if ever, used for the assessment of micropollutant removal.

Process based models, that simulate the key treatment mechanisms, although far more reliable and transferable (Loucks et al, 2005), are very rarely used in stormwater practice. One of the rare examples is STUMP (Vezzaro et al., 2010), characterized by a simplified water mass balance model, with pollutant fate governed by the removal of Total Suspended Solids (TSS). The model has not yet been tested for organic micropollutant removal by stormwater biofilters, but showed good results when tested for the removal of heavy metals by a biofilter (Vezzaro et al., 2010) and organic micropollutants (iodopropynyl butylcarbamate - IPBC, benzene, glyphosate and pyrene) at a stormwater pond (Vezzaro et al., 2011).

Another example of a mechanistic model is a model by He and Davis (2009), which has been set up for bioretention water quality in COMSOL Multiphysics to simulate the fate of naphthalene and pyrene in single events. The flow model is based on Richard's Equation with Van Genuchten soil-water parameters, while the water quality model includes only linear sorption. This model showed good results, but is missing the ability to simulate pollutant degradation, and therefore has not been tested for continuous simulations.

2.4.3 Water quality models potentially applicable to stormwater organic micropollutant modelling

While stormwater treatment literature is very limited on this subject, a literature review has been done on micropollutant removal processes and their modelling in soil-based media (especially in the field of bioremediation) and wastewater treatment systems. Among the many diverse types of micropollutants found in soil media literature, pesticides and PAHs have been studied most frequently, with a substantial number of process-based models being set up to include leaching, sorption, aerobic and anaerobic degradation, uptake by plants, and volatilization at different scales – column, field, and catchment (e.g. Mulder et al., 2001, Tao et al., 2003, Köhne et al., 2009). Most of the models follow the interaction between water and soil (sorption-desorption), and present processes as different sink terms in the pollutant mass conservation partial differential equation (PDE). Depending on how the water flow is solved (Richards's equation, Philips infiltration, etc.) the PDE is accordingly discretised.

Particularly interesting are the models for Vertical Flow Constructed Wetlands; though used for wastewater treatment, they share several operating principles with stormwater biofilters, such as inlet spraying to the surface of the filter media, presence of macrophytes, vertical flow to the drainage zone, etc. It should be noted that there is a major difference between wetlands and biofilters: wetlands are permanently wet systems, while biofilters' dry weather treatment processes are crucial for their performance (e.g. Hatt et al., 2009). This makes the loading rates (eWater, 2009) and selection of plants (Read et al, 2008) for the two types of systems very different.

The models used for Vertical Flow Constructed Wetlands range from simple first-order decay lumped models (Kadlec and Knight, 1996), to more complex process-based

multicomponent reactive transport models (e.g. CW2D (Langergraber and Šimůnek, 2005), FITOVERT (Giraldi et al., 2010)). The former have been assessed as inadequate by Kadlec himself (e.g. Kadlec, 2000), while the latter have been adapted from Activated Sludge Models (Henze et al., 2000) and therefore include complex and intertwined cycles of substances such as oxidation of carbon sources, organic matter hydrolysis, nutrient transformation, etc.

CW2D (Langergraber and Šimůnek, 2005) was developed for HYDRUS-2D software to model the biochemical transformation and degradation processes. The HYDRUS-2D software numerically solves the Richard's equation for saturated/unsaturated water flow and the advection–dispersion equation for heat and solute transport using finite-elements. The water flow equation incorporates a sink term to account for water uptake by plant roots. The transport equations include advective–dispersive transport in the liquid phase, diffusion in the gaseous phase, as well as non-linear non-equilibrium reactions between the solid and liquid phases – sorption (Šimůnek et al., 1999). To demonstrate the complexity of the CW2D module, its 12 components and 9 processes are listed:

- Components: dissolved oxygen, organic matter (inert, slowly and readily degradable), ammonium, nitrite, nitrate, and nitrogen gas, inorganic phosphorus, and heterotrophic and two species of autotrophic micro-organisms;
- Processes: hydrolysis, mineralization of organic matter, nitrification (modelled as a two-step process), denitrification, and a lysis process (as the sum of all decay and loss processes) for the microorganisms.

Organic nitrogen and organic phosphorus are modelled as nutrient contents of the organic matter (they are calculated as a percentage of COD). The biochemical elimination and transformation processes are based on Monod-type expressions used to describe the process rates. This adds up to a total of 46 model parameters.

As CW2D has been set up for nutrient analysis, most studies have been successfully carried out with that particular purpose (e.g. Toscano et al., 2009; Langergraber et al., 2009). To the best of author’s knowledge, no modelling studies have been performed with heavy metals or organic micropollutants. This is not surprising having in mind the

number of parameters, and the available data on these pollutants: it should be noted that only very recent studies present the behaviour of heavy metals and organic pollutants in constructed wetlands (e.g. Schmitt et al., 2015; Gao et al., 2015).

FITOVERT (Giraldi et al., 2010) was developed as a more practical tool for the design and operation optimization of vertical flow constructed wetlands. The complexity of the model is lower than that of the CW2D module. The flow is considered to be dominantly vertical and is described by the Richard's equation. Biochemical transformation processes are similar to the CW2D module, as they both come from the standard Activated Sludge Models (Henze et al., 2000). FITOVERT is able to handle the porosity reduction due to bacteria growth and accumulation of particulate components. This means that the clogging process is also simulated: hydraulic conductivity decreases with the pore size reduction. Although current settings of FITOVERT are not applicable to heavy metal or organic micropollutant modelling, it is anticipated that its philosophy will be useful for the biofilter model set up.

Another important constructed wetland model type is the RSF_Sim model (Meyer et al., 2008; Meyer and Dittmer, 2015). The RSF_Sim model is a simple phenomenological model that describes purification processes in retention soil filters (RSFs). It was designed to be combined with sewer quality models (e.g. SWMM, Mike Urban, InfoWorks) in long term simulations. The RSF_Sim model works with three complete stirred tanks in vertical series:

- Ponding: the retention layer provides the water storage on top of the process layer,
- Filter layer: the process layer describes the sand/gravel layer (saturated during feeding, drained afterwards) in which the treatment occurs,
- Drainage layer: improves the volume balances.

Descriptions of treatment performances are kept very simple. The total COD is separated into two fractions: particulate COD is reduced by filtration (down to a background concentration), and dissolved COD is reduced by a treatment efficiency factor (varies with temperature, outflow limitation rates and the duration of antecedent

dry periods). The retention of NH_4-N is calculated with a steady-state two-stage linear sorption isotherm, and nitrification with 1st order kinetics.

The simplicity of the RSF_Sim model allows for very successful calibrations and validations, and usage in general. However, it should be noted that detailed predictions of treatment failures are not possible.

2.4.4 Process modelling

Since treatment systems include pollutant flow, it is first necessary to define the transport processes. The movement of pollutants in the fluid or porous media is driven by three distinct processes: advection, dispersion and diffusion (Pinder and Celia, 2006). Advection is a transport mechanism of mass (or a conserved property like temperature) achieved by fluid's bulk motion: it is a movement by the average fluid stream velocity. Dispersion is pollutant movement by means of small-scale velocity variations e.g. due to porous media chaotic structure and/or non-uniform velocity profile. Diffusion is transport due to the existence of the concentration gradient. As diffusion and dispersion are *similar* in that they cause *spreading* of the pollutant, they are usually combined in models, and their bulk parameter is the hydrodynamic dispersivity (Pinder and Celia, 2006). The most commonly used transport process modelling concepts are (1) the advective-dispersive equation and (2) the tank-in-series approach. The former is considered a scientific notation of the substance conservation principle (Hirsch, 2007). The latter, although it represents a conservation principle, is not considered a "true" transport model: it is a chemical reactor model designed to contain chemical reactions. However, the tank-in-series or the continuous-stirred-tank-reactors (CSTRs) are capable of mimicking the advective-dispersive transport for one-dimensional problems i.e. the input pollutograph can be transformed using CSTRs so as to have a time-lag (consequence of advection) and a decrease in the amplitude or spreading (consequence of dispersion). This is achieved by the proper selection of tank layouts, and is commonly used for modelling ponds and constructed wetlands (Kadlec and Knight, 1996).

Biofilter ecosystems can be divided into five phases: air, water, sediments (particulates settled in the ponding zone), filter media and plants. Table 2-4 shows the anticipated

physical, physico-chemical or bio-chemical processes affecting the mass balance of pollutants in the five phases. Some processes are only phase exchanges (e.g. sedimentation, resuspension, straining, sorption/desorption, volatilization) while others represent pollutant mass sinks (e.g. hydrolysis, photodegradation, biodegradation, plant uptake). Biodegradation and plant uptake are considered mass sinks, because they usually include transformation processes where the "original" pollutant species is lost, while its metabolites are formed.

Table 2-4 Processes anticipated in stormwater biofilters and their impact on pollutant mass balance in each of the phases

Process	Phase	air	water	sediments	filter media	plants
			physical			
sedimentation			-	+		
resuspension			+	-		
straining			-		+	
volatilization		+	-		-	
			physico-chemical			
adsorption			-	+	+	+
desorption			+	-	-	-
hydrolysis			-			
photodegradation		-	-		-	
			bio-chemical			
aerobic biodegradation			-		-	
anaerobic biodegradation				-	-	
plant uptake			-		-	+

Some of the key treatment processes (e.g. sorption, degradation) have been extensively studied in biofilters and soil-water environments, and there is a number of fairly detailed and robust models (e.g. Šimůnek and Van Genuchten, 2008, Sniegowski et al., 2009). Other processes, e.g. volatilization from stormwater biofilter treatment ponds, have not been studied, and knowledge transfers need to be done from other types of treatment systems containing a free water surface such as conventional wastewater systems (Lee et al., 1998) or free surface constructed wetlands (Kefee et al., 2004; De Biase et al., 2011). Some of the relevant processes for the identified key stormwater

micropollutants are shown in Table 2-5. Table 2-7 shows some of the common equation types used for process modelling.

Table 2-5 Some of the key stormwater micropollutants' properties relevant for fate processes

Category	Compound	Volatile[(1)]	Sorbable[(2)]	Mobile[(3)]	Persistent[(4)]
Halogenated Aliphatics	Dichloromethane	++	--	+++	No
	Chloroform	++	--	++	Slightly
PAHs	Benzo(a)pyrene	-	++	---	Yes
	Naphthalene	+	+-	+	Slightly
	Pyrene	-	++	---	Yes
Pesticides	Chlordane	-	+-	--	Very
	Pentachlorophenol (PCP)	-	++	--	Slightly
	Glyphosate	--	+-	---	Varies
	Atrazine	--	+-	++	Slightly
	Simazine	--	+-	++	Slightly
PCBs	Total PCBs	+	++	---	Slightly
	PCB 118	+	++	---	Slightly
Phthalates	Diethylhexyl phthalate (DEHP)	-	++	---	No
Other MOCs	Benzene	++	--	++	Varies

[1)]Volatility is based on the Henry's constant, H [Pa m^3 mol^{-1}] (Sebastian, 2013): "++" highly volatile: > 100; " +-" volatile 1 - 100; "-" non vol. 0.003 - 1; "--" non vol. < 0.003

[2)]Sorbability is based on the octanol-water partitioning coefficient $logK_{ow}$ (Sebastian., 2013): "++" high > 4; " +-" moderate 2.5 - 4; "--" low < 2.5

[3)]Mobility is based on soil-water partitioning coefficient normalized to organic carbon content K_{oc} (Rogers, 1996): "+++" very high 0-50; "++" 50-150; "+" 150-500; "-" 500-2000; "--" 2000-5000; "---" very low >5000

[4)]Persistence is based on degradation half-life $T_{1/2}$ [day]: No < 100, Yes > 100, Slightly ~ 100

Sedimentation and resuspension are movements of suspended solids from water to the bottom of the biofilter's pond and vice versa. Since a major drive of these processes is a combination of gravity vs. fluid viscosity vs. particle shape, most of the models contain a settling velocity (e.g. Stokes' law) and water depth. A very versatile model is

proposed in a ScorePP deliverable on Unit Process Models for Fate of Priority Pollutants (Vezzaro et al., 2009) which proposes sedimentation to be modelled as a 1st order kinetic process affecting the particulate phase of micropollutants (i.e. mass sorbed to the Total Suspended Solids), assuming there is a fraction of a non-settleable concentration.

Straining or filtering, in the domain of this work, is a mechanical process of separating solid matter from liquids by the attenuation of small particles by large one in the porous media. In a broader sense, filtration involves three different types of processes as per Table 2-6, where *straining* is equivalent to *mechanical filtration.* According to some researchers, large particles follow the fluid streamlines but are stopped in the passageways too narrow for passage (crevices and constrictions). The resulting particle deposits continuously reduce the size of the free passage and eventually can cause blockage (Herzig et al., 1970).

Table 2-6 Deep filtration types with possible capture mechanisms and decolmatage characteristics (after Herzig et al., 1970)

Filtration type	Particle size	Retention sites	Retention forces	Capture mechanism	Spontaneous decolmatage	Provoked decolm.
Mechanical	≥ 30 µm	Constrictions, crevices, caverns	Friction, fluid pressure	Sedimenta-tion, direct inter-ception	Improbable	Flow direction reversal
Physico-chemical	~ 1 µm	Surface sites	Van der Waals forces, electrokinetic forces	Direct inter-ception	Possible	Increase in flowrate
Colloidal	< 0.1µm	Surface sites	Van der Waals forces, electrokinetic forces, chemical bonding	Direct inter-ception	Possible	Increase in flowrate

Yao et al. (1971) identifies three different transport processes of particles: (1) gravitational pull of small particles by larger ones, which is referred to as *interception*, (2) net effect of buoyant weight vs. fluid drag force, or *sedimentation*, and Brownian movement of small particles influenced by surrounding molecules in the fluid, which can be described as *diffusion*. In the domain of mechanical filtration, capture processes are sedimentation and direct interception due to (1) the fluid pressure holding a particle immobilized against the opening at a constriction site, and/or (2) the friction force keeping a particle moving from being wedged in a crevice (Herzig et al., 1970). Filtration is, therefore, influenced by the ratio of suspended solids particle size to filter bed pore size, but also water depth, flow rate, filter and suspended solids material, filter bed specific surface, temperature, pore structure, etc.

Model types used for straining range from simple empirical (regression) models like Siriwardene et al. (2007), across moderately complex kinetical process models like models by Yao et al. (1971) and Altoé et al. (2006), to complex kinetical models that include both particle and liquid flow coupled with an increased pressure drop due to particle retention, like presented by Herzig et al. (1970). Complex models are based on the probability theory, where retention is described using a *collision efficiency factor*, as in the Yao model, or a *retention probability*, as in the work of Herzig et al. (1970). These probability coefficients are proportional to the rate of suspended solids removal, and are used in kinetic first-order rate equations.

Table 2-7 Some of the common equation forms/models in environmental modelling

Equation forms		Process type
1. Equilibrium processes		
$c_1 = K \cdot c_2^n + c_e$	c_i - concentration in "*i*" phase K – "driving" coefficient (e.g. partitioning coeff.) n - exponent c_e – non reacting fraction	non-limited process e.g. sorption isotherm; c_e= 0, Freundlich isotherm
$c_1 = \frac{K \cdot c_{\max}}{1 + K \cdot c_{\max}} c_2$	c_i - concentration in "*i*" phase K – "driving" coefficient (e.g. partitioning coeff.) c_{max} – limiting factor (e.g. max. adsorption conc.)	limited process e.g. Langmuir isotherm

Equation forms		Process type
2. Kinetic processes		
$\frac{dc}{dt} \propto K_0$ $\frac{dc}{dt} \propto K_1 \cdot c$ $\frac{dc}{dt} \propto K_2 \cdot c^2$	*c* – concentration K_x – kinetic rate coefficient (x = 0, 1, 2 – zero, first, second order)	kinetic – rate process e.g. first order rate: sedimentation, straining, volatilization, sorption, hydrolysis, photodegradation, biodegradation e.g. second order rate: sorption
$steady\ flux \propto D_0 \frac{\partial c}{\partial x}$ $\frac{dc}{dt} \propto D_1 \frac{\partial c}{\partial x}$ $\frac{dc}{dt} \propto D_2 \frac{\partial^2 c}{\partial x^2}$	*c* – concentration D_x – diffusive rate coefficient (x = 0, 1, 2 – steady, advection, dispersion)	Fick's law – processes e.g. plant uptake, volatilization, D_1 – advection, D_2 – dispersion and diffusive fluxes
$\frac{dc}{dt} \propto k \cdot X \cdot \frac{c}{K_s + c}$	*c* – pollutant concentration *X* – catalyst amount *k* – specific process rate – "driving" K_s – half saturation coeff. – "limiting"	catalyst limited process e.g. biodegradation: Michaelis-Menten, volatilization (Lee et al., 1998), photodegradation - Langmuir-Hinshelwood
$\frac{dc}{dt} \propto \frac{\mu_{\max}}{Y} \cdot X \cdot \frac{c}{K_s + c}$ $\frac{dX}{dt} = \mu_{\max} \cdot \frac{c}{K_s + c} \cdot X$	*c* – pollutant concentration *X* – catalyst amount μ_{max} – maximum rate *Y* – catalyst yield μ_{max}/Y – spec. process rate – "driving" K_s – half saturation coeff. – "limiting"	catalyst limited – catalyst evolving process e.g. biodegradation: Monod growth model

Volatilization is a physical process in which a volatile substance dissolved in water is released and transferred to the atmosphere. In the simplest way, the contact between the water surface and the atmosphere can be described by four layers: (1) well-mixed, turbulent, bulk air, (2) thin stagnant layer of air, (3) thin stagnant layer of water and (4) well-mixed, turbulent, bulk water below the interface region. The transfer is believed to occur between the two stagnant thin layers of water (3) and air (2) by molecular diffusion. It is also assumed that resistances in the air and the water film are additive, although they are of different magnitudes. These two concepts are the basis of the two-

film theory published by Lewis and Whitman (1924), usually used for the description of the process of volatilization.

The model consists of pollutant mass transfer through the two layers with a combined water-air diffusion mass flux (mass-transfer). The equilibrium condition for this theory is expressed in terms of the Henry's law. The mass balance is a dynamic steady-state that does not allow for pollutant mass accumulation in any of the two layers. Volatilization is influenced by pollutant properties, such as the Henry's constant and solubility, and by water and air properties such as temperature, viscosity, partial pressure, etc. *Two-film models* have successfully been used for modelling of volatile organic compounds in primary and secondary settling tanks (e.g. Lee et al., 1998) and constructed wetlands (e.g. Keefe et al., 2004). It should be mentioned that for more turbulent environments, models have been developed that do not have a stagnant boundary between air and water. These include (1) *the surface renewal model* (Higbie, 1935) – in which new surfaces are formed by breaking waves, air bubbles entrapped in the water, and water droplets ejected into the air, and (2) *the boundary layer model* (Deacon, 1977) – an upgrade to the two-film model that includes a continuous diffusivity profile and transport of turbulence (kinematic viscosity).

Sorption is a complex physico-chemical process by which one substance (e.g. dissolved in fluid) becomes attached to another (e.g. mineral surface). This is achieved by absorption (when substance is incorporated into the volume of another), adsorption (surface adhesion) and/or ion-exchange. Sorption of pollutants is influenced by pollutant's intrinsic properties (hydrophobicity, polarity, aromaticity etc.) and soil physico-chemical characteristics (e.g. pH, cation exchange capacity, ionic strength, surface area, soil organic matter, water temperature, etc.) (Langmuir, 1997).

Sorption is usually described using a plot of the sorbate versus concentration in solution measured at a constant temperature when equilibrium is reached (a.k.a. a sorption isotherm). The two most commonly used isotherm models for fluid solutions are (Langmuir, 1997):

- Freundlich – which assumes an infinite supply of unreacted sorption sites, and
- Langmuir – which assumes a finite supply of sorption sites.

Sorption isotherms are not always adequate to describe sorption processes, even in simple cases such as batch-experiments, as they lack information on process kinetics. This is where e.g. adsorption kinetic models come in place. Qiu et al. (2009) made an extensive critical review of adsorption kinetic models, grouping them into:

- Adsorption reaction (e.g. pseudo-first-order rate eq., pseudo-second-order rate eq., Elovich's eq.) and
- Adsorption diffusion models (e.g. liquid film, intraparticle, double-exponential).

Although both types can fit the kinetic data in batch tests, Qiu et al. (2009) give slight preference to adsorption diffusion models. This is due to their capability of representing the *real* adsorption course "more reasonably", while the diffusion parameter determined from these models can be useful for system design (e.g. flow-through treatment systems). Similar conceptual kinetic models exist for both absorption and ion-exchange.

Stepping up from batch tests to pollutant flow through the porous media, it is necessary to formulate conceptual models of mass transport which include both transport and sorption processes. In these cases, isotherms are modified (simplified) and/or combined with kinetic models, allowing for non-equilibrium models.

The simplest model is the equilibrium K_d – model (a linear Freundlich isotherm) with parameter estimates compiled in most textbooks (e.g. Langmuir, 1997; Schwarzenbach et al., 2003; Mackay, 2006). The K_d parameter is not pollutant specific, but a lumped parameter that depends on the porous media composition and conditions at which it is determined, which is why most compilations include this metadata as well. There are attempts to "break" the K_d parameter into pollutant-specific and media-specific parts e.g. K_d for organic pollutants is described as a product of the soil-water partitioning coefficient normalized to organic content, which is pollutant-specific, and soil organic carbon content (Karickhoff et al., 1979; Karickhoff, 1984). The equilibrium K_d – model is usually used with the advective-dispersive transport equation, while K_d as a parameter is present in many non-equilibrium models.

Probably the most extensive review on non-equilibrium sorption-transport in the variably saturated porous media is given by Šimůnek and van Genuchten (2009). The models are grouped in:

- Conceptual physical non-equilibrium for water flow and solute transport and
- Conceptual chemical non-equilibrium models for reactive solute transport.

Both types of models try to compensate for simplifications made with the porous media, which is assumed to be structurally and chemically homogeneous. Physical non-equilibrium models compensate for assumed structural homogeneity (Figure 2-2). They are derived from a so-called uniform flow model (the original version of the transport equation, with bulk parameters such as hydraulic conductivity and porosity), by assuming that the soil particles have their own microporosities. These micropores allow (1) dissolved pollutants to move in-and-out by diffusion (Mobile-Immobile Water model) or (2) both water and dissolved pollutants to move in-and-out (Dual-Porosity model). More complex models include the Dual-Permeability models that assume existence of two types of pores: (1) large a.k.a. interporosity domain with fast fluid and solute movement and (2) small a.k.a. intraporosity domain with slow fluid and solute movement, and can be combined with "stationary" pores (such as in Mobile-Immobile water). Physical non-equilibrium models may be considered to account for pollutant absorption to soil, although that is not their primary intent. The motivation for their development comes from laboratory column experiments with uniform flow and conservative tracers which show extensive tailing in the pollutograph, indicating structural heterogeneity.

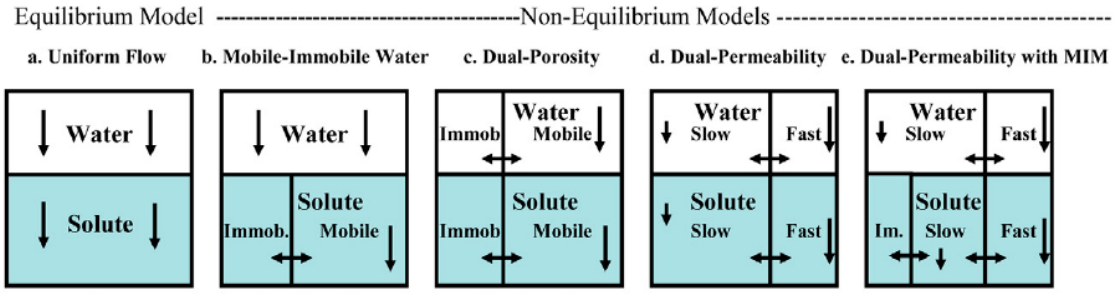

Figure 2-2 Conceptual physical non-equilibrium models for water and solute transport (after Šimůnek and van Genuchten, 2009)

Chemical non-equilibrium models compensate for assumed chemical homogeneity. These are: (1) One Kinetic Site – assuming kinetic nature of sorption and modelled using any of the kinetic models (usually the first order rate) (2) Two-Site – assuming instantaneous sorption to one fraction of sorbing sites and kinetic to the rest, modelled

using a combination of sorption isotherms and kinetic models, and (3) Two Kinetic Sites models – assuming two natures of sorption sites, each modelled by a kinetic model (Figure 2-3). When dealing with pollutants in real systems, it is natural to expect both physical and chemical non-equilibrium. Combination models, such as the Dual-Porosity with One Kinetic Site or the Dual-Permeability with Two-Site sorption, should be used when the two processes are of equal intensity (Šimůnek and van Genuchten, 2009).

The desorption process is implicitly accounted for in equilibrium sorption modelling, since sorption isotherm parameters depict net-sorption (sorption-desorption). In non-equilibrium sorption models, desorption is a kinetic process with identical or different kinetical model than sorption. Desorption kinetical models are usually first order rate models (e.g. STUMP byVezzaro et al., 2009).

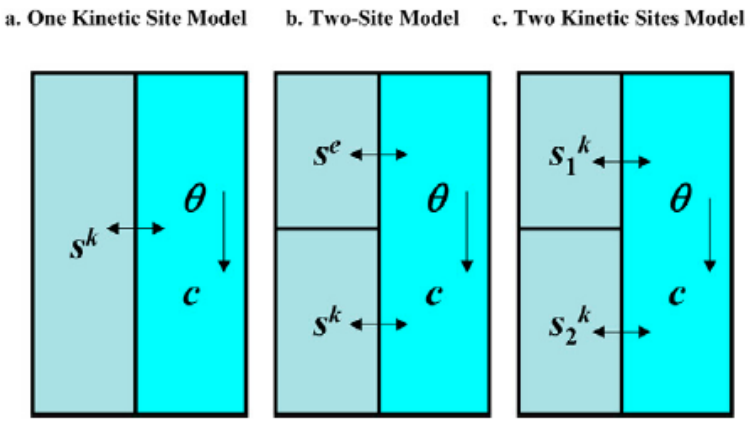

Figure 2-3 Conceptual chemical non-equilibrium models for reactive solute transport (θ – soil water content, c – pollutant concentration in water, s^e – pollutant concentration sorbed on soil at equilibrium, s^k – pollutant concentration sorbed on soil kinetically (after Šimůnek and van Genuchten, 2009)

Hydrolysis is a chemical process in which water molecules break existing bonds in substances and form new molecules: e.g. hydrolysis of organic molecules, RX, includes reaction with water where anion group X^- is substituted by OH^-, changing the water acidity. However, hydrolysis is sometimes used as a prototype reaction for any of the chemical decomposition or displacement reactions in which a nucleophile (electron-rich species) attacks an electrophilic atom (an electron-deficient reaction centre) (Schwarzenbach et al., 2003). Hydrolytic reactions are catalysed by acids, bases and, to some extent, water. Hydrolytic type reactions are usually modelled using kinetic:

- Pseudo-first order rate equations, when nucleophile is water or its concentration is constant or unknown, or
- Second order rate equations, when nucleophile concentration is changing and known (Schwarzenbach et al., 2003).

In most cases, the nucleophile is assumed to be water, and first-order rate is determined based on experimental data using reaction rate constants. Environmental compilations, such as Mackay et al. (2006), include hydrolysis "half-life" parameters in various environmental compartments, which are easily transformed to hydrolysis rates.

Photodegradation is a process of pollutant transformation following light absorption. This is also referred to as the direct photolysis (Schwarzenbach et al., 2003). Indirect photolysis, on the other hand, includes light excitation of photosensitive chemicals that easily react with organic species e.g. hydroxyl radicals, singlet oxygen, or ozone are formed in the presence of light. Although, indirect photolysis is induced by light absorption, it is usually neglected in the presence of other degradation mechanisms, due to its minor impact on the overall degradation rate. Photodegradation is a kinetic process that depends on (1) solar radiation intensity and wavelength, (2) suspended matter, colour and other factors influencing the penetration of light through water, (3) pollutant sensitivity to different wavelengths, and (4) the quantum yield – fraction of adsorbed photons that result in a chemical reaction (Schwarzenbach et al., 2003).

The kinetics of photodegradation of organic compounds is usually best described using a Langmuir-Hinshelwood scheme (Gaya and Abdullah, 2008). This is because a plateau type kinetic profile is observed where the initial rate (increased with longer irradiation time) changes to zero over time. According to the Langmuir-Hinshelwood model, the photocatalytic reaction rate is proportional to the reaction rate constant, organic compound concentration and the Langmuir adsorption constant. However, this scheme simplifies to a first order rate when applied to micropollutants (at low concentrations). Reaction rate constant is determined from experimental data, or can be calculated using pollutant specific data such as the quantum yield, and site-specific data such as water-depth, irradiation intensity, and water media light attenuation property (ScorePP, Vezzaro et al., 2009). Mackay et al. (2006) report experimentally determined photodegradation "half-life" parameters in various water bodies.

Biodegradation is a chemical process of substance dissolution catalysed by microorganisms: bacteria, viruses, fungi, protozoa or parasites. In this reaction, microorganisms profit as they receive carbon, nitrogen and energy necessary for their metabolism. Biodegradation may occur with or without oxygen, depending on the catalyst microorganism, and can be classified as aerobic or anaerobic. Biodegradation depends on the availability of microorganisms and substance (e.g. sorbed substance may be unavailable to microorganisms), but also on redox conditions, pH, temperature, or any other environmental parameter that limits the metabolism of microorganisms (e.g. oxygen) (Corapcioglu and Hossain, 1990). Biodegradation can be modelled using some of the simpler models, such as the zero order rate (constant) or first order rate kinetics model, or growth – models that include information on microorganisms, which are usually based on Monod (Monod, 1949) or Michaelis-Menten type kinetics (Johnson and Goody, 2011). Growth models include relationships between microorganism growth and substrate (i.e. substance being degraded). Monod type kinetics assume that the substance being degraded is a *limiting* factor in microorganism growth, while Michaelis-Menten type kinetics assumes that microorganism growth is either constant, or not influenced by the substrate itself: it is an equation developed for enzyme kinetics. This is why Monod may be more applicable to nutrient degradation modelling, while Michaelis-Menten may be more suitable for micropollutants. However, there are multiple cases where Monod kinetics have been used for pollutants that are not apparent nutrients, such as pesticides (Cheyns et al., 2010; Sniegowski et al., 2009), but the purpose was to model pesticide-degrading bacteria. Mackay et al. (2006) report experimentally determined half-life estimates (assuming first-order rate kinetics) for different environmental compartments such as different soils, surface water, groundwater etc.

Plant uptake (and storage) of organic compounds is one of the important steps in the global cycling of persistent pollutants (Collins et al., 2006). There is a substantial amount of evidence of plant contamination with a diversity of toxic organic pollutants, like accumulation of volatile substances in mosses, lichens, and higher plants due to air-plant interactions (e.g. Thomas et al., 1984) or phenanthrene and pyrene by soil-plant interactions (e.g. Gao and Zhu, 2004). Major plant uptake pathways are identified as follows: (1) passive and active uptake from soil into plant roots, (2) particulate

depositions followed by desorption into leafs and (3) gaseous interchanges at leaf levels (additionally influenced by transport of pollutants within the xylem) (Figure 2-4). The processes depend on the pollutant, plant and soil specific properties like sorption mechanisms (include octanol-water and octanol-air partitioning coefficients), solubility, plant lipid content, plant metabolism, temperature, etc. Simple process modelling, which is usually used for non-nutrient type pollutants, is based on partitioning models at root or leaf levels (Chiou et al., 2001; Collins et al., 2006), to calculate the plant uptake factor (PUF) as a driving force for either first-order kinetic rate (driven by concentration) or diffusive fluxes (driven by the concentration gradient). The *Nye-Tinker-Barber model*, used for nutrient type substances, uses a heuristic Michaelis-Menten kinetics to model nutrient uptake at root level (Roose, 2000). In addition to the root uptake, nutrient models include transport through the xylem, and transpiration fluxes.

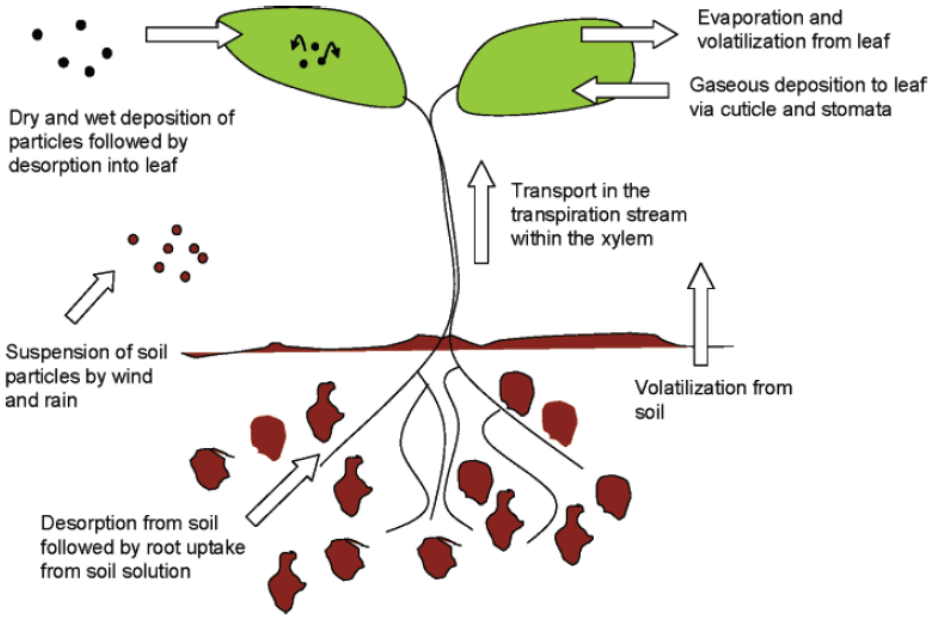

Figure 2-4 Major uptake processes of organic substances by plants (after Collins et al., 2006)

2.5 Uncertainty analysis

2.5.1 Introduction

Uncertainty is present in every modelling process, with sources ranging from decisions on model conceptualisation, to data collection, calibration and verification. By mapping

and analysing sources of the uncertainty, especially by quantifying their impact on modelling (e.g. estimating confidence intervals), model predictions can become more reliable i.e. less uncertain. Additionally, by knowing the impact of a particular error source on the overall simulation uncertainty, it is possible to decide on investing resources in improving the quality of that particular source e.g. if it is the input data that has the highest impact on the total simulation uncertainty, then the right decision would be to work on the data collection system, rather than to increase model complexity or improve calibration techniques (Vrugt, 2008). This section presents some of the methods for uncertainty assessment and uncertainty sources identified in the literature.

2.5.2 Uncertainty assessment

A fair number of studies investigated the uncertainty in groundwater, hydrological or environmental modelling in the past few decades (e.g. Beck, 1987; Beven and Binley, 1992; Kuczera and Mroczkowski, 1998; Kuczera and Parent, 1998; Muleta and Nicklow, 2005; Refsgaard et al, 2007). In the beginning, the research was directed primarily toward parameter uncertainty (Kuczera and Mroczkowski, 1998), then toward calibration induced uncertainty (McCarthy, 2008), only to find its way to the model structure (Gupta et al., 2012). Urban drainage modelling studies, on the other hand, do not have such a long history of uncertainty assessment (e.g. Kleidorfer et al., 2009; Lindblom et al., 2011; Vezzaro et al, 2012; Dotto et al., 2012), but have mostly acquired frameworks developed for hydrological models. Many of the uncertainty assessment concepts have been developed into commercial software models, where methods range from formal Bayesian like the Markov-Chain Monte-Carlo approaches (e.g. MICA by Doherty (2003), DREAM by Vrugt (2008)), to less formal likelihood methods as the Generalized Likelihood Uncertainty Estimation (GLUE by Beven and Binley, 1992). Either concept is used for (1) simple sensitivity analysis (usually qualitative study on parameters), (2) structural study of uncertainties by examining prior and posterior parameter distribution while propagating errors through the modelling process, and (3) evaluating predictive uncertainty using confidence intervals.

2.5.2.1 Methods for Uncertainty Assessments

Many methods for uncertainty assessment are developed for automatic model calibration. These methods solve an inverse problem and are based on a Bayesian

approach: (1) prior probability distribution function (PDF) of model parameters is estimated based on the best-available-knowledge (usually a uniform distribution), which is then (2) readjusted by sampling data and a likelihood function to obtain a posterior parameter PDF. The shape of the posterior PDF indicates uncertainty, with extremes being:

- Total certainty – defined as a Dirac δ function at the parameter value, and
- Total uncertainty – represented by a uniform PDF over $(-\infty, +\infty)$ (Kottegoda and Rosso, 2008).

Deletic et al. (2012) identify the most commonly used methods for uncertainty assessment in urban drainage modelling to be the Generalized Likelihood Uncertainty Estimation – GLUE (Beven and Binley, 1992), Shuffled Complex Evolution Metropolis Algorithm – SCEM-UA (Vrugt et al., 2003), Multi-objective calibration algorithm – AMALGAM (Vrugt and Robinson, 2007), and MICA (Doherty, 2003).

GLUE is considered a non-formal Bayesian method, due to its lack of a formal likelihood function, and its brute-force algorithm for parameter space exploration. GLUE is based on Monte-Carlo simulations, where model parameters sets are sampled *randomly* from their prior PDFs. A user defined likelihood function is used to compare model results with observations. Model parameter sets with "low" likelihood values are discarded, while the ones retained are used for formation of a posterior PDF. A "low" likelihood function is a user defined threshold. The major advantage of this method is its lack of assumptions on the error distribution function. However, the method may be computationally costly, and suffers from modeller's subjectivity on the choice of a threshold value for the likelihood function.

MICA belongs to the group of Markov-Chain Monte-Carlo methods (MCMC). Markov-Chain methods sample from a random walk which adapts to the true posterior distribution and in such way decreases the number of Monte-Carlo runs:

- Initial parameter sets are randomly sampled from the prior PDF;
- Model runs from these sets are evaluated by using the likelihood function;

- Subsequent parameter sets (a.k.a. proposed) are sampled from an updated parameter PDF function which depends on the values of the previously generated parameter sets;
- Proposed parameter sets can be accepted or rejected based on the comparison between their likelihood function with that of the previous set.

The Metropolis-Hastings algorithm (Metropolis et al., 1953; Hastings, 1970) is one such MCMC, where proposed parameter sets can be accepted even when they have a lower likelihood function than their parent sets, allowing for a broader parameter space search (avoiding local optima). MICA uses Bayes' theorem for calculation of posterior distributions, and assumes normal distribution of errors. The acceptance of parameter sets is not based on subjective threshold criteria for the likelihood function, but on the Metropolis-Hastings algorithm and assumed likelihood function.

SCEM-UA is a hybrid between GLUE and MICA: it explores the parameter space using the Metropolis-Hastings algorithm, but finalizes the posterior parameter PDFs by selecting those parameter sets with likelihood values above user defined threshold. AMALGAM is a complex 4-step algorithm that includes a genetic algorithm, Metropolis search, and GLUE-like cut-off. Both have a major advantage over the brute-force method (like GLUE) in that they can explore larger parameter spaces, with small computer costs, by focusing only on areas with high likelihood values. However, both have issues with subjective criteria for the likelihood functions.

Dotto et al. (2012) explored these four uncertainty techniques on simple water quantity and quality models, and concluded that all of them generated similar posterior PDFs and predictive uncertainties (confidence intervals on model results). The compromise is between the need for a strict theoretical description of uncertainty (e.g. MICA), which requires extensive modeller's knowledge, simplicity (e.g. GLUE) and computer time (SCEM-UA and AMALGAM are very time efficient algorithms).

2.5.3 Sources of uncertainty in stormwater quality models

Deletic et al. (2012) presents development of a conceptual framework for uncertainties assessment in urban drainage modelling: a Global Assessment of Modelling Uncertainties (GAMU). In this framework, three key groups of uncertainty sources are

identified: (i) Model input uncertainties, (ii) Calibration uncertainties, and (iii) Model structure uncertainties.

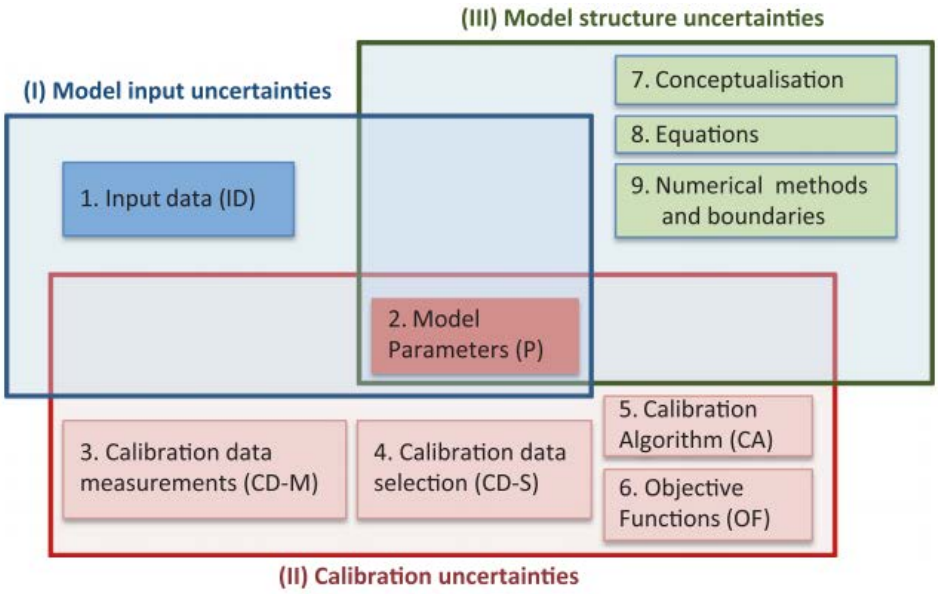

Figure 2-5 Key sources of uncertainties in urban drainage models and links between them (after Deletic et al., 2012)

Model input uncertainties are mostly associated with measured data uncertainties, and are caused by systematic and/or random errors. This type of uncertainty is usually defined as a dispersion of measured values. A probabilistic approach for expressing uncertainty is a probability density function associated with input data (and this does not necessarily have to be a normal distribution). Sometimes, it is not possible to find input data probability distribution functions due to an insufficient amount of available measured data. In this case, estimates can be made based on the-best-available-knowledge (e.g. information on the accuracy in the equipment used and assuming normal error distribution) or the Monte Carlo method to propagate probability distribution of the least restrictive type (e.g. uniform). In either case, uncertainties are propagated by running the model multiple times to obtain confidence intervals on model results. If these intervals are narrow, then it is safe to assume that input uncertainties do not play an important part in the overall uncertainty. Uncertainties in input data have been addressed by some urban drainage modelling studies in two ways: (1) “simply” – by propagating errors through the model by keeping the model parameters fixed (e.g. Rauch et al., 1998) or (2) “in-depth” – by assessing the impact of input data

uncertainties on model parameters and model results (e.g. Kleidorfer et al., 2009; Dotto et al., 2014).

Calibration uncertainties arise due to any of the selections made in the calibration process: (1) calibration dataset selection, (2) calibration algorithm or (3) the objective function. In addition to having similar uncertainties as the input data (due to measurements), calibration dataset should be selected to fit the purpose of the model's application. McCarthy (2008) showed that the microorganism model gave better predictions when it was calibrated using instantaneous concentrations instead of microorganism fluxes. In addition, many studies dealt with the selection of data for calibration and model verification (e.g. Vaze and Chiew, 2003). Todorovic (2015) studied the impact of the calibration period on parameter estimates in conceptual hydrological models. She found that with an increase in the length of the calibration period, variability of the parameters slightly decreases. Multiple studies have addressed the impacts of calibration and uncertainty analysis methods, along with a choice of different objective functions, on model predictions (e.g. Dotto et al., 2012; Kleidorfer et al., 2012). It was shown that different calibration methods can lead to different parameter sets, while still having a similarly good fit between measured and modelled data. This can happen due to difficulties in finding the global optimum, particularly pronounced in complex systems with a multi-modal objective function surface. It can also be the case that the model is "ill-posed" (Dotto et al., 2009), and that some of the model parameters are not "true", but rather compensate for the neglected or ill-conceptualized processes. The concept that a unique optimal parameter set exists is something that many researchers do not hold for granted, but rather accept the concept of "equifinality", introduced by Beven (2009), in which more than one parameter set may be able to provide an equally good fit between the model predictions and measurements.

Model structure uncertainties can be associated with (1) conceptualization (conceptual model), or determination of relevant processes to be modelled, (2) equation selection (mathematical model) or (3) solving technique (computational model) (Deletic et al, 2012; Gupta et al., 2012). Inspired by the idea that "we must be able to establish whether a model structure is adequate to the task of simulating system behaviours under

past, current, and potential future conditions for both similar and relatively different locations and/or modelling conditions", Gupta et al. (2012) performs an in-depth analysis on model structural adequacy and synthesizes current knowledge from several different modelling communities: groundwater (GW), unsaturated zone (UZ), terrestrial hydro-meteorology (THM), and surface waters (SW), suggesting a five-step framework for model evaluation (Figure 2-6). Although, model structure uncertainties are recognized to be relevant, there are not that many studies which actually address their impact on modelling results. A rare example is a study by Blumensaat et al. (2014) performed on river water quality models. In addition to presenting the assessment framework, it shows that model structure and parameter uncertainties are of the same order of magnitude.

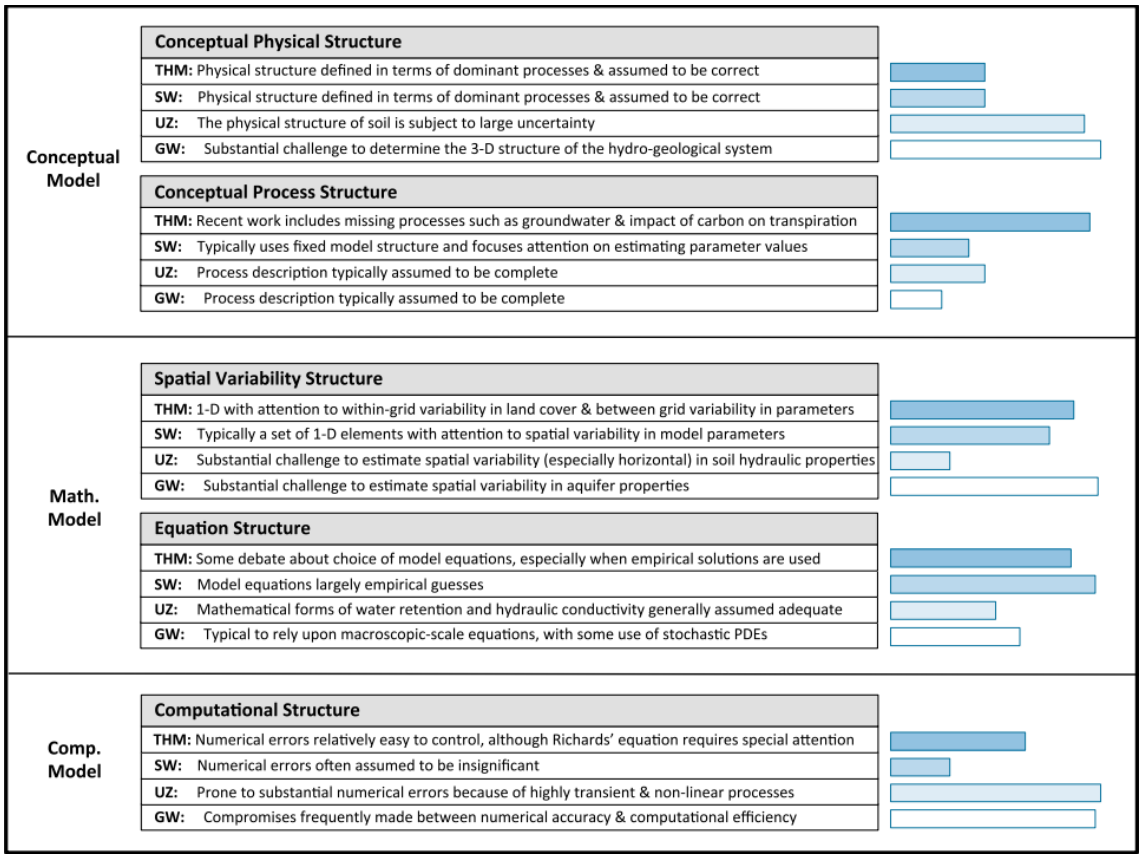

Figure 2-6 Subjective assessment of the emphasis (indicated by the length of bars) given by different modelling communities to various sources of model inadequacy (after Gupta et al., 2012)

2.6 Conclusion: Identification of key knowledge gaps

There is a fair number of stormwater quality studies that provide good insight into possible stormwater compositions. However, the mechanisms of pollutant transport and fate across the catchment, and particularly treatment systems, are not fully known. Even though a large number of studies have been performed specifically studying the behaviour of various pollutants in stormwater biofiltration systems, they have rarely included the most common stormwater micropollutants. This opens certain research questions:

- Are biofilters capable of treating micropollutant rich stormwater? If so, under which conditions?
- What are the key transport and fate mechanisms for micropollutants in biofilters?

Since the data on micropollutant behaviour in stormwater biofilters is scarce, it is only natural that models capable of reproducing their behaviour are also rare or non-existent. A literature review indicates that there are only a few models that can be adjusted to be used for micropollutants in biofiltration systems. These models either have very simple water dynamics, or lack some of, what is believed to be, key mechanisms. As such, the literature review indicates that:

- A new model is required that can adequately predict micropollutant behaviour in stormwater biofiltration systems.

This model can benefit from the reviewed models' algorithms e.g. a hydrodynamic module based on MUSIC (eWater, 2012) may be useful, or a treatment module adapted from RSF_Sim (Meyer et al., 2008; Meyer and Dittmer, 2015) or from the Hydrus family (Šimůnek et al., 1999).

There is a wide range of uncertainties that can impact the modelling results. It is, however, not standard practice to acknowledge and evaluate these uncertainties. This is particularly the case with urban drainage water quality models, which is why this research will attempt to perform such analysis on the developed model.

2.7 Research aims and objectives

The literature review found that significant knowledge and data gaps exist and in order to develop a new biofilter micropollutant model, a number of these gaps need to be filled. The overall aim presented above will be accomplished by completing a number of smaller, more specific, aims/objectives and hypotheses as follows:

1. To develop a transport and fate model for organic micropollutants in stormwater biofilters:

- It is hypothesized that micropollutants can be grouped according to their chemical structure and nature into a few groups, and that a good "representative" can be selected from each group, whose transport and fate models can be "transferred" to each member of the group.
- It is hypothesized that the complex hydrodynamic behaviour of urban stormwater in WSUD systems can be conceptualized by a multiple reservoir approach (one-dimensional model with dominant vertical flows).
- It is hypothesized that transport of micropollutants in the biofilter can be predicted by a linear advective dispersive transport equation (vertical), while conceptual 1^{st} and 2^{nd} order decay models could be used to assess the removal processes that may be physical/chemical/biological in nature (settling, straining, volatilization, photodegradation, hydrolysis, aerobic/anaerobic biodegradation, adsorption, and desorption).

2. To conduct controlled lab and field tests to refine the model component that simulates the micropollutant treatment in biofilters:

- It is hypothesized that a large amount of data should be collected to ensure accurate testing and verification of the newly developed model.

3. To calibrate, validate, and assess uncertainties in the model using field data from two stormwater systems (biofilters with different designs):

- It is hypothesized that uncertainty analysis (using two different field data sets) will point to sensitive parameters and provide insightful information about the processes.

2.8 Methodology used to complete the research aims

There is a total of seven chapters in this thesis, with each one contributing to the above listed aims. Chapter 2 is a literature review which should result in a better understanding of micropollutants present in stormwater, their transport and fate processes through the biofiltration systems and assess available micropollutant and similar models potentially useful in the development of the future model. Chapter 3 presents experimental methodology and collection of data for model development and testing. Chapter 2 and 3 provide necessary knowledge and data for the development of the model in Chapter 4. Chapter 5 presents calibration and verification of the model developed in Chapter 4 using data presented in Chapter 3. The data used for model testing includes field data, laboratory column and batch test data. Chapter 6 includes uncertainty analysis of the developed model, and its result should point to sensitive parameters. Chapter 7 gives a summary of conclusions, evaluation of research aims, and further research ideas.

Major parts of the overall thesis include field and laboratory studies as well as model development and testing. The information from data analysis and literature review will assist in the development of the micropollutant model. The models' code will be written using Python language, which was selected on the basis of its widespread use as a scripting language in commercial and open source programs. Model calibration, verification and uncertainty analysis will be conducted using an array of available softwares.

CHAPTER 3: EXPERIMENTAL DATA

3 EXPERIMENTAL DATA

3.1 Introduction

This chapter presents the data collection methodology used in this study. Data collected through laboratory and field experiments is used for the development and testing of a micropollutant transport and fate model in biofiltration units.

The chapter begins with a description of the field experimental site, where both tracer and micropollutant spiking tests were performed. This is followed by an explanation of the measuring system for flow and meteorological data, as well as sample collection and analysis methods. The tracer test is complemented with an Electrical Resistivity Tomography to visualise the vertical flow field, and the field measurements are accompanied by laboratory batch and column studies. The collected data is presented with its statistical measures, and a brief estimate of possible data uncertainty is provided.

3.2 Field experimental site

Field data was collected from the Monash Car Park Biofilter built inside Monash University (Australia) campus, which harvests stormwater from a nearby multi-level parking lot for irrigation of a sports oval (Figure 3-1). This biofiltration system consists of three separate cells (all lined), with different configuration of the filtration layers and plant covers. Although the biofilter has been in operation for 9 years, it is not in its original state. The biofiltration system were reconfigured in 2009, when barriers were placed between cells (to avoid fluid mixture among cells) and middle cell has been filled with media following the Guidelines for Soil in Filter Media in Biofiltration Systems (FAWB, 2009). This study was performed on only two of the cells, as the third cell experienced a high degree of clogging.

Cell 1 is a biofilter which is made with loamy sand and planted with *Carex appressa* (Table 3-1). The loamy sand that is used has a nutrient content well above the best design practice (FAWB, 2009), with on average 1600 mg/kg total nitrogen (TN) and 320 mg/kg total phosphorus (TP). There is an abundance of soil organic matter (SOM), 4.6% on average, and the soil's pH value of below 7.5 is considered to be normal

according to the same guidelines. Loamy sand is placed at a depth of 50 cm, and below it was a drainage layer consisting of small gravel and sand. There is no transitional layer. The drainage layer also has a central sloping (1%) PVC perforated pipe. The pipe is placed at the bottom of the cell, made out of an impermeable concrete, which extends all the way to the sides of the cell, isolating the cell from the surrounding soil media. The outlet of the PVC pipe is at the same level as the cell bottom, so the filter media can drain completely. This pipe is the outlet of the biofilter. There is an extended detention zone, provided by the placement of a security weir at a height of approximately 40 cm above the ground level (Figure 3-2).

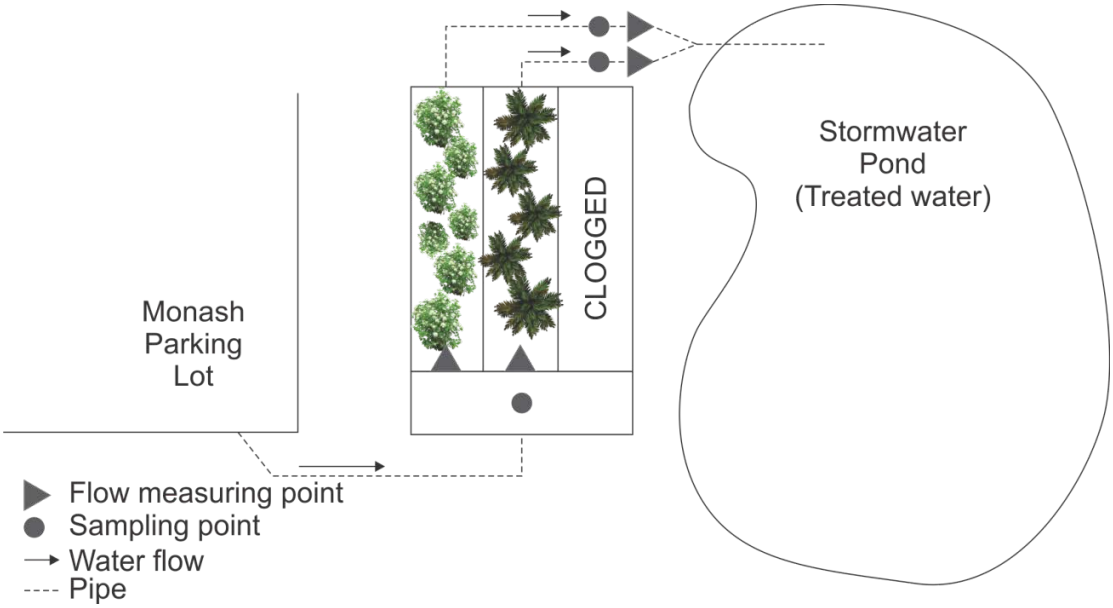

Figure 3-1 The Monash Car Park Biofiltration system – a scheme

Cell 2 is a biofilter which is made with sand and planted with *Melaleuca ericifolia* (Table 3-1). The sand used has a nutrient content in accordance with the best design practice (FAWB, 2009), having on average 850 mg/kg TN and 255 mg/kg TP. The SOM, 2.2 % on average, and soil's pH value of below 7.5 are also considered to be normal (FAWB, 2009). Sand is placed at a depth of 70 cm, with the material between 50 and 70 cm being at the same time a drainage layer and a submerged zone with extra organic content provided by the presence of woodchips and dry peat. Similarly to Cell 1, the drainage layer also has a central sloping (1%) PVC perforated pipe, placed at the bottom of the cell, but the outlet of the pipe is 20 cm above the cell bottom, allowing for submerged zone to be formed. This cell is also completely isolated from the surrounding soil by an impermeable concrete. There is an extended detention zone,

provided by the placement of a security weir at a height of approximately 40 cm above the ground level (Figure 3-3).

Table 3-1 Soil Characteristics and configurations of the two field biofilters, Nov 2013

		Cell 1 (loamy sand, no submerged zone)		Cell 2 (sand, with submerged zone)	
Soil Characteristics					
Sampling point (sample ID) depth[(1)]		10 cm	30 cm	10 cm	30 cm
Soil texture	sand (0.063 – 2.0 mm)	91.4%	92.8%	95.3%	99.4%
	silt (0.002 – 0.063 mm)	6.10%	4.10%	3.70%	0.30%
	clay (≤ 0.002 mm)	2.50%	3.10%	0.10%	0.30%
pH		7.10	7.40	7.10	7.20
Bulk Density (g/cm^3)		1.58	1.61	1.56	1.59
Soil Organic Matter, SOM (%)		5.30	3.90	4.20	0.350
Total Phosphorus, TP (mg/kg)		470	260	420	30.0
Total Nitrogen, TN (mg/kg)		2,000	1,200	1,400	300
Average Soil Porosity		0.35		0.40	
Geometry					
Length (m)		9.65		9.65	
Width (m)		1.35		1.35	
Ponding depth (m)		0.41		0.41	
Filter depth (m) – design value		0.50		0.50	
Drainage layer (m) – design value		0.20		0.20 (coincides with submerged zone)	
		sand and small gravel		filter material mixed with woodchips and dry peat	
		perforated PVC pipe Ø100		perforated PVC pipe Ø100	
Submerged zone depth (m)		No		0.20	
Plant species		*Carex appressa*		*Melaleuca ericifolia*	

(1) Depth measured from the soil surface during dry period

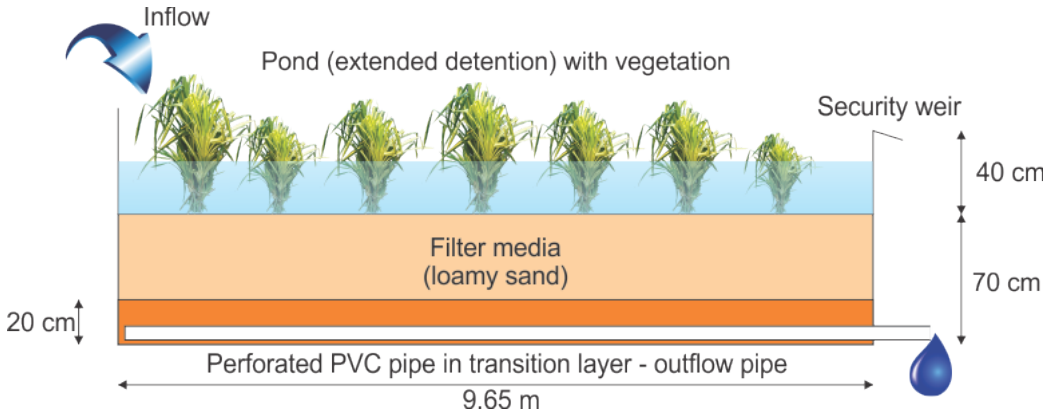

Figure 3-2 Cell 1 at the Monash car park biofiltration system – a scheme

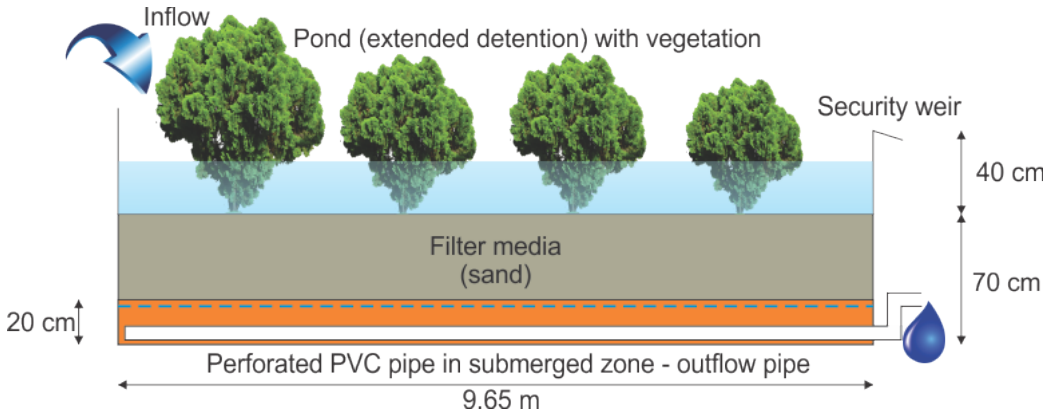

Figure 3-3 Cell 2 at the Monash car park biofiltration system – a scheme

3.2.1 Measuring and sample collection system

Water quantity data. The biofiltration system is equipped with flow measuring devices for inflow - I, outflow - D (drainage pipe), and overflow – O (flow over the security weir) (Figure 3-4).

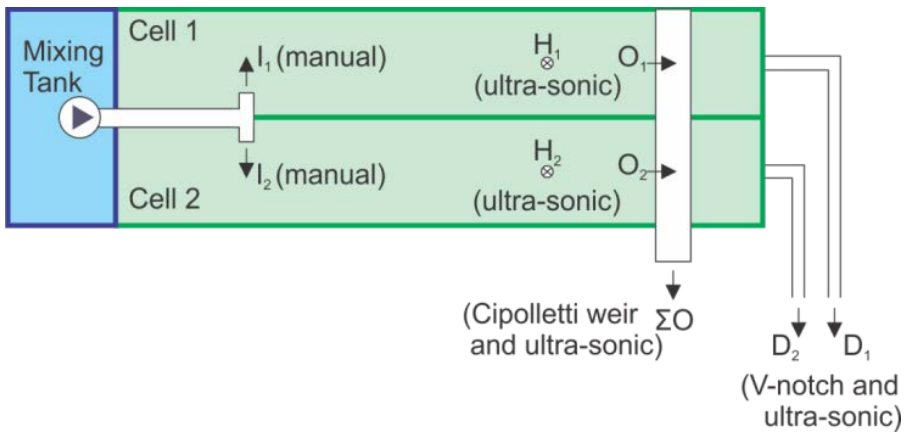

Figure 3-4 The flow measuring system scheme

The measuring system for flow is composed of V-notch weirs for inflow and outflows, trapezoidal (Cipolletti) weir for overflows, equipped with an open channel flow meter - Siemens Milltronics OCM III. Data was logged using the dataTaker ® 500 which connects to a PC via the DeLogger software.

The OCM III emits ultrasonic pulses that echo off the water surface and get captured by its transducer (supplied with velocity, auxiliary head and temperature sensors). The measured time for the echo is temperature compensated and converted into a measurement of head for a given zero reading (Instruction Manual PL-505, 2001). The range of the measurements is 0.3 m min to 1.2 m max, and the resolution is 0.2 mm.

Although the Siemens Milltronics flow meter can provide flow measurements using its velocity sensor, in this biofilter setup it was used as an ultrasonic depth measuring device, and the measured water depth was converted to flow using a calibration equation. The equation is Kindsvater and Shen's formula (USBR, 1997) of the following form:

$$Q = C_e \cdot \frac{8}{15} \cdot \sqrt{2g} \cdot \tan\left(\frac{\theta}{2}\right) \cdot \left(H + k\right)^{5/2} \tag{3.1}$$

where Q is the flow in the function of water head – H [L], and V-notch angle θ [deg]. C_e is the flow coefficient, and k [L] is the head correction, both functions of θ (C_e is additionally a function of the flow regime over the weir e.g. fully contracted flow). All V-notch weirs on site have a θ equal to 30°.

Figure 3-5 The Theta Probe – soil moisture sensor type ML2x

Since, it was found out that the ultrasonic depth sensors were not functioning properly at the inflow weir – I, the flow was additionally measured manually (discrete measurements) by a volumetric method.

Measurements of the water depth near the overflow Cipolletti weirs were at the same time measurements of water depth in the ponding zone of the biofilter – marked as H in Figure 3-4. The ultra-sonic depth measurements were averaged on a 30-sec interval for all measuring points (the sampling rate was 10 Hz).

Soil moisture measurements were taken with the Theta Probe sensors (Figure 3-5) placed horizontally at multiple sections and different depths of the biofilter as can be seen in Figure 3-6. The probe sends an output voltage proportional to the difference in amplitude of the standing wave in two point of the transmission line. The standing wave is produced by the emission and the reflection of the 100 MHz sinusoidal signal sent via a transmission line ending with an array of four rods in the soil. The change in the impedance of the rod array is influenced by the dielectric constant of the continuum between the rods, and since the dielectric of water is much higher than both soil and air (40 – 80 times), therefore, it can be completely attributed to the water content (Theta-Probe USER Manual, 1999). The probe output, which is in mV, is converted to volumetric water content via the following equation:

$$\theta = \frac{\left(1.1 + 4.44\frac{output\ [mV]}{1000}\right) - a_o}{a_1}\ \left[\frac{m^3}{m^3}\right] \tag{3.2}$$

where a_o and a_1 are calibration coefficients specific to soil, and for these biofilter cells are: a_o = 1.3727, a_1 = 9.6992. The full measurement range is 0.0 to 1.0 m^3m^{-3}, but the accuracy of ±0.01 m^3m^{-3} applies to the range 0.05 – 0.6 m^3m^{-3} (0 - 40°C) (Theta-Probe USER Manual, 1999).

The placement of the probes was optimized to capture variations of soil moisture profile with distance from the inlet and with depth. Data from the soil probes was stored using the dataTaker ® 600 in 15-min intervals (this was selected due to the not so dynamic change in soil moisture, as seen with previous experiments, and to save memory to allow for long term observations).

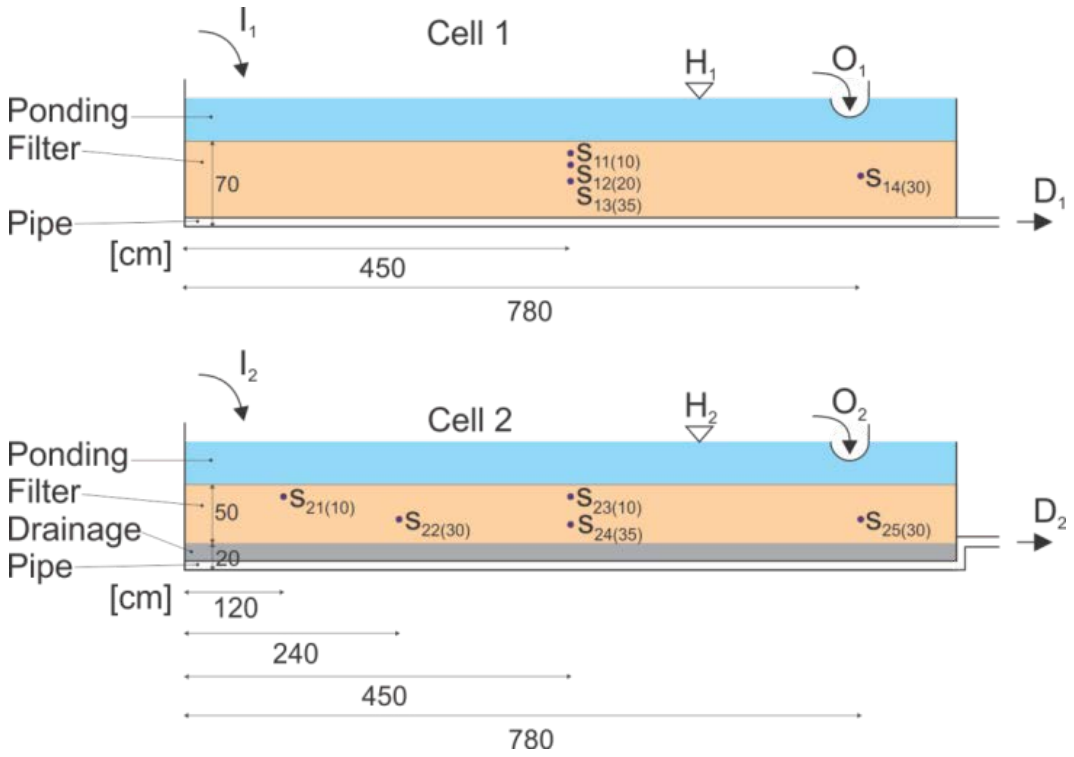

Figure 3-6 Soil moisture probes scheme

Water quality data. To assess the water quality in field experiments, two types of discrete samples were taken at both inflow, I, and outflow points, D: high frequency small volume and low frequency large volume samples. The small volume samples were taken to measure temperature and electrical conductivity (EC) with a multi – parameter probe PCSTestr 35 (temperature range 0 – 50°C, accuracy ±0.5°C; EC range 200 – 2000µS/cm, accuracy ±1%), while large volume samples were collected in standardized bottles (plastic, dark glass etc.), kept on ice during the experiment, and taken to the laboratory for further analysis (pH, EC, nutrients, organic matter, micropollutants etc.). Inflow samples were *grab* samples, taken by sterile containers and transferred to smaller bottles (standards and replicates for laboratory analysis), while samples at the outflow were collected using a *peristaltic pump*, with the hose set in the lower ¼ of the outflow pipe and directly poured in bottles. The samples were taken at a faster rate in the rising part of the breakthrough curve (e.g. every 200 to 500 L of cumulative outflow volume) and less frequently toward the end of an event (1000 to 1500 L), as can be seen in Figure 3-7 (this is important for calculations of EMCs – event mean concentrations).

Depending on the experiment type, the samples brought to the lab were analysed for pH, turbidity, fluorescein concentration, and EC. The pH and EC were checked with the HACH sensION+ MM374 multi-parameter benchtop meter. The measurement range for EC with this meter is 0.2 mS/cm to 200 mS/cm with an accuracy of ≤0.5%, and for the pH is 0 to 14 pH with an accuracy of 0.002 pH. Turbidity measurements were done with a HF Scientific Micro TPI portable turbidimeter.

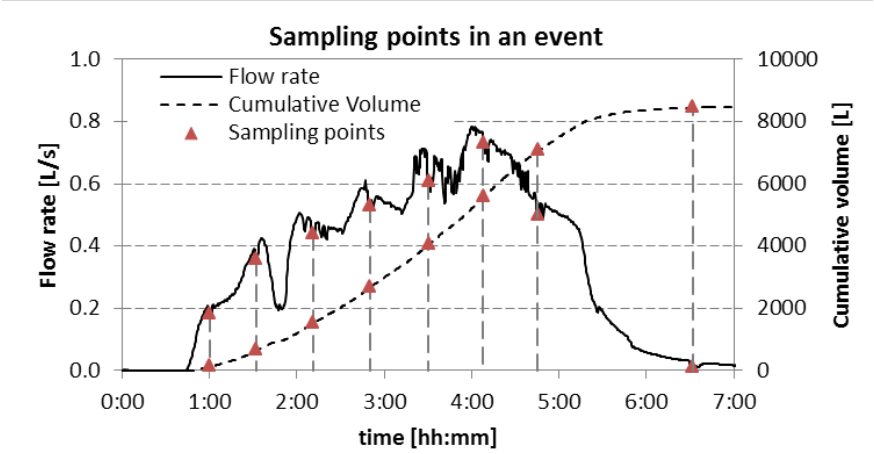

Figure 3-7 The sampling points showing the custom sampling procedure

AQUAFluor® was used for measurements of fluorescein concentration in water samples with a linear detection range between 0.4 to 400 ppb (equivalent to µg/L). Linear detection range provides that the reading of the AQUAFluor is directly proportional to the content of fluorophore. The device can be used for sample temperatures between 5 and 40°C, but since the readings are very sensitive to temperature, it is important to assure that the readings done on samples are temperature compensated to the temperature of the calibration standard. Fluorescence readings are also pH dependant, so each data point needed to be accompanied by a measurement of the pH value.

Once collected, the water samples were stored on ice, after which they were delivered to a NATA accredited laboratory (NATA – National Association of Testing Authorities, Australia) for analysis. All the samples were analysed for THMs, phenols, phthalates, PAHs and triazines using GCMS, for glyphosate using HPLC and for TPHs using GC FID (USEPA SW 846 Rev 2007) (see Table 3-2). The limit of report (LOR) for THMs, phenols, PAHs and phthalates was 1 µg/L. The LORs for glyphosate, triazines and

TPHs were 30 µg/L, 2 µg/L, and 100 µg/L, respectively. Electric conductivity (EC) was measured for all samples using a HACH sensION 378. The total dissolved solid (TDS) were then calculated based on a correlation between the EC and TDS determined by laboratory experiments.

Table 3-2 Summary of the µPs' physico-chemical properties, 95th percentile stormwater concentrations, measured inflow concentrations, Australian drinking water guideline (ADWG) values, and analytical methods used to quantify the pollutants in the collected water samples and their associated Limits of Reporting (LOR).

Pollutants		Physico-chemical properties[1)]		95th percentile concentration[2)] [µg/L]	Measured mean inflow value ± STD (n=9-12) [µg/L]	ADWG [µg/L]	Analysis method	LOR [µg/L]
		S [mg/L]	K_{OC}					
TPHs	Sum of TPH >C10-C40	-	-	147 Diesel in 5KL	5800±392	-[3)]	GC FID	100
PAHs	Pyrene	0.1	4.81	100	9.7±3.6	150	GCMS	1
	Naphthalene	32.2	2.74	250	16.2±6.9	70		
Herbicides	Glyphosate	12000	3.90	2000	1600±205	1000	HPLC	30
	Atrazine	29.8	2.09	60	49.5±9.4	20	GCMS	2
	Simazine	5.7	2.13	60	43.3±6.2	30		
	Prometryn	48.0	2.38	60	47.2±4.9	20		
Phthalates	DBP	9.9	2.20	60	41.3±4.4	35	GCMS	5
	DEHP	0.029	4.50	60	17.0±8.6	10		
THMs	Chloroform	8452	1.75	250	55.1±11.3	200	GCMS	1
Phenols	PCP	18.9	3.50	60	27.1±6.1	10	GCMS	1
	Phenol	83119	1.34	200	203.3±40.8	-[3)]		

[1)] mean values compiled from Mackay et al (2006)

[2)] Equates to target or challenge concentration

[3)] no Australian Drinking Water Guideline (ADWG) value

In addition to the micropollutant concentrations, all water samples were analysed for potential surrogates' concentrations (total suspended solids (TSS), total phosphorus (TP), total nitrogen (TN), ammonia, mono nitrogen oxides (NOx), dissolved organic carbon (DOC), and UV absorption at 254 nm (UVA).

Soil samples were taken at both cells during the 2nd test series from both the surface (5cm) and deep (15cm) soil layers. A sample for one cell and one depth was made in a 250 ml glass jar as a composite from three points: upstream, at 1.5 m, middle, at 4.8 m, and downstream, at 8.15 m (all distances measured from the wall at inflow end). The LOR for the pollutants was as follows: TPHs 20 mg/kg, phthalates, phenols and chloroform 5 mg/kg, triazines and PAHs 1 mg/kg. Glyphosate was not analysed.

3.3 Field tracer testing

A series of in-situ tests were conducted, named "challenge tests", involving pumping multiple pore volumes (PVs) of water from an adjacent stormwater pond spiked with 120 µg/L of fluorescein (1st and 2nd spiking tests) or without fluorescein (1st and 2nd flushing tests) into each biofilter. The inflow concentration of 120 µg/L was selected as it was best suited to the detection range of the measurement device – the AquaFluor® Handheld Fluorometer (Turner) (0.4 - 200 µg/L), and it allowed for visualisation of fluorescein in the water.

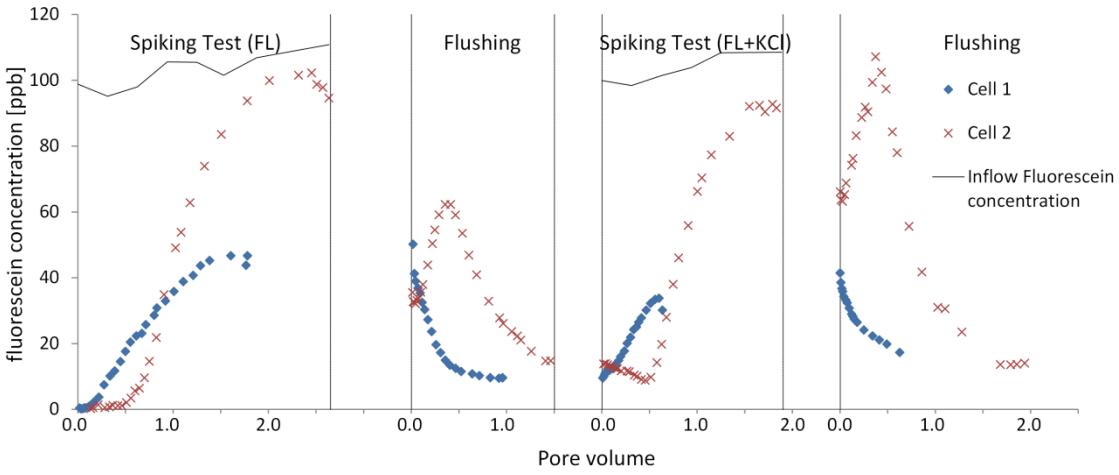

Figure 3-8 Pollutographs of fluorescein during tracer tests at Cell 1 and Cell 2

The 1st spiking test was conducted with 2.5 PVs inflow dosed into each biofilter, while the 2nd spiking test was conducted with 2.0 PVs. Before and after the 2nd spiking test, each biofilter was flushed by 2 PVs of un-spiked stormwater (1st flushing test and 2nd flushing test), which were aimed to flush the fluorescein in biofilters. Zhang et al. (2014) previously determined 2 - 3 PVs of inflow as being suitable for a challenge test for these biofilters. During the tests, about 10 discrete inflow samples and over 20 discrete outflow samples were collected for each test. Samples were analysed for

fluorescein concentration using a fluorometer, which was tested and validated for fluorescein detection in laboratory using standard fluorescein concentrations (10 µg/L and 100 µg/L) (Figure 3-8).

In spite of identical fluorescein infow concentrations, a substantial difference in fluorescein outflow concentrations was measured at Cell 1 and Cell 2 (Figure 3-8). Fluorescein outflow concentrations at Cell 1 were mostly lower than measured at Cell 2, which is hypothesized to be due to higher organic content of filter media in Cell 1, and presumable higher sorption of fluorescein in this cell.

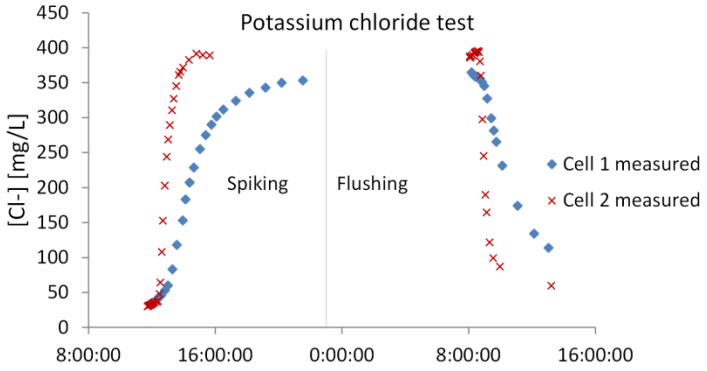

Figure 3-9 Pollutograph of KCl during the tracer test at Cell 1 and Cell 2

The conservative tracer testing was performed by pumping 2 PVs stormwater with a chlorine ion (Cl^-) concentration of 400 mg/L, followed by 2 PVs of stormwater (no tracer spiked) (Figure 3-9). Cl^- was analysed using a FIA Automated Ion Analyser (QuickChem 8500).

The difference in measured outflow concentration of Cl^- in Cell 1 and Cell 2 was attributed to a substantial decrease in hydraulic conductivity observed at Cell 1. This change in hydraulic conductivity was attributed to soil swelling (Dif and Bluemel, 1991) that happened due to the introduction of salt ions in an organic rich soil. Soil swelling is a phenomenon known to occur in the area, and it additionaly changes the porous structure of the filter media.

3.4 Field Electro Resistive Tomography (ERT)

3.4.1 Introduction

The main aim of the Electro Resistive Tomography (ERT) field experiments was to explore the dimensionality of the water flow i.e. whether one-dimensional flow was a

too high level of problem abstraction. Additionally, the collected data complemented the field tracer test data to uncover possible routes of short circuiting i.e. preferential flow paths.

3.4.2 About the method

Electro-Resistive Tomography for subsurface imaging is one of the non-invasive geophysical imaging methods that measures electrical resistivity distribution in soils. Because it is rarely the case that the subsurface is a homogeneous and steady continuum, but rather contains different soil materials with variable porosity, moisture and ionic content, measurement of resistivity allows for differentiation between them. This method can be used in both static characterizations of the subsurface, as well as to obtain a dynamic representation – series of images showing changes in resistivity caused by e.g. change in water saturation of pores. Since the resistivity of water is more than 8 times smaller than resistivity of air (at 20°C: water $2x10^2$ Ωm, air $2x10^{16}$ Ωm), a local increase in soil resistivity can be attributed to increase in air content in pores i.e. drying out.

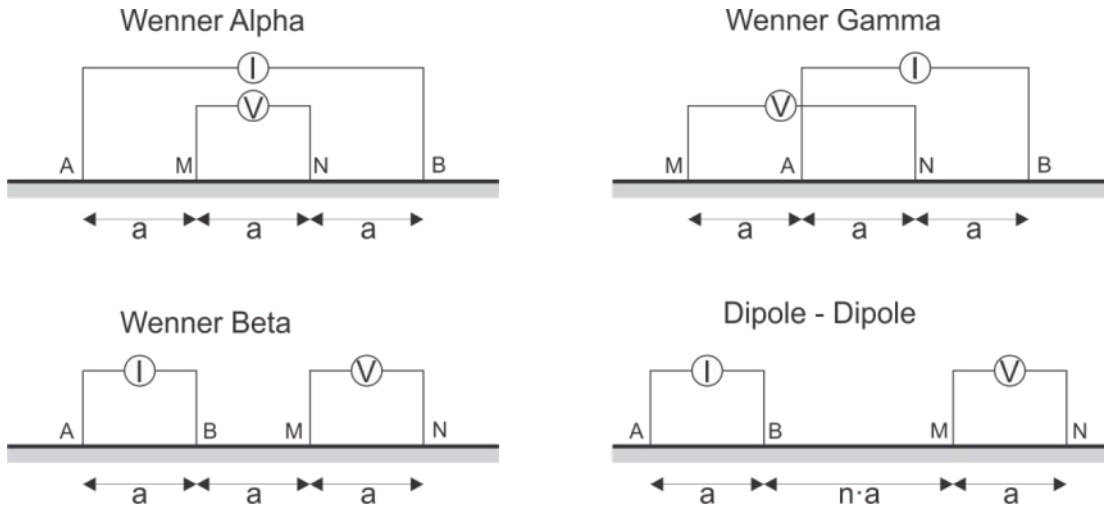

Figure 3-10 Sample electrode array placement and measurement points for ERT (after Keller and Frischknecht, 1996)

Measurements for the ERT are done so that a direct current I (Figure 3-10) is supplied via one pair of electrodes (electrodes A and B, placed in the subsurface zone) and a potential difference V (voltage drop) is measured at another pair of electrodes (electrodes M and N, also placed in the subsurface zone). Usually a large *even* number

of electrodes is placed, and electrodes are interchangeably used for supplying the current (only one pair at a time) and measurement of voltage drop (between pairs of remaining electrodes). For this purpose, a cable is placed from a High-Speed Data Acquisition System to all the electrodes, and so is formed an electrode array. Depending on the spacing of the electrodes, the measurement scale can go from a few centimetres to a few kilometres and can produce 2D or 3D images of the subsurface resistivity distribution. Also, depending on which pair of electrodes measures the voltage drop, the measurement point can be closer or further from the soil surface.

The raw measurements present an apparent resistivity (due to the heterogeneity of the subsurface) and need to be converted applying local boundary conditions to Poisson type equation (Garré et al., 2011) to get the calculated resistivity:

$$\nabla \cdot \left(EC_b \nabla \varphi \right) - \nabla \cdot j_s = 0 \tag{3.3}$$

Where EC_b is the bulk soil electrical conductivity ($\Omega^{-1}m^{-1}$), φ is the electric potential (V), and j_s is the source current density (Am^{-2}). Solving of the equation can be done using some of the state-of-the-art inversion algorithms e.g. error-weighted, smoothness constraint Occam type algorithm as per Garré et al. (2011).

3.4.3 Field setup

The two biofilter cells at Monash Carpark were equipped each with 30 metal rods, stabbed verticaly 5 cm in the subsurface at an equidistance of 30 cm. The electrodes were placed in the middle longitudinal cross section of the cell, as seen in Figure 3-11, and connected to the ABEM Terrameter LS device – a high speed data acquisition system for resistivity measurements (ABEM, 2012). ABEM Terrameter LS is supplied with a high power true current transmitter (output power 250 W; maximum output current 2.5 A; maximum output voltage ± 600 V), and a sensitive receiver that allows for high resolution data recording with 4, 8 or 12 galvanically separated channels (input impedance 200 MΩ, precision 0.1%), and is set to use a dipole – dipole electrode array (ABEM, 2012). ERT measurements were conducted in an experiment setting very similar to the first two events of the 2012 Challenge Test (see 0): with identical inflow dynamics of treated stormwater, from a nearby pond, with added fluorescein tracer. The rationale behind that was to obtain soil resistivity/moisture distribution throughout the

spiking test, but avoiding simultaneous experiments as ERT might induce electrolysis of micro-pollutants. Soil moisture probes were removed prior to the experiment, to avoid possible electrical damage. The tracer was used to serve as a reference between the two experiments (the same tracer was used for spiking tests as well).

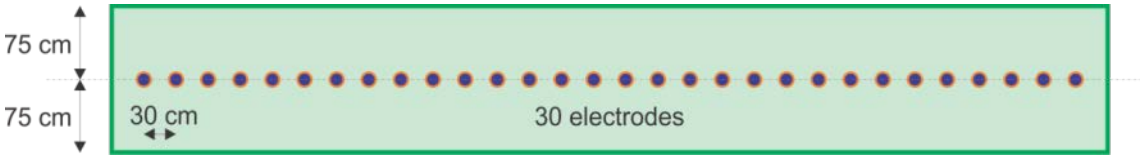

Figure 3-11 Electrode placement at the biofilter site - Monash Carpark

Prior to the actual experiment, the biofilter system was conditioned in a similar way as before the second challenge test: the system was saturated with 2.5 pore volumes of "clean" stormwater and left to freely drain for a period of two days. In that way, the starting saturation for the actual testing days was around 75% for Cell 1 and 55% for Cell 2. On the first testing day a total of 3 pore volumes was introduced in both cells with a constant average concentration of 112 μg/L of fluorescein (background concentration was 1.2 μg/L; concentration in deionized water was 0.3 μg/L). Ten hours following the end of the ponding phase of the first testing day, a second test was conducted: a total of 1.8 pore volumes were introduced in Cell 1 and 3 pore volumes in Cell 2 with an average fluorescein concentration of 119 μg/L. The water was dosed so that all the water was treated (nothing flowed over the security weir), which is the reason why Cell 1 only received 60% of the planned inflow water quantity.

Measurements included flow measurements at inflow and outflow pipes, depth of water at the ponding site, EC (Hach probe) and fluorescein concentration (AquaFluor Fluorometer) (see section 3.2.1. for details).

3.4.4 Results and Discussion

The inverted ERT data i.e. resistivity in Ohms, is shown in Figure 3-12 as a time lapse in a 10 minute increment for Cell 1 on 9/11/2012 and in Figure 3-13 for Cell 2 on 8/11/2012.

The resistivity fields in Figure 3-12 and Figure 3-13 show that it took Cell 1 around 20 minutes and Cell 2 around 50 minutes to become steady i.e. spatial heterogeneity of the

resistivity field, closely linked to the water saturation level, becomes “uniformly layered” at these times. This means that the change in resistivity (and, by assumption, the soil water content) becomes gradual in the vertical direction i.e. becomes one-dimensional.

It should be noted that the biofilters were not fully saturated prior to the test start and that inflow pattern was such that flows were very low (0.1 – 0.2 L/s). Even in these conditions 20 or 50 minutes is seen as a short period when compared to the total duration of the spiking tests (3 – 5 h). It is, therefore, safe to assume that the one-dimensional flow model can be used for spiking tests.

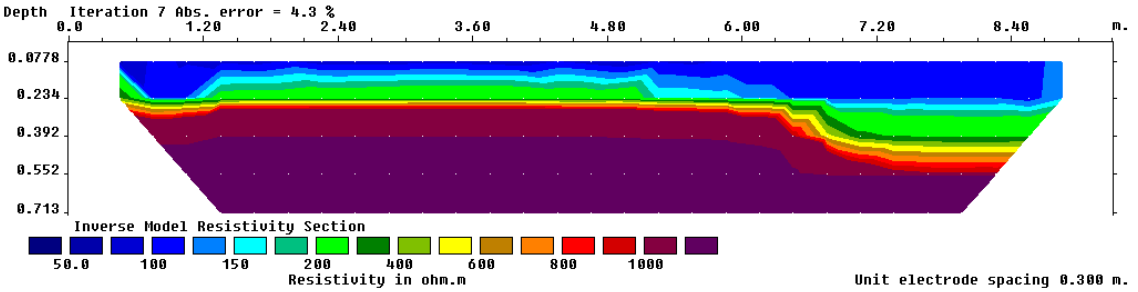

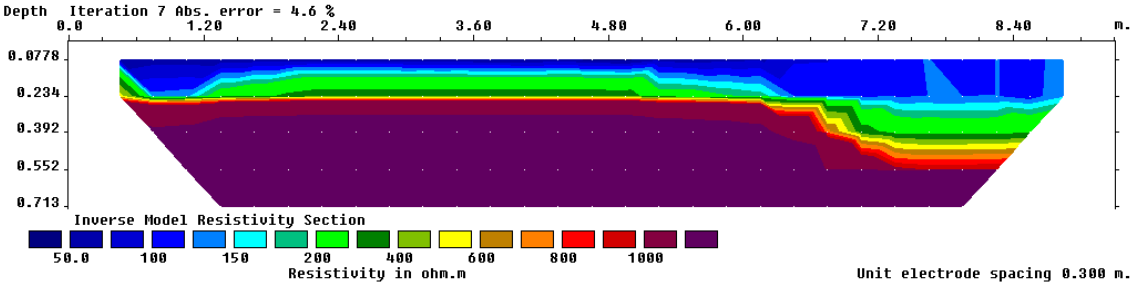

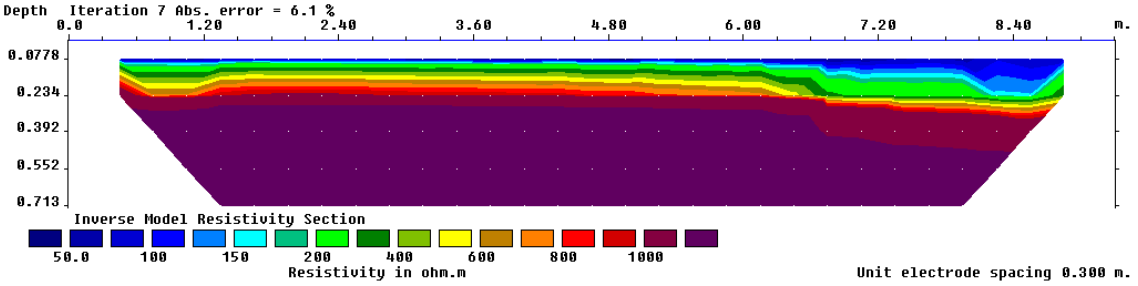

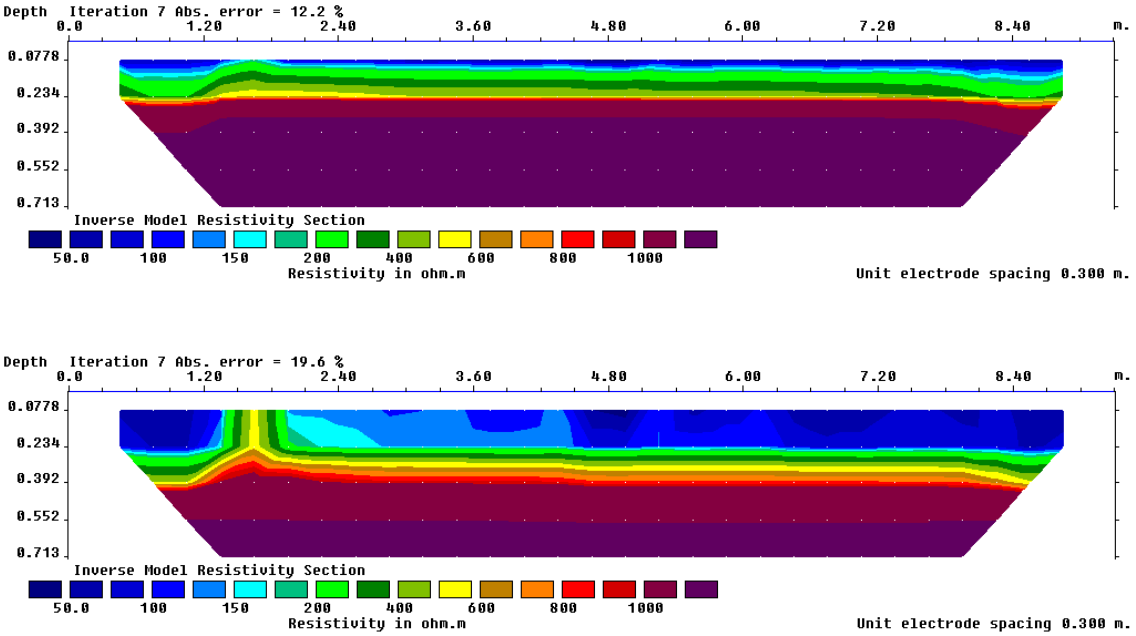

Figure 3-12 Time lapse of ERT inverted data for Cell 1 on 9/11/2012 (10 min inverval)

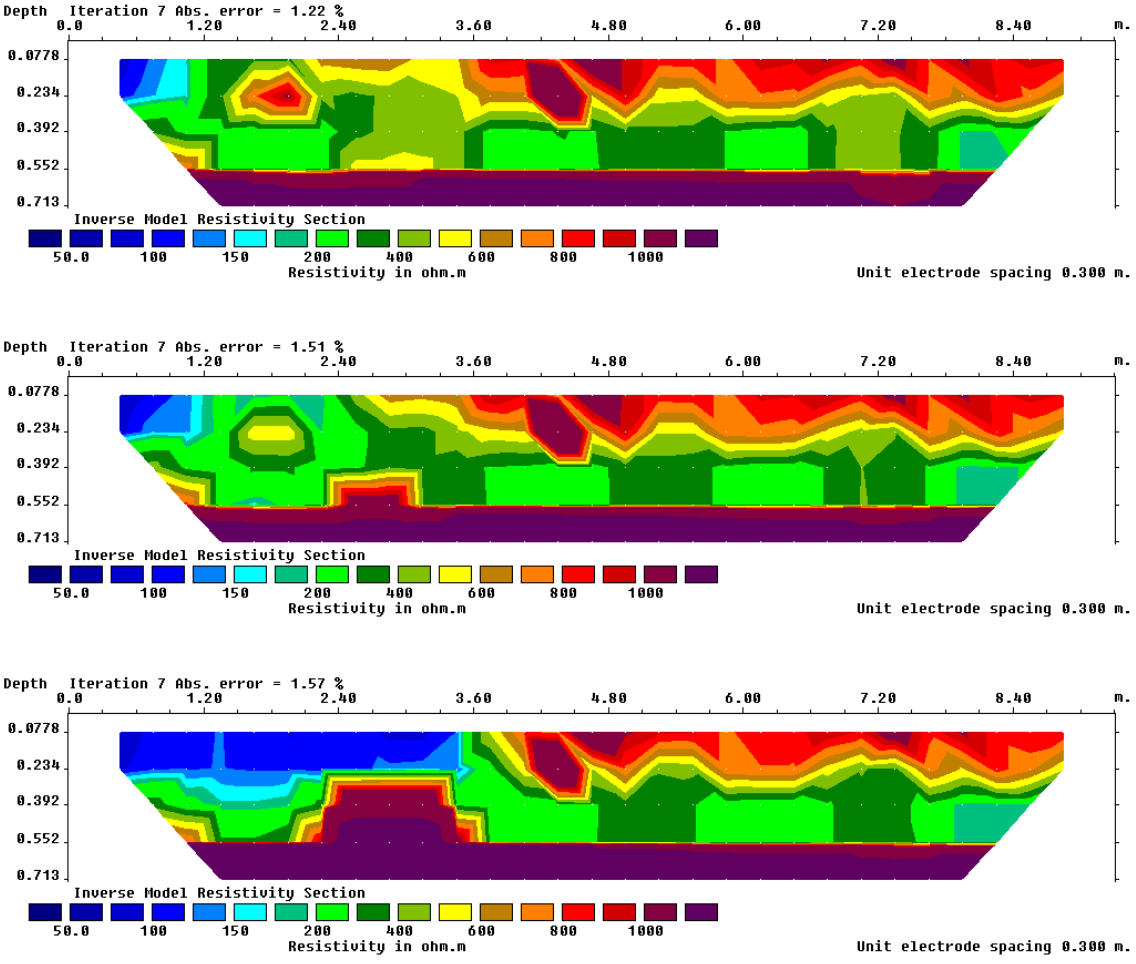

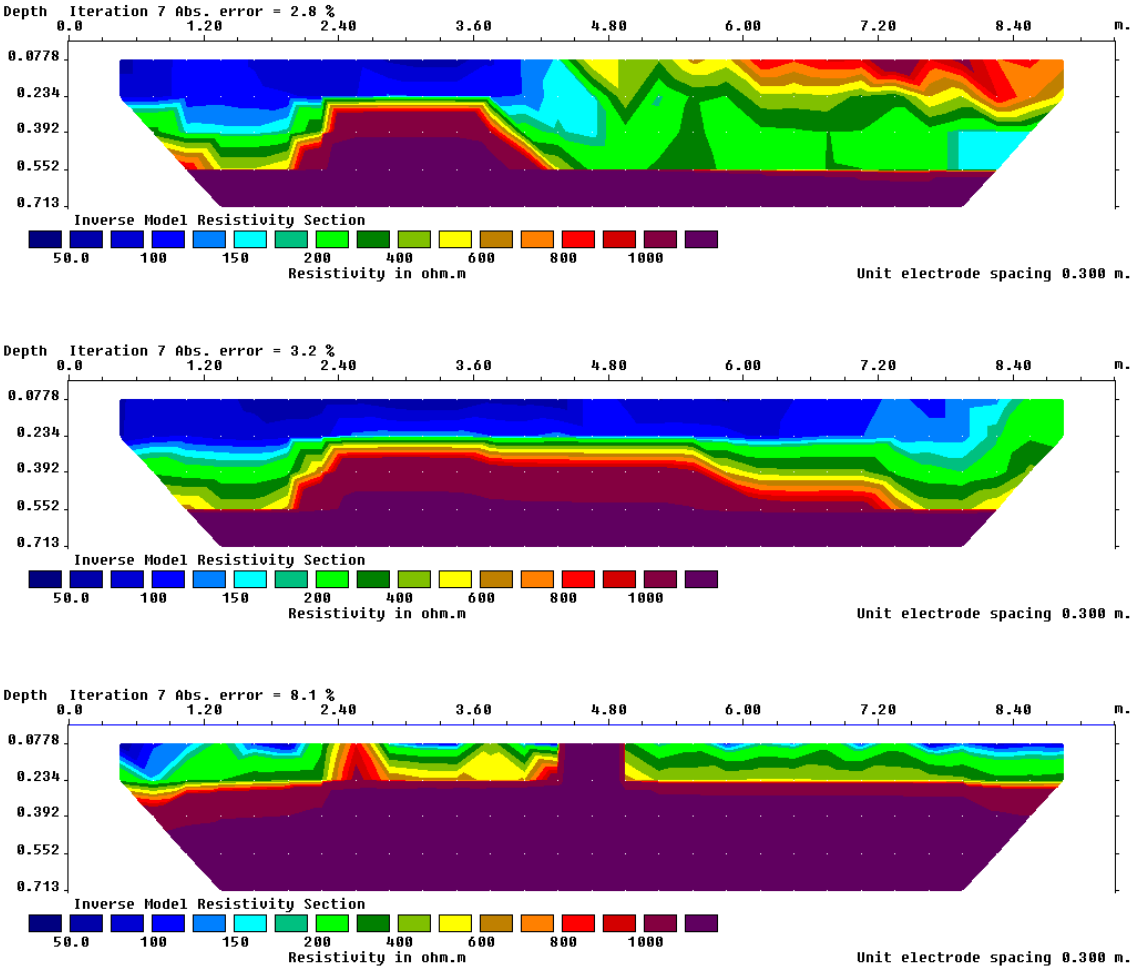

Figure 3-13 Time lapse of ERT inverted data for Cell 2 on 8/11/2012 (10 min inverval)

3.5 Field “spiking” testing

The field “spiking” tests (a.k.a. challenge tests) were carried out at the Monash Carpark biofiltration system described in detail in Chapter 3.2. The main aim of the tests was to provide sufficient data for model development, while at the same time allowing for the development of the validation framework (see Zhang, 2015). The tests were performed under challenging conditions: these included high target concentrations of micropollutants in the inflows, as well as extreme (the systems were run at their full infiltration capacity, but without any overflow) and highly variable operational conditions that biofilters could be exposed to (e.g. different drying/wetting regimes).

3.5.1 Experimental setup

A total of seven groups of micropollutants were selected to be checked in challenging conditions at Monash Carpark biofilter, as various studies report them to be present in stormwater (e.g. Cole et al., 1984; Makepeace et al., 1995; Duncan, 1999; Göbel et al., 2007; Zgheib et al., 2012) (For more details see Chapter 2.2.3). These include total petroleum hydrocarbons (TPHs), polycyclic aromatic hydrocarbons (PAHs), glyphosate, triazines (simazine, atrazine and prometryn), phthalates (dibutyl phthalate, di-(2-ethylhexyl) phthalate), trihalomethanes (THMs) and phenols (phenol, pentachlorophenol). Table 3-3 shows details regarding these micropollutants, with their classification according to groups, physico-chemical properties (solubility in water, K_{oc} – soil water partitioning coefficient normalized to organic carbon content, Henry's constant, pK_a – acid dissociation constant as logarithmic value, and half-life in soil), expected removal process in biofilters, and target concentration during tests. The target concentration was selected based on reported concentrations found in the literature. Event mean concentration (EMC) from each publication was considered where possible (measured values of single samples were not considered). In this way at least 15 EMC values were gathered for each micropollutant and the 95th percentile concentrations were calculated. The 95th percentile was adopted as the challenge concentration for consistency with the validation of pathogen removal in wastewater recycling schemes (DHV, 2013). Since some reports included very low micropollutant concentrations (that were far below the Australian Drinking Water Guideline (ADWG)), a value of twice the ADWG value was set as the target concentration (e.g. for naphthalene, glyphosate, DBP, chloroform). The idea behind the choice of target concentration values was to simulate operational conditions that may cause hazard to humans or other biota, and with full acknowledgment that stormwater data regarding micropollutants is scarce and usually does not include extreme conditions.

Regarding the operational conditions, literature review indicates the following are important (Zhang, 2015):

1) The total volume of water to be treated per event – e.g. Li et al. (2012) conclude that the residual water in the submerged zone and in soil voids affects the treatment performance;

2) Extreme wet conditions – e.g. Zhang et al. (2014) show that the occurrence of two or more large consecutive events within a short period can lead to breaking of the system function during the later events in which the system cannot provide reliable treatment;
3) Infiltration rate (velocity of water filtrating through soil media) – e.g. Chandrasena et al. (2012) show it is of little importance in the removal of nutrients, while Li et al. (2012) show high importance for pathogen removal;

Table 3-3 Summary of the micropollutants' physico-chemical properties, expected removal processes in biofiltration system, and target concentrations during tests

Pollutants		Physico-chemical properties[1)]					Expected removal processes in biofilter	target conc.[2)] [µg/L]
		Solubility [mg/L]	$logK_{OC}$	K_{Henry} [Pa m^3/mol]	pK_a	Half-lives in soil [d]		
TPHs		-[3)]	-	-	-	-	Volatilisation Adsorption	29.4 ml/L Diesel
PAHs	Pyrene	0.1	4.8	1.3	-	346	Adsorption,	100
	Naphthalene	28	3.2	54.9	-	36	Adsorption Biodegradation	140
Herb.	Glyphosate	12425	3.1	1.4×10^{-5}	0.8	47	Adsorption Biodegradation	2000
	Atrazine	38	2.1	3.9×10^{-4}	1.7	75		60
	Simazine	6	2.3	1.8×10^{-4}	1.7	77		60
	Prometryn	41	2.7	9.5×10^{-4}	4.1	60		60
Phthal.	DBP	10	2.9	0.2	-	16	Adsorption Biodegradation	70
	DEHP	15	5.1	0.8	-	65		50
THMs	Chloroform	8452	1.8	330.2	-	51	Adsorption Biodegradation Volatilisation	400
Phenols	PCP	19	3.2	0.1	4.9	48	Adsorption Biodegradation	60
	Phenol	83119	1.7	0.9	10.0	4.9		200

[1)]median values compiled from Mackay et al;

[2)]Equates to 95th percentile concentration (DEHP, PCP and phenol) or doubled ADWG values;

[3)]physico-chemical properties vary dramatically with different petroleum chemicals therefore not presented;

4) Duration of dry periods between successive storm events – longer dry periods decrease nitrogen removal (e.g. Hatt et al., 2008), while pathogen removal is decreased with very short dry periods (e.g. Chandrasena et al., 2012);

5) Temperature – an important variable that influences the rate of some of the processes in the biofilters (e.g. biodegradation, Blecken et al., 2010).

Operational conditions listed under (1), (2) and (4) were determined using data included in the MUSIC 5.1 software for modelling of urban stormwater systems using water sensitive urban design (eWater, 2012). The model was set up to simulate long term performance of the Monash Carpark biofilter – it included a highly urbanized (100% impervious) catchment with a surface area equal to the one of the Monash Car parking lot (4000m^2) that drains into the biofilter (characteristics of Cell 2, see Table 3-1). The model was run continuously for data between 1980 and 2010 (31 years of data, with 1980 being a model "warm-up" sequence). This included 6 minute rainfall data and measured monthly evaporation data for Melbourne. To determine the duration of the dry periods, a probability distribution function (log-normal) was applied to estimate the 95th percentile of the biofilter *inflows*. The inflow dataset was previously pre-processed and low inflow volumes were removed (i.e. everything below 1% of the maximum outflow-rate was discarded, as these events do not have the potential to saturate the biofilter, and to produce enough outflow to be measured). The challenging dry period length for Melbourne climate was found to be 21 days.

As for the wet weather events, two challenge scenarios were proposed: (1) the challenge volume of a single wet weather event and (2) the challenge volumes of two consecutive events, within 12 hours of each other. The two consecutive rainfall events with only 12 hours of dry period were seen as an extreme condition, since the system was not able to recover completely i.e. the system is saturated and barely drains before the second storm commences. The statistics were formulated on *outflows*, rather than on inflows, because: (i) many events were either too small (having no outflow) or too large (leading to overflow), and are seen as outliers in terms of this analysis; and (ii) treated water is more important in terms of stormwater harvesting, therefore to be on the safe side, the use of outflows for estimations was favoured. Again, 1% of the maximum outflow-rate of the system was used as a cut-off to determine when outflow begins or ends. This cut-off value was determined with reference to experience from previous biofilter field tests (maximum measurable flow). For the first case, the 95th percentile cumulative volume for a single event was 4 pore volumes (PV where a PV roughly equals to 3.5 m^3 for

each biofilter). For the second scenario, the 95th percentile of two consecutive events that occur less than 12 hours apart was 3 PVs for each event (3 PVs, followed by 12 hours of dry period, and another 3 PVs). These events correspond to 2nd test series in Table 3-4.

Another sequence of events was also tried as part of the challenge with more natural and higher probability events. These are 85th percentile single event outflow water volumes, and 40th, 90th, and 80th percentile dry period durations. This second series of events were selected arbitrary and corresponds to the 1st test series in Table 3-4.

The infiltration rate (4) is a biofilter intrinsic property that can change with age (Hatt et al., 2007), and is not a plausible parameter to change during a challenge test. Because of that, the challenge test was done on two biofiltration units that have different infiltration rates (different filter media and plant content).

Although the analysis was done to determine (5) the challenging temperature, it was not possible to control this feature during the actual field testing. Using 30 years of minimum and maximum daily temperature data from Bureau of Meteorology (BOM) (station No. 86232 in Melbourne) cumulative distribution curves were created and extreme values (5th percentiles of the minimum daily data as well the 95th percentiles of the maximum daily data) were determined to be 5°C / 33°C. The 5th / 95th percentile is selected since it is usually acquired as the cut off in other validation procedures (DHV, 2013).

3.5.2 Challenge tests characteristics

Two series of *in-situ* experiments were conducted, each consisting of three separate challenge tests (i.e. six challenge tests in total). These challenge tests covered different operational conditions, ranging from the above selected challenge scenario conditions to more typical operational conditions (Table 3-4).

The 1st series of challenge tests (TESTS 1-3) was conducted during the winter of 2011, whereas the 2nd series (TESTS 4-6) was performed during the summer 2012. Between TEST 1 and TEST 2 and after TEST 6, the biofilters received two natural stormwater events (Table 3-4).

Table 3-4 Detailed information of challenge tests

		Date	Inflow volume [m^3] /percentile[1)]	Preceding dry periods [h] /percentile[1)]	Daily Air Temperature
1^{st} series	TEST 1	16-08-2011	8.4 (2.4PVs) /85^{th}	84/40^{th}	10.9-19.2
	TEST 2	31-08-2011	8.4 (2.4PVs) /85^{th}	352/90^{th}	8.2-15.2
	Natural events	-[2)]	17.3 (5 PVs)	-	-
	TEST 3	22-09-2011	8.4 (2.4PVs) /85^{th}	240/80^{th}	11.5-22.9
2^{nd} series	TEST 4	19-11-2012	10.5 (3PVs) /95^{th}	66/30^{th}	6.8-23.6
	TEST 5	20-11-2012	Cell 1: 6.3 (1.8 PVs)/80^{th} Cell 2: 10.5 (3PVs) /95^{th}	10/<1^{st} [3)]	8.6-27.4
	TEST 6	11-12-2012	14 (4PVs) /95^{th}	496/95^{th}	9.0-27.3
	Natural Event 1[4)]	15-12-2012	2.1 (0.60PV)	89	18.6-23.1
	Natural Event 2[4)]	19-12-2012	2.2 (0.63PV)	84	16.2-30.8

[1)] Corresponding percentile value of 30-year rainfall statistic using MUSIC.

[2)] 3 rainfall events observed on 09-09-2011 (10.6mm), 10-09-2011 (3.11mm) and 11-09-2011 (4.2mm) but no samples were taken during this period.

[3)] <1st percentile of dry periods, extreme wet condition; [4)] 3.2mm rainfall observed on 15-12-2012 and 4.8mm on 19-12-2012.

Semi-synthetic stormwater (water quality is shown in Table 3-5) was prepared in the distribution tank (net volume of 4.2 m^3) using water from an adjacent stormwater pond. The stormwater sediment (from a local wetland inlet basin), raw sewage (from a local wastewater treatment plant – Pakenham), commercial diesel fuel (from a local fuel station; according to the Australian *Fuel Standard (Automotive diesel) determination 2001* contains a maximum of 11% m/m PAHs) and selected micropollutants (from Sigma-Aldrich) were added and then well mixed manually to attain the target concentrations (Table 3-3). As most of the micropollutants were in solid state (powder), special preparation was done before the actual experiment: concentrated solutions of micropollutants were prepared using deionized water in special glass vials that were added directly into the distribution tank. This was done to assure the homogeneity of the mixture.

During each test, in order to simulate challenge infiltration rates and make the biofilters work under full capacity, attempts were made to control the ponding depth of each biofilter to a stable level of 470±10mm from the surface of the biofilter (which was

close to the overflow weirs). In the outlet, outflow rates were recorded by using v-notch weirs equipped with ultrasonic depth sensors (Siemens Milltronics), which were calibrated using manual flow measurements before and during the tests.

Table 3-5 Water quality of the semi-synthetic stormwater in the challenge tests

Parameters		T (°C)	pH	EC (µs/cm)	TSS (mg/L)	TP (mg/L)
Mean value± STD (n=3-9)	1st series	19.2±1.2	7.4±0.1	419.9±6.1	52.7±11.0	0.88±0.02
	2nd series	10.2±1.6	7.3±0.2	NA[1)]	70.0±11.9	1.1±0.1
Parameters		TN (mg/L)	NH_3 (mg/L)	NO_X (mg/L)	DOC (mg/L)	UVA
Mean value ± STD (n=3-9)	1st series	2.7±0.1	0.29±0.09	0.12±0.03	19.7±1.1	0.551±0.09
	2nd series	3.1±0.5	NA	NA	NA	NA

[1)] NA: Not analysed

3.5.3 Sampling and analysis

In the 1st series of challenge tests, a flow-weighted composite sample of the inflow water was collected, while during the 2nd series, three composite inflow samples (each consisting of three discrete samples) were collected during the course of each event. In addition, 10 discrete outflow samples were taken over the course of the test from each cell in both series. During the natural events of the 2nd Series (after Test 6), natural stormwater grab samples were taken from the distribution tank; outflow samples were collected using autosamplers (Sigma 900). The autosamplers were triggered by flow measurements (cumulative volumes), so samples were taken as flow-weighted discrete samples. This sampling was completed after two rainfall events, after which time the micropollutant concentrations returned to below reporting limits in both the inflow and outflow samples.

To obtain an estimate of the 'overall' effluent quality for an entire event, the pollutant concentrations from 10 discrete samples were used alongside flow measurements to calculate the Event Mean outflow Concentration (EMC).

The samples were distributed in multiple plastic, transparent and colored flasks to prevent any type of degradation. The samples were stored on ice until they were delivered to a NATA accredited laboratory for analysis (see Chapter 3.2.1). It should be noted that in cases where the concentrations were lower than the detectable limits, half

of the lowest detectable limit was taken as the concentration for determination of EMC and mass balances.

Soil samples were taken during the 2nd test series only. Table 3-6 shows the soil sampling date and time, and the soil sample type: surface (5 cm) or deep (15 cm).

Table 3-6 The soil sampling sequence and sample type

sample type	Surface	Deep	Surface	Deep	Surface	Deep
date	Nov. 19th		Nov. 20th		Nov. 22th	
time	11:00 AM		7:00 AM		3:30 PM	
sample type	Surface	Deep	Surface			
date	Nov. 26th		Dec. 3rd			
time	10:50 AM		3:30 PM			
sample type	Surface	Surface	Deep			
date	Dec. 11th		Dec. 11th			
time	6:00 AM		4:30 PM			
sample type	Surface	Deep	Surface			
date	Dec. 13th		Dec. 17th			
time	2:20 PM		11:00 AM			

3.5.4 Challenge test: Results and Discussion

3.5.4.1 Hydraulic Performance

A water balance (including measured inflow and outflow volumes, estimated storage change and evaporation and vegetation-uptake) was produced for each biofilter over each series of challenge tests (see Table 3-7). The estimated errors of the water balance were between 2.3-5.9% of the total inflows, with higher errors estimated for cell 1 (loamy sand).

Figure 3-14 presents the inflow and outflow rates measured during the 1st and the 2nd test series of the spiking tests. Cell 1 shows a significant decrease in the infiltration rate during Test 5, and it was not able to treat the entire targeted volume (it treated only 6.3 m^3 instead of 10.5 m^3) in the selected timeframe without overspills. The reduction in the hydraulic rate is linked to a prolonged wetting period (there were only 10 hours between Tests 4 and 5) which might have caused soil swelling due to high clay content

(Dif and Bluemel, 1991). The 1st test series does not hold similar behaviour of Cell 1, as the wetting conditions were not as challenging (e.g. the minimum dry period was 84h, meaning that the system had time to recover before the subsequent wet weather period). On the other hand, Cell 2, designed according to the FAWB guidelines, had a consistent hydraulic rate during all of the tests (under varying conditions).

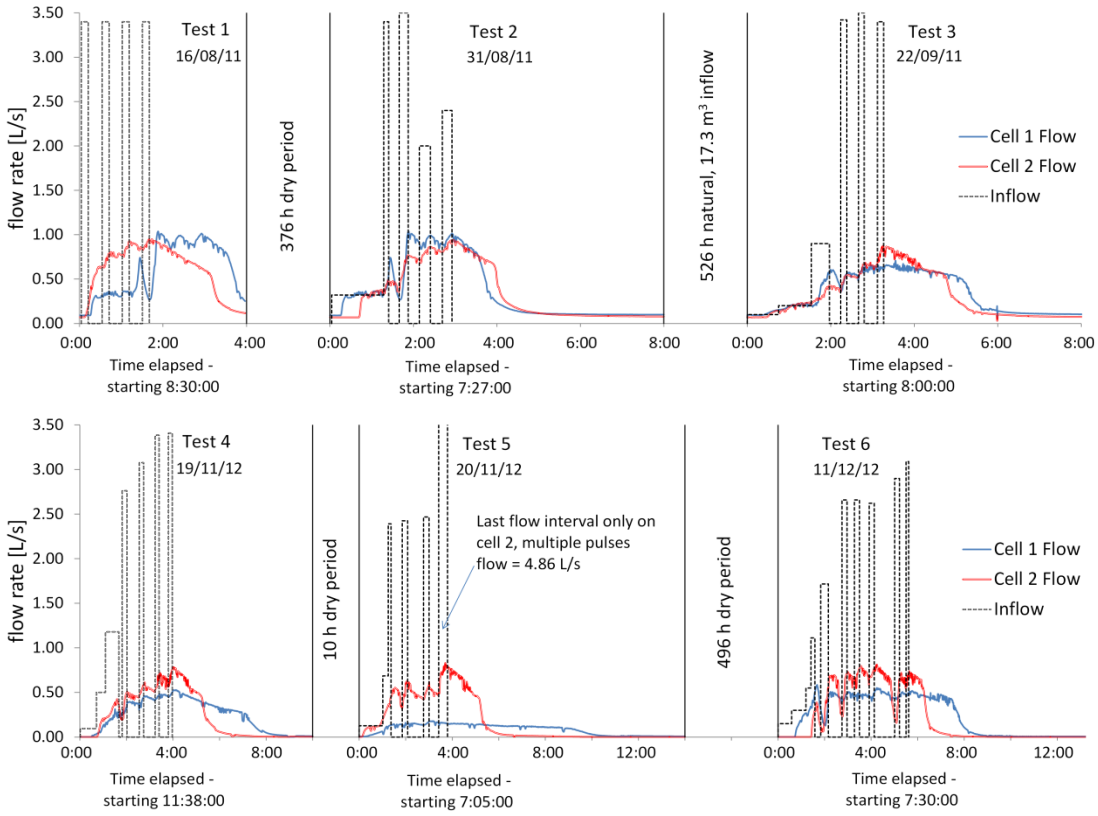

Figure 3-14 Inflow and outflow rates measured during the 1st (top) and the 2nd (bottom) test series

3.5.4.2 Treatment Performance

Table 3-8 presents the results of the measured inflow concentrations and outflow Event Mean Concentrations (EMCs), while Table 3-9 shows calculated mass balances of the tested micropollutants for the two series of challenge tests. The attempt is made to estimate uncertainties in the mass balance as follows:

- 1st Test series – by assuming that the pollutant mass balance error equals the water balance error:

$$\begin{matrix}\text{uncertainty}\\ \text{in the mass balance}\end{matrix} = \begin{matrix}\text{pollutant mass}\\ \text{reduction}\end{matrix} \times \begin{matrix}\text{water balance}\\ \text{error}\end{matrix}$$

- 2nd Test series – by using TDS as a measure of mass balance uncertainty, assuming it is a conservative quantity:

$$\text{uncertainty in the mass balance} = \text{pollutant mass reduction} \times \text{TDS balance error}$$

Table 3-7 The water balance of the two test series of challenge tests: Unit m^3

	Cell	Test	Inflow	Outflow	change in storage [1)]	Evaporation & plants uptake during dry periods [2)]	Total error[3)]	Water balance error (% of total inflow)
1st Series	1	Test 1	8.4	7.5	0.315	1.43		
		Test 2	8.4	8.1				
		Natural Events	11.6	10.5				
		Test 3	8.4	8.1				
		Subtotal	36.8	34.2	0.315	1.43	**1.49**	4.0%
	2	Test 1	8.4	7.5	0.14	1.6		
		Test 2	8.4	8.1				
		Natural Events	11.6	10.8				
		Test 3	8.4	8.1				
		Subtotal	36.8	34.5	0.14	1.6	**0.84**	2.3%
2nd series	1	Test 4	10.5	9.5	0.26	1.29		
		Test 5	6.3	5.4				
		Test 6	14	13.1				
		Natural Event	2.1	1.9				
		Natural Event	1.9	1.8				
		Subtotal	34.8	31.7	0.26	1.29	**2.07**	5.9%
	2	Test 4	10.5	9.6	0.115	2.2		
		Test 5	10.5	9.8				
		Test 6	14	13.1				
		Natural Event	2.1	1.8				
		Natural Event	1.9	1.7				
		Subtotal	39.0	36.0	0.115	2.2	**0.92**	2.3%

[1)] Estimated by calculating the change of soil moisture before and after that series of tests;

[2)] Estimated by calculating the change of soil moisture during dry days;

[3)] Inflow – outflow + change in storage - evaporation & plants uptake: if there is no error, should be equal to zero

The micropollutants were generally classified according to the removal efficiencies:

- excellent removal (removal>80%) e.g. TPHs, glyphosate, DBP, DEHP, pyrene and naphthalene;
- good removal (50% < removal < 80%) e.g. phenol and PCP in Cell 2);
- intermediate removal (20% <removal<50%) e.g. Chloroform
- and poor removal (removal<20%) e.g. atrazine and simazine in Cell 2.

Generally, the removal performance of biofilters in the 1st series tests was better than that in the 2nd series, especially for triazines (that can be grouped into intermediate category in the 1st series), a fact mainly due to the more challenging conditions conducted in the 2nd series. Also, it can be noted that the removal performance is higher or equal in Cell 1 than the removal in Cell 2. This is hypothesized to be due to the higher soil organic matter content of Cell 1: 4.6% compared to 0.4%.

The removal of pollutants is significantly influenced by adsorption. Soil organic matter (SOM) content is particularly important for adsorption of organic compounds, such as micropollutants used in this study, since most of them are dominated by apolar groups: aliphatic and/or aromatic. This fact is used to calculate the *theoretical maximum* of micropollutant mass that can adsorb prior to the breakthrough:

$$\textit{theoretical maximum adsorbed mass} = K_{oc} \cdot f_{oc} \cdot c_{inflow} \cdot M_{soil} \qquad (3.4)$$

Where SOM value is the organic carbon content, f_{oc}; K_{oc} is the soil-water partitioning coefficient (Table 3-3); c_{in} is the micropollutant inflow concentration; and M_{soil} is the total mass of soil in a biofilter cell.

TPHs, pyrene and phthalates (DEHP and DBP) were bellow detection limits for all outflow samples (see TPHs are a mixture of petroleum-based chemicals, some of which volatilize quickly (e.g. benzene K_{Henry}= 500 Pa·m^3/mol) while several others attach to the soil easily (e.g. benzo(a)pyrene logK_{oc}=6.1). Pyrene and DEHP have a high K_{oc} value (log K_{oc} > 4), meaning they also have a strong tendency to adsorb. The mass reduction of pyrene, DEHP and DBP was lower than the maximum adsorption mass, indicating that the biofilters still have a capacity to absorb more of these micro-pollutants. For the adsorbed micropollutants, other removal processes (e.g.

biodegradation) may also be occurring during dry periods, allowing the regeneration of adsorption sites. Zhao et al. (2004) reported that adsorption and biodegradation influenced the removal of DBP in a vertical flow constructed wetland. Naphthalene was also well removed: it has a moderate adsorption tendency ($logK_{oc}$=2.74) and is prone to biodegradation in soils ($T_{1/2}$=36d).

Glyphosate showed good removal (>80% in all tests) by biofilters. Glyphosate attaches to soil readily ($logK_{oc}$=3.1) and the mass reduction was lower than predicted by K_{oc} values. Glyphosate is also possibly degraded by soil microorganisms with a half-live averaging on 47d.

Biofilter cells were not so successful in removing triazines (especially Cell 2). This was attributed to their moderate tendency to adsorb ($logK_{oc}$=2.1-2.7), and low biodegradation rate ie. quite slow and variable, with half-lives in different soils varying from weeks to a year (Mackay et al., 2006). Although biodegradation is highly unlikely to occur during the biofilter's residence time (around 3h), there is a possibility for it to happen during dry periods (EMCs lower after prolonged dry periods).

Chloroform was removed between 26.9 and 61.5%: it has a low biodegradation rate ($T_{1/2}$>50d) and is weakly adsorbed to soil (log K_{oc}=1.8), however it is quite volatile (K_{Henry} =330.2 $Pa \cdot m^3/mol$), which may have contributed to its removal.

PCP has good removal in both biofiltration cells: it sorbs well (log K_{oc}=3.2), but has a low biodegradation rate ($T_{1/2}$=49d). EMC values of PCP in Cell 2 during Test 5 and Test 6 were much higher than that in Test 4. It is hypothesized that this could be because the adsorption sites were limited in this sandy media and these were mostly occupied during Test 4, leaving fewer sites for adsorption to occur during Test 5 and Test 6.

Cell 1 showed better removal (>80%) of phenols as compared with Cell 2 (50-80%). Phenol is very mobile in soil systems (log K_{oc} =1.7) and biodegrades quickly ($T_{1/2}$=4.9d). However, phenol outflow concentrations peaked during Test 6. It is hypothesized that the peak is caused by short-circuiting through cracks formed in the filter media after prolonged dry period (and pollutants high mobility).

Table 3-8 Measured inflow concentrations and outflow event mean concentrations (EMCs) for micropollutants during the two challenge tests

	Measured concentrations						
	Inflow±STD	Outflow EMC (µg/L)					
	(µg/L)	Cell 1			Cell 2		
1st series tests		T1.1	T1.2	T1.3	T2.1	T2.2	T2.3
TPHs	12700±707	<100	<100	<100	<100	<100	<100
Glyphosate	1950±353	NA	54	100	NA	41	105
Atrazine	55±13	14	34	17	32	65	23
Simazine	47±6	3	11	6	7	25	7
Prometryn	53±4	4	9	2	13	26	5
DBP	33±5	<1	<1	<1	<1	<1	<1
DEHP	24±10	<1	<1	<1	<1	<1	<1
Chloroform	43±15	9	24	19	15	49	28
2nd series tests		T1.4	T1.5	T1.6	T2.4	T2.5	T2.6
TDS [ppm]	214	210	210	212	210	210	214
TPHs	4300±220	<100	<100	<100	<100	<100	<100
Pyrene	10±2.6	<1	<1	<1	<1	<1	<1
Naphthalene	17±6.6	2	2	2	3	1	3
Glyphosate	1600±100	99	116	187	29	106	70
Atrazine	48±6	25	28	27	35	42	49
Simazine	42±3	22	32	24	33	49	43
Prometryn	50±4	11	14	15	20	29	32
DBP	42±4	<1	<1	<1	<1	<1	<1
DEHP	17±8	<1	<1	<1	<1	<1	<1
Chloroform	59±7	32	38	40	40	47	49
PCP	27±6	1	6	4	2	19	11
Phenol	203±15	2	1	18	1	3	106

Legend for Table 3-9:

[1)] Uncertainties in mass reduction = pollutant mass reduction x water balance error (1st test series) and = pollutant mass reduction x TDS balance error (2nd test series), percentage removal in parentheses;

[2)] Max adsorption: theoretical maximum mass of micropollutants that can be adsorbed onto the organic carbon of biofilter soils before breakthrough (equals to $K_{OC}*f_{OC}*C_{inflow}$*Mass of soil);

Table 3-9 Calculated mass balances for micropollutants during the two challenge tests

Calculated mass balances								
	Cell 1				Cell 2			
1st series tests	In	Out	Reduction[1)]	Max Ad.[2)]	In	Out	Reduction[1)]	Max Ad.[2)]
TPHs	324.7	1.2	323.5±12.9 (99.6%)	-	324.7	1.2	323.5±19.1 (99.6%)	-
Glyphosate	32.8	1.3	31.5±1.3 (96.0%)	1168.7	32.8	1.2	31.5±1.9 (96.0%)	144.1
Atrazine	1.76	0.52	1.24±0.05 (70.5%)	3.3	1.76	0.95	1.24±0.05 (70.5%)	0.4
Simazine	0.94	0.16	0.78±0.03 (80.3%)	4.5	0.94	0.31	0.78±0.04 (83.0%)	0.6
Prometryn	1.02	0.12	0.90±0.04 (88.2%)	12.6	1.02	0.35	0.90±0.04 (88.2%)	1.6
DBP	0.45	0.01	0.44±0.02 (97.8%)	12.5	0.45	0.01	0.44±0.03 (97.2%)	1.5
DEHP	0.6	0.01	0.59±0.02 (98.3)	1438.4	0.6	0.01	0.59±0.03 (98.3%)	177.3
Chloroform	1.09	0.42	0.67±0.03 (61.5%)	1.3	1.09	0.74	0.67±0.02 (61.5%)	0.2
2nd series tests	In	Out	Reduction[1)]	Max Ad.[2)]	In	Out	Reduction[1)]	Max Ad.[2)]
TDS [ppm]	7441.9	6744.4	697.5 (9.4%)	-	8336	7630.3	705.7 (8.5%)	-
TPHs	148.3	1.6	146.7±13.8 (98.9%)	-	160.9	1.8	159.1±13.5 (98.9%)	-
Pyrene	0.3	0.02	0.28±0.03 (93.3%)	300.4	0.33	0.02	0.31±0.03 (93.9%)	37
Naphthalene	0.56	0.06	0.50±0.05 (89.3%)	12.8	0.62	0.08	0.54±0.05 (87.1%)	1.6
Glyphosate	47.5	4	43.5±4.1 (91.6%)	958.9	54.2	2.2	52.0±4.4 (95.9%)	118.2
Atrazine	1.45	0.77	0.68±0.06 (46.9%)	2.9	1.67	1.44	0.23±0.02 (13.8%)	0.4
Simazine	1.3	0.72	0.58±0.05 (44.6%)	4	1.49	1.4	0.09±0.01 (6.0%)	0.5
Prometryn	1.39	0.4	0.99±0.09 (71.2%)	11.9	1.6	0.94	0.66±0.06 (41.3%)	1.5
DBP	1.28	0.02	1.26±0.12 (98.4%)	15.9	1.45	0.02	1.43±0.12 (98.6%)	2
DEHP	0.58	0.02	0.56±0.05 (96.6%)	1018.8	0.63	0.02	0.61±0.05 (96.8%)	125.6
Chloroform	1.85	1.1	0.75±0.07 (40.5%)	1.8	2.08	1.52	0.56±0.05 (26.9%)	0.2
PCP	0.8	0.1	0.70±0.07 (87.5%)	20.4	0.94	0.36	0.58±0.05 (61.7%)	2.5
Phenol	6.1	0.65	5.45±0.51 (89.3%)	4.8	7.02	1.53	5.86±0.50 (78.2%)	0.6

3.5.4.3 Intra-event variability

Figure 3-16 – Figure 3-18 show how the concentrations of selected micropollutants vary over the duration of the challenge tests. Micropollutants were well removed at the very beginning of the series. The outflow concentrations increased over the duration of each test, and then dropped towards the end. This drop is probably due to low infiltration rates through the biofilter (after inflows stopped, the hydraulic head decreases), resulting in longer residence times (2-4 hours longer) and therefore better removal (due to adsorption).

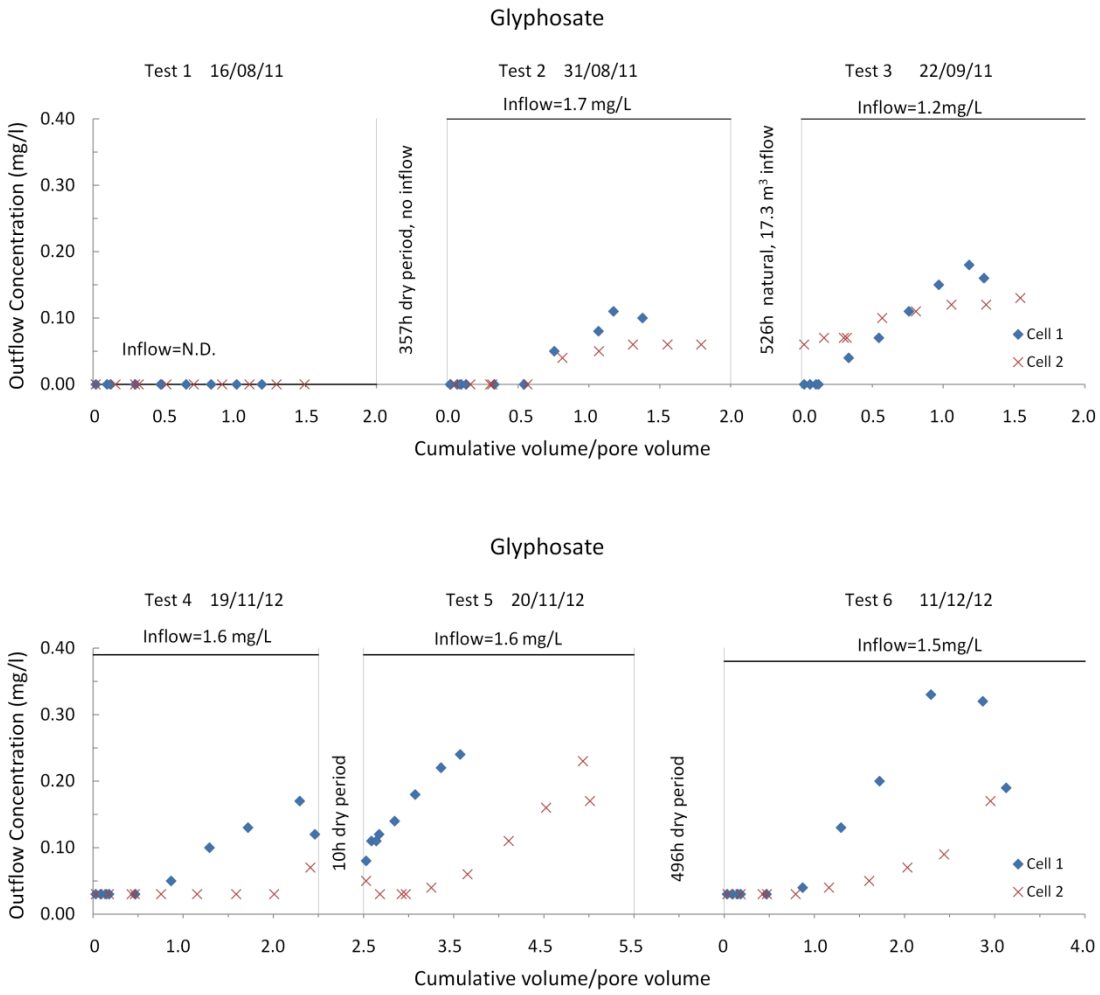

Figure 3-15 Pollutographs of glyphosate during 1st test series (top) and 2nd test series (bottom) for Cell 1 and Cell 2

The starting outflow concentrations of Tests 2 and 3 were lower than ending concentrations of Test 1 for all pollutants. This indicates that micropollutant biodegradation occurred between these events. The starting outflow concentrations of

Test 5 were within the range of the finishing concentrations of Test 4 for the majority of micropollutants. This suggests that micropollutants were retained in the biofilters during Test 4 and no significant degradation occurred during the short dry period of 10h before the start of Test 5. As a result, Cell 2 showed a net production of simazine (i.e. outflow concentrations > inflow concentrations) recorded during Test 5 and Test 6 (the so called "production" can be seen with chloroform in Tests 2 and 3, atrazine and prometryn in Tests 5 and 6).

Figure 3-19 and Figure 3-20 show pollutographs for naphthalene, PCP and phenol (detected in the outflow only during the 2nd test series).

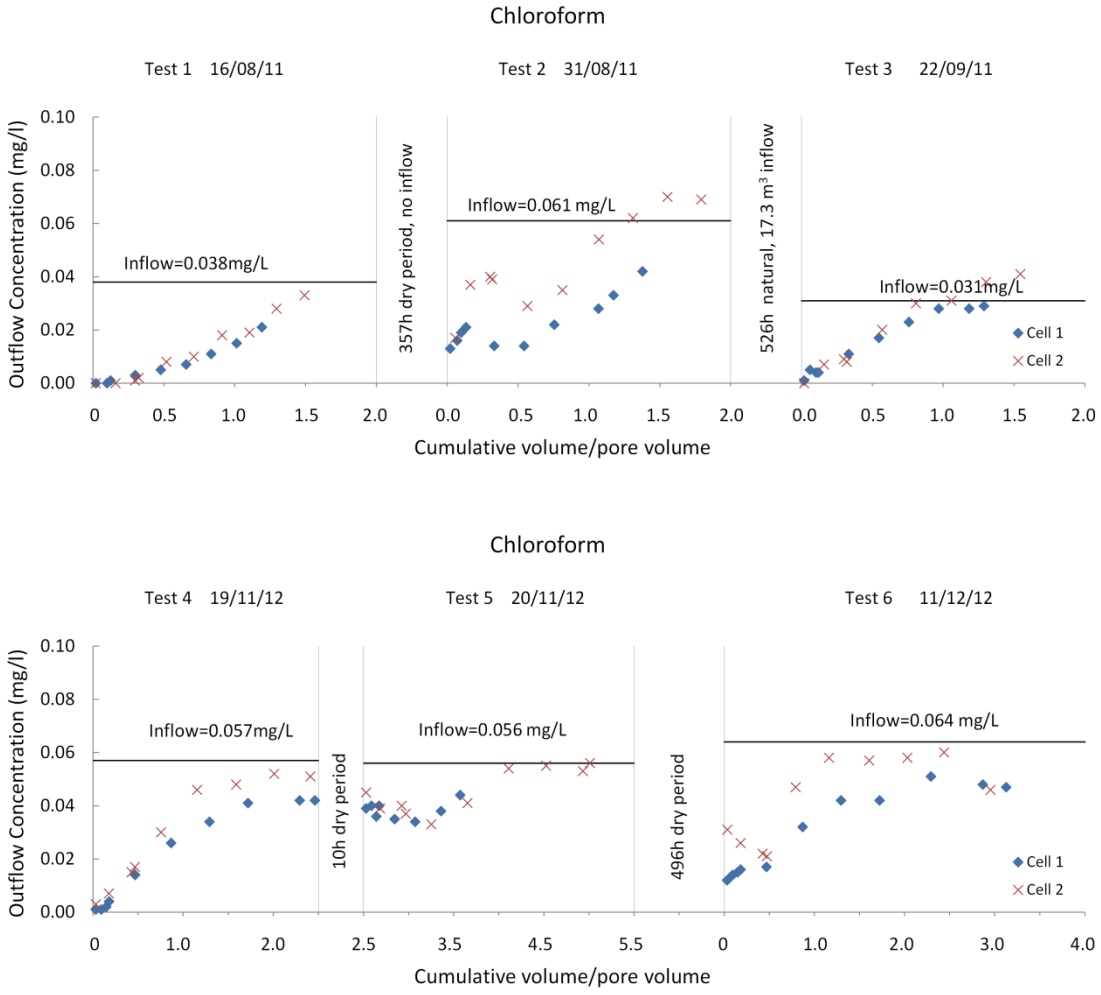

Figure 3-16 Pollutographs of chloroform during 1st test series (top) and 2nd test series (bottom) for Cell 1 and Cell 2

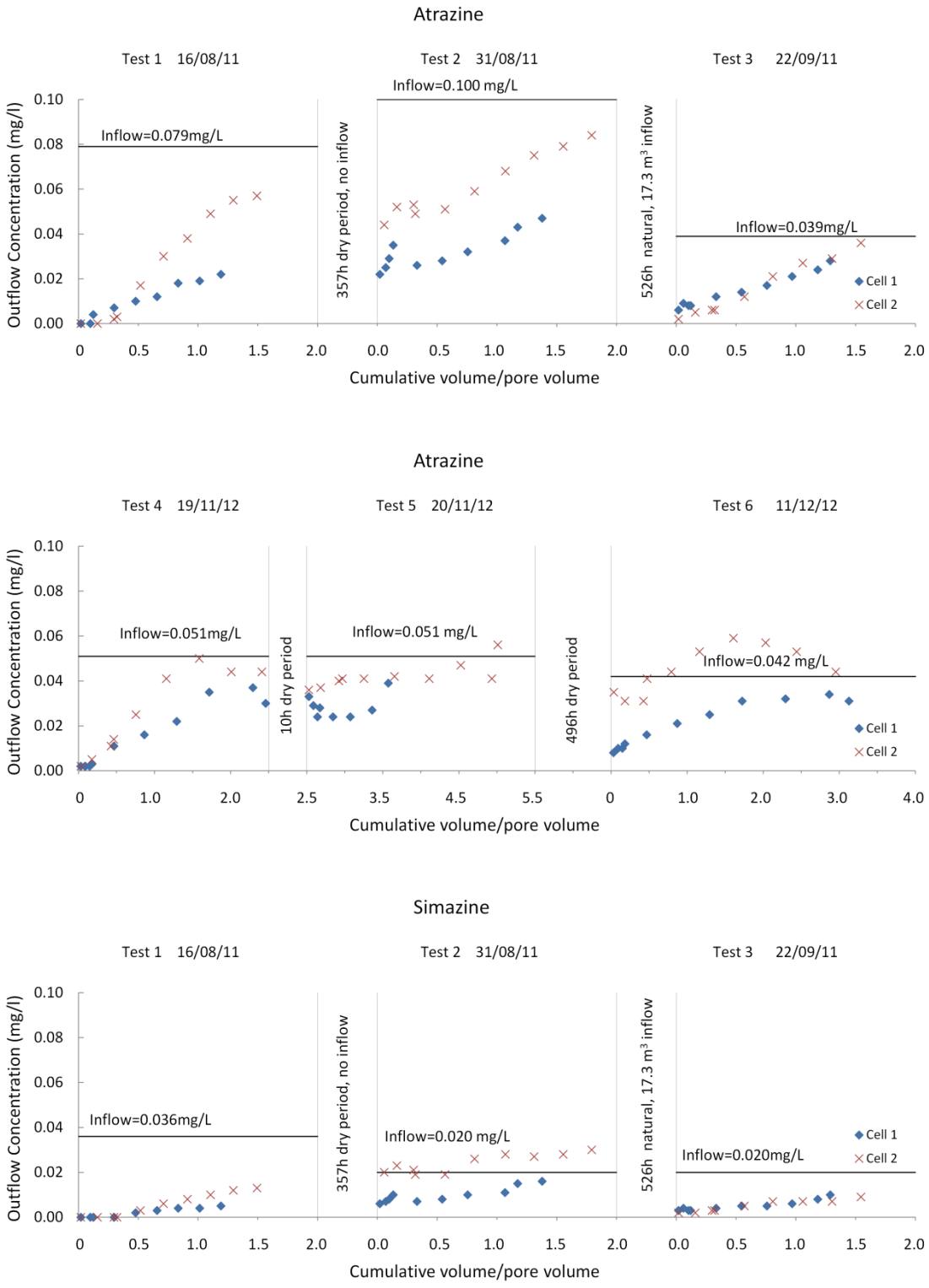

Figure 3-17 Pollutographs of atrazine during 1st test series (top) and 2nd test series (middle) and of simazine during 1st test series (bottom) for Cell 1 and Cell 2

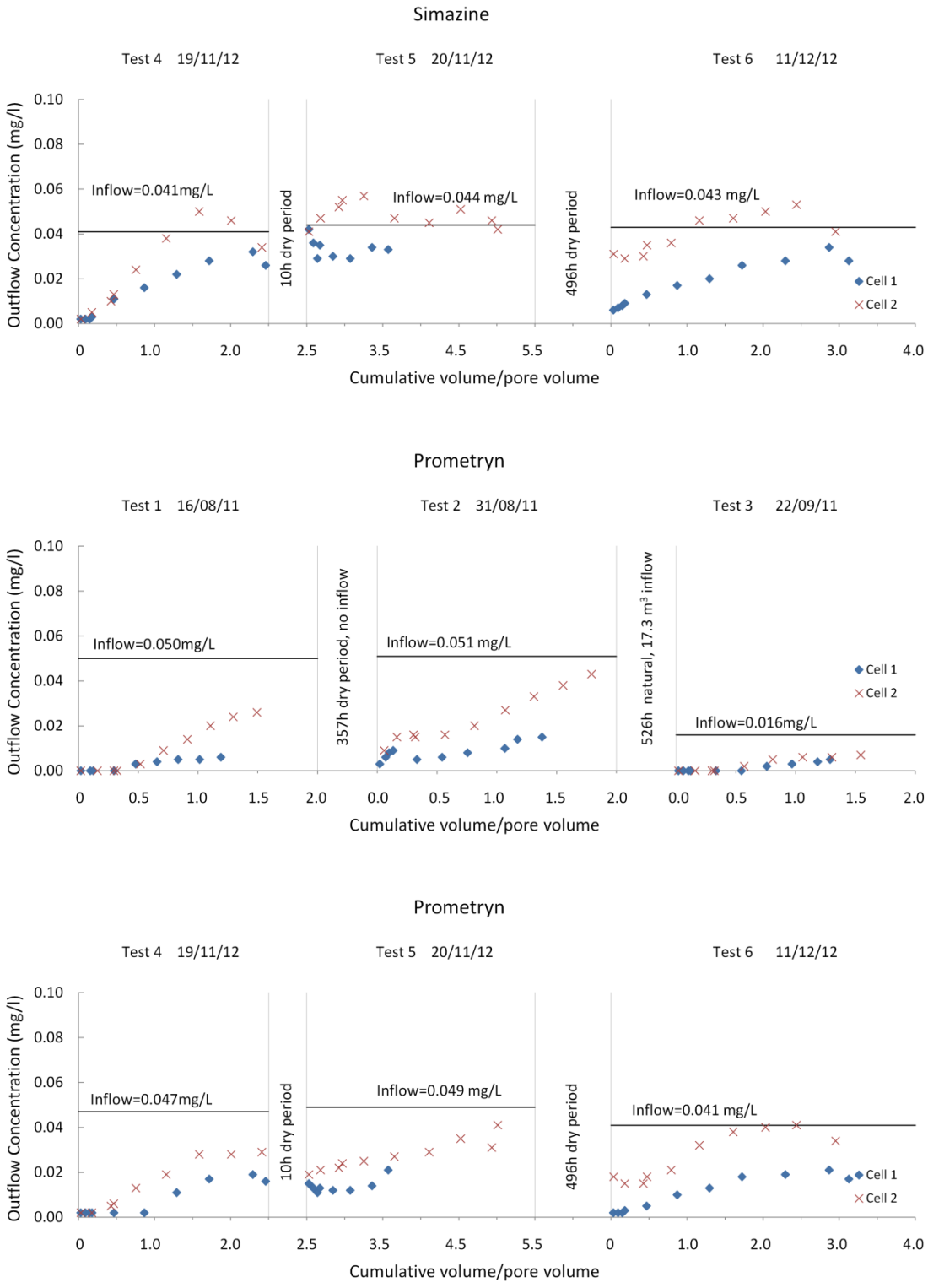

Figure 3-18 Pollutographs of simazine during 2nd test series (top) and of prometryn during 1st test series (middle) and 2nd test series (bottom) for Cell 1 and Cell 2

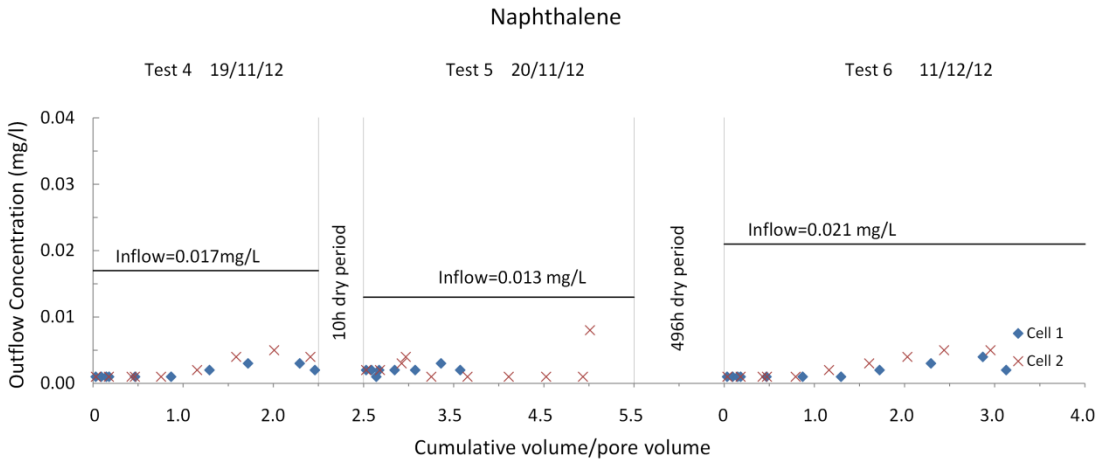

Figure 3-19 Pollutographs of naphthalene during 2nd test series for Cell 1 and Cell 2

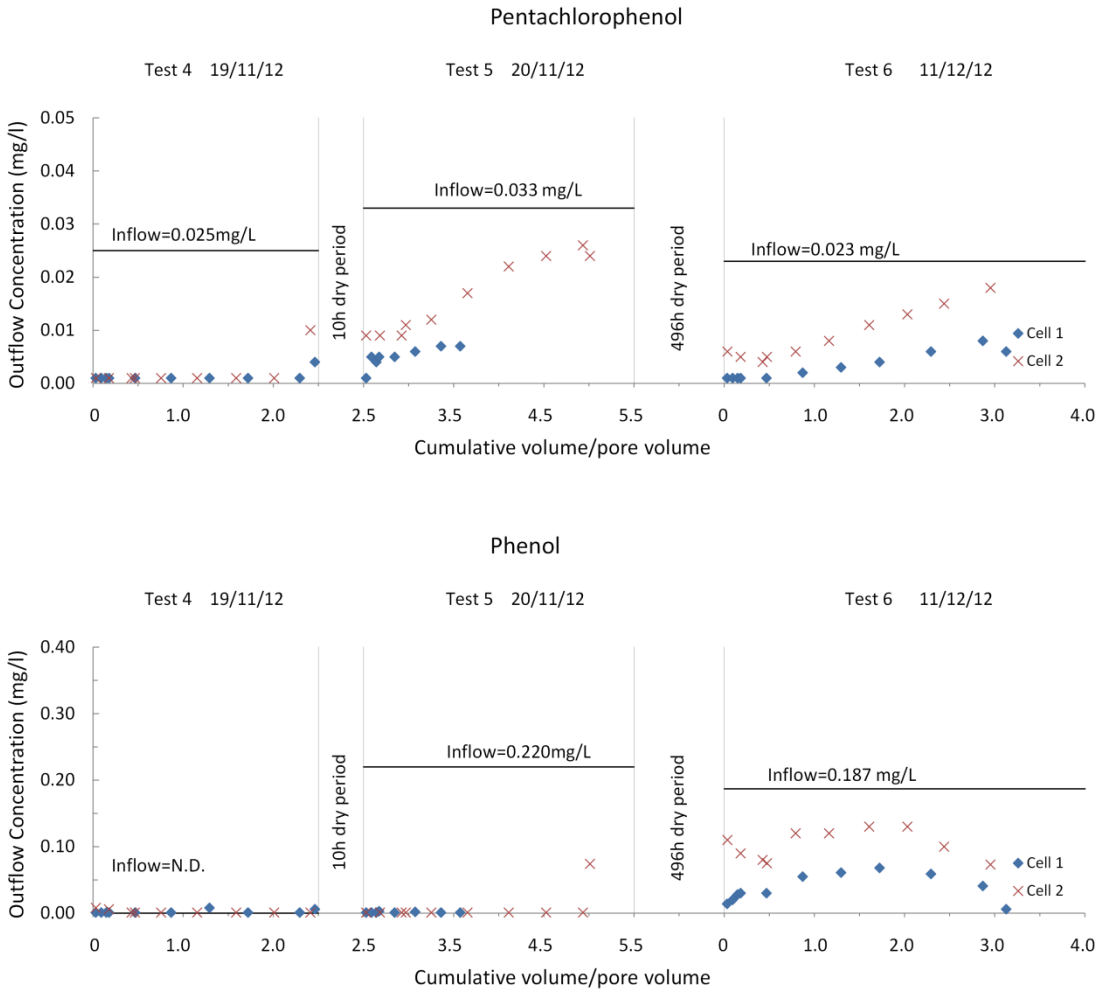

Figure 3-20 Pollutographs of PCP and phenol during 2nd test series for Cell 1 and Cell 2

3.5.4.4 Soil sample analysis results

TPHs, pyrene and DEHP are the only pollutants that were detected in the *surface* soil samples (although, they were not detected in deep); concentrations of all the other micropollutants were below the limit of report.

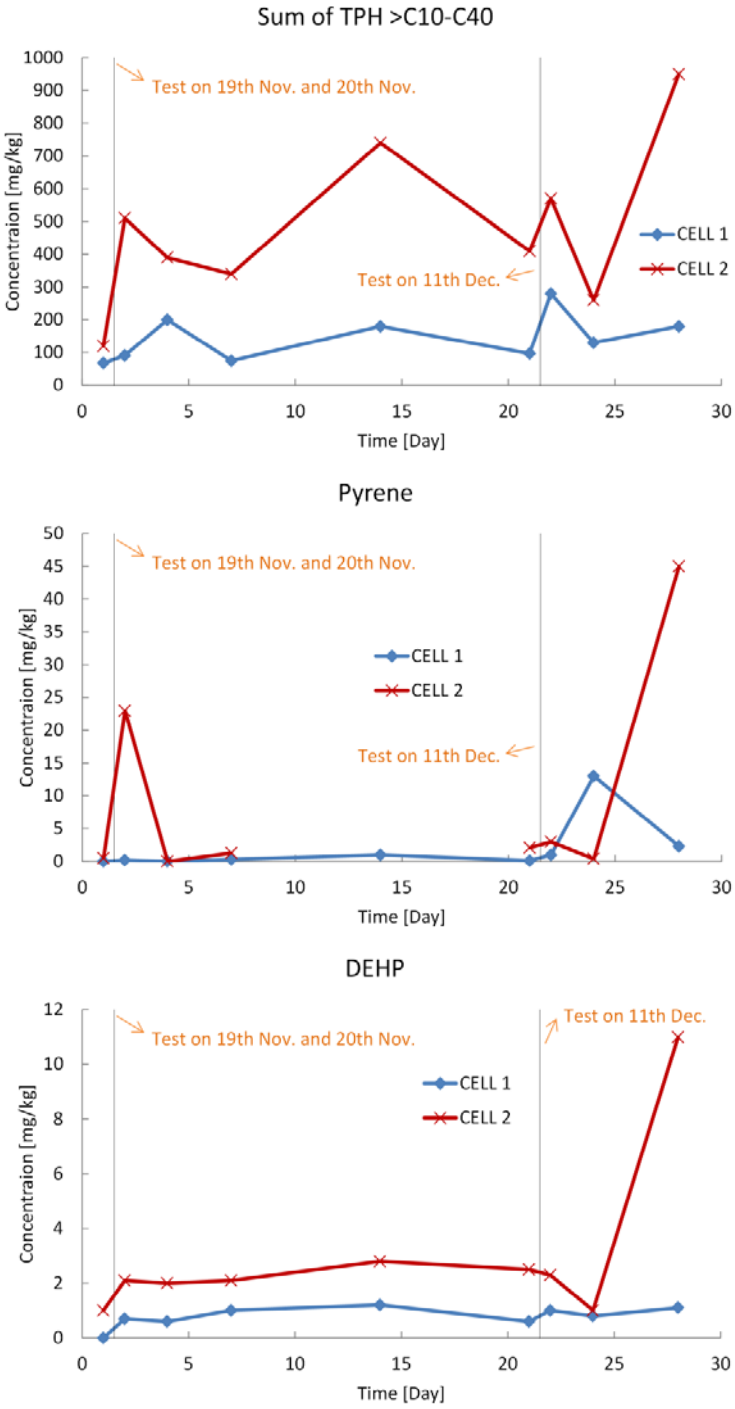

Figure 3-21 TPHs, pyrene and DEHP concentration detected in soil samples taken from surface soil at Cell 1 and Cell 2 during the 2nd test series

However, it should be noted that soil samples have a higher limit of report than water samples (mg/kg compared to µg/L, see Chapter 3.2.1). Figure 3-21 shows TPHs, pyrene and DEHP concentrations found in soil samples taken from surface soil at Cell 1 and Cell 2 during the 2nd test series. The results are not surprising for these three chemicals, as they were removed well in both cells (high above 90%). The fact that they were detected in surface samples only agrees with other studies reported in literature that most of the removal is happening in the upper most layer of the biofilter media (the hummus zone).

Interestingly, Cell 2 soil samples showed a higher micropollutant content than Cell 1's samples. It is hypothesized that this is due to plant litter formed in the upper zone (more profound with Melaleuca ericifolia, than with Carex appressa).

3.5.4.5 Summary

The following is a summary of the challenge test results:

- Extreme wet conditions could be of high importance for hydraulic performance, but only in systems in excess of certain clay content, whereas it seems that it should not be a problem for well-designed biofilters;
- Cell 1 is better or equal than Cell 2 in removing micropollutants;
- Good removal was achieved for TPHs, glyphosate, DBP, DEHP, pyrene and naphthalene;
- Moderate removal was achieved for PCP and chloroform;
- Poor removal was achieved for triazines;
- TPHs, pyrene and DEHP were the only pollutants detected in surface soil samples;
- Formation of cracks during long dry periods caused short-circuiting and enlarged EMCs.

3.6 Laboratory batch and column testing

This chapter presents the methodology of conducted batch and column tests. Obtained results and data analysis are presented in Chapter 5.3.2. It should be noted that most of the testing was performed by Kefeng Zhang.

3.6.1 Batch studies

The batch technique is a very popular procedure for estimating the capacity of soils to remove chemicals from a water solution. The procedure includes mixing a water solution of known composition (and concentration) with a known quantity of soil (adsorbent) for a given period of time. The solution is then separated from the adsorbent (e.g. by centrifuging) and analysed for solute concentration. The difference between this and the initial concentration is assumed to have been sorbed on the soil. The method is highly influenced by contact time, method of mixing, soil to solution ration, solution pH, hydrolysis, biodegradation, photodegradation etc. (US EPA, 1992).

Batch tests conducted as part of this research were done with fluorescein only (as a model micropollutant) and included two types of experiments: (1) adsorption and (2) biodegradation. The adsorption experiments included sterilization of the soil samples. The biodegradation experiments were done on non-sterilized soil, and showed influences of both adsorption and biodegradation. Methodology on how to extract data on biodegradation only is presented in Chapter 5.3.2.

Detailed experiment methodology

The laboratory tests were done on surface (top 5 cm) and deep soil samples collected from the two biofilters (Cell 1 and Cell 2 at Monash Car park site, see Chapter 3.2). Before the test, soil samples were air dried and then sieved (< 5.6 mm).

Adsorption experiments were performed using 200 mL amber glass bottles containing 10 g of sterilised soil (autoclaved at 120°C for 30 min, three times), mixed with 45 mL synthetic stormwater (according to the procedure described previously by Blecken et al. (2009)) spiked with 120 µg/L fluorescein. The bottles were shaken on a rotatory shaker at 100 rpm for 32 hours at 15 ± 0.5°C in the dark. Samples were taken at 0, 0.5, 3, 6, 9, 24 and 32 hours and centrifuged at 4000 rpm for 10 min. The centrifuging speed and time were tested to be enough to settle the sediment from the mixture. The supernatants were then analysed for fluorescein concentrations. All the experiments were performed in triplicate. Positive and negative controls were prepared at the same time.

Biodegradation experiments were conducted in 500 mL amber glass bottles containing 10 g non-sterile soil and 45 mL synthetic stormwater spiked with 120 µg/L fluorescein.

The bottles were incubated at 15 ± 0.5°C in the dark without shaking for 21 days to mimic the biodegradation of fluorescein during dry periods. The temperature (15 ± 0.5°C) was derived from the average soil temperature according to a year of online monitoring of the two field biofilters in 2011 (Monash Carpark Meteo Station: internal data). Samples were taken at 0, 0.25, 1, 2, 3, 7, 14 and 21 days. The bottles were shaken for 1 min at each sampling point. Collected samples were centrifuged and the supernatants were analysed for fluorescein as described above.

3.6.2 Column studies

Three replicate stainless steel columns were packed with filter media collected from the two biofilters used in the field challenge test. The soil profile of the columns (diameter 99mm; total depth 706±2mm; submerged zone depth 200mm), the porosity (0.39), and bulk density (1.59 g/cm^3) were very similar to the field biofilter a total depth 700mm, submerged zone depth 200mm, porosity 0.39 and bulk density 1.59 g/cm^3. The filter media were air dried and then sterilized by gamma irradiation at 25 kGy before column packing. Once packed, the columns were flushed using 12 x 2L pulses of deionised water to remove finer particles that results from column packing and to allow the media to settle. Up-flow flushing (5L) was performed to remove air bubbles and to ensure the columns were fully saturated at the beginning of the experiment. The columns were then equilibrated with synthetic stormwater without herbicides until the outflow electrical conductivity (EC) and pH values were stable (EC ~400 µS/cm and pH ~7.1).

Sorption column experiments were performed using a flow rate of ~21 ± 0.6 mL/min (hydraulic conductivity of 164 ± 5 mm/hr which was similar to the field condition which had an average of 155 mm/hr). Two series of experiments were conducted:

- the first involved dosing 4 PVs of synthetic stormwater with atrazine, simazine and prometryn, and
- the second series involved passing 10 PVs of the same synthetic stormwater with 1,900 ± 20 µg/L glyphosate.

Previous work showed that the sorption rate of glyphosate to stormwater biofilter media is much higher than the triazines and is reflected in the K_{oc} values (Zhang et al., 2014), e.g. after up to 3 PVs inflow, the outflow concentrations of triazines showed

breakthrough while that of glyphosate was just ~25% of inflow. A further limitation was the relatively small column used, which was not able to produce enough sample for co-analysis of glyphosate and triazines in the same test. Three composite inflow samples were collected during the dosing periods while 8-10 discrete outflow samples were collected over the entire experiment. All the samples were analysed for the selected herbicides.

3.7 Conclusions

This chapter presented experimental methodology and some experimental results for tests conducted at Monash Car Park field site, and laboratory batch and column tests. Field data included conservative and reactive tracer tests, electro-resistive tomography, and micropollutant challenge tests.

Tracer test and ERT data showed that Cell 1 of Monash Car Park biofiltration system has a lower hydraulic conductivity than Cell 2, and is prone to soil swelling. Additionally, ERT data demonstrated that the flow in both cells becomes predominantly one-dimensional in a relatively short period of time.

Challenge test results showed that micropollutants with similar structures exhibited similar fate in biofiltration cells (e.g. triazines had comparable behaviour). Pollutant mass balance during all conducted tests clearly showed that pollutants were being retained in the biofiltration cells by either sorption, degradation or other removal processes. Some pollutants (e.g. atrazine, simazine) had outflow concentrations that were higher than the inflow ones, indicating that the pollutant mass is being retarded i.e. the pollutant mass is being sorbed by the biofilter media and/or plants. This evidence indicates that the future model needs to have at least sorption and degradation to be able to reproduce the measured data.

CHAPTER 4: MODEL DEVELOPMENT

4 MODEL DEVELOPMENT

4.1 Introduction

For biofilters to be used as an effective stormwater management measure, it is important to model their performance, since only through continuous simulations of their hydraulic and treatment efficiencies the long-term impact on the reduction of stormwater pollution levels and loads can be predicted.

Bearing in mind all the strengths and weaknesses of models reviewed under Chapter 2.4, the aim of this study was set to develop a general treatment model of stormwater biofilters that is applicable to a wide range of micropollutants and allows for long-term simulations when combined with integrated stormwater models. The latter requires the model concept to make a compromise between the little available data and the needed complexity to accurately describe the nature of the system, i.e. practical useability versus scientific rigour. The model needs to be able to simulate the key treatment processes within stormwater biofilters, i.e. volatilisation, sorption, and bio-chemical degradation. It can therefore be easily applied to any micropollutant if its key removal mechanisms are known (e.g. for removal of pesticides sorption and biodegradation are predominate processes, while volatilisation can be neglected). This chapter presents the development of the MPiRe model (MicroPollutants In RaingardEns – quality model).

4.2 Model structure selection

In order to make the model applicable to a wide range of micropollutants and allow for long-term simulations when combined with integrated stormwater models, the following key model structure elements needed to be defined as per McCarthy (2008):

1) Scale of the problem, that includes both the timestep and the space conceptualization;
2) Governing equations should be easily transferrable to other biofiltration systems, and should capture the essence of transport and fate so to be adaptable to other pollutants;

3) Preferred model outputs should be micro-pollutant concentrations, to estimate peaks, and micro-pollutant loads, to estimate long term performance;
4) Model data requirements should be easily fulfilled, to secure usability.

When choosing the appropriate time-step, it is necessary to consider the real time response of the stormwater systems to rainfall events, and the modelling purpose: event modelling or long-term system effects. The choice for the MPiRe model was to be able to deal with events, but also to be scalable. As rainfall events usually occurr in a sub-daily time frame, with most urban stormwater quality models being set up to run in minutes to perform well (e.g. MUSIC Model – Wong et al., 2006, SWMM – EPA, 2007, FITOVERT – Giraldi et al., 2010, STUMP – Vezzaro et al, 2012), it was natural to choose minute-resolution for the MPiRe model as well. The model was set in a way where it is possible to change the timestep, and it can give stable results with a far larger time-step (e.g. 1 hour, 2 hours, etc.), but for the results to make sense, especially for the quality component, it is advisable to use minutes. For most of the testing procedures, the actual timestep is set as to as low as 30-seconds to follow the data collection system's resolution (see Chapter 3.2.1).

The space conceptualization is selected to be one-dimensional in the vertical direction. The dimensionality of flow in the biofilter has been tested using tracers in combination with ERT (see Chapter 3.4).

The governing equations were selected to be mechanistic, rather than regression based, as this should assure that the model is transferrable between different biofiltration systems, and among different pollutants. The water quality set of equations is based on pollutant water and soil concentrations, as intensive quantities. However, as the water quality model is coupled with a water flow model, it is possible to calculate the model outputs as pollutant loads. Most of the water quality legislation (Clean Water Act, EU WFD, etc.) is written so to prescribe maximum allowable concentrations. However, from the managerial point of view, it is important to estimate total pollutant loads.

The model is written in the Python programming language, and is set to be compatible with CITY DRAIN © (Achleitner et al, 2007). CITY DRAIN © is an open source toolbox for integrated modelling of urban drainage systems realized in

Matlab/Simulink, and is capable of being extended with different subsystems, such as this one – a biofiltration system. The modelling environment is set to calculate all blocks simultaneously. Fluxes (water, pollutant) between different blocks (e.g. from a catchment to biofilter) are sent at the end of each time interval, so all blocks need to be set to have calculations *explicit in time*.

4.3 Fluid flow

The water flow module was not developed, but rather adapted, with some small changes, from Lintern et al. (2012) and eWater (2009). This was done because that type of a model has performed quite well among different types of biofilters, and especially on the Monash Car Park site.

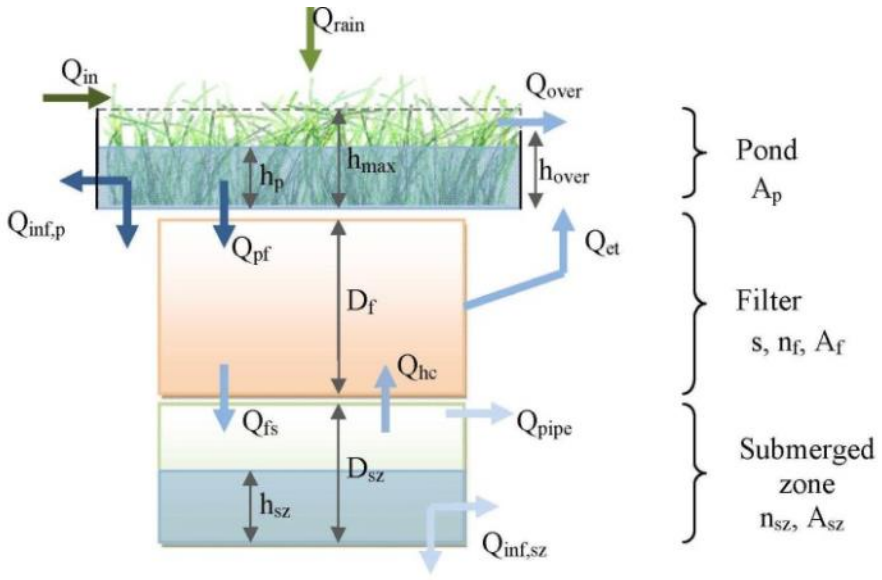

Figure 4-1 The main biofilter zones and flow scheme

When stormwater enters a biofilter it can form a temporary pond on top of the filter media (Figure 4-1), which depends on the dynamic of its inflow and the ability of the system to filtrate. While the water infiltrates through the biofilter media (from which it is collected by a drainage pipe) any excessive water will overflow over a security weir. The system can be lined or unlined (therefore promoting infiltration), and can contain a submerged zone, usually formed by a riser pipe that is connected to the drainage pipe. These processes are modelled using so called the 'three tank' approach (also known as a

bucket approach), where the tanks represent (1) the ponding zone, (2) the filter media, and (3) the submerged zone.

The key variables that are modelled are:

- water depth in the ponding zone, h_p,
- saturation of the filter media, S, and
- depth in the submerged zone, h_{sz} (if this zone exists).

At the same time the following flow rates are calculated using the equations listed in Table 4-2 with their parameters listed in

Table 4-3: infiltration flows (Equations 4.1, 4.2, 4.4, 4.8, 4.11), overflowing flows (Eqs. 4.3, 4.12), capillary rise flow (Eq. 4.6) and evapo-transpiration (Eq. 4.9).

Infiltration flows are governed by Darcy's law if the media is saturated, or by modified Darcy's law with the relative hydraulic conductivity presented with S^b (Eq. 4.8) according to Dingman (2002). Flow over the weir is calculated by a weir discharge equation. The capillary rise and the evapotranspiration are both represented with empirical functions derived by Daly et al. (2009). Equations 4.5, 4.10, and 4.13 present water mass balance equations in each of the buckets, which are solved for the key variables.

Flow equations 4.2, 4.4, 4.6, 4.7, 4.8, 4.9, 4.11, and 4.12 are solved explicitly in time, therefore a special care needs to be given to the physical conditions – mass conservation, so each flow is a minimum of (i) what is physically possible, (ii) what is available at the upstream tank, and (iii) what is available at the downstream tank for a particular moment in time. Flow over the weir is the only flow that is solved implicitly; i.e. the flow at a time step t is dependent upon depth in the pond in the same time *t*, so that the mass balance equation in the pond (Eq. 4.5) has to be solved iteratively. This is done with using the false position method.

Stability of the model under different time steps was extensively tested, showing excellent results (not included in the thesis). However, it is recommended to use the model with sub-hourly time steps, due to the dynamic nature of the key modelled

processes. It can be noted that the model does not show the position of the wet front in the filter media, but rather assumes average saturation over the entire porous media.

Table 4-1 Biofilter geometry and state variables

Pond	
A_p	Horizontal area of the pond [L^2]
h_p	Pond water depth [L]
h_{max}	Max. depth of water in pond [L]
h_{over}	Weir height [L]
Filter	
A_f	Horizontal area of the filter [L^2]
n_f	Filter material porosity [-]
D_f	Filter depth [L]
S	Filter water saturation [-]
Submerged zone	
A_{sz}	Horizontal area of subm. zone [L^2]
n_{sz}	Submerged zone porosity [-]
D_{sz}	Depth of the submerged zone [L]
h_{sz}	Water depth in the subm. zone [L]

Table 4-2 Water flow model equations

Water Flow Model Equation	Eq. No.
General form of equations $Flow = \min(\text{physically possible, available upstream, available downstream})$	
Max. infiltration to surrounding soil through filter and submerged zone $Q_{\text{inf},sz}^{\max} = \begin{cases} 0 \text{ , if biofilter is lined} \\ K_s\left(A_f + C_s \cdot P_{sz}\right) \end{cases}$	(4.1)
Ponding zone tank Infiltration from pond to filter media $Q_{pf} = \min\left(K_f \frac{h_p + D_f}{D_f} A_f, \frac{1}{\Delta t}\left(h_p A_p + \int_t^{t+\Delta t} Q_{in} dt\right), \frac{1}{\Delta t}\left((1-S) n_f D_f A_f + \left(1 - \frac{h_{sz}}{D_{sz}}\right) n_{sz} D_{sz} A_f\right) + Q_{\text{inf},sz}^{\max}\right)$	(4.2)
Weir overflow (rectangular weir) $Q_{over} = \min\left(C_Q B \sqrt{2g\left(h_p - h_{over}\right)^3}, \frac{1}{\Delta t}\left(\left(h_p - h_{over}\right) A_p + \int_t^{t+\Delta t} Q_{in} dt - \int_t^{t+\Delta t} Q_{pf} dt\right), -\right), \; h_p > h_{over}$	(4.3)

Water Flow Model Equation	Eq. No.

Infiltration from pond to surrounding soil (4.4)

$$Q_{\inf,p} = \min\left(K_s\left[\left(A_p - A_f\right) + C_s \cdot P_p\right], \frac{1}{\Delta t}\left(h_p A_p + \int_t^{t+\Delta t} Q_{in}dt - \int_t^{t+\Delta t} Q_{pf}dt - \int_t^{t+\Delta t} Q_{over}dt \right), - \right)$$

Water mass balance in the ponding zone (4.5)

$$\frac{d\left(h_p A_p\right)}{dt} = Q_{in} - Q_{pf} - Q_{over} - Q_{\inf,p}$$

Filter zone tank

Flow due to capillary rise (4.6)

$$Q_{hc} = \min\left(A_f C_r \left(S - S_s\right)\left(S_{fc} - S\right), \frac{n_{sz} h_{sz} A_f}{\Delta t}, \frac{1}{\Delta t}\left(\left(1 - S\right) n_f D_f A_f - \int_t^{t+\Delta t} Q_{pf}dt \right) \right),$$

when $S_s \le S(t) \le S_{fc}$, otherwise $Q_{hc} = 0$, $C_r = \dfrac{4E_{\max}}{2.5\left(S_{fc} - S_s\right)^2}$

Estimated saturation at time level n+1 (4.7)

$$S_{est} = \min\left(S^n + \frac{Q_{pf}^n \Delta t}{n_f A_f D_f}, 1.0 \right),$$ where n denotes beginning of time interval Δt

Infiltration from filter to submerged zone (4.8)

$$Q_{fs} = \min\left(A_f K_f \frac{\left(h_p + D_f\right)}{D_f} S_{est}^b, \frac{1}{\Delta t}\left(\left(S - S_h\right) n_f D_f A_f + \int_t^{t+\Delta t} Q_{pf}dt + \int_t^{t+\Delta t} Q_{hc}dt \right), - \right)$$

Flow due to evapotranspiration (4.9)

$$Q_{et} = \min\left(\begin{cases} 0, S_{est} \le S_h \\ A_f E_w \dfrac{S - S_h}{S_w - S_h}, S_h < S_{est} \le S_w \\ A_f\left(E_w + \left(E_{\max} - E_w\right)\dfrac{S - S_w}{S_s - S_w} \right), S_w < S_{est} \le S_s \\ A_f E_{\max}, S_s < S_{est} \le 1 \end{cases}, \frac{\left(S - S_h\right) n_f D_f A_f + \int_t^{t+\Delta t} Q_{pf}dt + \int_t^{t+\Delta t} Q_{hc}dt + \int_t^{t+\Delta t} Q_{fs}dt}{\Delta t}, - \right)$$

Water mass balance in the filter zone (4.10)

$$\frac{d\left(S n_f D_f A_f\right)}{dt} = Q_{pf} + Q_{hc} - Q_{fs} - Q_{et}$$

Submerged zone tank

Infiltration from submerged zone to surrounding soil (4.11)

$$Q_{\inf,sz} = \min\left(K_s\left(A_{sz} + C \cdot P_{sz}\right), \frac{1}{\Delta t}\left(n_{sz} h_{sz} A_{sz} + \int_t^{t+\Delta t} Q_{fs}dt - \int_t^{t+\Delta t} Q_{hc}dt \right), - \right)$$

Water Flow Model Equation	Eq. No.
Flow through drainage pipe	(4.12)
$Q_{pipe} = \min\left(-, \frac{1}{\Delta t}\left(\left(h_{sz} - h_{pipe}\right) n_{sz} A_{sz} + \int_{t}^{t+\Delta t} Q_{fs} dt - \int_{t}^{t+\Delta t} Q_{hc} dt - \int_{t}^{t+\Delta t} Q_{\inf,sz} dt\right), -\right)$, if $h_{sz} \geq h_{pipe}$	
Water mass balance in the submerged zone	(4.13)
$\frac{d\left(n_{sz} h_{sz} A_{sz}\right)}{dt} = Q_{fs} - Q_{hc} - Q_{\inf,sz} - Q_{pipe}$	

Table 4-3 Water flow model parameters

Water flow model parameters	
K_s	Hydraulic conductivity of the surrounding material [L T^{-1}]
C_s	Side infiltration coefficient [-]
P	Unlined perimeter [L]
K_f	Hydraulic conductivity of the filter material [L T^{-1}]
B	Length of overflow weir [L]
C_Q	Weir overflow coefficient [-]
S_s	Filter material saturation at plant "stress" water content [-] = 0.22[(1)] (no saturated zone), 0.37[(1)] (saturated zone)
S_{fc}	Filter material saturation at field capacity [-] = 0.37[(1)] (no saturated zone), 0.61[(1)] (submerged zone)
E_{max}	Potential evapotranspiration [L T^{-1}]
S_h	Filter material saturation at hygroscopic water content [-] = 0.05[(1)]
b	Relative hydraulic conductivity coefficient dependent on soil type [-]:sand – 11, loamy sand – 13, sandy loam – 13, loamy clay – 14, clay – 14
S_w	Filter material saturation at wilting point [-] = 0.11[(1)]
E_w	Evapotranspiration at wilting point [L T^{-1}] = 0.001[(1)] md^{-1}

[(1)]According to Daly et al. (2009)

4.4 Pollutant transport and fate

The pollutant transport module simulates advection and dispersion of micro-pollutants, as well as the three key treatment processes that occur in biofilters: volatilization, sorption and degradation. Exchange of pollutant mass between stormwater and atmosphere in the process of volatilization is assumed to happen only through the

surface area of the ponded water. Sorption and degradation are assumed to occur both in the filter and submerged zones, but not in the pond, because the filter media has far larger sorption capacity than plants submerged within the pond, and is characterized by longer stormwater retention time than the ponding zone (at least two times).

Table 4-4 Pollutant transport model equations

Pollutant Transport Model Equation	Eq. No.
Ponding zone tank	
Pollutant mass balance in the ponding zone	(4.14)
$\frac{d\left(c_p h_p A_p\right)}{dt} = c_{in} Q_{in} - c_{p,out}\left(Q_{pf} + Q_{over} + Q_{\inf,p}\right) - h_p A_p K_{vol} c_p ,$ assuming fully mixed $\Rightarrow\ c_p^{n+1} = c_{p,out}^{n+1}$	
Volatilization model	(4.15)
$\frac{d\left(c_p h_p A_p\right)}{dt} = -h_p A_p \underbrace{K_L a_{sur,p} \frac{H_c'}{H_c' + \left(k_L / k_G\right)_{sur,p}}}_{K_{vol}} \cdot c_p$	
Filter zone tank	
Continuity condition at pond – filter interface	(4.16)
$c_{p,out} = c_{f,in}$	
Pollutant mass balance in the filter zone	(4.17)
$\frac{\partial\left(S \cdot n_f c_f\right)}{\partial t} + \rho \frac{\partial s^e}{\partial t} + \rho \frac{\partial s^k}{\partial t} = \frac{\partial}{\partial z}\left(S \cdot n_f D \frac{\partial c_f}{\partial z}\right) - \frac{\partial\left(q c_f\right)}{\partial z} - S \cdot n_f k_{bio} c_f$	
Sorbed concentration at instantaneous sites at equilibrium	(4.18)
$s^e = f_e \cdot K_d \cdot c_f \ ;\ K_d = K_{oc} f_{oc}$	
Sorbed concentration at kinetic sites at equilibrium	(4.19)
$s_e^k = (1 - f_e) \cdot K_d \cdot c_f$	
Kinetic sorption model	(4.20)
$\rho \frac{\partial s^k}{\partial t} = \alpha_k \cdot \rho \cdot \left(s_e^k - s^k\right)$	
Biodegradation constant with Arrhenius eq.	(4.21)
$k_{bio} = \frac{\ln 2}{T_{1/2}} e^{\kappa\left(T - 20^\circ C\right)}$ where κ is Arrhenius constant corresponding to temperature T = $20^\circ C$	

Pollutant Transport Model Equation	Eq. No.
Average unit flow through the filter media	(4.22)
$q = \frac{Q_{net}}{A_f} = \frac{\alpha Q_{pf} + \beta Q_{fs}}{A_f}$, where $\alpha + \beta = 1$, and $\alpha = 1$ at upper boundary, $\beta = 1$ at lower boundary	
Dispersion coefficient	(4.23)
$D = \alpha_L \cdot q$	
Submerged zone tank	
Continuity condition at filter – submerged zone interface	(4.24)
$c_{f,out} = c_{sz,in}$	
Pollutant mass balance in the submerged zone	(4.25)
$\frac{d\left(c_{sz} n_{sz} h_{sz} A_f\right)}{dt} + \rho \frac{d\left(s^e h_{sz} A_f\right)}{dt} + \rho \frac{d\left(s^k h_{sz} A_f\right)}{dt} = c_f Q_{fs} - c_{sz,out}\left(Q_{hc} + Q_{pipe} + Q_{\inf,sz}\right) - k_{bio} c_{sz} n_{sz} h_{sz} A_f$, assuming fully mixed $\Rightarrow c_{sz}^{n+1} = c_{sz,out}^{n+1}$	

Similar to the water flow module, the transport module simulates transport and removal to occur within a series of connected tanks, where each tank represents one of the biofilter zones (Figure 4-1). All adopted transport equations are listed in Table 4-4 for each of the tanks, with their main parameters presented in Table 4-5. The pond is assumed to be fully mixed with volatilisation being the only sink (Eq. 4.14). Volatilization is modelled using Lee et al. (1998) approach (Eq. 4.15), but only for pollutants that have a high Henry's constant. Although there is no universal threshold value of this constant that can indicate whether volatility is important or not for a pollutant, the model assumes that this threshold is 100 Pa m^3 mol^{-1} as per Byrns (2001). This was regarded as a sufficiently robust approach, because the key volatile micropollutants occur in very low concentrations in stormwater, and therefore the mass transfer between liquid and gas is controlled by the liquid phase.

The processes within the filter media and the submerged zone tanks are modelled using a one-dimensional vertical advection-dispersion model for saturated/unsaturated soil. Presence of the plant root system is accounted for through an equivalent porosity, which is a bulk parameter representing the biofilter media as specified by Hatt et al. (2009).

Table 4-5 Pollutant transport model parameters

Pollutant transport model parameters	
c	Concentration in water phase [ML^{-3}]
s^e	Sorbed concentration that would be reached at equilibrium with the liquid phase concentration at instantaneous sorption sites[M M^{-1} soil]
s^k	Sorbed concentration of the kinetic sorption sites [M M^{-1} soil]
s_e^k	Sorbed concentration at equilibrium with the liquid phase concentration at kinetic sorption sites [M M^{-1} soil]
ρ	Bulk soil density [ML^{-3}]
q	Unit/specific flow [L T^{-1}]
α_L	Dispersivity [L]
D	Dispersion coefficient [L^2 T^{-1}]
k_{bio}	Biodegradation rate constant [T^{-1}]
$T_{1/2}$	Biodegradation half-life [T]
f_e	Fraction of exchange sites assumed to be in equilibrium instantaneously
α_K	Kinetic sorption rate [T^{-1}]
K_d	Soil water partitioning coefficient [L^{-3} M soil]
K_{oc}	Soil water partitioning coefficient normalized to organic carbon [L^{-3} M soil],
f_{oc}	Soil organic carbon content [-]
H_c`	Non dimensional Henry's constant [-]
$(k_I/k_G)_{sur,p}$	Mass transfer between liquid and air through pond surface area (volatilization)
$K_L a_{sur,p}$	Overall surface-desorption gass-transfer coefficient for pond
T_{vol}	"Half-life" for the process of volatilization defined by K_{vol} (eq. 4.15) [T]

Sorption of organic pollutants is influenced by pollutant's intrinsic properties (hydrophobicity, polarity, aromaticity etc.) and soil physico-chemical characteristics (e.g. pH, cation exchange capacity, ionic strength, surface area, soil organic matter and water temperature, as per Delle Site, 2001). In a review of pesticides' soil sorption parameters, Wauchope et al. (2002) identified three scales of sorption processes (1) rapid, reversible sorption to "accessible" sites of soil surfaces driven by diffusion, that can be reasonably be assumed to be instantaneous (2) slower exchange of pollutant between water and soil phases, with equilibrium being achieved in the order of hours to a couple of days, and (3) very slow exchange in the order of days to years, that is irreversible and not easily distinguishable from degradation. To simulate these

phenomena, a chemical non-equilibrium two-site model of sorption is used (Van Genuchten and Wagenet, 1989; Šimůnek and Van Genuchten, 2008), as per Eqs. 4.19-4.20. The model assumes instantaneous sorption to one fraction of sites, f_e, following linear sorption isotherm (Eq. 4.18). Soil organic matter content is used to estimate soil-water partitioning coefficient, K_d. Kinetic sorption is assumed to occur on the other fraction of sites, $(1-f_e)$, also following the linear sorption isotherm with identical soil-water partitioning coefficient, and allowing simulation of the desorption process.

The process of biodegradation is dependent on two main factors: the amount of pollutant, and the amount of degrading biomass present. Although Monod-based biodegradation models are expected to be more accurate (e.g. Plosz et al., 2010), a simple first order decay model was selected (Eq. 4.21) due to difficulties in estimation of biomass parameters (it is also hypothesised that the influence of micropollutant mass that can accumulate in stormwater systems is negligible for biomass production). Degradation is assumed to affect only the dissolved phase of the micropollutant in the filter media and the submerged zone, as it is the practice in the vast majority of published micropollutant models (Pommies et al. 2013).

The transport equations listed in Table 4-4 are solved sequentially, with all time dependent equations (Eqs. 4.14, 4.17, 4.20, 4.25) being solved explicitly. Advection term in Eq. 4.17 is calculated by upwind or central differences depending on the value of Peclet number, while dispersion term is approximated by central differences (Hyakorn and Pinder, 1983).

CHAPTER 5: MODEL TESTING

5 MODEL TESTING

5.1 Introduction

This chapter presents the testing of the MPiRe model developed in Chapter 4. The two modules, the water flow module and the pollutant transport module were tested and calibrated separately and verified against field data. Since the water flow module has been extensively tested, the calibrated values of its key parameters were compared to previously determined values of these parameters (previous studies, e.g. Lintern et al., 2012).

The transport module was, however, tested under different scenarios, as the aim was to delevelop a model that would be usable under variable data accessibility. The transport module was tested under the following scenarios:

- Field data exists: calibrated against field data and predictions tested against separate set of field data (simple 50:50 split);
- Laboratory data exists: calibrated on laboratory data (batch and column studies) and predictions tested against field data.

The aim of this chapter is to gain insight on how the model performed with different pollutants in different availabilities of calibration data.

5.2 Model testing settings and procedures

5.2.1 Input data and boundary conditions

The model testing was done by running the entire model continuously for the each test series on a 30-second time-step. The input data included, beside inflow rates, meteorological (daily values of potential evapotranspiration and rainfall) and geometry data, as shown in Table 5-1. Rainfall data for naturally occurring events was taken from a local rain gauge (as explained in Chapter 3.5.1). Daily evapotranspiration data was obtained from the Bureau of Meteorology (BOM, 2011, 2012 – www.bom.gov.au) for station No. 86071 in Melbourne (Melbourne Regional Office). This station is 16 km northwest of the measuring site (Figure 5-1). The evapotranspiration rates were

calculated using the FAO Penman-Monteith equation (Allen et al., 1998). The flow module was additionally run for 6 weeks prior the challenging series to "warm up the model", i.e. to ensure that the antecedent soil and submerged zone conditions for the test period are simulated well (Table 5-1). Six weeks was chosen as an arbitrary period, where the main objective was to have at least one large-volume rain event, that will saturate the biofilter and "reset" its moisture content from that point onwards (make it unrelated to antecedent period).

The boundary conditions included defining flows and pollutant fluxes at all "boundaries" i.e. drainage to the surrounding soil, exchange to the atmosphere (evaporation) and possible outflows (flow over the weir, flow through the pipe). Most of these conditions were defined by geometry e.g. the shape of the weir and its elevation defined the overflow (see Eq. 4.3). Since the tested biofilters were lined, there was no water or pollutant mass flow toward the surrounding soil. Exchange with the atmosphere was via evaporation for water, where the pollutant itself concentrated in the remaining water (does not evaporate itself), or in case where the pollutant was volatile, it may have passed to the atmosphere via volatilization (again not carried by the water itself).

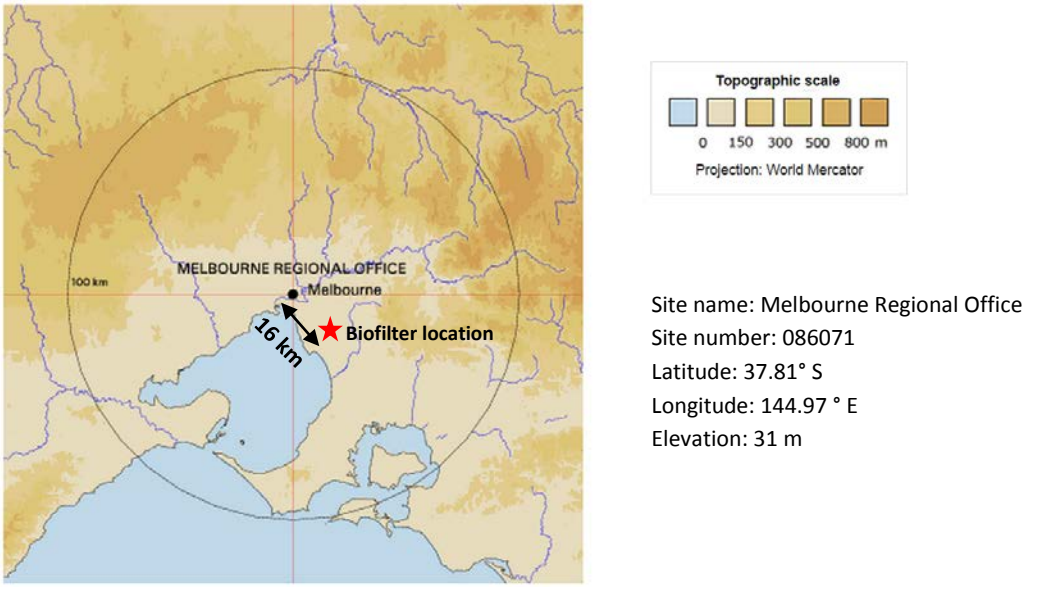

Figure 5-1 The meteorological station no. 086071 distance from the biofilter location (adapted from www.bom.gov.au)

The initial conditions for the transport module assumed that the biofilter cells were "free" of micropollutant presence: micropollutant concentrations were zero in all zones of the biofilter, in both the water and soil phase as per Table 5-1.

Table 5-1 Biofilter characteristics and initial conditions for the two test series

Biofilter characteristics		Cell 1		Cell 2	
Length [m]		10		10	
Width [m]		1.5		1.5	
Filter depth [m]		0.7		0.5	
Ponding depth [m]		0.41		0.41	
Saturated zone depth[m]		0		0.2	
Porosity [-]		0.35		0.49	
[1)]Dispersivity [m]		0.29		0.14	
Initial conditions		16/08/2011	19/11/2012	16/08/2011	19/11/2012
Pond	hp [m]	0	0	0	0
Filter	S [-]	0.5	0.6	0.8	0.5
Saturated zone	hsz/Dsz [-]	-	-	1	1
Conc. of pollutant in water [mg/L]		0	0	0	0
Conc. of pollutant on soil [mg/kg]		0	0	0	0

[1)]Determined from separate conservative tracer tests – see Chapter 5.2.4

5.2.2 Calibration procedure

PEST (Doherty, 2013) was selected as a tool for automatic model calibration: it minimises the objective function (sum of equally weighted residuals i.e. squared deviations between model and measurements a.k.a observations) using the Gauss-Marquardt-Levenberg algorithm. The objective function favours the peaks in values and is of the following form:

$$\Phi = \sum_{i=1}^{m} \left(w_i r_i \right)^2 , \; r_i = \left(\text{'model output value' - 'measurement'} \right) \tag{5.1}$$

Where r_i are residuals, w_i weight, and m is the number of measurement. The weights are inversely proportional to the standard deviation of the observation they are associated

with (Doherty, 2013). In case all measurement belong to the same population (i.e. measurements include only flow rates, or only pollutant concentrations), then the weight of each observation is the same, and can be set to 1. The weight can also be manually changed to be higher for measurements that are more favoured e.g. when instead of the peaks, which is inherent to the objective function, the aim is to model well the low values. The calibration algorithm minimises the Φ function (Eq. 5.1).

Initially, the model was manually calibrated, to get a first insight into the model behaviour. This included choosing specific values for input parameters, running the model and checking agreement with measured data by visual inspection or some likelihood measure like the Nash-Sutcliffe coefficient (Nash and Sutcliffe, 1970). Manual calibration results were then used for setting the parameter range in the PEST control file. The PEST control file communicates with both input and output template files to write input parameter value-sets and to read the output model data (after model execution) and calculate selected objective function until finding the best parameter set (Figure 5-2).

Calibration was performed separately for the flow and transport module. The objective function for the flow module contains non-transformed measurements of outflow rates at 30-sec interval. The only parameter that was calibrated for the water flow module was hydraulic conductivity, K, as the porosity (the only other flow parameter, Table 5-1) was set to its measured value determined in 2011 (Lintern et al, 2012). It was assumed that the porosity did not change over time, since the biofilters had more than 5 years of establishing (Le Coustumer et al., 2012).

The objective function for the pollutant transport module was made with non-transformed concentration measurements at the outflow pipe (cca. 10 measurements per each event). The following pollutant transport model parameters were calibrated for each of the micropollutants:

- the three sorption coefficients, K_{oc}, f_e, and α_K,
- the degradation coefficient (half-life, $T_{1/2}$), and
- volatilization coefficient (half-life T_{vol}) for pollutants with high value of the Henry-constant.

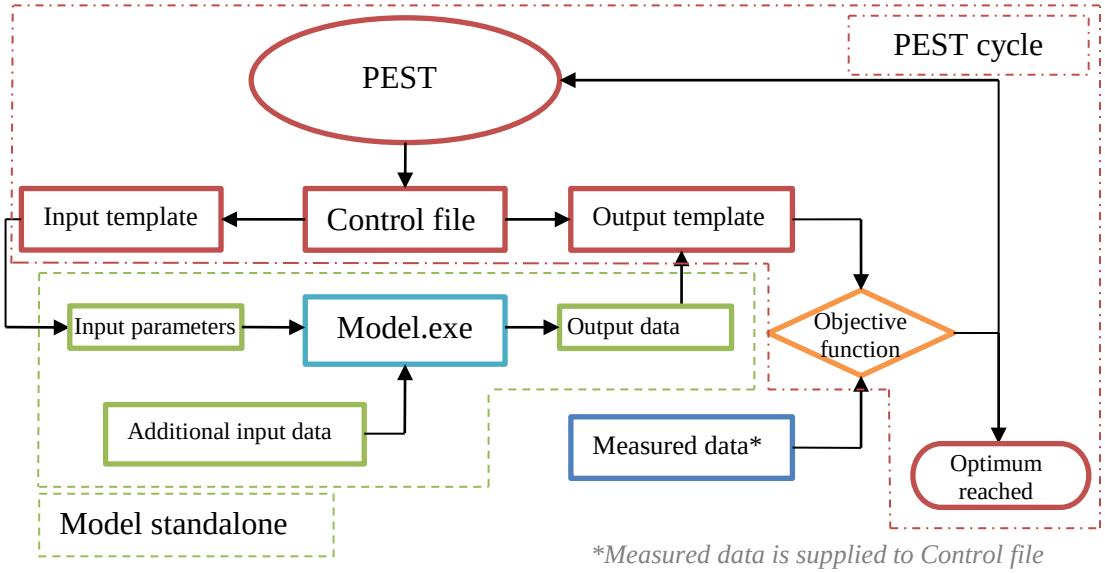

Figure 5-2 Scheme of PEST "wrapping-up" the standalone model

The calibration was done using the measured concentrations of the five pollutants (not their flux), as this was suggested by previous investigations of McCarthy (2008). When calibration is done on the pollutant flux, the objective function is minimizing the residuals between composite and not directly measured quantities which include both variability of the flow rate and the pollutant concentration. Advection/dispersion terms in Eq. 4.17 were applied and estimated (dispersivity) using conservative tracer test data (Potassium chloride, KCl) from an experiment performed on the two biofilter cells in a separate event (see Chapter 3.3).

5.2.3 Model performance assessment

The model results are presented graphically as:

- time series flow rates, pollutant concentrations and pollutant fluxes,
- scatter plots of measured vs. modelled event mean concentrations (EMCs) for pollutants, and
- scatter plots of measured vs. modelled event loads for pollutants.

The event mean concentration and event load were calculated in the same manner for both measured and modelled values as per Eqs. 5.2 and 5.3, where ΔV_i is the outflow volume corresponding to the measured/modelled concentration c_i, and m is the number of measurements.

$$EMC = \frac{\sum_{i=1}^{m} \Delta V_i c_i}{\sum_{i=1}^{m} \Delta V_i} = \frac{\sum_{i=1}^{m} \Delta V_i c_i}{V_{total}} \ \left(mg / L\right) \tag{5.2}$$

$$Event\ Load = \sum_{i=1}^{m} \Delta V_i c_i \ \left(mg\right) \tag{5.3}$$

Additionally, the model assessment was performed numerically calculating the value of the Nash-Sutcliffe coefficient (E, Eq. 5.4) for both time-series and scatter plots, and the adjusted coefficient of determination (R^2, Eq. 5.5) for scatter plots only. The Nash-Sutcliffe coefficient indicates how well the model outputs represent the measurements when compared to the mean value of measurements (E = 1 is a perfect match; E = 0 model predictions are as accurate as the mean value of measurements; E < 0 the mean value of measurements is a better predictior than the model; E > 0.6 is considered acceptable in hydrology). The adjusted coefficient of determination takes into account the low number of observations (i.e. there is a maximum of 12 events for one pollutant – 6 per cell), and uses the variance, instead of the square residuals only (R^2 = 1 is a perfect match). The variances (Var_{res}, Var_{tot}) were calculated in an unbiased manner as per Eqs. 5.6 where *m* is the number of measurements, and *p* is the degree of freedom: in this case p = 1 (1 degree of freedom in terms of regression is the vector of measured values) (Montgomery and Runger, 2010).

$$E = 1 - \frac{\sum_{i=1}^{m} \left(meas_i - mod_i\right)^2}{\sum_{i=1}^{m} \left(meas_i - \overline{meas}\right)^2}, \ (-\infty, 1] \tag{5.4}$$

$$R^2 = 1 - \frac{Var_{res}}{Var_{tot}}, \ (-\infty, 1] \tag{5.5}$$

$$Var_{res} = \frac{\sum_{i=1}^{m} \left(meas - mod\right)^2}{m - p - 1}, \ Var_{tot} = \frac{\sum_{i=1}^{m} \left(meas - \overline{meas}\right)^2}{m - 1} \tag{5.6}$$

5.2.4 Conservative tracer test analysis

The longitudinal dispersivity (α_L) was estimated from the in-situ study with a conservative tracer, potassium chloride, using Eq. 4.17 without the adsorption and

biodegradation terms. The Nash-Sutcliffe coefficient, E, was used as a measure of calibration performance (see Chapter 5.2.2).

Calibration was very successful for Cell 2, with E value of 0.96, and acceptable for Cell 1, with E value of 0.86. The dispersivity, α_L, was found to be 0.29 m for Cell 1, and 0.14 m for Cell 2.

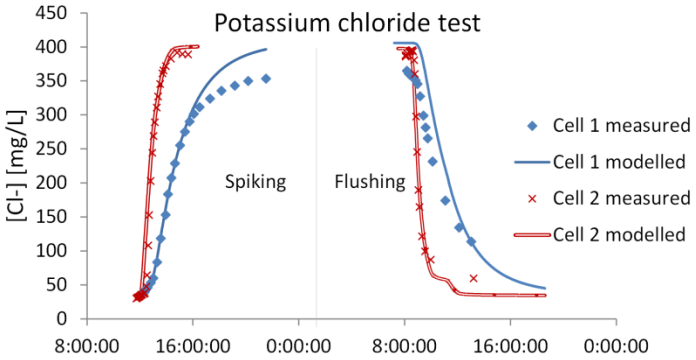

Figure 5-3 Pollutographs of KCL for Cells 1 and 2 - estimation of dispersivity

5.2.5 Model calibration and verification with field data

The model was calibrated against field tests explained in Chapter 3.5.4. The data from the two series was split, so that one half is used for calibration and the second half for validation. The 2nd test series (challenging tests 4-6) was used for calibration, because it had more reliable flow and soil moisture measurements. First step involved calibration of the key model parameter (hydraulic conductivity) for the flow module, and then in the second step the key model parameters for the transport module were calibrated using the modelled flows and moisture contents. This was done for all the detected micropollutants (atrazine, prometryn, simazine, glyphosate and chloroform). The calibrated model was then verified using the data from the 1st test series (challenge tests 1-3).

Additionally, the calibrated hydraulic conductivities of both cells were compared to previously measured and estimated values by Lintern et al, (2012), while the calibrated transport module parameters were compared to the literature values (fate process parameters). To assess the robustness of the model, the Nash-Sutcliffe coefficient (Nash and Sutcliffe, 1970) was calculated between the modelled and measured values (of both

calibration and verification data series) for the following variables: the filter moisture content, the outflow rates and the concentrations of the 5 micropollutants.

5.2.6 Model parameter estimation from batch studies data

The sorption and biodegradation parameters (K_d, f_e, α_k and K_{bio} (or $T_{1/2}$)) were determined through laboratory batch studies for fluorescein, here used as a micropollutant-surrogate (a.k.a. reference micropollutant). Fluorescein as it is low in cost and easy to use (easy detection method). Although fluorescein is commonly used as a tracer, it has been criticized due to its relative high potential for sorption onto soils and biodegradation (Smart and Laidlaw, 1977; Sabatini, 2000). These characteristics make fluorescein a very good surrogate or reference micro-pollutant that can be used to study sorption and biodegradation process in biofilters. Although fluorescein is prone to photolysis, it was assumed that it did not occur in the vegetated biofilters as exposure to sunlight is negligible because of the dense plants above. Fluorescein was hydrolytically stable in stormwater: concentration change of fluorescein (200 µg/L and 340 µg/L) in stormwater was within ± 2.0% under different temperatures (4, 15 and 30°C) for over 5 days.

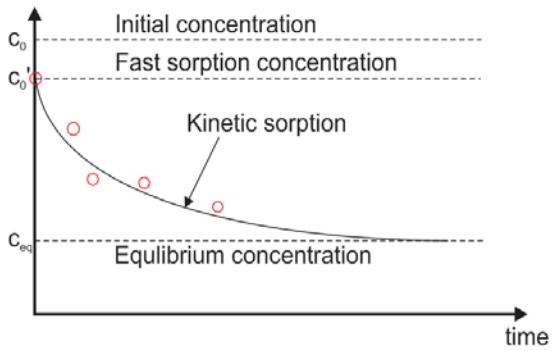

Figure 5-4 Example plot of laboratory sorption data with characteristic concentrations used for determination of sorption parameters in the transport module

Soil samples for these tests were collected from surface (top 5 cm) and deep soil samples from the two biofilters (Monash Car park site, see Chapter 3.2). Since the tests were done to sterile samples (no microbes) and non-sterile samples, it was possible to determine both sorption and degradation parameters. Volatilization was not studied in these tests (fluorescein is not prone to it).

The sorption parameters from Eq. 4.17 (i.e. K_d, f_e and α_k) were estimated from data plots from the sorption laboratory (batch) tests (Figure 5-4). The plot shows the approximation of the laboratory data with an exponential function of the following form:

$$c(t) - c_{eq} = \left(c_0' - c_{eq}\right) \cdot e^{-K_{slow} \cdot t} \tag{5.7}$$

Where *c(t)* is the pollutant concentration in water phase at time *t* (mg/L), c_{eq} is concentration reached at equilibrium (mg/L), c_0' is pollutant concentration after fast sorption has happened (mg/L), and K_{slow} is kinetic sorption rate (s^{-1}). This format is taken as a generalization of various sorption kinetic models reviewed by Qiu et al., (2009).

$$K_{fast} = \frac{c_0'}{c_0}, \quad K_{eq} = \frac{c_{eq}}{c_0}, \quad \text{where } c_0 \text{ is initial pollutant concentration in water (mg/L)} \tag{5.8}$$

Introducing K_{fast} and K_{eq} as fast sorption coefficient and equilibrium sorption coefficient, respectively, as per Eq. (5.8), and rearranging Eq. 5.7, the following equations for pollutant concentrations in water phase (Eq. 5.9) and soil phase (Eq. 5.10) are obtained:

$$c(t) = c_0 \cdot \left(K_{eq} + \left(K_{fast} - K_{eq}\right) \cdot e^{-K_{slow} \cdot t}\right) \tag{5.9}$$

$$s(t) = \frac{water}{soil} \cdot \left(c_0 - c(t)\right) = \frac{water}{soil} \cdot c_0 \cdot \left(1 - K_{eq} - \left(K_{fast} - K_{eq}\right) \cdot e^{-K_{slow} \cdot t}\right) \tag{5.10}$$

Where $\frac{water}{soil}$ is ratio of water solution (L) to soil sample (kg). Similarly, s_0' or pollutant concentration in soil that is instantaneously sorbed can be expressed as:

$$s_0' = \frac{water}{soil}\left(c_0 - c_0'\right) = \frac{water}{soil} \cdot c_0 \cdot \left(1 - K_{fast}\right) \tag{5.11}$$

Eq. 5.11 can be compared with Eq. 4.18, here written again for convenience, to make a relation between (1) experimental and (2) two-site chemical non-equilibrium model parameters as per Eq. 5.12.

$$s_0' = s^e = f_e \cdot K_d \cdot c_0 \tag{4.18}$$

$$\underbrace{\frac{water}{soil}\left(1 - K_{fast}\right)}_{\text{experimental parameters}} = \underbrace{f_e \cdot K_d}_{\substack{\text{two-site chemical} \\ \text{non-equilibrium} \\ \text{model parameters}}} \tag{5.12}$$

Similar can be done with kinetic-sorption equation from the two-site chemical non-equilibrium model: Eq. 5.13 is written with Eqs. 4.19 and 4.20. The derivative in the new equation is changed to the total derivative since the batch is homogeneous across volume (assumption), so the pollutant concentrations in water (or soil) phase change only with time. Eq. 5.13 is solved (integrated) with known initial condition: no pollutant in the soil phase at t = 0 (Eq. 5.14). The final form of the sorbed concentration at the kinetic sorption sites, $s^k(t)$, for the two-site chemical non-equilibrium model is given with Eq. 5.15. Its counterpart written in terms of batch experimental parameters is written as Eq. 5.16. Comparing the two, Eq. 5.15 and Eq. 5.16, using Eq. 5.12, the relationship is established between model and experimental parameters as per Eq. 5.17.

$$\frac{ds^k}{dt} = \alpha_k \left(\left(1 - f_e\right) \cdot K_d \cdot c_0 - s^k \right) \tag{5.13}$$

$$\int \frac{ds^k}{\left(1 - f_e\right) \cdot K_d \cdot c_0 - s^k} = \int \alpha_k dt \qquad \text{solving with } s^k\left(t = 0\right) = 0 \tag{5.14}$$

$$s^k\left(t\right) = \left(1 - f_e\right) \cdot K_d \cdot c_0 \cdot \left(1 - e^{-\alpha_k \cdot t}\right) \tag{5.15}$$

$$s^k_{\text{exp}} = s\left(t\right) - s_0' = \frac{water}{soil} \cdot c_0 \cdot \left(1 - K_{eq} - \left(K_{fast} - K_{eq}\right) \cdot e^{-K_{slow} \cdot t} - \left(1 - K_{fast}\right)\right) \tag{5.16}$$

$$K_d = \frac{water\ solution(L)}{soil(kg)}\left(1 - K_{eq}\right);\ f_e = \frac{1 - K_{fast}}{1 - K_{eq}};\ \alpha_k = K_{slow} \tag{5.17}$$

Fast sorption and equilibrium concentration (c_0' and c_{eq}) were estimated as concentration values at 0.5 h and 32 h respectively (the first measured and the last from the dataset). When these concentrations were determined, K_{fast} and K_{eq} were calculated using Eq. 5.8. K_{slow} was estimated using the least-squares method while fitting Eq. 5.9

with experimental data. Model parameters (K_d, f_e, α_k) were then determined using relations in Eq. 5.17.

To estimate biodegradation rates (K_{bio}), fluorescein concentrations from non-sterile samples were adjusted to the concentrations of sterile control ones to account for the effects of sorption. Once data was prepared, the kinetic rate was estimated using the least-squares method while fitting the first order decay equation to adjusted experimental data.

The model was first applied to the field challenge tests with parameters estimated from the laboratory batch experiments (K_d, f_e, α_k and K_{bio}) and dispersivity (α_L) estimated from separate conservative tracer tests performed on site (see Chapter 3.3). The model was set as to differentiate between surface (first 10 cm) and deep filter media (>10cm), as batch experiments were separately done on the two types of soils. Dispersivity was, however, taken to be constant throughout the filter media. The Nash-Sutcliffe coefficient was used to assess the model performance: E was calculated for modelled and measured outflow concentrations.

Additionally, the model was calibrated against field data from the fluorescein tracer test (see Chapter 3.3) to estimate model parameters (K_d, f_e, α_k and K_{bio}) that give the best fit with the measured data. To avoid over-parameterization, this model setup did not differentiate between surface and deep soils. The calibration was done using PEST software, as explained in Chapter 5.2.2. During the calibration, all the other parameters (i.e. bulk density, soil organic matter and porosity) were fixed at measured values as per Table 5-1. This “field calibration” was done to compare the best fitted parameters with estimated from the batch studies i.e. to analyse the transferability of batch experiment results to field conditions.

5.2.7 Model parameter estimation from column studies

The sorption parameters (K_d, f_e, and α_k) were determined through laboratory column studies for herbicides: glyphosate, atrazine, simazine and prometryn. It was not possible to study the process of degradation due to short duration of the experiments. However, discrete samples were collected at the outflow, so the developed pollutant transport

model was used to estimate the sorption parameters. This was done in a two-step process:

- Estimation of the conservative transport parameters using tracer test's results
- Estimation of the reactive transport parameters using herbicide tests' results.

Both steps were done using the developed model and the calibration procedure (Chapter 5.2.2).

5.3 Model testing results and discussion

5.3.1 Model calibration and verification with field data

5.3.1.1 Flows

The model was mostly capable of predicting flow rates for both cells and both test series (Figure 5-5, Figure 5-6). However, events following long dry periods (e.g. TESTS 1-6, 2-6) showed some disagreement i.e. the model was "late" and failed to predict high initial peak in the flow rate, which can probably be attributed to the cracking of the soil in both cells (which was not represented by the model itself).

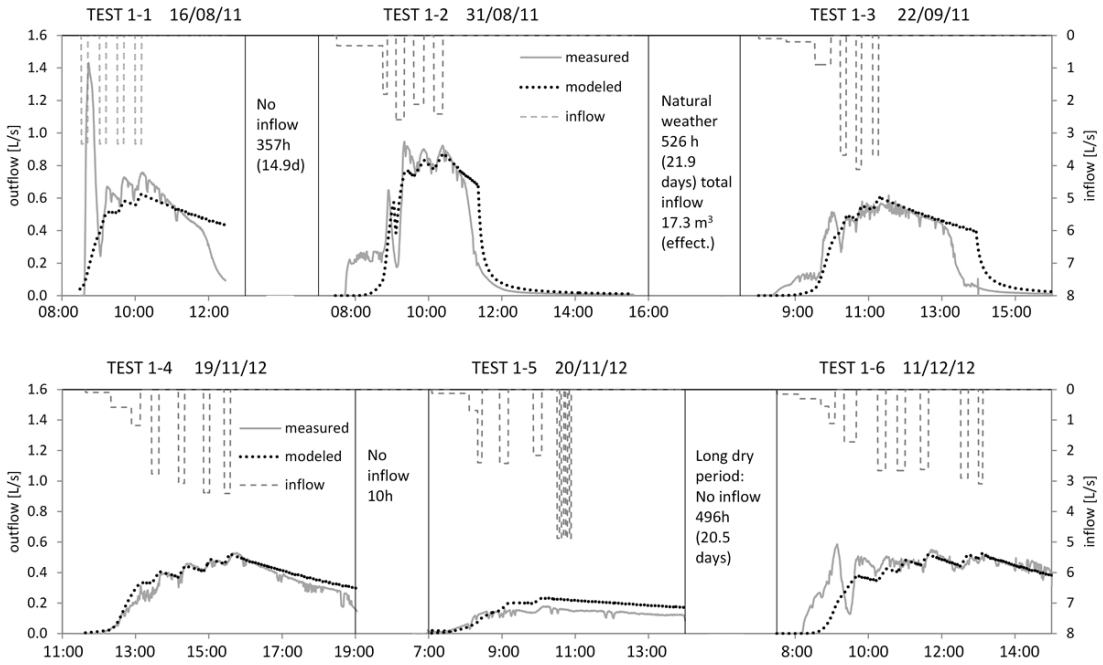

Figure 5-5 Inflow, measured and modelled flow at the outflows of Cell 1 for the two test series: calibration data from 2012, E = 0.876 (bottom), verification data from 2011, E = 0.611 (top). Nomenclature TEST X-Y: X – cell number, Y – test number

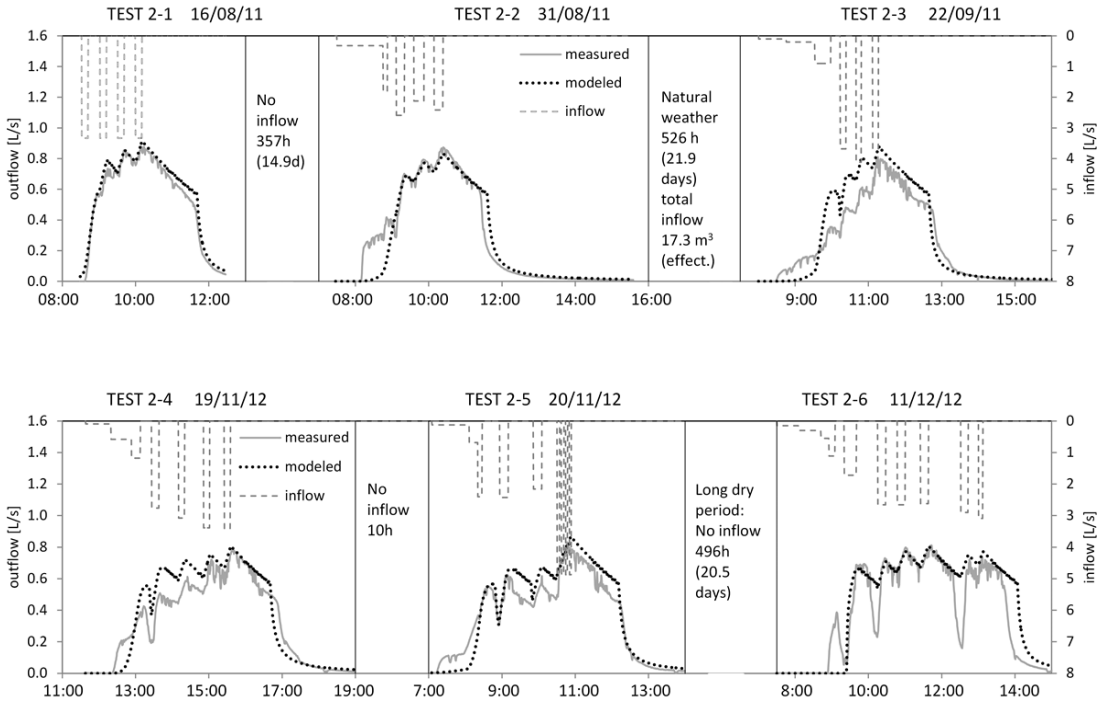

Figure 5-6 Inflow, measured and modelled flow at the outflows of Cell 2 for the two test series: calibration data from 2012, E = 0.881 (bottom), verification data from 2011, E = 0.904 (top)

The slight difference between simulated and measured flows was also evident with events that start with low inflows (e.g. TESTS 1-2, 1-3, 2-2, 2-3). This was very likely a consequence of biofilters not behaving as one-dimensional systems (variably saturated along cross-section), which was the main assumption of the flow module. Cell 1 had an additional peculiar event, which started with high inflow (TEST 1-1), where model failed to predict the extremely high initial flow peak (again, possible short-circuiting due to high organic content soils' tendency to crack when dry; similar was not seen with soil in TEST 2-1).

5.3.1.2 Micropollutants

Figure 5-7 to Figure 5-16 show the agreement between simulated and measured concentrations and fluxes in outflows for glyphosate, atrazine, prometryn, simazine, and chloroform in Cells 1 and 2. Table 5-2 shows the Nash-Sutcliffe model efficiency coefficient, E, for concentrations for both calibration and verification events, as well as the calibrated model parameters and their literature values (as per Mackay et al., 2006).

The modelled glyphosate concentrations followed well the measured calibration data for Cell 2 (e.g. the model efficiency was 0.736), but slightly underestimated outputs for the verification series (E = 0.611/0.486) (Figure 5-8). Although, E value of 0.611 might indicate good agreement, E value of 0.486, calculated for TESTS 2-2 and 2-3 only (excluding 2-1, where measured outflow concentrations were below the detection limit), is a more reliable performance indicator. The concentrations in both TESTS 2-2 and 2-3 were underestimated and one reason can be the failure to detect any inflow concentration in TEST 2-1 i.e. the absence of glyphosate in the inflow might be a measurement fault, since the inflow tank was dosed with the same amount of pollutant as in the other tests (Table 3-3). If this was the case, then the mass is not balanced for the field test data i.e. the modelled biofilter is "supplied" with less inflow pollutant mass than the actual biofilter.

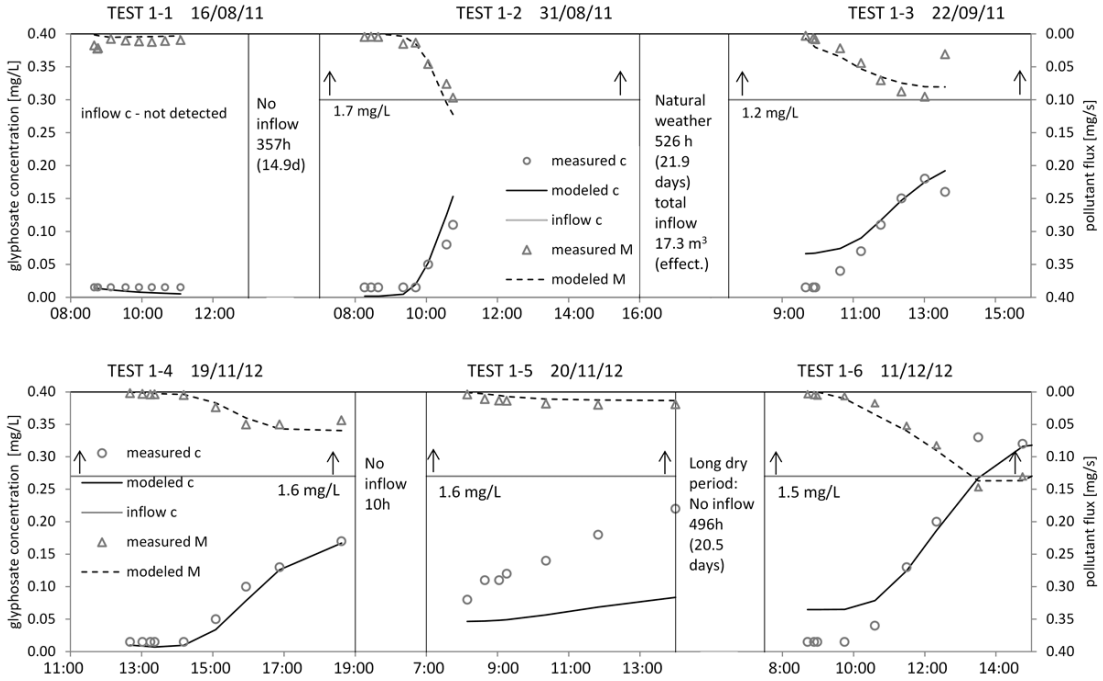

Figure 5-7 Inflow and outflow concentration and pollutant flux time series for glyphosate and Cell 1: calibration, E = 0.575 (bottom), verification, E = 0.545 (top)

On the other hand, it is possible that not all the processes relevant to the glyphosate removal were presented by the model: e.g. biomass growth/die off, or some sorption related phenomena (Figure 5-7). Biomass dynamics was willingly excluded from the

model, as it would require large amount of additional data. On the other hand, peculiar behaviour of glyphosate (unexpectedly high outflow concentrations i.e. leaching) was observed even in controlled laboratory conditions with non-vegetated columns (e.g. Magga et al., 2012), so it might be that for reliable per-event prediction sorption model would need additional leaching component (desorption is already present). Although alteration can be done to the model for it to be more precise, the simplicity (low data requirements) and good performance indicators (E values mostly above 0.5) go in its favour. This is additionally confirmed with Cell 1, where the model efficiency was 0.575 for 2012, and 0.545 for 2011 (Table 5-2), with model equally under- and over-estimating concentrations.

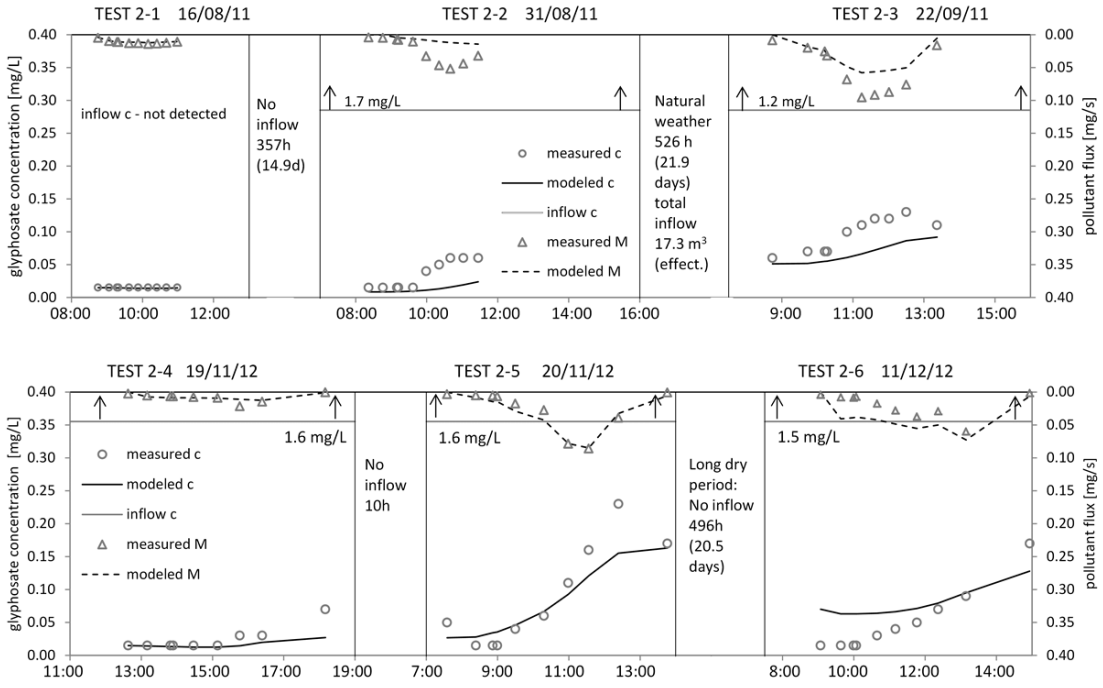

Figure 5-8 Inflow and outflow concentration and pollutant flux time series for glyphosate and Cell 2: calibration, E = 0.736 (bottom), verification, E = 0.611 (top)

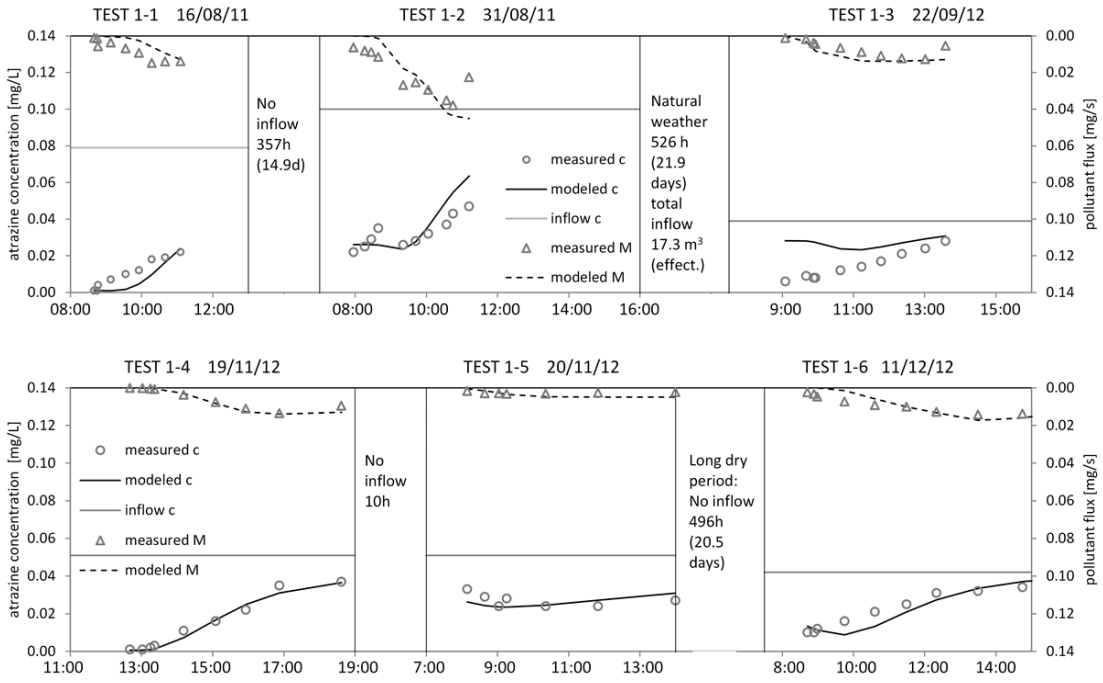

Figure 5-9 Inflow and outflow concentration and pollutant flux time series for atrazine in Cell 1: calibration, E = 0.876 (bottom), verification, E = 0.536 (top)

The model was successful in replicating the fate of all three triazines (E value well above 0.5), with well simulated starting and ending concentrations and its variability/trend during most events (except simazine). Events where outflow concentrations were underestimated consistently among pollutants were the ones following long dry periods (e.g. 2-3, 2-6 or 1-3 seen in Figure 5-10, Figure 5-12, Figure 5-14 or Figure 5-9, Figure 5-11, Figure 5-13). It is hypothesized that this was a consequence of inflow applied in pulses, rather than continuous flow (Figure 5-5, Figure 5-6), on the dry filter media (that must have contained some cracks), which emphasized flow along preferential paths with decrease in the residence time. The two E values reported for Cell 1 for prometryn and simazine (Table 5-2) were for: (1) the entire test series (negative) and (2) TEST 1-1 and 1-2 only. TEST 1-3 was found to decrease the model performance indicator substantially, as the outflow concentrations were very low, therefore, slight difference in modelled and measured concentrations (e.g. order of measurement precision) gave a high relative error. A visual inspection, however, assured that the modelled outputs were following trends in the measured data.

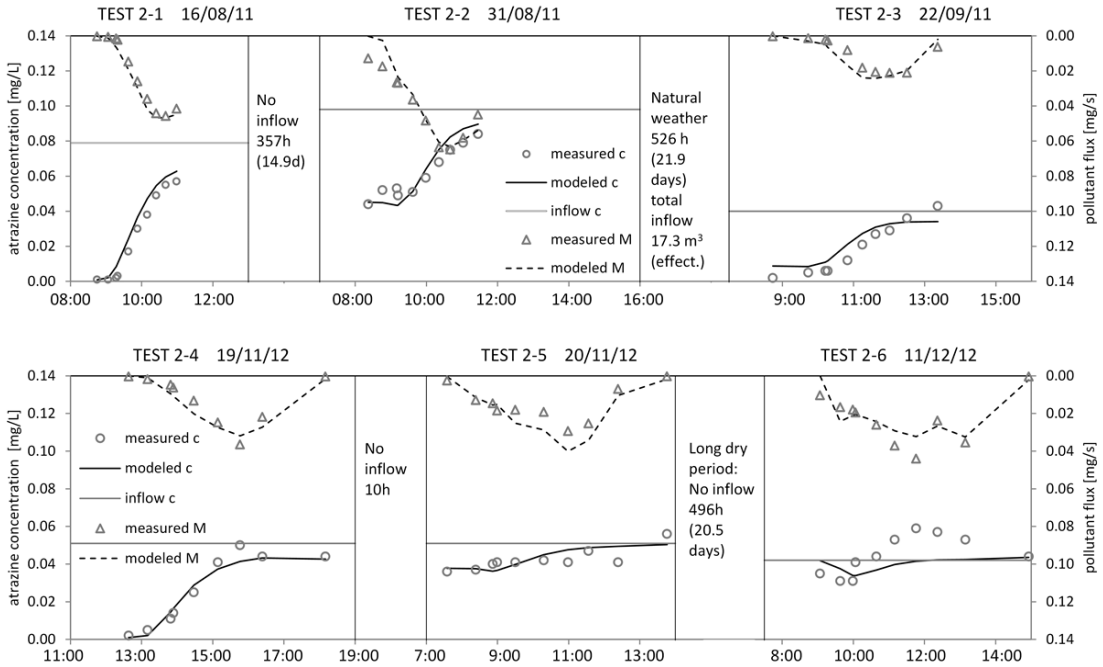

Figure 5-10 Inflow and outflow concentration and pollutant flux time series for atrazine in Cell 2: calibration, E = 0.776 (bottom), verification, E = 0.941 (top)

Chloroform was the only pollutant where modelling of volatilization was included. The model's performance was excellent, with high values of E high: for calibration series being above 0.9, and verification around 0.7 (Table 5-2). On TESTS 2-2 and 2-3 (Figure 5-16), as well as on 1-2 and 1-3 (Figure 5-15), outflow concentrations were slightly underestimated which was, again, hypothesized to be a consequence of cracks formed after long dry periods.

The calibrated pollution transport parameters are in the range of reported literature values (Table 5-2), with Cell 1 being characterized by lower sorption parameter values (literature median) and longer degradation half-life (literature maximum) than Cell 2. Glyphosate was found to be very persistent in Cell 1 ($T_{1/2}$ = 198) and somewhat degradable in Cell 2 ($T_{1/2}$ = 51). It was also found to be sorbable (logK_{oc} = 2.87/4.39) and somewhat prone to kinetic sorption: greater fraction of sites is prone to kinetic sorption in Cell 1 (89% compared to 67%), with kinetic sorption rate also being higher (1.5 compared to 0.18E-05 s^{-1}). The three triazines showed similar sorption characteristics, with prometryn having the highest soil-water partitioning coefficient of the three (logK_{oc} = 2.30/3.34), and simazine, on average, being the most prone to kinetic

sorption (60-70% of sites, 0.5 to 7E-05 s^{-1} kinetic sorption rate). The similar behaviour of triazines is not unusual, as they share similar molecular structure.

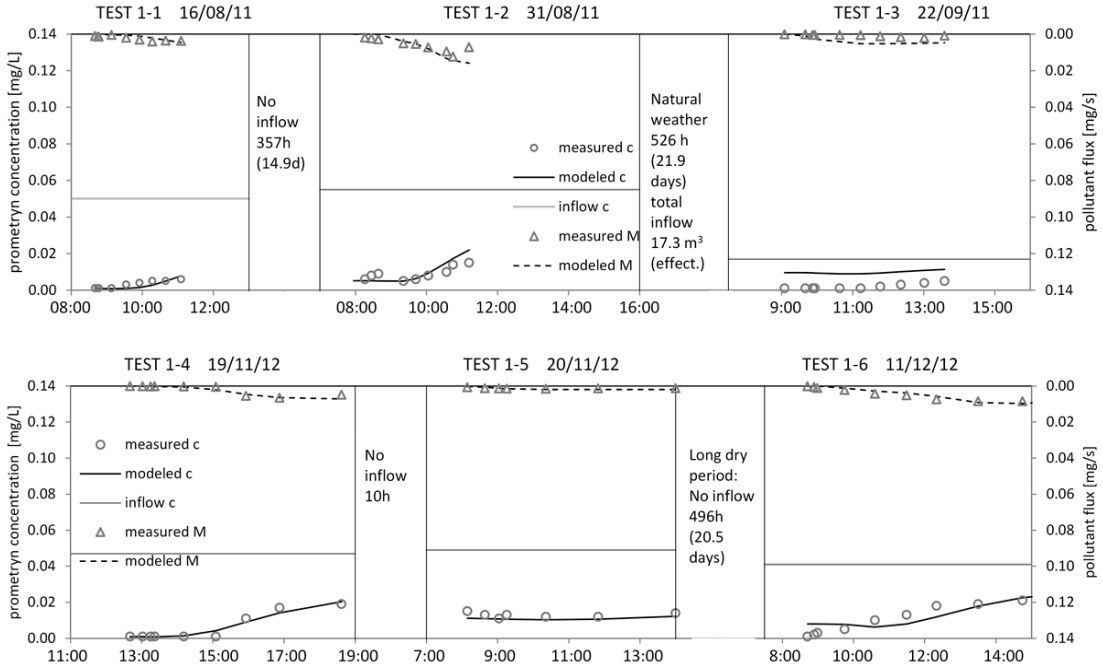

Figure 5-11 Inflow and outflow concentration and pollutant flux time series for prometryn in Cell 1: calibration, E = 0.730 (bottom), verification, E = 0.782(0.595) (top)

As for the degradation, atrazine and prometryn were found to be persistent in Cell 1 ($T_{1/2}$ around 140 days), unlike simazine ($T_{1/2}$ = 61 days), while all three were prone to degradation in Cell 2 ($T_{1/2}$ is 23 to 37 days). Calibrated parameters showed that chloroform was almost completely prone to kinetic sorption (99% of sites), with high soil-water partitioning coefficient (close to simazine). Chloroform was found to be degradable in both cells ($T_{1/2}$ = 35/24 days). As for volatilization, chloroform half-life in a biofilter system was longer than what is reported in literature, and that may be because data is reported for far larger water bodies with higher horizontal velocities than found in biofiltration ponds (e.g. horizontal water velocity in the tested cells would be close to zero for most of the experiments). The volatilization time is almost identical for the two cells, which is expected, since ponding zone was identical for the two (same surface, same depth).

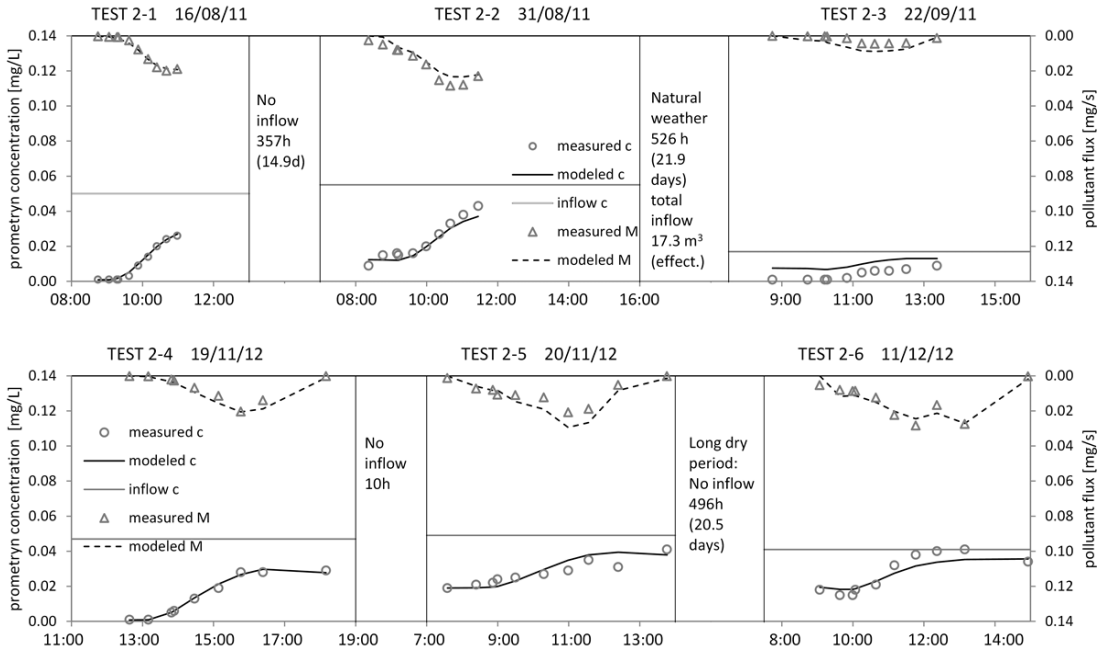

Figure 5-12 Inflow and outflow concentration and pollutant flux time series for prometryn in Cell 2: calibration, E = 0.907 (bottom), verification, E = 0.893 (top)

Comparing Cells 1 and 2, it can be concluded that pollutants experience higher degradation rate in Cell 2, which might seem unexpected since this cell has the filter media material with smaller specific surface (i.e. lower content of clay and silt), and lower nutrient content – both factors that can cause a decrease in biomass growth. Cell 2, unlike Cell 1, has a submerged zone, which is shown to maintain soil moisture regime capable of sustaining both plant and microbial activity especially during prolonged dry periods (Zinger et al, 2013). It is interesting to note the difference in K_{oc} values between the two cells for the same pollutant (higher in Cell 2), as this parameter is usually assumed to be only pollutant specific. It is hypothesized that the difference is due to the neglect of sorption to other matter other than organic carbon that is present in the soil (e.g. cations, dissolved organic content etc.), meaning that the sorption is not driven by f_{oc} only (so that K_{oc} value obtained is not the "real" K_{oc} value, and therefore not constant for a single pollutant). It can also be noted that the soil pH values of the two cells did not differ enough (Cell 1: pH=7.1, and Cell 2: pH=7.4) to cause the difference in K_{oc} values (as suggested by Jeppu et al., 2012).

Table 5-2 The Nash-Sutcliffe values between the measured and modelled concentration, E, and the model parameter values as calibrated and reported by Mackay et al. (2006)

		Literature values				
			$logK_{oc}$		$T_{1/2}$	T_{vol}
		Lower	Median	Upper	[d]	[d]
	Glyphosate	1.22	3.1	4.38	20, 47, 100	
	Atrazine	0.7	2.1	4.2	36, 75, 150	
	Prometryn	1.77	2.3	3.24	40, 60, 150	
	Simazine	1.68	2.7	3.66	30, 75, 180	
	Chloroform	1.4	1.8	2.8	10, 50, 100	0.5, 1

				Calibrated model parameters				
		E		fe	$logK_{oc}$	α_K	$T_{1/2}$	T_{vol}
	Cell	2012	2011	[-]		[s^{-1}]	[d]	[d]
Glyphosate	1	0.575	0.545	0.107	2.87	1.51E-05	198	
	2	0.736	0.611	0.326	4.39	0.18E-05	51	
Atrazine	1	0.876	0.536	0.375	1.81	1.02E-05	142	
	2	0.776	0.941	0.095	2.83	5.66E-05	23	
Prometryn	1	0.730	-0.782 (0.595)	0.179	2.30	0.53E-05	143	
	2	0.907	0.893	0.201	3.34	3.79E-05	27	
Simazine	1	0.700	-0.286 (0.293)	0.294	1.76	0.49E-05	61	
	2	0.511	0.285	0.378	2.87	6.99E-05	37	
Chloroform	1	0.967	0.705	0.010	1.05	52.8E-05	35	5.11
	2	0.947	0.685	0.011	3.03	0.43E-05	24	5.14

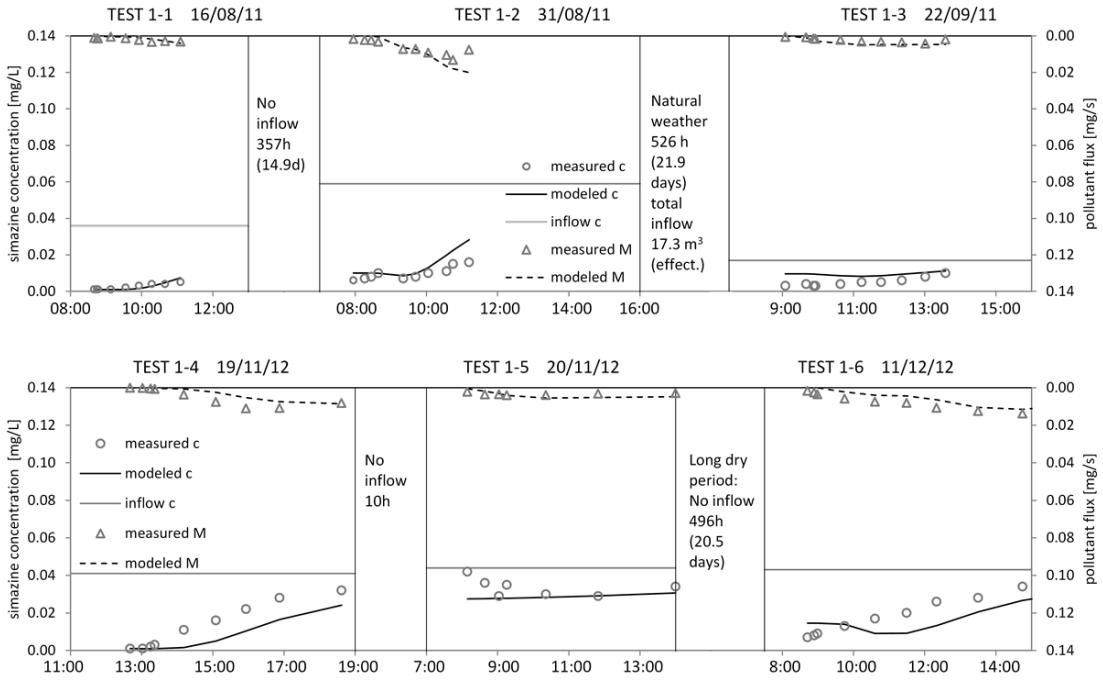

Figure 5-13 Inflow and outflow concentration and pollutant flux time series for simazine in Cell 1: calibration E = 0.700 (bottom), verification E = 0.286(0.293) (top)

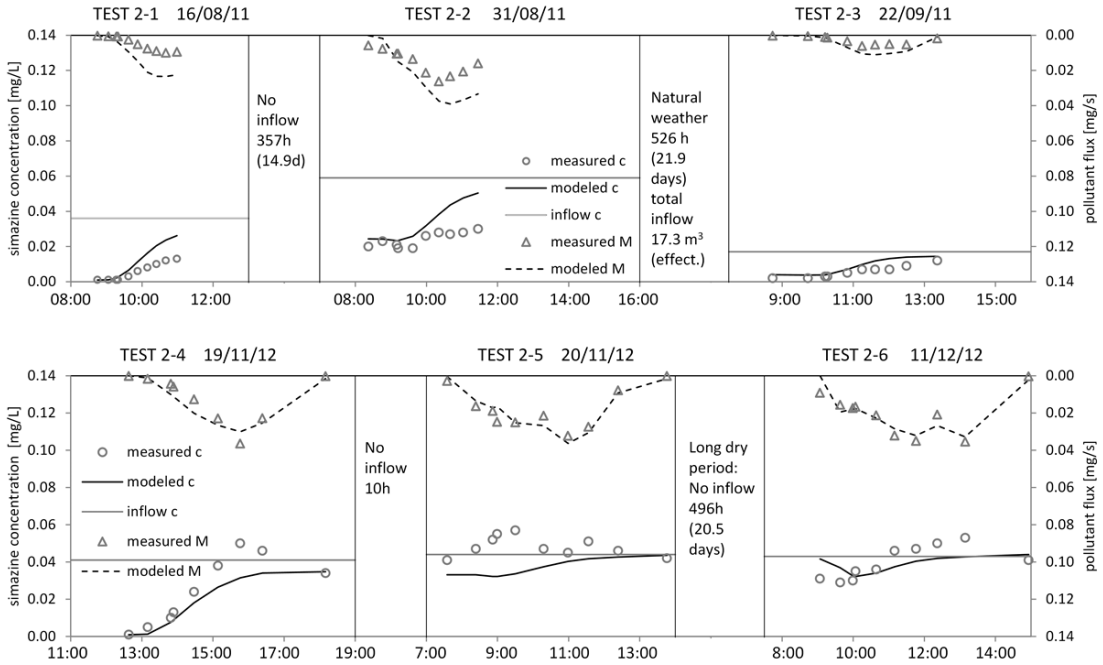

Figure 5-14 Inflow and outflow concentration and pollutant flux time series for simazine in Cell 2: calibration, E = 0.511 (bottom), verification, E = 0.285 (top)

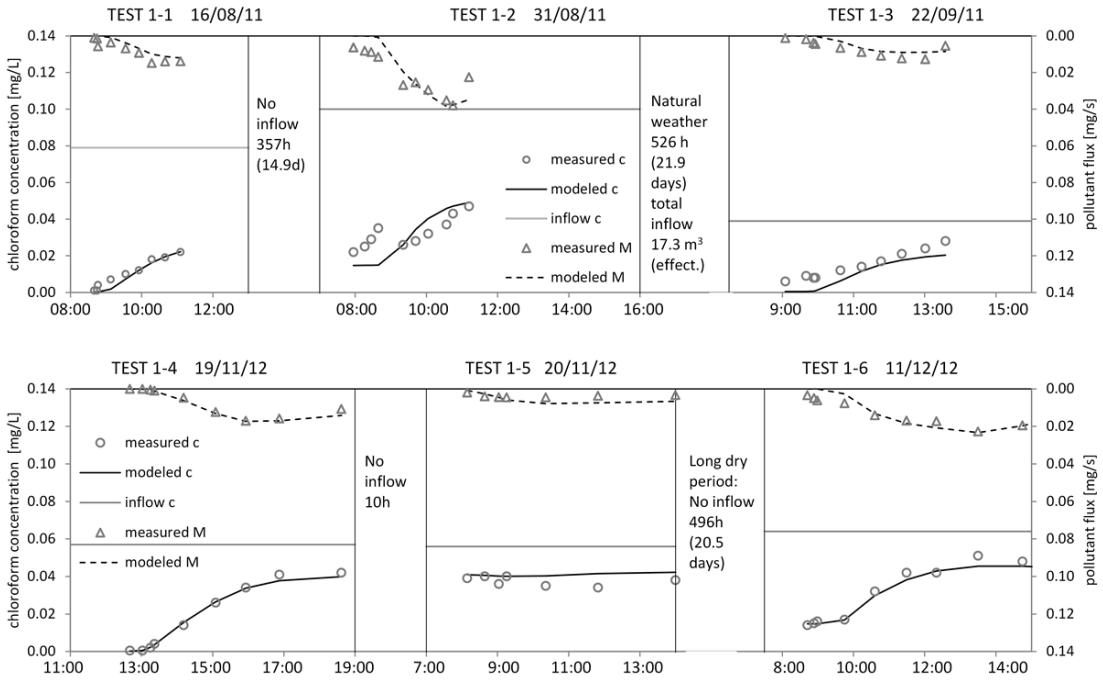

Figure 5-15 Inflow and outflow concentration and pollutant flux time series for chloroform in Cell 1: calibration, E = 0.967 (bottom), verification, E = 0.705 (top)

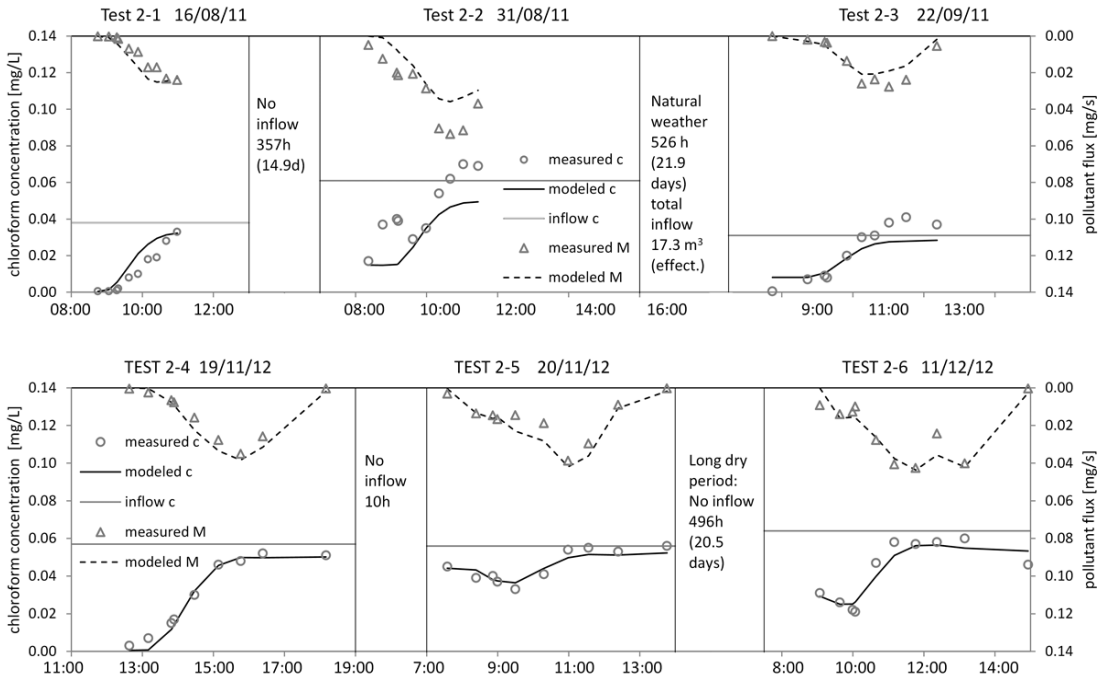

Figure 5-16 Inflow and outflow concentration and pollutant flux time series for chloroform in Cell 1: calibration, E = 0.947 (bottom), verification, E = 0.685 (top)

5.3.1.3 Performance assessment

To get a more general performance assessment, scatter plots of measured vs. modelled event mean concentrations and event loads were made. The 1:1 line separates the zones where the model is overestimating – below the line, from where it is underestimating EMCs (or event loads) – above the line, as can be seen in Figure 5-17.

Figure 5-18 to Figure 5-20 show scatter plots of measured vs. predicted EMCs (in mg/L) and event loads (in mg) for atrazine, prometryn, simazine, glyphosate and chloroform for both cells and 6 separate events giving a total of 12 events per micropollutant. Additionally, graphs include E and R^2 values, showing how well the two (measured and modelled) agree.

Figure 5-18 to Figure 5-20 show the performance of model on the triazines: atrazine and prometryn have very high values of E and R^2 for both EMCs and event loads, while model was slightly underestimating simazine, equally for both cells 1 and 2. The E values are still quite high (above 0.77), so the model is still considered to do a good job.

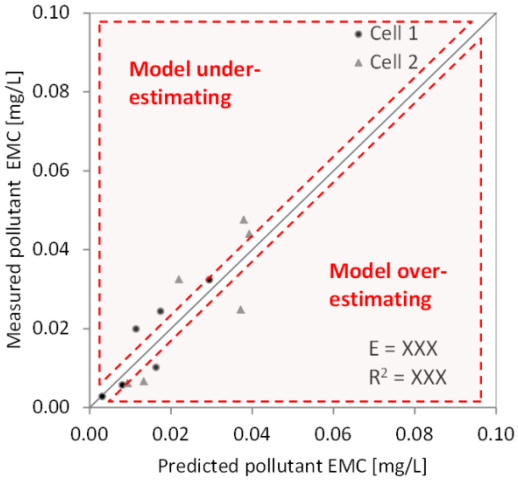

Figure 5-17 The predicted and measured pollutant Event Mean Concentration (EMC) with marked zones where the model is under and over estimating EMCs

Glyphosate EMCs were probably predicted the worst by the model, as can be seen in Figure 5-19 - bottom, where major underestimate is evident for Cell 1 – and this is related to TEST 1-5 (Figure 5-7). This only complements the discussion on page 118 regarding the unpredictable behaviour of glyphosate. Although the event loads of glyphosate seem to be well predicted, since the values of E and R^2 are above 0.8, this is misleading. The actual source of the high numeric values is the peculiar high event in cell 1 (event load above 2000 mg). Without this event, the actual values of E and R^2 are 0.616 and 0.605 respectively, which still can be considered rather high.

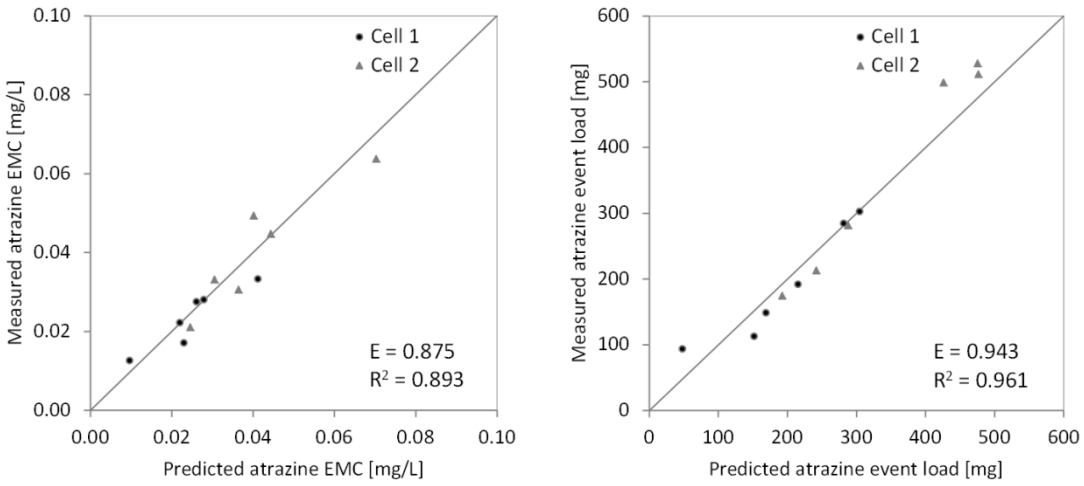

Figure 5-18 Predicted and measured pollutant Event Mean Concentration (EMC) in mg/L (left) and event load in mg (right) for atrazine

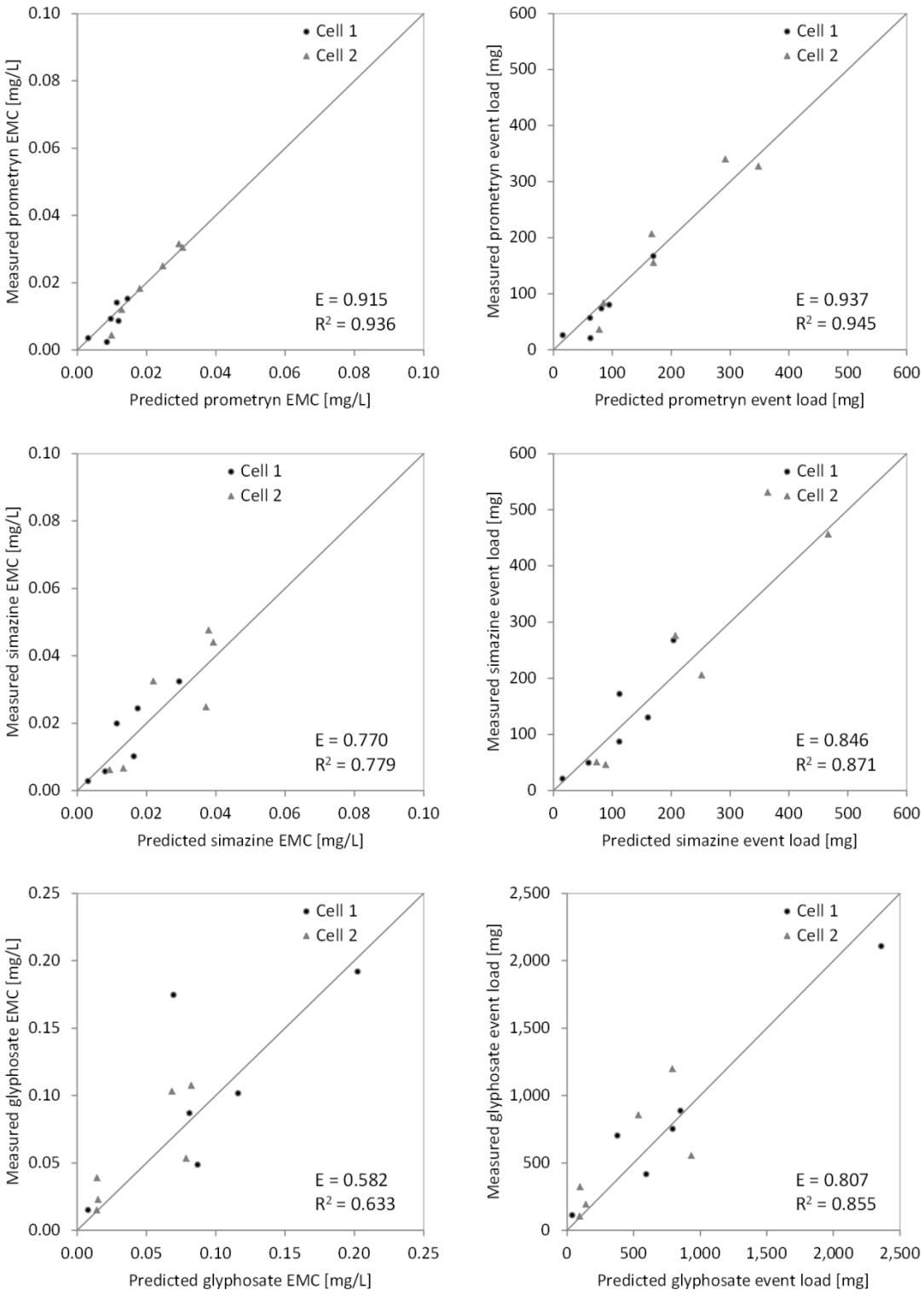

Figure 5-19 Predicted and measured pollutant Event Mean Concentration (EMC) in mg/L (left) and event load in mg (right) for prometryn (top), simazine (middle) and glyphosate (bottom)

As for the chloroform, the model shows good predictive capabilities, as most of the EMCs and event loads are estimated well (Figure 5-20).

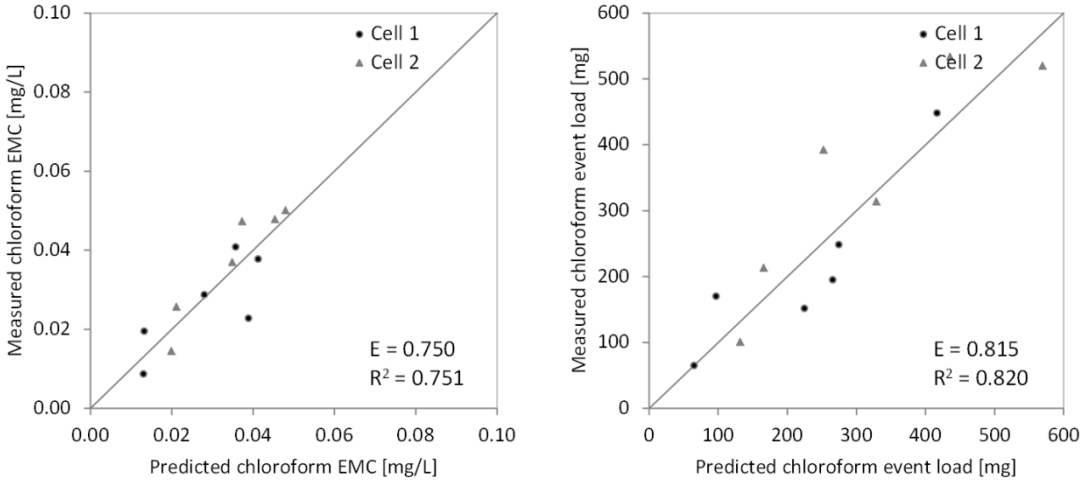

Figure 5-20 Predicted and measured pollutant Event Mean Concentration (EMC) in mg/L (left) and event load in mg (right) for chloroform

5.3.2 Model parameter estimation via laboratory testing

5.3.2.1 Pollutant transport module parameters estimation from batch tests

Figure 5-21 shows the results of performed batch experiments as the change of fluorescein concentration in the water phase (*c(t)*, left) and the change of fluorescein concentration in the soil phase (*s(t)*, right) for experiment duration. The latter one was derived from the mass balance and the known soil-water ratio.

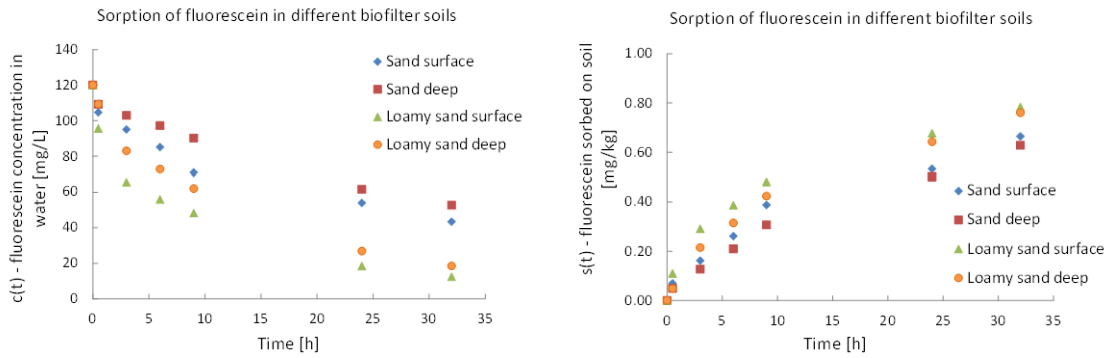

Figure 5-21 Batch test results: sorption of fluorescein in different biofilter soils – fluorescein concentration in water (left) and fluorescein concentration on soil (right)

The sorption kinetics exhibited a two-step process: the initial step was quite rapid (< 0.5 hr), while the second step was slower and exhibited equilibration. It was assumed

in this study that instantaneous sorption occurred in the first rapid step while the first-order sorption occurred in the second step (as per Eq. 5.7). The sorption parameters (f_e, α_k and K_d) were estimated as explained in Figure 5-4 and Eqs. 5.8 and 5.17. Figure 5-22 depicts estimation of kinetic sorption rate, as well as R^2 values obtained for each soil.

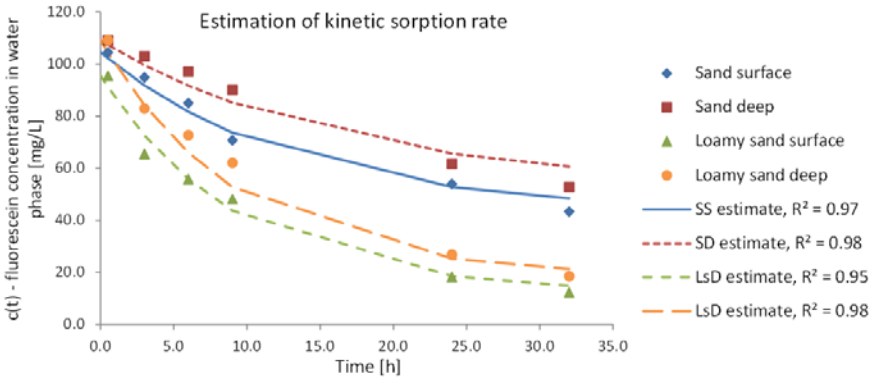

Figure 5-22 Batch test results analysis: estimation of kinetic sorption rate of fluorescein in different biofilter soils

Table 5-3 Transport and fate model parameters for fluorescein obtained from laboratory batch studies and model calibration

Model parameters	Parameters estimated from laboratory experiments				Calibrated parameters to achieve the best fit to *in-situ* data[2]	
Model type	Cell 1		Cell 2		Cell 1	Cell 2
	S	D	S	D	S/D	S/D
Instantaneous sorption fraction, f_e [-]	0.23	0.21	0.20	0.16	0.19	0.13
Kinetic adsorption rate, α_k [h^{-1}]	0.11	0.11	0.078	0.061	0.085	0.055
Soil water partit. coefficient K_d [L kg^{-1}]	2.2	1.4	0.45	0.33	2.7	1.5
Biodegradation rate, K_{bio} [h^{-1}]	2.5E-03	1.5E-03	3.0E-03	2.9E-03	2.9E-03	9.0E-03
Nash-Sutcliffe coefficient, E	-1.2 / -0.54[1]		0.67 / 0.88[1]		0.69	0.90

[1] E value based on the whole part of the test/E value based only on spiking part of the test;

[2] combined calibrated parameters of surface and deeps soils were obtained to avoid over-parameterization.

Table 5-3 shows transport and fate model parameters for fluorescein obtained from laboratory batch studies and model calibration. The f_e, α_k and K_d values of loamy sand (average 0.22, 0.11 h^{-1} and 1.8 L kg^{-1}, respectively) were higher than that of sand media (average 0.18, 0.070 h^{-1} and 0.39 L kg^{-1}, respectively), which may be due to the higher

clay and organic matter content in loamy sand media compared to sand media (Table 3-1). It has been reported that higher soil organic matter content may contribute to higher sorption capacity (René and Schwarzenbach, 1993). Similarly, these parameter values in surface media were higher than that in the deep media. The first order kinetic rate (α_k) in this study was much lower than that was found by Abdus-Salam and Buhari (2014) who used pseudo-first order to describe the kinetic adsorption of fluorescein (α_k =3.36h^{-1}). The K_d value estimated in this study (average 0.39 L kg^{-1} for sand and 1.8 L kg^{-1} for loamy sand) were lower than the reported value (K_d = 10.3 L kg^{-1}) by Omoti and Wild (1979) who used loamy sand (~85% sand, ~10% clay) to study fluorescein adsorption equilibrium through column experiments. However, the values of this study were close to reported value (K_d = 0.33L kg^{-1}) by Sabatini and Austin (1991) who used aquifer sand (97.3% sand, 2.2% silt and 0.5% clay) to study adsorption characteristics of fluorescein using batch experiments. The differences between soil properties of the studied biofilter media (Table 3-1) and other studies may be attributed to the different K_d values.

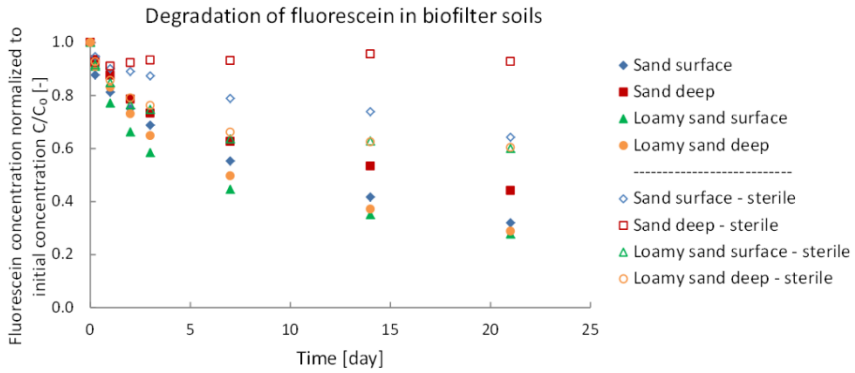

Figure 5-23 Batch test results: degradation of fluorescein in different biofilter soils

Figure 5-23 shows changes of fluorescein concentration in different soils during performed degradation-batch experiments: sterile soils were assumed to experience sorption only, while regular samples were assumed to experience a combination of sorption and degradation. Fluorescein concentration dropped in all the soils during the entire experiment (~21 days). As anticipated, the decrease in concentration was lower for the sterile-soils when compared with regular ones, with the least decrease in sterile sand deep soil (~10% reduction). Figure 5-24 presents estimation of a degradation rate

from the trend in fluorescein concentration change: the concentrations from the experiments were first adjusted, so to show net-degradation (without sorption). The change was assumed to follow first-order kinetics. The numerical values are shown in Table 5-3. From these results, it is evident that the degradation process was having a much slower pace than the sorption kinetics. However, degradation cannot be neglected, especially during the dry weather periods that occur between storm events, as some of these periods can be up to 500 hours (more details in Zhang et al., 2014). As can be seen in Figure 5-23, the drop in fluorescein concentration for long dry periods (> 500 h) due to degradation only can be up to 30% for the deep loamy sand or sand soils. Slightly higher biodegradation rates were found in the sand media (3.0×10^{-3} h^{-1} for surface and 2.9×10^{-3} h^{-1} for deep) compared to the loamy sand media (2.5×10^{-3} h^{-1} for surface and 1.5×10^{-3} h^{-1} for deep).

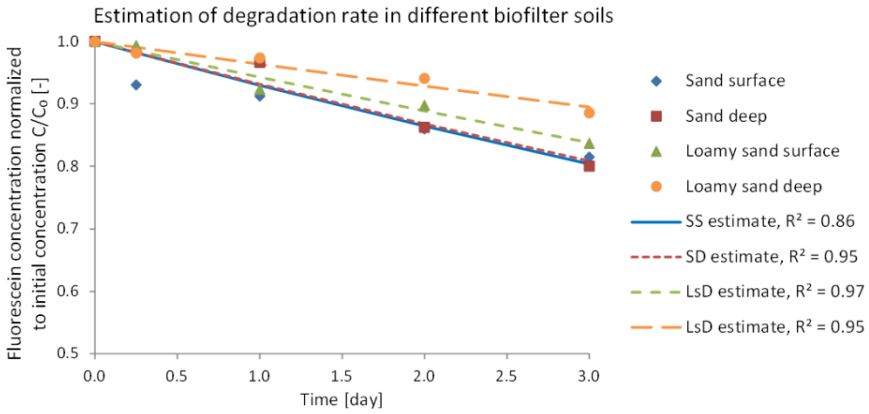

Figure 5-24 Batch test results analysis: estimation of degradation rate of fluorescein in different biofilter soils

Figure 5-25 shows how the model fits the measured outflow rates during the fluorescein field test. While the model was quite successful for Cell 2 (E = 0.709), it was not as much with Cell 1 (E = 0.284). The major difference occurred on day when both KCl and fluorescein were introduced at the same time. It is hypothesized that KCl interacted with the clay in the filter media, and actually changed the apparent soil structure, influencing the hydraulic conductivity to change as well (decrease) (as seen in other studies e.g. Shainberg et al., 1981, Yilmaz et al., 2008). Unfortunately, this discrepancy influences the pollutant modelling substantially, so conclusions made on Cell 1 should be taken with reservations.

The model parameters estimated from the batch experiments were used in a predictive mode against the field fluorescein data, and results showed good agreement with Cell 2 (E = 0.67) and poor agreement with Cell 1 (E = -1.27) (Figure 5-26).

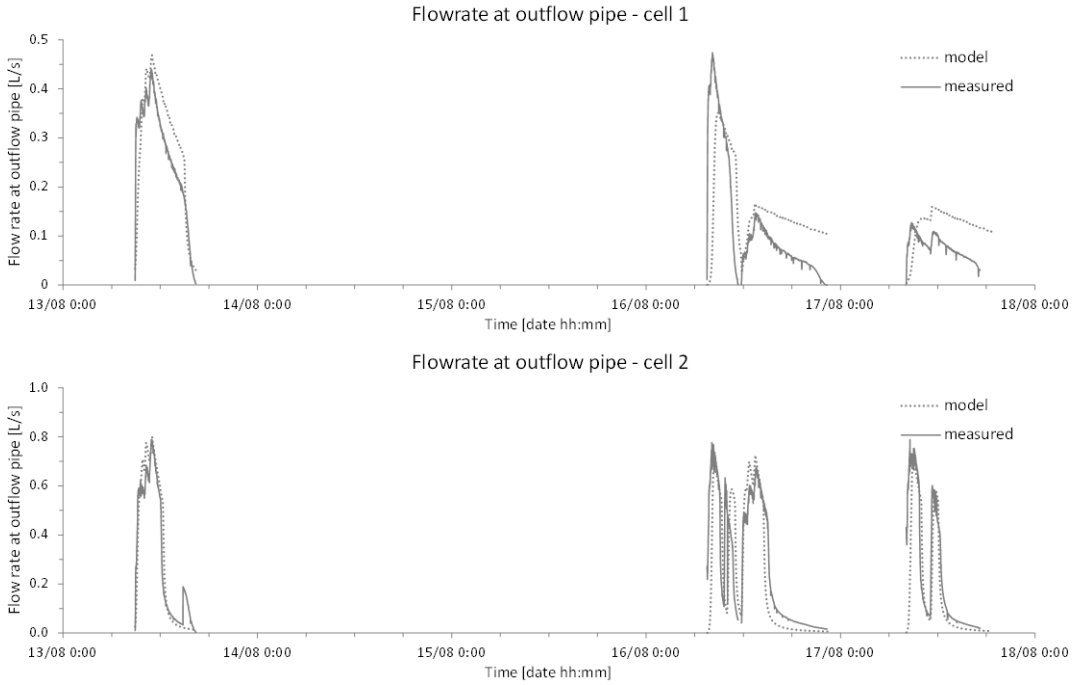

Figure 5-25 Measured and modelled flow at the outflow pipe for fluorescein test: Cell 1 (top), E = 0.284 and Cell 2 (bottom), E = 0.709

The model struggled to predict well the starting concentrations of flushing part of the test, when presumably desorption wass occurring (this holds for both cells). The high starting concentration of the flushing event could also be attributed to underestimated degradation rate. Once the initial phase of desorption occured, the model was quite successful in replicating the measured concentrations for Cell 2. As for the Cell 1, the model struggled even during events when hydraulics was well modelled (first spiking, first flushing, Figure 5-26). Since the model was overestimating outflow concentrations in all events, it is concluded that analysis of results of batch studies underestimates both sorption and degradation parameters (applicable to field conditions).

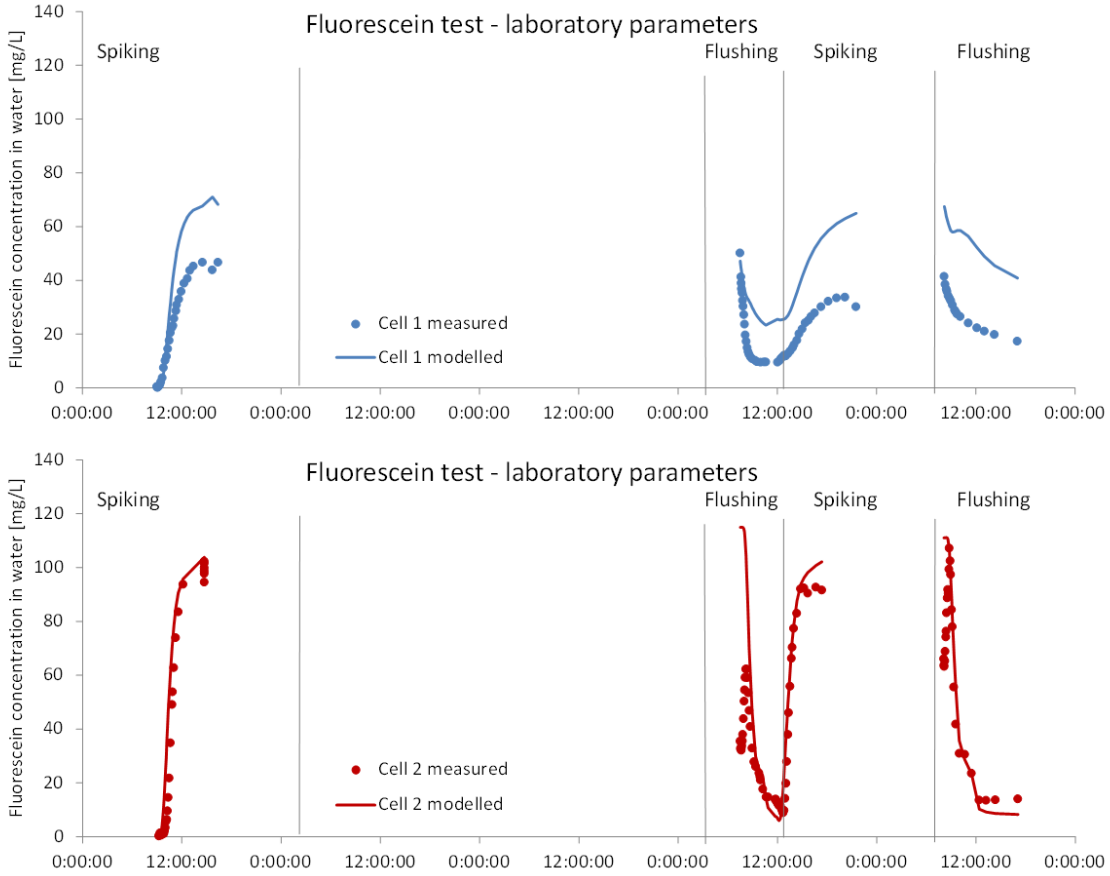

Figure 5-26 Batch test results application: measured and modelled fluorescein outflow concentration for *in-situ* test for Cell 1 (top), E = -1.27, and Cell 2 (bottom), E = 0.67. Field model parameters estimated from batch test results

The model was also calibrated with field data for both cells and the results are shown in Figure 5-27 and Table 5-3. High values of Nash-Sutcliffe are evidence of good fit (E = 0.69 for Cell 1, E = 0.90 for Cell 2). The field calibrated sorption parameters indicate a more kinetic sorption with higher soil-water partitioning coefficient when compared to estimates with batch experiments. The degradation rate is also higher, eventually producing lower starting concentrations for flushing events.

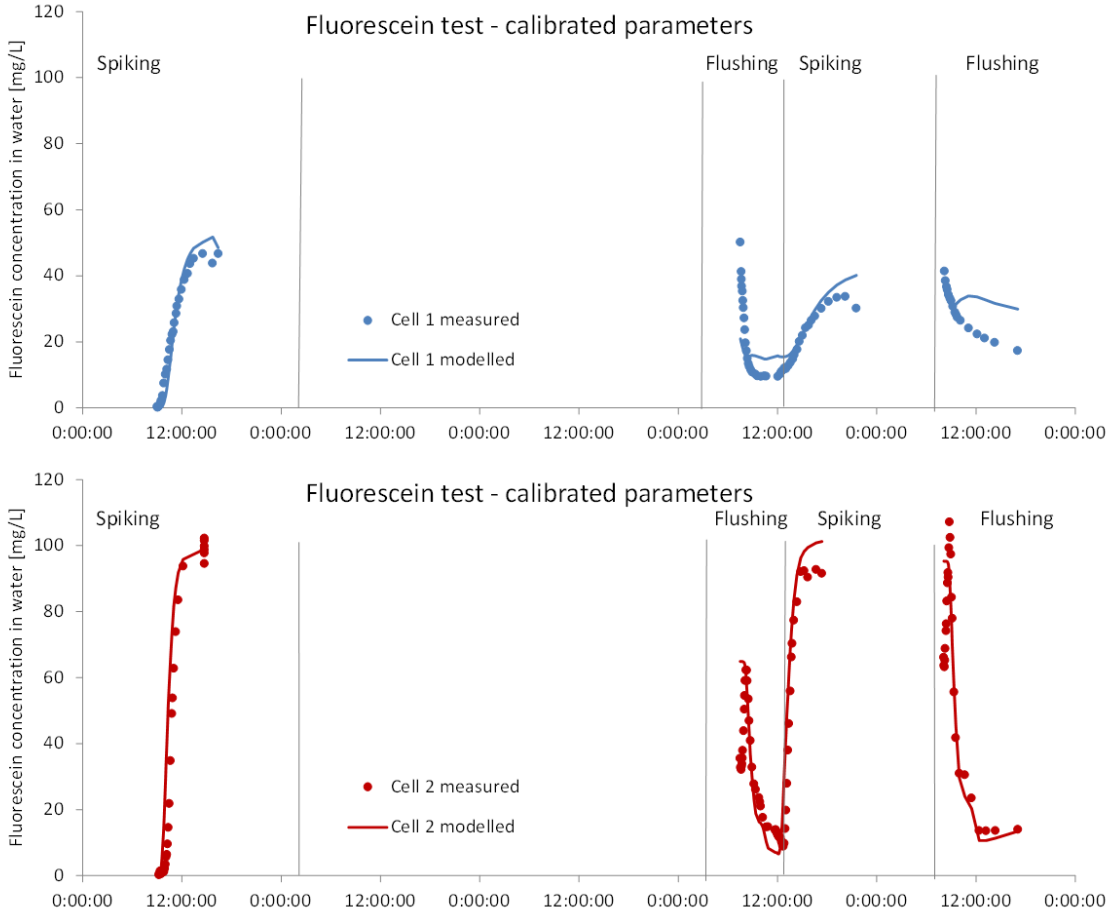

Figure 5-27 Measured and modelled fluorescein outflow concentration for *in-situ* test for Cell 1 (top), E = 0.69, and Cell 2 (bottom), E= 0.90. Field model parameters calibrated on field data

5.3.2.2 Pollutant transport module parameters estimation from column tests

As explained in Chapter 3.6.2, three replicates of columns were set up. The samples were taken simultaneously and the average concentration was reported. Figure 5-28 presents results from tracer test along with modelled values assuming conservative transport (no sorption, no degradation). A high value of the Nash-Sutcliffe coefficient (E = 0.97) indicates a very good agreement between measured and modelled concentrations, and therefore high reliability in estimated transport parameter for the conservative transport. The dispersivity (used for calculation of dispersion coefficient) was found to be quite low (α_L = 0.007 m), indicating that the flow in the columns was predominantly advective. It is hypothesized that this might be due to the uniform packing that was accomplished while setting up the columns, as well as the rinse-out of the smallest particles (see Chapter 3.6.2 for column establishment procedure).

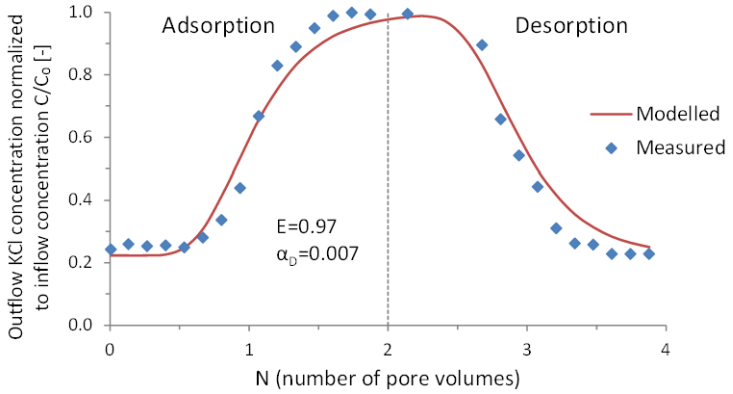

Figure 5-28 Measured and modelled outflow concentrations of KCl during column test normalized to initial concentration C/C_0

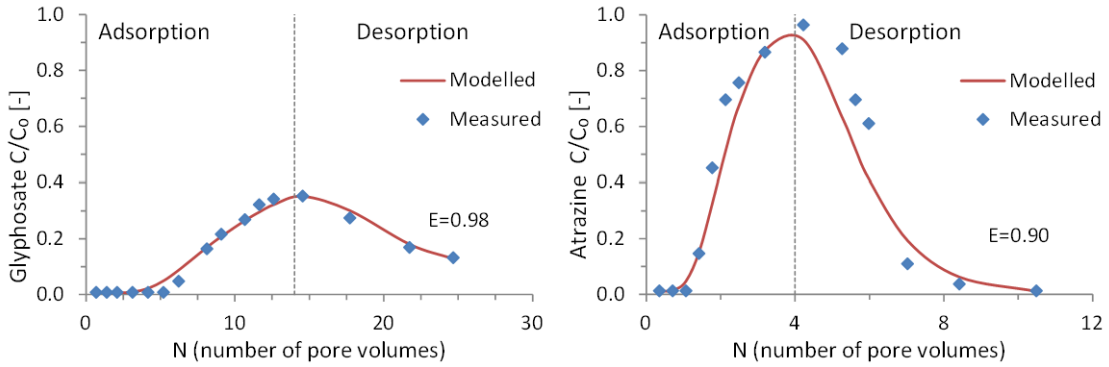

Figure 5-29 Measured and modelled outflow concentrations of glyphosate (left) and atrazine (right) normalized to initial concentration C/C_0

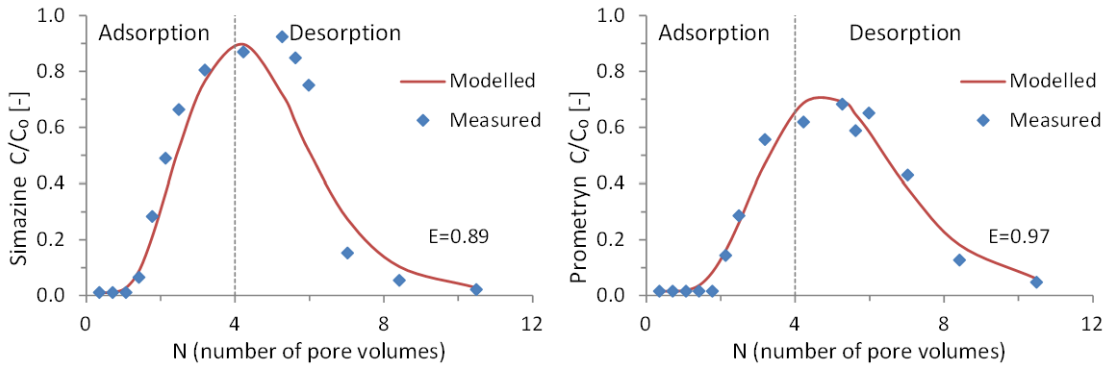

Figure 5-30 Measured and modelled outflow concentrations of simazine (left) and prometryn (right) normalized to initial concentration C/C_0

For the second step, the model was calibrated against outflow concentrations for column tests with herbicides. Figure 5-29 and Figure 5-30 show measured and modelled outflow concentrations for glyphosate, atrazine, simazine, and prometryn, as well as the performance measure (Nash-Sutcliffe). The values of E are quite high, having a range

from 0.89 (simazine) up to 0.98 (glyphosate), indicating very good estimates of sorption parameters made with column study's results.

Once the dispersivity and sorption model parameters have been estimated (Table 5-4), the model was used in predictive mode against the field data (Chapter 3.5.4). Since the degradation process was not studied in the column tests, half-life for model predictions was taken as field-calibrated values from Table 5-2. Figure 5-31 to Figure 5-34 show model predictions against field measured pollutant concentrations and fluxes for all tested herbicides. In addition to the column test estimated parameters, Table 5-4 includes E values for the column test (calibration) as well as E values for field data for both 2011 and 2012.

Table 5-4 Values of sorption model parameters calibrated on column test for herbicides; E values for column test (calibrated) and field tests (prediction)

Herbicides	E value - column test	E value – field		Calibrated parameters			Field*
		2011	2012	Log K_{oc} [log L/kg]	f_e [-]	α_k [s^{-1}]	$T_{1/2}$ [day]
Glyphosate	0.98	0.205	-1.410	4.31	0.193	6.53E-06	51
Atrazine	0.90	0.929	0.478	2.60	1.000	5.95E-05	23
Simazine	0.89	0.193	0.502	2.74	1.000	1.15E-05	37
Prometryn	0.97	0.736	0.452	3.26	0.476	1.28E-05	27

*Degradation half-life is taken from the field calibration

Model outputs for glyphosate show overestimates for both years, with especially high values obtained for 2012 (Figure 5-31, bottom). Therefore, one can assume that the column testing analysis appears to underestimate the sorption parameter values. Triazines outflow concentrations, however, were not substantially overestimated by the model for neither 2011 nor 2012. Atrazine and prometryn concentrations were modelled reasonably well, with E values being lower than field-calibrated but still around and above 0.5 (Figure 5-32, Figure 5-33). Simazine outflow concentrations were slightly overestimated, but are comparable to the field-calibrated results: E values were as follows for the two testing periods: 2011 – 0.193 for column compared to 0.285 for field and 2012 – 0.502 compared to 0.511 (Figure 5-34).

Table 5-5 Comparison of field and column calibrated sorption parameters' values

Herbicides	Field calibrated parameters			Column calibrated parameters		
	log K_{oc} [log L/kg]	f_e [-]	α_k [s^{-1}]	log K_{oc} [log L/kg]	f_e [-]	α_k [s^{-1}]
Glyphosate	4.39	0.326	0.18E-05	4.31	0.193	0.65E-05
Atrazine	2.83	**0.095**	5.66E-05	2.60	**1.000**	5.95E-05
Simazine	2.87	**0.378**	6.99E-05	2.74	**1.000**	1.15E-05
Prometryn	3.34	0.201	3.79E-05	3.26	0.476	1.28E-05

Once the column calibrated sorption parameter values were compared to the ones from the calibration against field data (Table 5-5), it was concluded that the kinetic sorption parameters (f_e, α_k) can be extremely different and still give similar results. That is, in the column tests, atrazine and simazine were found to be completely prone to instantaneous sorption, while field calibrated values point to substantial kinetic behaviour (most evident in f_e: 1.0 compared to 0.1 for atrazine, and 1.0 to 0.4 for simazine, Table 5-5).

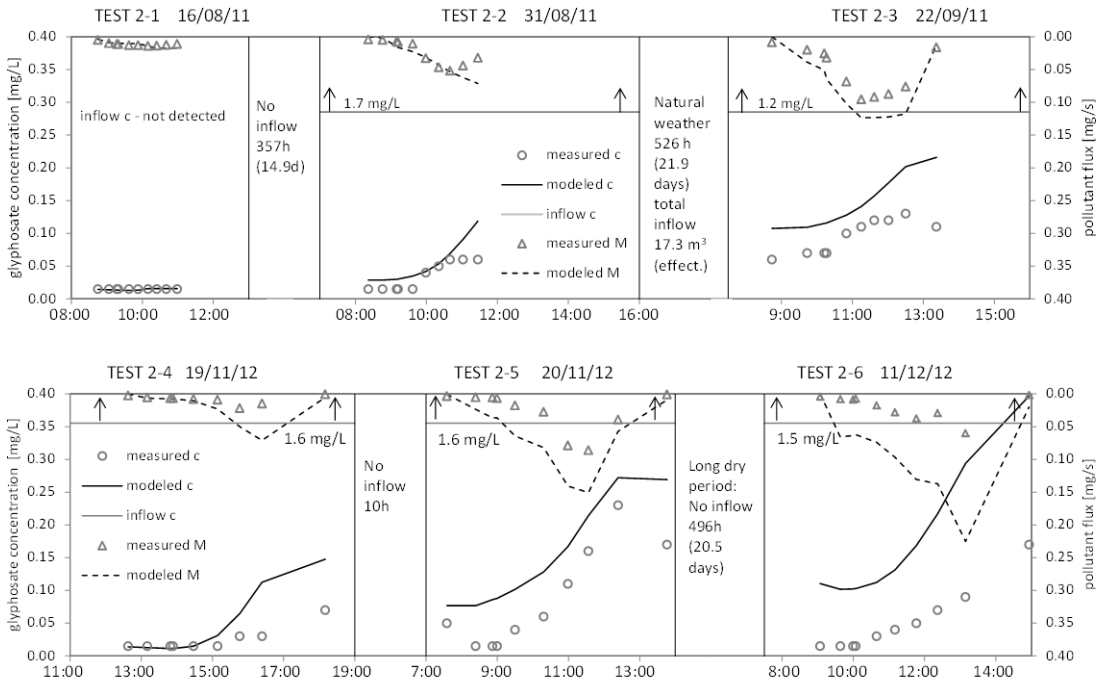

Figure 5-31 Inflow and outflow concentration and pollutant flux time series for glyphosate at Cell 2 using column test parameters: 2011, E = 0.205 (top), 2012, and E = -1.410 (bottom)

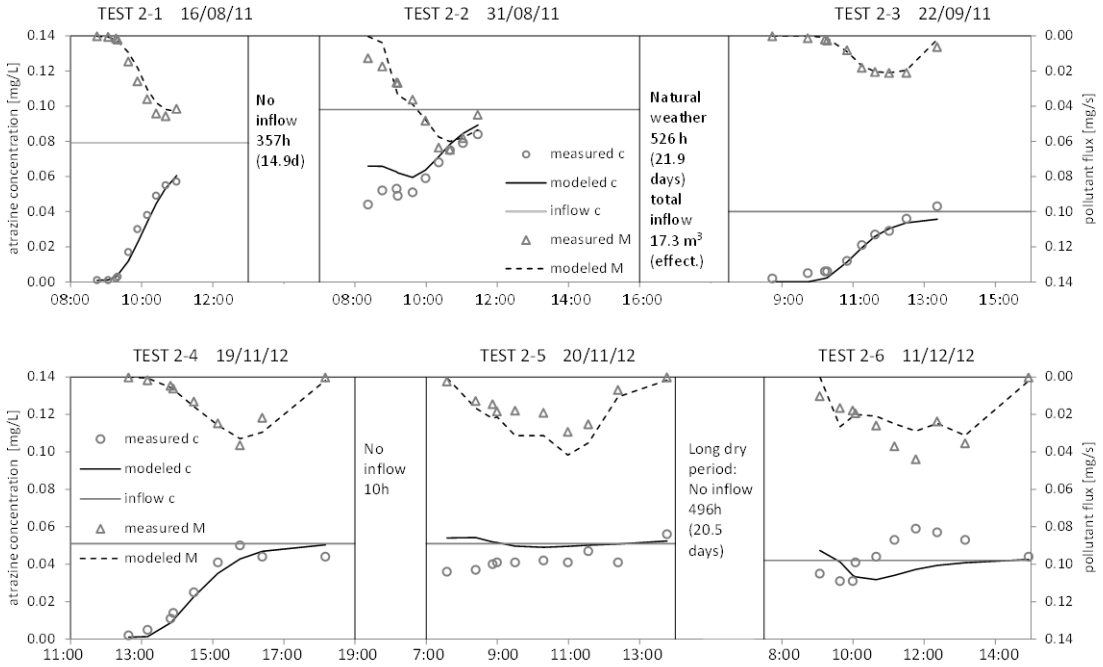

Figure 5-32 Inflow and outflow concentration and pollutant flux time series for atrazine at Cell 2 using column test parameters: 2011, E = 0.929 (top), 2012, and E = 0.478 (bottom)

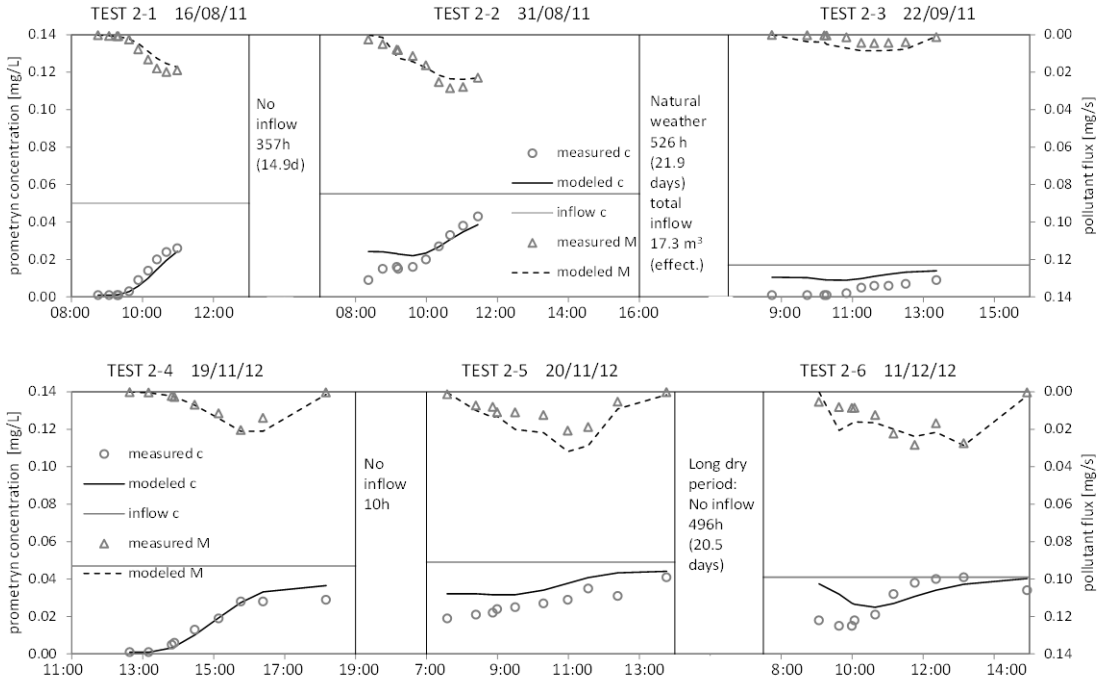

Figure 5-33 Inflow and outflow concentration and pollutant flux time series for prometryn at Cell 2 using column test parameters: 2011, E = 0.736 (top), 2012, and E = 0.452 (bottom)

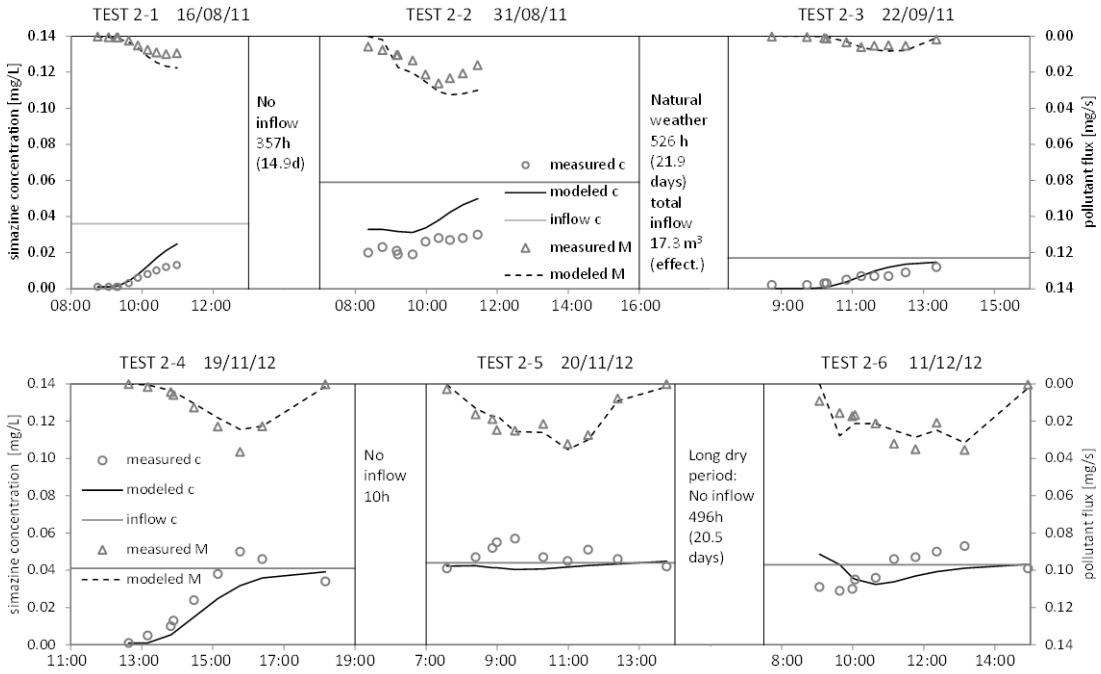

Figure 5-34 Inflow and outflow concentration and pollutant flux time series for simazine at Cell 2 using column test parameters: 2011, E = 0.193 (top), 2012, and E = 0.502 (bottom)

This is indication of the model's "equifinality" (Beven, 1993; Beven, 2006), or the absence of a unique parameter set, but rather several equally possible parameter sets. As noted by Dotto (PhD thesis, 2013) there are several possible reasons for this effect, and the mostly probable in this case are: (1) parameter space has several local minima regions and (2) parameters can exhibit a high degree of correlation. Since the effect of equifinality can substantially reduce confidence in the modelled results (Kuczera and Parent, 1998), it will be of outmost importance to perform a through uncertainty analysis of the model. Chapter 6 is, therefore, completely devoted to this subject.

5.4 Conclusions

Water flow was very well simulated for the well-designed Cell 2, but was not completely verified for Cell 1. This was attributed to profound cracking after dry periods of the Cell 1 media (which had high clay content). Most pollutants were well modelled in both cells, with the exception of simazine and prometryn for low inflow events after prolonged dry periods. Pollutants were found to sorb well in both cells, and exhibiting a more kinetic behaviour in Cell 1. Degradation was found to be more

dominant in Cell 2, and this is believed to be due to the presence of the submerged zone that sustains microbial activity during dry periods.

The model was run with laboratory data from batch studies (fluorescein as referent pollutant) and column studies (herbicides: atrazine, prometryn, simazine, glyphosate). A procedure was developed for the estimation of parameters from batch studies, and a regular calibration method was used for parameter estimation from column tests. Parameters for both sorption and degradation were found to be underestimated from batch studies. This is hypothesized to be due to differences in the water to soil ratio in batch studies, when compared to the field. The sorption parameters estimated from columns were also somewhat underestimated, and when used with the model produced higher outflow pollutant concentrations. This is especially the case with glyphosate, and only slightly with the triazines. Column studies also indicate less-kinetic-sorption behaviour when compared with the field data. It is hypothesized that kinetic sorption behaviour on the field may be apparent, and a consequence of the assumption that the flow is one dimensional, when in reality it is not, leading to conclusion that the kinetic behaviour is due to *structural* heterogeneity of the biofiltration material, rather than *chemical*. It is possible that the sorption process in the field is accounting for both micropollutant sorption to sorption and to the vegetation. This, however, can only be checked with additional laboratory column studies with *undisturbed* samples and vegetation.

The calibrated model parameters were in agreement with the available literature values, which makes the use of this model promising for the tested groups of organic pollutants.

CHAPTER 6: MODEL UNCERTAINTY ANALYSIS

6 MODEL UNCERTAINTY ANALYSIS

6.1 Introduction

Uncertainty is inherent to every modelling process and has multiple sources. By mapping and analysing sources of the uncertainty, especially their impact on modelling, one can make model predictions more reliable i.e. less uncertain. This chapter deals with the following: (1) Calibration data selection, and (2) General uncertainty.

The MPiRe model was applied to atrazine, simazine, prometryn, glyphosate and chloroform with data from Monash Car Park biofilter (field data). The uncertainty due to calibration data selection was assessed by choosing different parts of dataset for calibration, and comparing different optimal parameter sets. The general uncertainty assessment was performed using (1) GLUE (Beven and Binley, 1992) to create parameter probability distributions (PDs) and (2) to create 95^{th} percentile confidence intervals for modelling results.

6.2 Materials and methods

6.2.1 Calibration data selection uncertainty procedure

To assess the influence of used calibration dataset on model uncertainty, the available dataset of measurements was divided into several smaller datasets of different sizes. These smaller datasets were used for event-based model calibration. Calibration was done automatically using PEST (Doherty, 2013) against measured outflow rates and pollutant concentrations (as in Chapter 5.2.2). The Nash-Sutcliffe coefficient is used as model efficiency criteria. It should be noted that calibration uncertainty procedure was quite limited by the amount of data (number of events) available, and is just shown as a method. Additionally, calibration of separate events was done under constant degradation rate (calibrated), as the major impact of degradation is between events.

6.2.2 General uncertainty procedure

Sensitivity analysis (creation of probability density (PDs) histograms of model parameters) was done using Generalized Likelihood Uncertainty Estimation method (GLUE, by Beven and Binley, 1992), similar to other urban drainage water modelling

studies (e.g. Dotto et al, 2012, Mannina and Viviani, 2010, Vezzaro et al, 2012). GLUE is based on Monte-Carlo simulations, where parameters are sampled randomly from assumed prior PDs. Parameter sets are evaluated for their ability to reproduce measured data using a likelihood function - Nash-Sutcliffe coefficient for (1) flow measurements for hydraulic module and (2) pollutant concentrations for pollutant module. The accepted parameter sets – the ones with likelihood function above a certain threshold, are used to construct the density distribution histograms for each of the calibration parameters, as well as to examine their cross correlations.

Prior parameter PDs were assumed to be uniform on intervals. The ranges for parameters of the hydraulic module were: hydraulic conductivity, K_f 10 – 250 mm/h, porosity, n 0.15 – 0.55 and starting filter pore saturation s 0.0 – 1.0. The range for each parameter of the pollutant module was estimated using manual calibration and is shown in Table 6-1 with respective likelihood function thresholds. A total of 100 000 parameter sets is created for hydraulic module and each of the micropollutants using Latin Hypercube sampling (McKay et al., 1979).

Table 6-1 Parameter range for uniform prior PDs with the E - threshold

Parameter	Atrazine	Prometryn	Simazine	Glyphosate
$\log K_{oc}$	-1.6 – 3.6	-1.6 – 3.6	-1.6 – 3.6	0.4 – 5.0
f_e [-]	0 – 1	0 – 1	0 – 1	0 – 1
α_k [s^{-1}]	1e-7 – 1e-5	1e-7 – 1e-5	1e-7 – 1e-5	1e-7 – 1e-5
$T_{1/2}$ [day]	5 - 300	5 -300	5 - 300	5 - 300
E-threshold	0.4	0.6	0.4	0.6

Posterior PDs of parameter sets were then used to run the model and produce 95th percentile confidence intervals for micropollutant concentration in order to assess its robustness. It should be noted that the confidence interval is inversely proportional to the likelihood function threshold value: larger values produce narrower confidence intervals.

6.3 Results and discussion

6.3.1 Calibration data selection

Table 6-2 shows hydraulic module parameter values estimated for each of the test days alongside parameters estimated for the complete continuous series. The parameters of Cell 2 are found not to vary substantially when calibration is event-based for singular test days or when run as a continuous simulation, suggesting that the model could be successfully calibrated for Cell 2.

Table 6-2 Model parameter and Nash-Sutcliffe values for different periods for hydraulic module on Cell 2

	Test 1	Test 2	Test 3	Continuous series
K_f [mm/h]	141.8	151.9	160.0	155.5
n [-]	0.400	0.422	0.450	0.400
s [-]	0.498	0.843	0.283	0.406
E [-]	0.909	0.953	0.877	0.893

* Test 1 (19-11-2012), Test 2 (20-11-2012), Test 3 (11-12-2012)

Table 6-3 Model parameter and Nash-Sutcliffe values for different calibration periods for atrazine on Cell 2

	Test 1	Test 2	Test 3	Continuous series*
$logK_{oc}$ [logL/kg]	5.44	2.72	3.04	2.83
fe [-]	0.431	0.113	0.029	0.095
α_K [s^{-1}]	2.46e-05	1.35e-06	7.85e-05	5.66e-05
Nash-Sutcliffe (E)	0.721	0.899	0.857	0.776
	Test 4	Test 5	Test 6	Continuous series*
$logK_{oc}$ [logL/kg]	3.45	1.74	2.12	1.81
fe [-]	0.431	0.113	0.029	0.375
α_K [s^{-1}]	4.46e-06	5.43e-06	2.73e-05	1.02e-05
Nash-Sutcliffe (E)	0.897	0.698	0.887	0.876

* Continuous series are joined single events

Table 6-3 shows these pollutant module parameter values estimated for each of the test days and for the complete continuous test series for atrazine at Cell 2. The most sensitive parameter is found to be the soil-water partitioning coefficient normalized to organic carbon content, K_{oc}, which differs over 2 orders of magnitude (in logarithmic scale) between different calibration periods. The least sensitive is the kinetic sorption rate, α_K, with at most 3 times difference. Interestingly, Nash-Sutcliffe is increased when the calibration period is short (only one event), and is around 0.7 and above for all periods. Similar is found for all the other micropollutants (see Appendix): K_{oc} is the most sensitive, and α_K the least sensitive. However, it should have in mind that biodegradation rate is not evaluated in this study.

6.3.2 General uncertainty

Figure 6-1 shows matrix plot of cross-correlation scatter plots (off diagonal) between model parameters and model parameters and likelihood function (top row). Diagonal plots on Figure 6-1 are posterior parameter PDs.

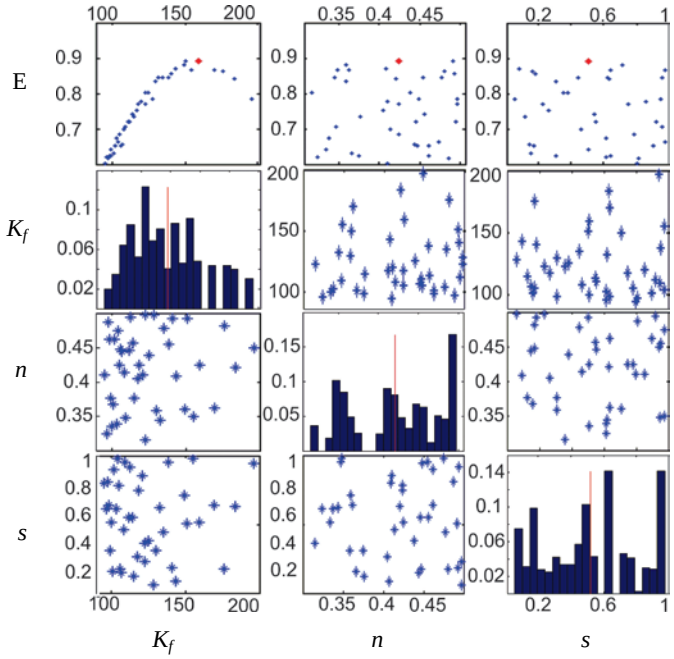

Figure 6-1 Matrix plot of cross-correlation scatter plots (off-diagonal) and posterior parameter probability density functions (diagonal) for flows at Cell 2 using GLUE and likelihood E > 0.6 (Prodanovic et al., 2014)

It is clear that there is only one sensitive parameter in the hydraulic module: the filtration coefficient (K_f), which has a clear peak value as seen in Figure 6-1. The model

is insensitive to changes in the value of parameters porosity (n) and saturation of the filtration layer (s). Cross-correlation scattered plots in Figure 6-1 also show that there is no apparent correlation between the parameters, additionally confirmed by correlation coefficient values in Table 6-4.

Table 6-4 Matrix of parameter cross-correlation coefficients for flows at Cell 2, using GLUE, E > 0.6

Hydraulics	E	K_f	n	s
E	1	0.361	-0.037	0.019
K_f		1	0.105	0.014
n			1	-0.048
s				1

Parameter mutual independence is highly valued in modelling, as the contrary signals an ill-posed model. (Dotto et al., 2012) From the above, it is concluded that the hydraulic module is well-posed.

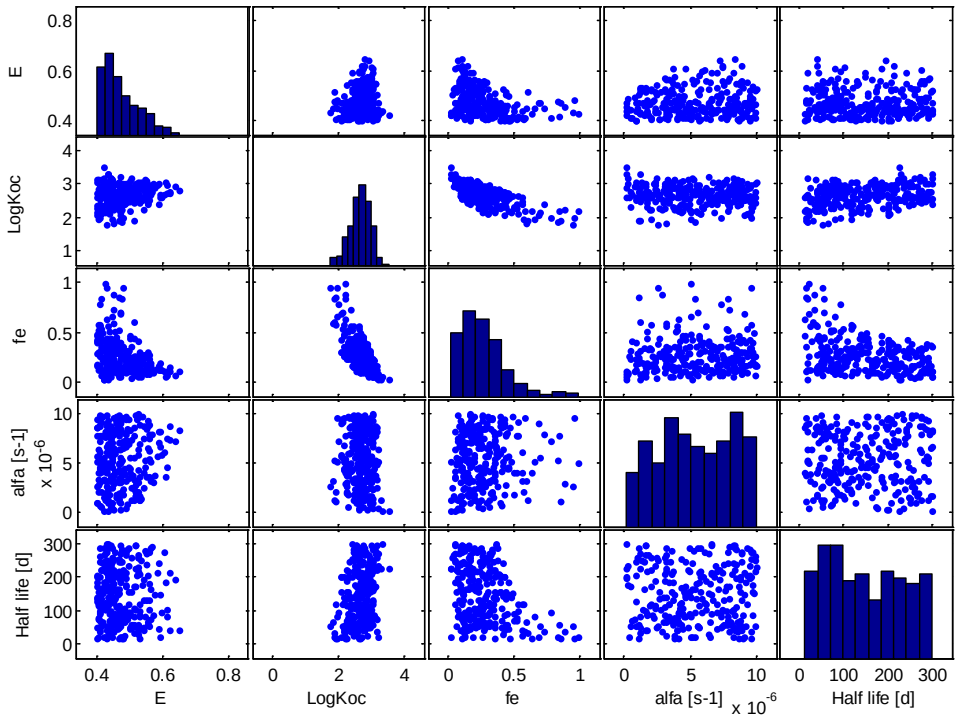

Figure 6-2 Matrix plot of cross-correlation scatter plots (off-diagonal), efficiency density(upper left corner) and posterior parameter probability density functions (diagonal) for atrazine concentrations at Cell 2 using GLUE and likelihood E > 0.4

Figure 6-2 shows the parameter sensitivity for atrazine at Cell 2 using GLUE with the likelihood function cut-off E > 0.4. The posterior parameter PDs show that the soil-water partitioning coefficient, K_{oc}, and fraction of instantaneous sorption sites, f_e, have clear peaks, indicating that their optimal values are easily identified. Posterior PDs for kinetic sorption rate, α_k, and degradation half-life, $T_{1/2}$, do not have clear peaks (they may be considered multi-modal, or almost uniform); therefore, their calibrated values have a high uncertainty.

Table 6-5, that includes parameter cross-correlation coefficients for atrazine at Cell 2, using GLUE with a cut-off E > 0.4, shows that parameters $logK_{oc}$ and f_e are substantially correlated, with R = -0.711. This means that the two compensate for each other: combination of high $logK_{oc}$ and low f_e produces similar sorption results to low $logK_{oc}$ and high f_e. This is expected, as the sorption model includes their mutual product. However, although they are correlated, it is not difficult to find their optimal values. The correlation and high peaks indicate that calibration would probably be better performed (with less uncertainty) for two unrelated parameters formed from the combination of K_{oc} and f_e such as (1) their product and (2) another relation derived from kinetic sorption model (Doherty, 2013).

Table 6-5 Matrix of parameter cross-correlation coefficients for atrazine at Cell 2, using GLUE, E > 0.4

Atrazine	E	LogKoc	fe	α_k	$T_{1/2}$
E	1	0.176	-0.377	0.099	-0.032
LogKoc		1	**-0.711**	-0.044	0.277
fe			1	0.084	-0.357
α_k				1	0.031
$T_{1/2}$					1

The likelihood function is most sensitive to $logK_{oc}$ and f_e, indicated by the narrowest distribution function, with a clear peak (Figure 6-2, top row) and high R values in Table 6-5. Insensitivity of the likelihood function to values of degradation half-life are anticipated to be consequences of (1) assumptions regarding degradation being relevant in dissolved micropollutant phase only (water pollutant concentration) and (2) low data for determination of this value. As it was previously concluded, degradation is a process

relevant between events (Chapter 5.3). Inter-event data is very scarce: there are only a few soil samples (usually not showing any detected concentration) and the major weight of the degradation rate estimation is held by two outflow concentration points (ending of one event, and start of the next event). It is hypothesized that longer continuous series of measured outflow pollutant concentrations (with more events) would decrease uncertainty regarding this parameter, and show that it is a well-chosen model parameter.

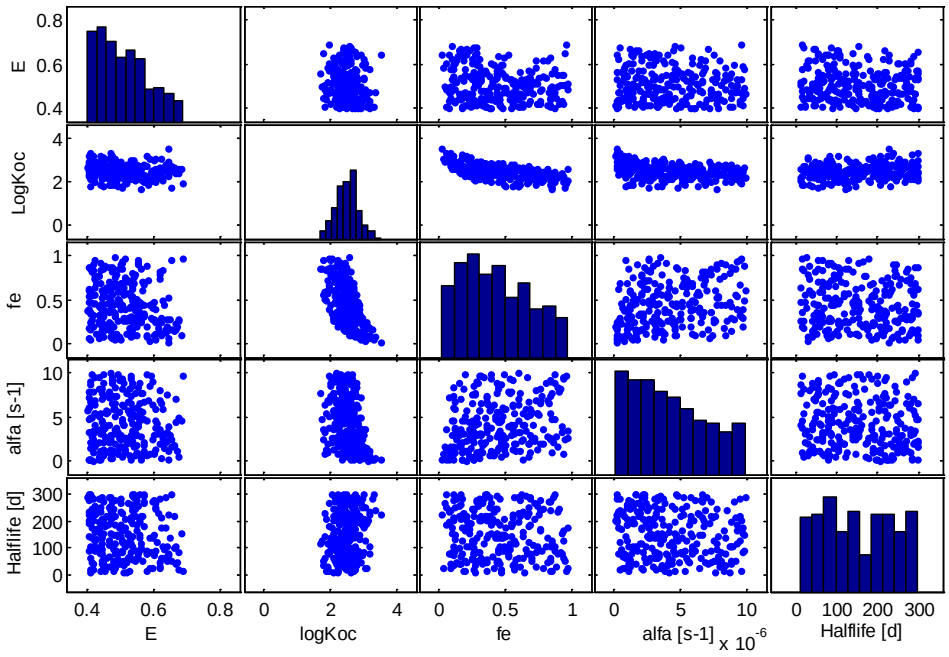

Figure 6-3 Matrix plot of cross-correlation scatter plots (off-diagonal), efficiency density(upper left corner) and posterior parameter probability density functions (diagonal) for simazine concentrations at Cell 2 using GLUE and likelihood E > 0.4

Table 6-6 Matrix of parameter cross-correlation coef. for simazine at Cell 2, using GLUE, E > 0.4

Simazine	E	LogKoc	fe	α_k	$T_{1/2}$
E	1	-0.178	-0.170	-0.026	-0.131
LogKoc		1	**-0.638**	-0.359	0.121
fe			1	0.268	-0.083
α_k				1	-0.119
$T_{1/2}$					1

Figure 6-4 and Figure 6-5 shows the parameter sensitivity for simazine and prometryn at Cell 2 using GLUE with the likelihood function cut-off E > 0.4 and E>0.6, respectively. Parameter cross-correlation scatter plots and parameter probability density functions for simazine and prometryn are very similar to atrazine. Similarity can be seen in correlation values, as well (Table 6-6, Table 6-7): $logK_{oc}$ and f_e are strongly correlated, but due to the narrowness of their probability distributions, it is easy to determine their optimal values. The kinetic sorption rate, α_k, and degradation half-life, $T_{1/2}$, do not have a clear peak in PDs. (Figure 6-4, Figure 6-5) The Nash-Suttcliffe coefficient is mostly influenced by $logK_{oc}$ for both simazine and prometryn.

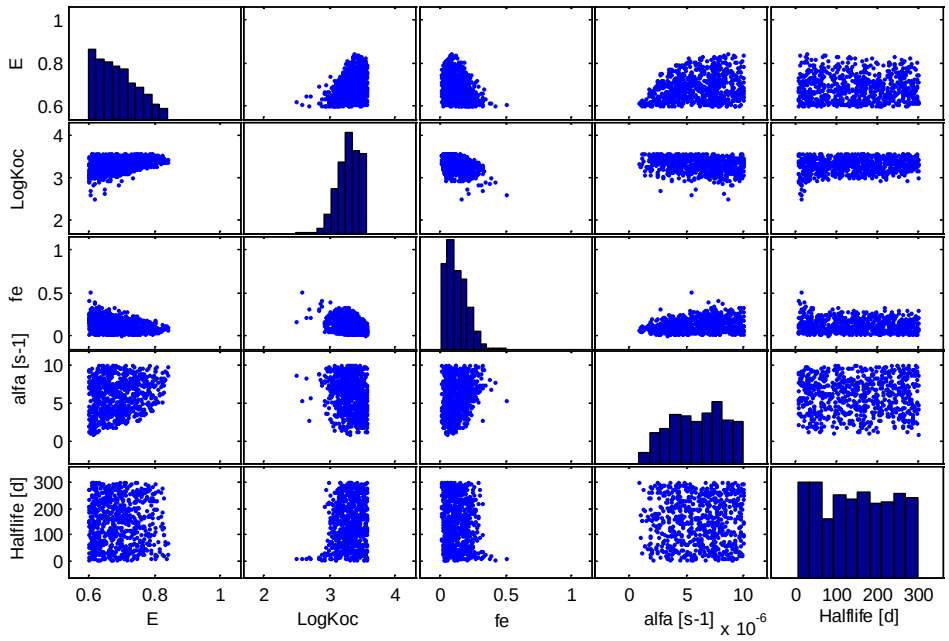

Figure 6-4 Matrix plot of cross-correlation scatter plots (off-diagonal), efficiency density(upper left corner) and posterior parameter probability density functions (diagonal) for prometryn concentrations at Cell 2 using GLUE and likelihood E > 0.6

Table 6-7 Matrix of parameter cross-correlation coef. for prometryn at Cell 2, using GLUE, E > 0.6

Prometryn	E	LogKoc	fe	α_k	$T_{1/2}$
E	1	0.390	-0.307	0.224	-0.014
LogKoc		1	**-0.403**	-0.215	0.162
fe			1	0.232	-0.130
α_k				1	-0.009
$T_{1/2}$					1

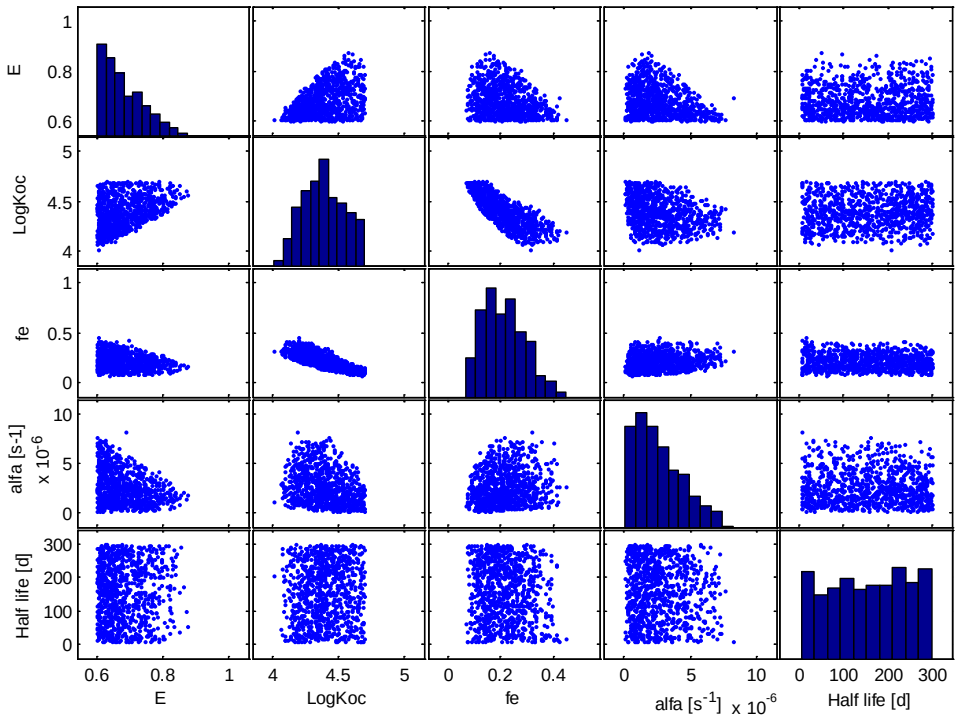

Figure 6-5 Matrix plot of cross-correlation scatter plots (off-diagonal), efficiency density(upper left corner) and posterior parameter probability density functions (diagonal) for glyphosate concentrations at Cell 2 using GLUE and likelihood E > 0.6

Table 6-8 Matrix of parameter cross-correlation coef. for glyphosate at Cell 2, using GLUE, E > 0.6

Glyphosate	E	LogKoc	fe	α_k	$T_{1/2}$
E	1	0.399	-0.240	-0.309	0.008
logKoc		1	**-0.789**	-0.273	0.073
fe			1	0.149	-0.099
α_k				1	-0.037
$T_{1/2}$					1

Figure 6-5 shows the parameter sensitivity for glyphosate at Cell 2 using GLUE with the likelihood function cut-off E > 0.6. The posterior parameter PDs show that the soil-water partitioning coefficient, K_{oc}, and fraction of instantaneous sorption sites, f_e, have clear peaks, indicating that their optimal values are easily identified. But unlike the rest of micropollutants, kinetic sorption rate, α_k, shows a clear peak in posterior PD, meaning that the calibrated value is with low uncertainty. There is a slight correlation between sorption parameters f_e and α_k, and again a strong correlation between $\log K_{oc}$

and f_e. (Table 6-8) The degradation half-life exhibits the same behaviour as with the other pollutants and the same is hypothesized about the need for longer continuous series of measured outflow pollutant concentrations (with more events).

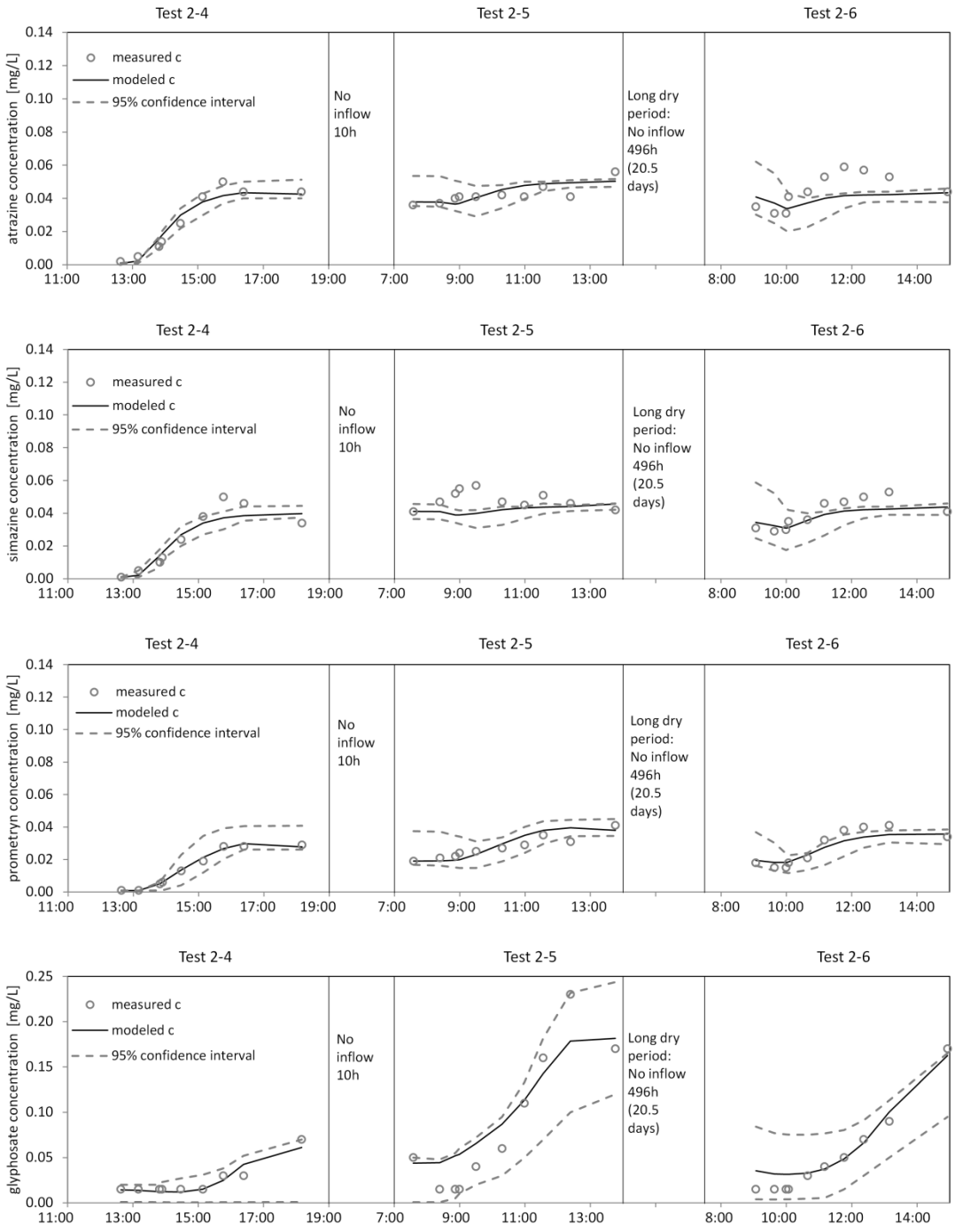

Figure 6-6 Atrazine, simazine, prometryn and glyphosate (top-bottom) pollutographs at biofilter outflow pipe with measured and modelled concentrations including a 95% confidence interval from GLUE analysis

Figure 6-6 shows pollutographs at biofilter outflow pipe with measured and modelled concentrations and a 95% confidence interval for atrazine, simazine, prometryn and glyphosate at Cell 2. Most of measurements fall well between the confidence intervals that suggests that the model is well-posed: 76% for atrazine, 66% for simazine, 90% for prometryn and 97% for glyphosate. It can be observed that ending and starting event concentrations have the widest confidence interval, meaning they have the highest uncertainty (which further confirms the hypothesis about degradation half-life posterior PD).

6.4 Conclusions

The MPiRe model was checked with micropollutant data at Monash Car Park biofilter. The model was successfully calibrated, and then model uncertainty analysed. The following is concluded:

- Different calibration datasets produce different optimal model parameters, with soil-water partitioning coefficient (normalized to organic carbon content) being the most sensitive to this procedure.
- The longest dataset gives the most average values of parameters, and the lowest value of likelihood function.
- Uncertainty analysis performed with GLUE confirmed that the soil-water partitioning coefficient (normalized to organic carbon content) is the most sensitive model parameter, but also found correlation between sorption parameters, and high uncertainty in the degradation rate estimation. It is suggested that these procedure needs to be redone with longer continuous series of measured outflow pollutant concentrations (with more events).
- Additionally, the predictive uncertainty is assessed by making 95% confidence intervals for model predictions, and it suggests that the model is sound.

CHAPTER 7: CONCLUSIONS AND FURTHER RESEARCH

7 CONCLUSIONS AND FURTHER RESEARCH

7.1 Summary of conclusions

This main aim of this research was to develop a process based model that is capable of simulating water and micropollutant transport though stormwater biofilters. To get insight into the dimensionality of the flow, conservative tracer tests and ERT were performed on-site with two different biofiltration units. ERT data visually confirmed that the transition from two-dimensional to one-dimensional flow is fast when water is introduced into a variably saturated biofiltration system, and that transport is one dimensional. The tracer test measurement data was successfully simulated with the proposed one-dimensional model with conservative advective-dispersive transport.

The MPiRe model's final form included three key processes that govern behaviour of micropollutants in these systems: (1) sorption, (2) degradation and (3) volatilisation. The water flow contained at-least one calibration parameter (hydraulic conductivity) while the pollution transport required calibration of additional four or five parameters. The model was used to simulate the fate of five organic micropollutants (glyphosate, atrazine, simazine, prometryn, and chloroform) in two different biofiltration cells; one cell was designed according to the best Australian design practice (Cell 2) and the other cell has a high organic and clay content (Cell 1). The cells were tested under variable and challenging operational conditions. The model was calibrated and independently validated on two separate data series.

The water flow was very well simulated for the well-designed Cell 2, but was not completely verified for Cell 1. This was attributed to pronounced cracking after dry periods of the Cell 1 media (which had a high clay content). The model was successful in capturing pollutograph trends and peaks for most micropollutants. The exceptions were simazine and prometryn during low inflow events after prolonged dry periods, where outflow concentrations were underestimated. The pollutants were found to sorb better in Cell 1 (lower outflow concentrations), and exhibited a more sorption kinetic behaviour in Cell 2 (higher sorption rate for most pollutants). Degradation was also

found to be more dominant in Cell 2, and this is believed to be due to the existence of a submerged zone that sustains microbial activity during dry periods.

The model was run with laboratory data from batch studies (fluorescein as referent pollutant) and column studies (herbicides: atrazine, prometryn, simazine, glyphosate). A procedure was developed for the estimation of parameters from batch studies, and a regular calibration method was used for parameter estimation from column tests. Parameters for both sorption and degradation were found to be underestimated from batch studies. This is hypothesized to be due to differences in the water to soil ratio in batch studies, when compared to the field. The sorption parameters estimated from columns were also somewhat underestimated, and when used with the model produced higher outflow pollutant concentrations. This was especially the case with glyphosate, and only slightly with the triazines. Column studies also indicated less-kinetic-sorption behaviour when compared with the field data. It is hypothesized that kinetic sorption behaviour on the field may be apparent, and a consequence of the assumption that the flow is one dimensional, when in reality it is not. This leads to a conclusion that the kinetic behaviour is due to the structural heterogeneity of the biofiltration material, rather than chemical heterogeneity. It is also possible that the sorption process in the field accounts for both micropollutant sorption to soil and to vegetation. This, however, can only be checked with additional laboratory column studies with undisturbed samples and vegetation.

The calibrated model parameters were in agreement with the available literature values, which makes the use of this model promising for the tested groups of organic pollutants. Sensitivity and uncertainty analysis indicated that the most sensitive parameter of the water module is the hydraulic conductivity, while for the pollutant module it is the soil-water partitioning coefficient. The degradation rate was found to be an uncertainty parameter, and it is suggested that uncertainty analysis needs to be redone with longer continuous series of measured outflow pollutant concentrations (with more events) when data becomes available. The model's predictive uncertainty is not high, and most measurements fell well between the 95^{th} percentile confidence intervals.

7.2 Research aim evaluation

Goal 1: To develop a transport and fate model for organic micropollutants in stormwater biofilters.

1. It was hypothesized that micropollutants can be grouped according to their chemical structure and nature into a few groups, and that a good "representative" can be selected from each group, whose transport and fate models can be "transferred" to each member of the group.

   Atrazine, prometryn and simazine were considered to belong to the same group of pollutants as they share a similar structure (triazines). Modelling results from this research suggest that a similar model can be applied to all of them, giving satisfactory results (Chapter 5). Unfortunately, many of the micropollutants that were introduced into the biofiltration system were detected in the outflow (Chapter 3) so the conclusion made for triazines cannot be confirmed with other micropollutant groups. It is suggested that this hypothesis needs to be further confirmed when new data becomes available.
2. It was hypothesized that the complex hydrodynamic behaviour of urban stormwater in WSUD systems can be conceptualized by a multiple reservoir approach (one-dimensional model with dominant vertical flows).

   In order to check this hypothesis, and eventually develop a model based on it, a group of tests was performed on a biofiltration system (field site): tracer tests with conservative and non-conservative tracers and the ERT. A tracer test was successfully simulated using a proposed one-dimensional model with dominant vertical flows and the advective-dispersive equation (Chapter 5.2.4). ERT results gave visual evidence of a short transition from two-dimensional to one-dimensional flow when water is introduced in a variably saturated biofiltration system (Chapter 3.4.4).
3. It was hypothesized that the transport of micropollutants in the biofilter can be predicted by a linear advective dispersive transport equation (vertical), while conceptual 1^{st} and 2^{nd} order decay models could be used to assess the removal processes that may be physical/chemical/biological in nature (settling, straining,

volatilization, photodegradation, hydrolysis, aerobic/anaerobic biodegradation, adsorption, and desorption).

To check this hypothesis, and develop a model, a series of tests were performed with fluorescein – as a reference micropollutant that included: conservative tracer test, field fluorescein test, and laboratory batch and column studies. A model based on a one-dimensional bucket hydraulical module and advective-dispersive transport equation with processes modelled as two-site sorption model, and first order degradation (basis of the developed MPiRe model) as the water quality module, was successfully applied to measured data (Chapter 5.3.2), confirming this hypothesis.

Goal 2: To conduct controlled lab and field tests to refine the model component that simulates the micropollutant treatment in biofilters;

4. It was hypothesized that a large amount of data should be collected to ensure accurate testing and verification of the newly developed model.

   This hypothesis was confirmed with successful modelling results presented in Chapter 5, which included: (1) successful simulation of measured outflow concentrations in field conditions at two different biofiltration systems, and (2) successful simulation of measured outflow concentration in laboratory conditions (column studies), with parameters that can be transferred to the field. However, this hypothesis confirmation will benefit from results with additional measurement data.

Goal 3: To calibrate, validate, and assess uncertainties in the model using field data from two stormwater systems (biofilters with different designs).

5. It was hypothesized that uncertainty analysis (using two different field data sets) will point to sensitive parameters and provide insightful information about the processes.

   This was confirmed in Chapter 6 that presents the model parameter uncertainty analysis conducted using GLUE methodology. The most sensitive parameters are identified to be sorption parameters, in particular the soil-water partitioning

coefficient. Large uncertainty related to the degradation rate is evaluated to be due to scarce inter-event data.

7.3 Discussion on model development

The pollutant removal processes emphasised in the model development are sorption, biodegradation and volatilisation. These are most certainly important processes but why were other presumably relevant processes such as sedimentation and vegetative filtering excluded?

When the model was in its initial development stage, many other processes were included (such as stripping, sedimentation etc.). But attempts to calibrate the model were not very successful: (1) it was difficult to source the parameter values from the literature and (2) the model was overparametrized since there were more parameters than measured data points. Additionally, it was very encouraging to see that even with relatively small number of processes (parameters) the model was able to predicting the removal. Therefore, it is author's belief that it is not necessary (at this point) to add complexity to the model.

This is why all but the most dominant processes were taken out (sorption, degradation and volatilization). Sedimentation was neglected, as it was found that most of these pollutants are mostly dissolved rather than particulate (Zgheib et al., 2012) while in the water column, meaning they would sorb to the filter media rather than settle. As for the vegetative filtering (sorption to plants) it is hypothesized that due to relatively short contact time (only during ponding), this process has a low impact on the overall removal. This was further encouraged by the fact that stormwater biofilters are vertical flow systems, and very little if any water movement is horizontal, therefore the filtering is mostly through the soil media.

However, the author is completely aware that the neglected processes are compensated by the calibration coefficients e.g. sorption to grass (plants) and straining are fused with sorption to soil particles.

The usability of the model is very important for practical applications (both system sizing and validation monitoring), and there comes the tendency to keep it as simple as possible and still get meaningful results.

7.3.1 Model's usability in practical applications

The MPiRe model was developed as a tool to ease the management of stormwater biofiltration systems when they are used for water harvesting or to control the polluted urban runoff to water receiving bodies. The model can be used to predict biofilter's long-term performance in removal of some of the key stormwater micropollutants (glyphosate, triazines, chloroform). The model is an alternative to STUMP (Vezzaro et al., 2010, the only other available model in literature that can predict micropollutant behaviour in biofilters), but it allows a more accurate water flow modelling and can be used even when there is no information on suspended solids data. The model parameters for the tested herbicides and chloroform agree with the literature, suggesting that the model is physically sound. It was therefore hypothesized that the model can be easily extended for other types of micropollutants (PAHs, phenols, phthalates, etc.) by adjusting model parameters to their properties directly sourced from literature.

The way the MPiRe model is set up enables it to be implemented for exploration of (1) different biofilter designs (geometry, material composition etc.) and (2) testing of biofilters performance under different scenarios (e.g. variable wetting and drying periods, different inflow pollutant concentrations, etc.). These model traits would eventually lead to optimal designs and operational regimes of these systems.

The MPiRe model can also facilitate the validation monitoring of biofilter systems. Since full scale tests are usually expensive, and in most cases impractical for large stormwater biofilters, the alternative is to use the MPiRe model to complement the measured data and assess the biofilter performance. The MPiRe model has already been adopted and tested for this purpose, as discussed in Zhang et al. (2016); this work shows that the model can be used to optimize the monitoring procedure (that is necessary to demonstrate that the treatment processes are capable of achieving the required water quality objectives) by selecting only the most valuable data points to be collected, thereby minimizing the total expenses (number of measurements).

7.4 Future research

Although the research aims have been, for the most part, achieved, inevitably new research questions are opened, and are anticipated to be part of future research.

1. Testing the model on longer continuous series of measured outflow concentrations with extensive inter-event data

The major weakness of the model is found to be in the high uncertainty related to degradation process. This was identified to be due to scarce data on which this particular process is developed and modelled. It would be valuable to perform uncertainty analysis on longer measurement data series.

2. Calibration of the model using additional micropollutants

It would be valuable to truly check the 1st hypothesis regarding group – representative micropollutants. This would, inevitably, require more data on biofilter outflow concentrations. The model would also profit if the micropollutants are prone to other fate processes, such as photodegradation, straining, etc.

3. Re-evaluation of the sorption model

The model for sorption used in the model is found to give mostly good results, based on micropollutant behaviour in both laboratory and field conditions. Since, the aim was to develop a practically usable model, it was an imperative to make model that is easily transferred from laboratory to the field. However, due to differences in kinetic rates determined for pollutants in laboratory vs. field, it is hypothesized that the model would profit from another set of laboratory experiments involving *undisturbed* soil columns with vegetation. The model would also benefit from experiments with variable input concentrations to test whether competitive sorption plays a role in the process (a micropollutant being able to cause desorption of another pollutant due to its higher sorption ability).

4. Biofiltration system aging modelling

It would be interesting to see how the model parameter (both flow and pollutant) change over time, and whether it is possible to easily model such changes.

5. Further uncertainty analysis

A thorough uncertainty analysis should be conducted for the new micropollutant model, focusing on determining the impact of uncertainties in (1) input data (2) measurement data, and (3) model structural uncertainty. The first two questions can be addressed with additional data, while the third requires development of structurally different models for micropollutants in biofiltration systems.

8 REFERENCES

Abdus-Salam N. and Buhari M. (2014) Adsorption of Alizarin and Fluorescein Dyes on Adsorbent prepared from Mango Seed, The Pacific Journal of Science and Technology, vol. 15(1) pp. 232-234

ABEM (2012) User manual – Terrameter LS, ABEM Instrument AB, Sundbyberg, Sweden

Achleitner S., Möderl M., Rauch W. (2007) CITY DRAIN © An open source approach for simulation of integrated urban drainage systems, Environmental Modelling & Software, vol. 22(8), pp. 1184-1195

Active Beautiful Clean Waters – Design Guidelines. (2014) PUB, Singapore's national water agency

Allen R.G., Pereira L.S., Raes D., Smith M. (1998) Crop evapotranspiration – guidelines for computing crop water requirements. FAO Irrigation and drainage paper 56, Food and Agriculture Organisation of the United Nations

Altoé J.E., Bedrikovetsky P., Siqueita A.G., de Souza, A.L.S., Shecaira F.S. (2006) Correction of basic equations for deep bed filtration with dispersion. Journal of Petroleum Science and Engineering, vol. 51, pp. 68-84

Beck M.B. (1987) Water Quality Modeling: A Review of the Analysis of Uncertainty. Water Resources Research, vol. 23(8), pp. 1393-1442

Beven K.J. (1993) Prophecy, reality and uncertainty in distributed hydrological modelling. Advances in Water Resources, vol. 16, pp. 41-51

Beven K.J. (2006) A manifesto for the equifinality thesis. Journal of Hydrology, vol. 320, pp. 18-36

Beven K.J. (2009) Environmental Modelling: An Uncertain Future? Routledge, New York, USA

Beven K.J., Binley A. (1992) The future of distributed models: Model calibration and uncertainty prediction. Hydrological Processes, vol. 6(3), pp. 279-298

Beyer A., Biziuk M. (2009) Environmental fate and global distribution of polychlorinated biphenyls. Reviews of Environmental Contamination and Toxicology, vol. 201, pp. 137-158

Björklund K., Cousins A.P., Strömvall A.M., Malmqvist P.A. (2009) Phthalates and nonylphenols in urban runoff: Occurrence, distribution and area emission factors. Science of the Total Environment, vol. 407, pp. 4665-4672

Blecken G.T., Zinger Y., Deletic A., Fletcher T., Viklander M. (2009) Impact of submerged zone and a carbon source on heavy metal removal in stormwater biofilters. Ecological Engineering, vol. 35, pp. 769-778

Blecken G.-T., Zinger Y., Deletic A., Fletcher T.D., Hedström A., Viklander M. (2010) Laboratory study on stormwater biofiltration: Nutrient and sediment removal in cold temperatures. Journal of Hydrology, vol. 394 (3–4), pp. 507-514.

Blumensaat F., Seydel J., Krebs P., Vanrolleghem P.A. (2014) Model structure sensitivity of river water quality models for urban drainage impact assessment. Proceedings of the 7th International Congress on Environmental Modelling and Software, San Diego, USA

Boyd G.R., Palmeri J.M., Zhang S., Grimm D.A. (2004) Pharmaceuticals and personal care products (PPCPs) and endocrine disrupting chemicals (EDCs) in stormwater canals and Bayou St. John in New Orleans, Louisiana, USA. Science of the Total Environment, vol. 333 (1-3), pp. 137-148

Bressy A., Gromaire M.C., Lorgeoux C., Chebbo G. (2011) Alkylphenols in atmospheric depositions and urban runoff. Water Science and Technology, vol. 63(4), pp. 671-679.

Butler D., Davies J.W. (2011) Urban Drainage. Third edition. Spon Press, New York, USA

Byrns G. (2001) The fate of xenobiotic organic compounds in wastewater treatment plants. Water Research, vol. 35(10), pp. 2523-2533

Chandrasena G.I., Pham T., Payne E.G., Deletic A., McCarthy D.T. (2014) E.coli removal in laboratory scale stormwater biofilters: Influence of vegetation and submerged zone. Journal of Hydrology, vol. 519, pp. 814-822

Chandrasena, G.I., Deletic, A.; Ellerton, J.; McCarthy, D. T. (2012) Evaluating Escherichia coli removal performance in stormwater biofilters: a laboratory-scale study. Water Science & Technology, vol. 66 (5), pp. 1132-1138.

Cheyns K., Mertens J., Diels J., Smolders E., Springael D. (2010) Monod kinetics rather than a first-order degradation model explains atrazine fate in soil mini-columns: Implications for pesticide fate modelling. Environemental Pollution, vol. 158, pp. 1405-1411

Chiou C.T., Sheng G., Manes M. (2001) A partition-limited model for the plant uptake of organic contaminants from soil and water. Environmental Science and Technology, vol. 35, pp. 1437-1444

Clara M., Windhofer G., Hartl W., Braun K., Simon M., Gans O., Scheffknecht C., Chovanec A. (2010) Occurrence of phthalates in surface runoff, untreated and treated wastewater and fate during wastewater treatment, Chemosphere, vol. 78(9), pp. 1078-1084

Collins C., Fryer M., Grosso A. (2006) Plant uptake of non-ionic organic chemicals. Environmental Science and Technology, vol. 40, pp. 45-52

Cole R.H.; Frederick R.E., Healy R.P., Rolan, R.G. (1984) Preliminary Findings of the Priority Pollutant Monitoring Project of the Nationwide Urban Runoff Program. Journal (Water Pollution Control Federation), vol. 56 (7), pp. 898-908.

Corapcioglu M.Y., Hossain M.A. (1990) Theoretical modeling of biodegradation and biotransformation of hydrocarbons in subsurface environments. Journal of Theoretical Biology, vol. 142, pp. 503-516

Daly, E., Zinger, Y., Deletic, A. and Fletcher, T.D., (2009) A possible mechanism for soil moisture bimodality in humid-land environments, Geophysical Research Letters, vol. 36(7), pp. L07402

Davis, A.P. (2007) Field performance of bioretention: Water quality, Environmental Engineering Science, vol. 24(8), pp. 1048-1064

De Biase C., Reger D., Schmidt A., Jechalke S., Reiche N., Martínez-Lavanchy P.M., Rossell M., Van Afferden M., Maier U., Oswald S.E., Thullner M. (2011) Treatment of volatile organic contaminants in a vertical flow filter: Relevance of different removal processes. Ecological Engineering, vol. 37, pp. 1292-1303

Deacon E.L. (1977) Gas transfer to and across an air/water interface. Tellus, vol. 29(4), pp. 363-374

Deletic A., Dotto C.B.S., McCarthy D.T., Kleidorfer M., Freni G., Mannina G., Uhl M., Henrichs M., Fletcher T.D., Rauch W., Bertrand-Krajewski J.L., Tair S. (2012) Assessing uncertainties in urban drainage models. Physics and Chemistry of the Earth, vol. 42-44, pp. 3-10

Delle Site A. (2001) Factors affecting sorption of organic compounds in natural sorbent/water systems and sorption coefficients for selected pollutants. A review. Journal of Physical abd Chemical Reference Data, vol. 30(1), pp. 187-439

DHI (2009a) MOUSE Pipe flow reference manual, DHI Software, Hørsolm, Denmark

DHI (2009b) MOUSE TRAP Technical Reference Surface Runoff Quality Module, DHI Software, Hørsolm, Denmark

DHI (2009c) MOUSE User guide, DHI Software, Hørsolm, Denmark

DiBlasi C.J., Li H., Davis A.P., Ghosh U. (2009) Removal and fate of polycyclic aromatic hydrocarbon pollutants in an urban stormwater bioretention facility, Environmental Science and Technology, vol. 43(2), p. 494-502

Dif A., Bluemel W. (1991) Expansive soils under cyclic drying and wetting. GeotechnicalTesting Journal. vol. 14(1), pp. 96-102

Dingman, S.L. (2002) Physical Hydrology, Prentice Hall, Upper Saddle Hall, NJ.

Djukić A., Lekić B., Rajaković-Ognjanović V., Veljović Dj., Vulić T., Djolić M., Naunović Z., Despotović J., Prodanović D. (2016) Further insight into the mechanism of heavy metals partitioning in stormwater runoff. Journal of Environmental Management, vol. 168, pp. 104-110

Dodds L., King W., Allen A.C., Armson B.A., Fell D.B., Nimrod C. (2004) Trihalomethanes in public water supplies and risk of stillbirth. Epidemiology, vol. 15(2), pp. 179-186

Doherty J. (2003) Model Independent Markov Chain Monte Carlo Analysis - MICA, Watermark Numerical Computing and US EPA, US.

Doherty, J. (2013) PEST—Model-Independent Parameter Estimation—User Manual, Watermark Numerical Computing

Dotto C.B.S. (2013) Parameter sensitivity and uncertainty analysis in urban drainage modelling. Civil Engineering, Melbourne, Monash University, Australia. PhD Thesis

Dotto C.B.S., Kleidorfer M., Deletic A., Rauch W., McCarthy D.T. (2014) Impacts of measured data uncertainty on urban stormwater models. Journal of Hydrology, vol. 508, pp. 28-42

Dotto C.B.S., Mannina G., Kleidorfer M., Vezzaro L., Henrichs M., McCarthy D.T., Freni G., Rauch W., Deletic A. (2012) Comparison of different uncertainty techniques in urban stormwater quantity and quality modelling. Water Research, vol. 46(8), pp. 2545-2558

Duncan H. (1999) Urban stormwater quality: a statistical overview. CRC for Catchment Hydrology, Melbourne

ECE. (2008) Priority substances and certain other pollutants (According to Annex II of the Directive 2008/105/EC), European Commission Environment. [Online]. European Commission Environment. Available: http://ec.europa.eu/environment/water/water-framework/priority_substances.htm [Accessed 27 April 2012].

Eriksson E., Baun A., Mikkelsen P.S., Ledin A. (2005) Chemical hazard identification and assessment tool for evaluation of stormwater priority pollutants. Water Science and Technology, vol. 51(2), pp. 47-55

eWater CRC (2009) Model for urban stormwater improvement conceptualisation (MUSIC) (Version 4.0), Canberra: eWater Cooperative Research Centre.

FAWB. (2009) Adoption guidelines for Stormwater Biofilter systems. Facility for Advancing Water Biofiltration, Monash University

Feng, W., Hatt, B.E., McCarthy, D.T., Fletcher, T.D., Deletic, A. (2012) Biofilters for stormwater harvesting: Understanding the treatment performance of key metals that pose a risk for water use, Environmental Science and Technology, vol. 46(9), pp. 5100-5108.

Gao J., Zhang J., Ma N., Wang W., Ma C., Zhang R. (2015) Cadmium removal capability and growth characteristics of *Iris sibirica* in subsurface vertical flow constructed wetlands. Ecological Engineering, vol. 84, pp. 443-450

Gao Y., Zhu L. (2004) Plant uptake, accumulation and translocation of phenanthrene and pyrene in soils. Chemosphere, vol. 55, pp. 1169-1178

Gasperi J., Zgheib S., Cladière M., Rocher V., Moilleron R., Chebbo G. (2012) Priority pollutants in urban stormwater: Part 2 – Case of combined sewers. Water Research, vol. 46, 6693-6703

Gaya U.I., Abdullah A.H. (2008) Heterogeneous photocatalytic degradation of organic contaminants over titanium dioxide: A review of fundamentals, progress and problems. Journal of Photochemistry and Photobiology C: Photochemistry Reviews, vol. 9(1), pp. 1-12

Geissen V., Mol H., Klumpp E., Umlauf G., Nadal M., van der Ploeg M., van de Zee S.E.A.T.M, Ritsema C.J. (2015) Emerging pollutants in the environment: A challenge for water resource management. International Soil and Water Conservation Research, vol. 3(1), pp. 57-65

Gillbreath A.N. and McKee L.J. (2015) Concentrations and loads of PCBs, dioxins, PAHs, PBDEs, OC pesticides and pyrethroids during storm and low flow conditions in a small urban semi-arid watershed. Science of the Total Environment, vol. 526, pp. 251-261

Giraldi D., de Michieli Vitturi M., Iannelli R. (2010) FITOVERT: A dynamic numerical model of subsurface vertical flow constructed wetlands, Environmental Modelling and Software, vol. 25, p. 633-640

Göbel, P.; Dierkes, C.; Coldewey, W. G. (2007) Storm water runoff concentration matrix for urban areas. Journal of Contaminant Hydrology, vol. 91 (1-2), pp. 26-42.

Griffiths W.C., Camara P., Lerner K.S. (1985) Bis-(2-ethylhexyl) phthalate, an ubiquitous environmental contaminant. Annals of Clinical and Laboratory Science, vol. 15(2), pp. 140-151

Gupta H.V., Clark M.P., Vrugt J.A., Abramowitz G., Ye M. (2012) Towards a comprehensive assessment of model structural adequacy. Water Resources Research, vol. 48(8), W08301

Hastings W.K. (1970) Monte Carlo sampling methods using Markov chains and their applications. Biometrika, vol. 57, pp. 97-109

Hatt B.E., Fletcher T.D., Deletic A. (2007) Hydraulic and pollutant removal performance of stormwater filters under variable wetting and drying regimes. Water Science and Technology, vol. 56 (12), pp. 11-19

Hatt, B. E.; Fletcher, T. D.; Deletic, A. (2008) Hydraulic and Pollutant Removal Performance of Fine Media Stormwater Filtration Systems. Environmental Science & Technology, vol. 42(7), pp. 2535-2541.

Hatt, B. E.; Fletcher, T. D.; Deletic, A. (2009) Hydrologic and pollutant removal performance of stormwater biofiltration systems at the field scale, Journal of Hydrology, vol. 365 (3-4), pp. 310-321

He Z., Davis A.P. (2009) Unit process modeling of stormwater flow and pollutant sorption in a bioretention cell, World Environmental and Water Resources Congress 2009: Great Rivers, Conference proceedings ,p. 1622-1630

Henze M., Gujer W., Mino T., van Loosdrecht, M.C.M. (2000) Activated sludge models ASM1, ASM2, ASM2D and ASM3, IWA Scientific and Technical Report No. 9, IWA Publishing, London UK

Herzig J.R., Leclerc D.M., Le Goff P. (1970) Flow of suspensions through porous media – application to deep bed filtration. Industrial and Engineering Chemistry, vol. 62(5), pp. 8-35

Higbie R. (1935). The rate of adsorption of a pure gas into a still liquid during short periods of exposure. Transactions of the American Institute of Chemical Engineers, vol. 35, pp. 365-389

Hinman C. (2009) Bioretention soil mix review and recommendations for Western Washington, Washington State University, USA

Hirsch C. (2006) Numerical computations of internal and external flows – the fundamentals of computational fluid dynamics. Second Edition, Butterworth-Heinemann, Burlington, USA

Hong, E., Seagren, E.A., Davis, A.P. (2006) Sustainable oil and grease removal from synthetic stormwater runoff using bench-scale bioretention studies, Water Environment Research, vol. 78(2), pp. 141-155

Hunt, W.F., Jarrett A.R., Smith, J.T., Sharkey, L.J. (2006) Evaluating bioretention hydrology and nutrient removal at three field sites in North Carolina, Journal of Irrigation and Drainage Engineering, vol. 132(6), pp. 600-608

Hwang H.M and Foster G.D. (2006) Characterization of polycyclic aromatic hydrocarbons in urban stormwater runoff flowing into the tidal Anacostia River, Washington, DC, USA. Environmental Pollution, vol. 140, pp. 416-426

Hyakorn P.S., Pinder G.F. (1983) Computational methods in subsurface flow, Academic Press, New York

IARC (2015) IARC Monographs Volume 112: evaluation of five organophosphate insecticides and herbicides. International Agency for Research of Cancer – World Health Organization

Jeppu G.P., Clement T.P. (2012) A modified Langmuir-Freundlich isotherm model for simulating pH-dependent adsorption effects, Journal of Contaminant Hydrology, vol. 129-130, pp. 46-53

Johnson K.A., Goody R.S. (2011) The Original Michaelis Constant: Translation of the 1913 Michaelis–Menten Paper. Biochemistry, vol. 50(39), pp. 8264–8269

Kadlec R.H. (2000) The inadequacy of first-order treatment kinetic models, Ecological Engineering, vol.15, p. 105-119

Kadlec R.H., Knight R.L. (1996) Treatment wetlands. New York, USA: Lewis Publishers

Karickhoff S.W., Brown D.S., Scott T.A. (1979) Sorption of hydrophobic pollutants on natural sediments. Water Research, vol. 13, pp. 241-248

Karickhoff S.W. (1984) Organic pollutant sorption in aquatic systems. Journal of Hydraulic Engineering, vol. 110(6), 18939

Keefe S.H., Barber L.B., Runkel R.L., Ryan J.N. (2004) Fate of volatile organic compounds in constructed wastewater treatment wetlands. Environmental Science and Technology, vol. 38, pp. 2209-2216

Keller G.V., and Frischknecht F.C. (1996) Electrical methods in geophysical prospecting, Pergamon, London

Kleidorfer M., Deletic A., Fletcher T.D. and Rauch, W. (2009) Impact of input data uncertainties on stormwater model parameters. Water Science and Technology, vol. 60(6), pp. 1545 -1554

Kleidorfer M., Chen S., Dotto C.B.S., McCarthy D. (2012) Impact of objective function choice on model parameter sensitivity. 9th International Conference on Urban Drainage Modelling, Belgrade, Serbia

Köhne J.M., Köhne S., Šimůnek J. (2009) A review of model applications for structured soils: b) Pesticide transport, Journal of Contaminant Hydrology, vol. 104, p. 36-60

Kottegoda N.T., Rosso R. (2008) Applied Statistics for Civil and Environmental Engineers. Second Edition. Oxfor, United Kingdom, Blackwell Publishing

Kuczera G., Mroczkowski M. (1998) Assessment of hydrologic parameter uncertainty and the worth of multiresponse data. Water Resources Research, vol 34(6), pp. 1481-1489

Kuczera G., Parent E. (1998) Monte Carlo assessment of parameter uncertainty in conceptual catchment models: the Metropolis algorithm, Journal of Hydrology, vol. 211, pp. 69-85.

Langergraber G., Šimůnek J. (2005) Modeling variably saturated water flow and multicomponent reactive transport in constructed wetlands. Vadose Zone Journal, vol. 4(4), pp. 924-938

Langergraber G. (2008) Modeling of processes in subsurface flow construted wetlands – a review, Vadose Zone Journal, vol. 7(2), p. 830-842

Langergraber G., Giraldi D. , Mena J., Meyer D., Peña M., Toscano A., Brovelli A., Korkusuz E.A. (2009) Recent developments in numerical modelling of subsurface flow constructed wetlands. Science of the Total Environment, vol. 407(13), pp. 3931-3943

Langmuir D. (1997) Aqueous Environmental Geochemistry. Prentice Hall, New Jersey, USA

Le Coustumer S., Fletcher T.D., Deletic A., Barraud S., Poelsma P. (2012) The influence of design parameters on clogging of stormwater biofilters; a large-scale column study, Water Research, vol. 46(20), pp. 6743-6752

Lee K.C., Rittman B.E., Shi J., McAwoy D. (1998) Advanced Steady-State Model for the Fate of Hydrophobic and Volatile Compounds in Activated Sludge, Water Environment Research, vol. 70(6), pp. 1118-1131

LeFevre, G.H., Novak, P.J., Hozalski, R.M. (2012) Fate of Naphthalene in laboratory-scale bioretention cells: Implications of sustainable stormwater management, Environmental Science and Technology, vol. 46(2), pp.995-1002

Lewis W.K., Whitman W.G. (1924) Principles of Gas Absorbtion. Industrial and Engineering Chemistry, vol. 16(12), pp. 1215-1220

Li, H., Davis A.P. (2008a) Urban particle capture in bioretention media. I: Laboratory and field studies, Journal of Environmental Engineering, vol. 134(6), pp. 409-418

Li, H., Davis A.P. (2008b) Heavy metal capture and accumulation in bioretention media, Environmental Science and Technology, vol. 42(14), pp. 5247-5253

Li, Y.; Deletic, A.; Alcazar, L.; Bratieres, K.; Fletcher, T. D.; McCarthy, D. T. (2012) Biofilters for removal of microorganisms from urban stormwater. Ecological Engineering, vol. 49, pp. 137-145

Li. Y.L. McCarthy D., Deletic A. (2014) Stable cooper-zeolite filter media for bacterial removal in stormwater. Journal of Hazardous Materials, vol. 273, pp. 222-230

Lindblom E., Ahlman S. Mikkelsen P.S. (2011) Uncertainty-based calibration and predictionwith a stormwater surface accumulation-washoff model based on coverage of sampled Zn, Cu, Pb and Cd field data. Water Research, vol. 45(13), pp. 3823-3835.

Lintern A., Daly E., Deletic A. (2012) Verifying a stormwater biofiltration model. Paper presented at UDM Conference, Belgrade, Serbia

Loke E., Warnaars E.A., Jacobsen P., Nelen F., do Céu Almeida M. (1997) Artificial neural networks as a tool in urban storm drainage. Water Science and Technology, vol. 36, pp. 101-109

Loucks, D.P., van Beek, E.; Stedinger, J.R., Dijkman, J.P.M; Villars, M.T. (2005). Ch. 12 in: Water Resources Systems Planning and Management: An Introduction to Methods, Models and Applications, Paris: UNESCO

Mackay D., Shiu W.Y., Ma K.Ch., Lee S.Ch. (2006) Handbook of Physical-Chemical Properties and Environmental Fate for Organic Chemicals, second ed., CRC Press

Magga, Z., Tzovolou, D. N., Theodoropolou, M. A., Tsakiroglou, C. D., (2012) Combining experimental techniques with non-linear numerical models to assess the sorption of pesticides on soil, Journal of Contaminant Hydrology, vol. 129-130, pp. 62-69

Makepeace D. K.; Smith D. W.; Stanley S. J. (1995) Urban stormwater quality: Summary of contaminant data. Critical Reviews in Environmental Science and Technology, vol. 25 (2), pp. 93-139.

Mannina G., Viviani G. (2010). An Urban Drainage Stormwater Quality Model: Model Development and Uncertainty Quantification. Journal of Hydrology, vol. 381 (3-4), pp. 248–265.

Maryland Stormwater Design Manual, Volume I. (2009), Maryland Department of the Environment, USA (revised version)

Maryland Stormwater Design Manual, Volume II. (2009) Maryland Department of the Environment, USA (revised version)

McCarthy D.T. (2008) Modelling microorganisms in urban stormwater. Civil Engineering, Melbourne, Monash University, Australia. PhD Thesis

McKay M.D., Beckman R.J., Conover W.J. (1979) A comparison of three methods for selecting values of input variables in the analysis of output from a computer code. Technometrics, vol. 21(2), pp. 239-245

Metropolis N., Rosenbluth A.W., Rosenblulth M.N., Teller A.H., Teller E. (1953) Equation of state calculations by fast computing machines. Journal of Chemical Physics, vol. 21, pp. 1087-1092.

Meyer D., Langergraber G., Dittmer U. (2006) Simulation of sorption processes in vertical flow constructed wetlands for CSO treatment. Proceedings 10th International Conference on Wetland Systems for Water Pollution Control, Lisbon, Portugal

Meyer D., Dittmer U. (2015) RSF_Sim – A simulation tool to support the design of constructed wetlands for combined sewer overflow treatment. Ecological Engineering, vol. 80, pp. 198-204

Monod J. (1949) The growth of bacterial cultures. Annual Reviews of Microbiology, vol. 3, pp. 371–394.

Montgomery D.C., Runger G.C. (2010) Applied Statistics and Probability for Engineers, 5th Edition, Wiley

Morrison F., Gasperikova E. (2012) DC Resistivity and IP field systems, data processing and interpretation. Berkley course in applied geophysics – online notes

Muleta M.K., Nicklow J.W. (2005) Sensitivity and uncertainty analysis coupled with automatic calibration for distributed watershed model. Journal of Hydrology, vol. 306, pp. 127-145

Mulder H., Breure A.M., Rulkens W.H. (2001) Prediction of complete bioremediation periods of PAH soil pollutants in different physical states by mechanistic models, Chemosphere, vol. 43, p. 1085-1094

Murakami M., Shinohara H., Takada H. (2009) Evaluation of wastewater and street runoff as sources of perfluorinated surfactants (PFSs). Chemosphere, vol. 74, pp. 487-493

Nash J.E., Sutcliffe J.V. (1970) River flow forecasting through conceptual models. Part I – A discussion of principles, Journal of Hydrology, vol. 10, p. 282-290

Ngabe B., Bidleman T.F., Scott G.I. (2000) Polycyclic aromatic hydrocarbons in storm runoff from urban and coastal South Carolina. Science of the Total Environment, vol. 255, pp. 1-9

NHMRC-NRMMC. (2011) Australian Drinking Water Guidelines. National Health and Medical Research Council and Natural Resource Management Ministerial Council: Canberra.

NRMMC, EPHC & NHMRC. (2008) Australian guidelines for water recycling: managing health and environmental risks (Phase 2) Augmentation of drinking water supplies. Natural Resource Management Ministerial Council, the Environment Protection and Health Council and the National Health and Medical Research Council

Omoti U. and Wild A. (1979) Use of Fluorescent Dyes to Mark the Pathways of Salute Movement Through Soils Under Leaching Conditions: 1. Laboratory Experiments, Soil Science, vol. 128(1), pp. 28-33

Page D.W., Khan S.J., Miotlinski K. (2011) A systematic approach to determine herbicide removals in constructed wetlands using time integrated passive samplers. Journal of Water Reuse and Desalination, vol. 1(1), pp. 11-17

Pinder G.F., Celia M.A. (2006) Sursurface hydrology. First Edition, John Wiley and Sons, New Jersey, USA

Pitt R., Field R., Lalor M., Brown M. (1995) Urban stormwater toxic pollutants: assessment, sources and treatability. Water Environment Research, vol. 67 (3), pp. 260-275.

Plosz, B. G., Leknes, H., Thomas, K. V. (2010) Impacts of competitive inhibition, parent compound formation and partitioning behavior on the removal of antibiotics in municipal wastewater treatment, Environmental Science and Technology, vol. 44(2), pp. 734-742

Pomiès M., Choubert J.M., Wisniewski C., Coquery M. (2013) Modelling of micropollutant removal in biological wastewater treatments: A review, Science of the Total Environment, vol. 443, pp. 733 – 748

Prodanovic V., Randelovic A., Deletic A., Jacimovic N. (2014) Dealing with uncertainty in calibration of a stormwater biofilter model. Paper presented at the 13th International Conference on Urban Drainage, Sarawak, Malaysia

Qiu H., Lu L., Pan B., Zhang Q., Zhang W., Zhang Q. (2009) Critical review in adsorption kinetic models, Journal of Zhejiang University SCIENCE A, Vol. 10(5), pp. 716-724.

Rauch W., Thurner N., Harremoes P. (1998) Required accuracy of rainfall data for integrated urban drainage modeling. Water Science and Technology, vol. 37 (11), pp. 81–89

Read J., Wevill T., Flether T., Deletic A. (2008) Variation among plant species in pollutant removal from stormwater in biofiltration systems. Water Research, vol. 42, pp. 893-902

Refsgaard J.C., van der Sluijs J.P., Brown J., van der Keur P. (2006) A framework for dealing with uncertainty due to model structure error. Advances in Water Resources, vol. 29(11), pp. 1586-1597

René P.S. and Schwarzenbach R.P. (1993) Environmental organic chemistry, John Wiley & Sons, INC, New York.

Rogers H.R. (1996). Sources, behaviour and fate of organic contaminants during sewage treatment and in sewage sludges. The Science of the Total Environment, vol. 185(1-3), pp. 3-26.

Roose T. (2000) Mathematical model of plant nutrient uptake. PhD Thesis, Linacre College, University of Oxford, England, UK

Rossman L.A. (2010). Storm Water Management Model – User Manual V5.0. US EPA, Cincinnati, OH

Sabatini D.A., (2000) Sorption and Intraparticle Diffusion of Fluorescent Dyes with Consolidated Aquifer Media, Ground Water, vol. 38(5), pp. 651-656.

Sabatini, D.A. and Austin, T.A., (1991) Characteristics of Rhodamine WT and Fluorescein as Adsorbing Ground-Water Tracers, Ground Water, vol. 29(3), pp. 341-349

Schmitt N., Wanko A., Laurent J., Bois P., Molle P., Mosé R. (2015) Constructed wetlands treating stormwater from separate sewer networks in a residential Strasbourg urban catchment area: Micropollutant removal and fate. Journal of Environmental Chemical Engineering, vol. 3(4), pp. 2816-2824

Schnoor J.L., Licht L.A., McCutcheon S.C., Woolfe N.L., Carreira L.H. (1995) Phytoremediation of organic and nutrient contaminants. Environmental Science and Technology, vol. 29 (7), pp. 318A–323A

Scwarzenbach R.P., Gschwend P.M., Imboden D.M. (2003) Environmental Organic Chemistry. Second Edition, Wiley-Interscience, New Jersey, USA

Schwarzenbach R.P., Escher B.I., Fenner K., Hofstetter T.B., Johnson C.A. von Gunten U., Wehrli B. (2006) The Challenge of Micropollutants in Aquatic Systems. Science, vol. 313(5790), pp. 1072-1077

Sebastian C. (2013) Bassin de retenue des eaux pluviales en milieu urbain : performance en matière de piégeage des micropollutants. Ecole doctorale : Mécanique, Energétique, Génie Civil, Acoustique. L'institut national des sciences appliquées de Lyon, France. PhD Thesis

Shainberg I., Rhoades J.D., Prather R.J. (1981) Effect of Low Electrolyte Concentration on Clay Dispersion and Hydraulic Conductivity of a Sodic Soil, Soil Science Society of America Journal, Vol. 45(2), pp. 273-277

Šimůnek J., Šejna M., van Genuchten M.Th. (1999) The HYDRUS-2D software package for simulating the two-dimensional movement of water, heat, and multiple solutes in variably saturated media - Version 2.0. IGWMC - TPS - 53, International Ground Water Modeling Center, Colorado School of Mines, Golden, Colorado, USA

Šimůnek J., Van Genuchten M.Th. (2008) Modeling Nonequilibrium Flow and Transport Processes using HYDRUS, Vadose Zone Journal, vol. 7(2), pp. 782-797

Siriwardene N.R., Deletic A., Fletcher T.D. (2007) Modelling of treatment of solids through infiltration systems. Proceedings of the NOVATECH 2007 conference, Lyon, France

Smart P.L. and Laidlaw I.M.S. (1977) An evaluation of some fluorescent dyes for water tracing, Water Resources Research, vol. 13(1), pp. 15-33.

Sniegowski, K., Mertens, J., Diels, J., Smolders, E., Springael, D. (2009) Inverse modeling of pesticide degradation and pesticide-degrading population size dynamics in a bioremediation system: Parameterizing the monod model. Chemosphere 75, 726–731.

SoE (2011) State of the Environment report, Department of Environmment, Australian Government. Available: https://www.environment.gov.au/science/soe/2011-report/contents

Tao S., Cao H., Liu W., Li B., Cao J., Xu F., Wang X., Coveney R.M. Jr., Shen W., Qin B., Sun R. (2003) Fate modelling of phenanthrene with regional variation in Tianjin, China, Environemental Science and Technology, vol. 37, p. 2453-2459

Thomas W., Rühling Å., Simon H. (1984) Accumulation of airborne pollutants (PAH, chlorinated hydrocarbons, heavy metals) in various plant species and humus. Environmental Pollution (Series A), vol. 36, pp. 295-310

Todorovic A. (2015) Impact of calibration period on parameter estimates in the conceptual hydrologic models of various structures. Faculty of Civil Engineering, Belgrade, University of Belgrade, Serbia. PhD Thesis

Toscano A., Langergraber G., Consolia S., Cirellia G.L. (2009) Modelling pollutant removal in a pilot-scale two-stage subsurface flow constructed wetlands. Ecological Engineering, vol. 35(2), pp. 281-289

US Army Corps of Engineers (1977) STORM Storage, Treatment, Overflow Runoff Model – User's Manual, Hydrologic Engineering Center, Davis, CA

US EPA (1992) Batch-Type Procedures for Estimating Soil Adsorption of Chemicals, Technical Resource Document, US EPA, Washington, DC

US EPA (2009) Appendix A to Part 423 - 126 Priority Pollutants. Title 40 Code of Federal Regulations Part 423 – Steam Electric Power Generating Point Source Category. United States Environmental Protection Agency.

US EPA (2010) Assessment monitoring list 1 and Screening survey list 2. Basic Infromation about the Unregulated Contaminant Monitoring Rule 2 (UCMR 2). [online] United States Environmental Protection Agency. Available: http://water.epa.gov/lawsregs/rulesregs/sdwa/ucmr/ucmr2/basicinformation.cfm [Accessed 27 April 2012]

USBR (1997). U.S. Department of the Interior, Bureau of Reclamation. Water Measurement Manual

Van Genuchten M.Th., Wagenet R.J. (1989) Two site/two region models for pesticide transport and degradation: Theoretical development and analytical solutions. Soil Science Society of America Journal, vol. 53, pp. 1303 – 1310

Vaze J., Chiew F.H.S. (2003) Comparative evaluation of urban storm water quality models. Water Resources Research, vol. 39 (10), 1280

Vezzaro L., Gevaert V., Benedetti L., De Keyer W., Verdonck F., Vanrolleghem P.A., Boisson P., Mikkelsen P.S. (2009) Unit Process Models for Fate of Priority Pollutants, ScorePP Deliverable No: D7.2. Sixth Framework Programme, Sub-Priority 1.1.6.3, Global Change and Ecosystems, Project no. 037036, www.scorepp.eu

Vezzaro L., Eriksso E., Ledin A., Mikkelsen P.S. (2010) Dynamic stormwater treatment unit model for micropollutants (STUMP) based on substance inherent properties. Water Science and Technology, vol. 62(3), pp. 622-629.

Vezzaro L., Eriksson E., Ledin A., Mikkelsen P.S. (2011) Modelling the fate of organic micropollutants in stormwater ponds. Science of the Total Environment, vol. 409(13), pp. 2597-2606

Vezzaro L., Eriksson E., Ledin A., Mikkelsen P.S. (2012) Quantification of uncertainty in modelled partitioning and removal of heavy metals (Cu, Zn) in a stormwater retention pond and a biofilter. Water Research, vol. 46(20), pp. 6891-6903

Vrugt J.A. (2008) Markov chain Monte Carlo Simulation Using the DREAM Software Package: Theory, Concepts, and MATLAB Implementation. DREAM Manual. Updated version available on: http://faculty.sites.uci.edu/jasper/files/2015/03/manual_DREAM.pdf

Vrugt J.A., Gupta H.V., Bouten W., Sorooshian S. (2003) A Shuffled Complex Evolution Metropolis algorithm for optimization and uncertainty assessment of hydrologic model parameters. Water Resources Research, vol. 39(8). SWC1e1SWC1-16

Vrugt J.A., Robinson B.A. (2007) Improved evolutionary optimization from genetically adaptive multimethod search. Proceedings of the National Academy of Sciences, USA, vol. 104, 708-711.

Wauchope R.D., Yeh S. ,Linders J.BHJ., Kloskowski R., Tanaka K., Rubin B., Katayama A., Koerdel W., Gerstl Z., Lane M., Unsworth J.B., (2002) Pesticide soil sorption parameters: theory, measurement, uses, limitations and reliability, Pest Management Science, vol. 58(5), pp. 419-445

Wilkes C.E., Summers J.W., Daniels C.A. (2006) PVC Handbook, Hanser Gardner Publications, Cincinnati, USA

Wong T.H.F, Fletcher T.D., Duncan H.P., Jenkins G.A. (2006) Modelling urban stormwater treatment – A unified approach, Ecological Engineering, vol. 27(1), pp. 58-70

Wong, T.H.F., Allen, R., Brown, R.R., Deletic, A., Fletcher, T.D., Gangadharan, L., Gernjak, W., Jakob, C., O'Loan, Reeder, M., Tapper, N., Walsh, C.W., (2012). Stormwater Management in Water Sensitive City: blueprint 2012. The Centre for Water Sensitive Cities, Melbourne

Wood Ballard B., Wilson S., Udale-Clarke H., Illman S., Scott T., Ashley R., Kellagher R. (2015) The SuDS Manual (C753), CIRIA, London, UK

Yao K., Habibian M., O'Melia C. (1971) Water and waste water filtration: Concepts and applications. Environemental Science and Technology, vol. 5(11), pp. 1105 - 1112

Yilmaz G., Yetimoglu T., Arasan S. (2008) Hydraulic conductivity of compacted clay liners permeated with inorganic salt solutions, Waste Management and Research, Vol. 26(5), pp. 464-473

Zgheib S., Moilleron R., Chebbo G. (2012) Priority pollutants in urban stormwater: Part 1 – Case of separate storm sewers. Water Research, vol. 46(20), pp. 6683-6692.

Zhang K. (2015) Micropollutants validation framework for natural treatment systems. Civil Engineering, Melbourne, Monash University, Australia. PhD Thesis

Zhao W., Wu Z., Zhou Q., Cheng S., Fu G., He F. (2004) Removal of dibutyl phthalate by a staged, vertical-flow constructed wetland. Wetlands, vol. 24 (1), pp. 202–206.

Zinger Y., Blecken G.T., Fletcher T.D., Viklander M., Deletic A. (2013) Optimising nitrogen removal in existing stormwater biofilters: Benefits and tradeoffs of a retrofitted saturated zone, Ecological Engineering vol. 51, pp. 75-82.

Биографија аутора

Ања Ранђеловић је рођена 11. октобра 1983. године у Београду. Основну школу и гимназију је похађала у Србији, Перуу, и Сједињеним Америчким Државама, због чега одлично влада енглеским и шпанским језиком. 2007. године је дипломирала на Грађевинском факултету, Универзитета у Београду, као студент генерације са просечном оценом 9,51. Добитник је бројних стипендија и признања током школовања и студија.

После завршене четврте године студија, радила је на више пројеката Тексашке Агенције за заштиту животне средине, који су за циљ имали успостављање доброг водног статуса мерењем и контролом садржаја патогених индикатора у атмосферском отицају. Дипломски рад је радила на Институту за водопривреду „Јарослав Черни“, где је учествовала и на пројектима анализе хаварија на депонијама пепела и на студији о Београдском изворишту.

Уписивањем докторских студија на Грађевинском факултету постаје асистент на предметима из области Механика флуида и хидраулика и Еколошко инжењерство. Уједно, као сарадник на Институту за хидротехнику, Грађевинског факултета, учествује у разним пројектима, студијама и експертизама (водовод, канализација, заштита животне средине, санитарне депоније, рударски пројекти итд.)

Истраживачки рад на њеној докторској дисертацији је део научног пројекта ТР 37010 „Системи за одвођење кишних вода као део урбане и саобраћајне инфраструктуре”. Лабораторијске и теренске експерименте је урадила 2012./13. године током једногодишњег студијског боравка на Универзитету Monash, у Мелбурну, у сарадњи са истраживачком групом проф. Ане Делетић у оквиру центра „Water Sensitive Cities”. Аутор и коаутор је четири рада на SCI листи, као и већег броја радова у домаћим часописима, на међународним и домаћим конференцијама.

Прилог 1.

• Изјава о ауторству

Потписани-а Ања Ранђеловић

број индекса 928/07

Изјављујем

да је докторска дисертација под насловом

Modelling transport of micropollutants in biofiltration systems for stormwater treatment

(Моделирање транспорта микрополутаната у биофилтерским системима за третман кишних вода)

- резултат сопственог истраживачког рада,
- да предложена дисертација у целини ни у деловима није била предложена за добијање било које дипломе према студијским програмима других високошколских установа,
- да су резултати коректно наведени и
- да нисам кршио/ла ауторска права и користио интелектуалну својину других лица.

Потпис докторанда

У Београду, 13. април 2016.

Прилог 2.

- # Изјава о истоветности штампане и електронске верзије докторског рада

Име и презиме аутора	Ања Ранђеловић
Број индекса	928/07
Студијски програм	Грађевинарство
Наслов рада	Modelling transport of micropollutants in biofiltration systems for stormwater treatment
Ментор	доц. др Ненад Јаћимовић, дипл. грађ. инж.

Потписани/а Ања Ранђеловић

Изјављујем да је штампана верзија мог докторског рада истоветна електронској верзији коју сам предао/ла за објављивање на порталу **Дигиталног репозиторијума Универзитета у Београду.**

Дозвољавам да се објаве моји лични подаци везани за добијање академског звања доктора наука, као што су име и презиме, година и место рођења и датум одбране рада.

Ови лични подаци могу се објавити на мрежним страницама дигиталне библиотеке, у електронском каталогу и у публикацијама Универзитета у Београду.

Потпис докторанда

У Београду, 13. април 2016.

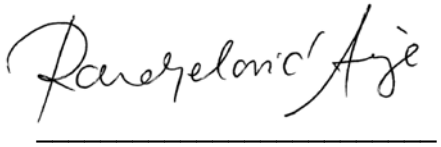

Прилог 3.

• Изјава о коришћењу

Овлашћујем Универзитетску библиотеку „Светозар Марковић“ да у Дигитални репозиторијум Универзитета у Београду унесе моју докторску дисертацију под насловом:

Modelling transport of micropollutants in biofiltration systems for stormwater treatment

(Моделирање транспорта микрополутаната у биофилтерским системима за третман кишних вода)

која је моје ауторско дело.

Дисертацију са свим прилозима предао/ла сам у електронском формату погодном за трајно архивирање.

Моју докторску дисертацију похрањену у Дигитални репозиторијум Универзитета у Београду могу да користе сви који поштују одредбе садржане у одабраном типу лиценце Креативне заједнице (Creative Commons) за коју сам се одлучио/ла.

1. Ауторство

2. Ауторство - некомерцијално

3. Ауторство – некомерцијално – без прераде

4. Ауторство – некомерцијално – делити под истим условима

5. Ауторство – без прераде

6. Ауторство – делити под истим условима

(Молимо да заокружите само једну од шест понуђених лиценци, кратак опис лиценци дат је на полеђини листа).

Потпис докторанда

У Београду, 13. април 2016.

1. Ауторство - Дозвољавате умножавање, дистрибуцију и јавно саопштавање дела, и прераде, ако се наведе име аутора на начин одређен од стране аутора или даваоца лиценце, чак и у комерцијалне сврхе. Ово је најслободнија од свих лиценци.

2. Ауторство – некомерцијално. Дозвољавате умножавање, дистрибуцију и јавно саопштавање дела, и прераде, ако се наведе име аутора на начин одређен од стране аутора или даваоца лиценце. Ова лиценца не дозвољава комерцијалну употребу дела.

3. Ауторство - некомерцијално – без прераде. Дозвољавате умножавање, дистрибуцију и јавно саопштавање дела, без промена, преобликовања или употребе дела у свом делу, ако се наведе име аутора на начин одређен од стране аутора или даваоца лиценце. Ова лиценца не дозвољава комерцијалну употребу дела. У односу на све остале лиценце, овом лиценцом се ограничава највећи обим права коришћења дела.

4. Ауторство - некомерцијално – делити под истим условима. Дозвољавате умножавање, дистрибуцију и јавно саопштавање дела, и прераде, ако се наведе име аутора на начин одређен од стране аутора или даваоца лиценце и ако се прерада дистрибуира под истом или сличном лиценцом. Ова лиценца не дозвољава комерцијалну употребу дела и прерада.

5. Ауторство – без прераде. Дозвољавате умножавање, дистрибуцију и јавно саопштавање дела, без промена, преобликовања или употребе дела у свом делу, ако се наведе име аутора на начин одређен од стране аутора или даваоца лиценце. Ова лиценца дозвољава комерцијалну употребу дела.

6. Ауторство - делити под истим условима. Дозвољавате умножавање, дистрибуцију и јавно саопштавање дела, и прераде, ако се наведе име аутора на начин одређен од стране аутора или даваоца лиценце и ако се прерада дистрибуира под истом или сличном лиценцом. Ова лиценца дозвољава комерцијалну употребу дела и прерада. Слична је софтверским лиценцама, односно лиценцама отвореног кода.